

OPERATION OF V.L.C.C.'S IN HEAVY WEATHER

BY

Civ.ing. Staffan Robertsson

A thesis submitted in partial  
fulfilment of the requirements  
for the Degree of Doctor of  
Philosophy of the C.N.A.A.  
(London).

School of Maritime Studies,

Plymouth Polytechnic,

Plymouth,

Devon, England.

PLYMOUTH POLYTECHNIC LIBRARY	
	Accn. No.
	Class No.
	Cat. No.

Plymouth, April, 1979.

STACK

PLYMOUTH POLYTECHNIC LIBRARY	
Accn. No.	5500013
Class. No.	T 623.88245 R103
Contl. No.	x70013869

DECLARATION

While registered as a candidate for the degree for which submission is made, I have not been a registered candidate for another award of the C.N.A.A. or of a University during the research programme.

No material contained in this thesis has been used in any other submission for an academic award.

*Staffan Robertsson*

Staffan Robertsson

## ACKNOWLEDGEMENTS

This project has been sponsored by Esso Petroleum Limited and I would like to thank <sup>the late</sup> Captain B. Garg for his co-operation. I would also like to thank Dr. R. Goodman, Mr. K. Taylor and staff at Lloyds Register of Shipping for helpful discussions and invaluable assistance by supplying me with the necessary transfer functions. For helpful discussions and supply of recorded full-scale measurements I am grateful to Dr. G. Ward and Mr. J. Vardon at British Ship Research Association.

I have been given full support, guidance and encouragement in every way by my supervisors Mr. Steve Dalzell and Mr. Roger Cheesley for which I am sincerely grateful. My thanks and appreciation also go to Dr. Moreby and all staff at the School of Maritime Studies who have made my stay such an enjoyable and memorable time.

Finally, my sincere thanks and admiration to Mrs. G. Day for her patient and excellent typing of a difficult manuscript.



# OPERATION OF V.L.C.C.'S IN HEAVY WEATHER

by

Staffan Robertsson

## ABSTRACT

A short review is presented of available instrumentation systems designed to assist the operation of ships in heavy weather by warning against dangerous wave loads. Some systems also give guidance to the master by predicting the outcome of evasive actions, and the bases on which such predictions are made, such as visual observations of the wave system, are questioned. A method is presented in which the motions of the ship are used to determine the sea state in the form of an "equivalent" wave spectrum.

Two investigations of the possibility of improving the guidance capability of warning instruments are described, in which the predictions are based on the equivalent wave spectrum. For this purpose, recorded full-scale data from a container ship and a tanker have been analysed and the two methods, spectrum analysis and a statistical method, are described.

Using the equivalent spectrum, predictions of the effect of a change of course and estimates of one response from another have been made and compared to measured values. The results of these comparisons, which are presented graphically and in the form of correlations between measured and predicted values, are discussed with respect to error sources and factors which limit the method's applicability.

The accuracy in predicting one response from another was found to be higher the closer the correlation between the responses, and correct estimations of the relative heading and the angular energy distribution of the wave system were found to be of importance.

Theoretical calculations of ship responses to irregular waves have been made by linear superposition of transfer functions and wave spectra and a new way of extrapolating the transfer functions is described.

# OPERATION OF V.L.C.C.'S IN HEAVY WEATHER

by

Staffan Robertsson

## ABSTRACT

A short review is presented of available instrumentation systems designed to assist the operation of ships in heavy weather by warning against dangerous wave loads. Some systems also give guidance to the master by predicting the outcome of evasive actions, and the bases on which such predictions are made, such as visual observations of the wave system, are questioned. A method is presented in which the motions of the ship are used to determine the sea state in the form of an "equivalent" wave spectrum.

Two investigations of the possibility of improving the guidance capability of warning instruments are described, in which the predictions are based on the equivalent wave spectrum. For this purpose, recorded full-scale data from a container ship and a tanker have been analysed and the two methods, spectrum analysis and a statistical method, are described.

Using the equivalent spectrum, predictions of the effect of a change of course and estimates of one response from another have been made and compared to measured values. The results of these comparisons, which are presented graphically and in the form of correlations between measured and predicted values, are discussed with respect to error sources and factors which limit the method's applicability.

The accuracy in predicting one response from another was found to be higher the closer the correlation between the responses, and correct estimations of the relative heading and the angular energy distribution of the wave system were found to be of importance.

Theoretical calculations of ship responses to irregular waves have been made by linear superposition of transfer functions and wave spectra and a new way of extrapolating the transfer functions is described.

## CONTENTS

	<u>Page</u>
TITLE	i
ACKNOWLEDGEMENTS	ii
ABSTRACT	iii
CONTENTS	iv
LIST OF FIGURES	vii
LIST OF TABLES	xiii
INTRODUCTION	1
CHAPTER 1	INSTRUMENTATIONS AS AID
	FOR OPERATION OF SHIPS IN
	HEAVY WEATHER .. .. . 4
CHAPTER 2	THEORY .. .. . 11
	Ship responses in irregular
	waves. .. .. . 11
	Wave spectrum. .. .. . 11
	Response amplitude operators. 16
	The principle of linear
	superposition. .. .. . 18
	Practical applications. .. .. . 24
	Significant values and
	expected max values. .. .. . 29
	Shipping of green water. .. 34
CHAPTER 3	WAVE SPECTRUM DERIVED FROM THE
	MOTIONS OF A SHIP .. .. . 37
	Equivalent wave spectra. .. .. . 38
CHAPTER 4	INVESTIGATION I. CONTAINERSHIP 42
	Introduction. .. .. . 42
	Wave data .. .. . 44

	<u>Page</u>
Measured responses. . . . .	47
Response calculations. . . . .	47
Derivation of equivalent wave spectra. . . . .	66
The use of the equivalent wave spectrum for predictions.	70
Conclusions. . . . .	73
CHAPTER 5	
INVESTIGATION II. TANKER	75
Introduction. . . . .	75
Data. . . . .	76
Analysis methods. . . . .	77
The manual method. . . . .	78
Mean response period. . . . .	84
Estimation of the spectrum width parameter $\epsilon$ . . . . .	85
Response values. . . . .	86
Comparison to the Rayleigh distribution. . . . .	86
Expected max values. . . . .	93
Spectrum analysis of the response signals. . . . .	102
Autocorrelation function. . . . .	102
The Fourier Transform and random processes. . . . .	103
Application. . . . .	109
Comparison of results from the spectral analysis and the manual method. . . . .	117

	<u>Page</u>
Estimation of one response from another. . . . .	132
Wave direction and spread.	132
Wave height and period of the equivalent spectrum. . .	135
Sensitivity to response periods in estimating wave heights. . . . .	141
Comparison of measured and predicted values. . . . .	146
Prediction of relative motion at the F.P. . . . .	157
Acceleration at the F.P. . .	162
Conclusions. . . . .	166
CHAPTER 6 DISCUSSION OF RESULTS . .	169
Derivation of the equivalent wave spectrum. . . . .	169
Using the equivalent spectrum for predictions. . . . .	171
Prediction of relative motion.	174
The manual method contra spectrum analysis. . . . .	174
Final conclusions. . . . .	175
REFERENCES	178
APPENDIX	A1
SYMBOLS	

LIST OF FIGURES

<u>Fig. No.</u>	<u>Page</u>
1	The relative range of wave spectrum and transfer functions for different wave periods and $\lambda/L = 0.05$ to $2.55$ .. .. . 28
2	Bridging of the gap between the transfer function and the asymptot by a power function .. .. . 30
3	Derivation of the equivalent spectrum .. .. . 40
4	Measurement manoeuvre. From Ref. [8] .. .. . 43
5	Comparison of the recorded spectrum and a spectrum of Pierson-Moskowitz type with the same $H_{1/3}$ and $T_2$ .. .. . 45
6	Comparison of measured angular energy spread and theoretical spread functions .. .. . 46
7	Recorded response spectrum for pitch $S_R(f)$ , and spectrum area $m_0$ and mean response period $T_R$ as functions of frequency .. .. . 48
8	Recorded response spectrum for vertical acceleration at the F.P. $S_R(f)$ , and spectrum area $m_0$ and mean response period $T_R$ as functions of frequency .. 49
9	Vertical acceleration at the F.P. for different headings, without spread .. .. . 51
10	Vertical acceleration at the F.P. for different headings, spread function 1 .. .. . 52
11	Vertical acceleration at the F.P. for different headings, spread function 2 .. .. . 53
12	Acceleration period for various headings without spread .. .. . 54

<u>Fig. No.</u>		<u>Page</u>
13	Acceleration period for various headings	
	spread function 1 .. .. .	55
14	Acceleration period for various headings	
	spread function 2 .. .. .	56
15	Pitch angle for various headings without spread	57
16	Pitch angle for various headings with spread	
	function 1 .. .. .	58
17	Pitch angle for various headings with spread	
	function 2 .. .. .	59
18	Pitch periods for various headings without spread	60
19	Pitch periods for various headings with spread	
	function 1 .. .. .	61
20	Pitch periods for various headings with spread	
	function 2 .. .. .	62
21	Allocation of weight to the transfer function for heading $\mu_3$ (shaded) when calculating response in heading $\beta$ .. .. .	63
22	The principle of how known values of $T_R$ and $R_{1/3}$ are used to determine $T_{P-M}$ and $H_{1/3}$ .. ..	67
23	Spectra derived from acceleration and pitch responses	69
24	Examples of the digitized response signals ..	79
25	Pitch signal compared to the Normal distribution	80
26	Roll signal compared to the Normal distribution	81
27	Acc. eng. compared to the Normal distribution	82
28	Example of output from the "manual method"	83
29	Distribution of maxima from pitch compared to the Rayleigh distribution .. .. .	90

<u>Fig. No.</u>		<u>Page</u>
30	Distribution of maxima from roll compared to the Rayleigh distribution .. .. .	91
31	Distribution of maxima from acc. eng. compared to the Rayleigh distribution .. .. .	92
32	Distribution of heights from pitch compared to the Rayleigh distribution .. .. .	94
33	Distribution of heights from roll compared to the Rayleigh distribution .. .. .	95
34	Distribution of heights from acc. eng. compared to the Rayleigh distribution .. .. .	96
35	Estimated versus recorded max-values for pitch. Regression line solid, ideal relationship broken line .. .. .	98
36	Estimated versus recorded max-values for roll. Regression line solid, ideal relationship broken line .. .. .	99
37	Estimated versus recorded max-values for acc. eng. Regression line solid, ideal relationship broken line .. .. .	100
38	Comparison between input spectra and corresponding spectra derived by different lag values .. .. .	113
39	Example of response spectrum of pitch .. ..	114
40	Example of response spectrum of roll .. ..	115
41	Example of response spectrum of acc. eng. ..	116
42	Recorded significant pitch versus estimated from the manual method with regression lines. X = without, O = with adjustment for spread. ..	119



<u>Fig. No.</u>		<u>Page</u>
43.	Recorded significant pitch versus estimated from the spectrum method, with regression lines. X = without, O = with adjustment for spread ..	120
44	Recorded significant roll versus estimated from the manual method. X = without, O = with adjustment for spread .. .. .	121
45	Recorded significant roll versus estimated from the spectrum method. X = without, O = with adjustment for spread .. .. .	122
46	Recorded significant acc. eng. versus estimated from the manual method. X = without, O = with adjustment for spread .. .. .	123
47	Recorded significant acc. eng. versus estimated from the spectrum method. X = without, O = with adjustment for spread .. .. .	124
48	Pitch periods obtained from spectrum analysis versus manual method with regression line ..	125
49	Roll periods obtained from spectrum analysis versus manual method with regression line ..	126
50	Acc. eng. periods obtained from spectrum analysis versus manual method with regression line. . . .	127
51	Pitch responses, broken lines and pitch periods, solid lines, for full load, 14 knots and spread function 2 .. .. .	128
52	Roll responses, broken lines, and roll periods, solid lines, for full load, 14 knots and spread function 2 .. .. .	129

<u>Fig. No.</u>	<u>Page</u>
53	130
Acc. eng. responses, broken lines, and acc. eng. periods, solid lines, for full load. 14 knots and spread function 2 .. .. .	130
54	137
Significant wave heights of the equivalent spectra obtained from pitch versus heights from roll = X and acc. eng. = 0. Full load .. ..	137
55	138
Significant wave heights of the equivalent spectra obtained from pitch versus heights from roll = X and acc. eng. = 0. Ballast .. ..	138
56	139
Mean wave periods of the equivalent wave spectrum obtained from pitch versus periods from roll = X and acc. eng. = 0. Full load .. .. .	139
57	140
Mean wave periods of the equivalent wave spectrum obtained from pitch versus periods from roll = X and acc. eng. = 0. Ballast .. .. .	140
58	143
Sensitivity of pitch to errors in the recorded pitch period. Full load, 14 knots .. .. .	143
59	144
Sensitivity of roll to errors in the recorded roll period. Full load, 14 knots .. .. .	144
60	145
Sensitivity of acc. eng. to errors in the recorded acc. eng. period. Full load, 14 knots ..	145
61	149
Measured pitch versus predicted from roll = X and from acc. eng. = 0, and regression lines. Full load .. .. .	149
62	150
Measured pitch versus predicted from roll = X and from acc. eng. = 0, and regression lines. Ballast .. .. .	150
63	151
Measured roll versus predicted from pitch = X and acc. eng. = 0, and regression lines. Full load	151

<u>Fig. No.</u>		<u>Page</u>
64	Measured roll versus predicted from pitch = X and acc. eng. = 0, and regression lines. Ballast	152
65	Measured acc. eng. versus predicted from pitch = X and roll = 0, and regression lines. Full load	153
66	Measured acc. eng. versus predicted from pitch = X and roll = 0, and regression lines. Ballast	154
67	Measured acc. eng. versus predicted by equivalent spectrum = X and by correlation to pitch = 0. Full load .. .. .	155
68	Measured roll versus predicted by equivalent spectrum = X and by correlation to pitch = 0. Full load .. .. .	156
69	Relative motion estimated from pitch versus estimates from roll = X and acc. eng. = 0. Full load .. .. .	158
70	Relative motion estimated from pitch versus estimates from roll = X and acc. eng. = 0. Ballast .. .. .	159
71	Relative motion period estimated from pitch versus estimates from roll = X and acc. eng. = 0. Full load .. .. .	160
72	Relative motion period estimated from pitch versus estimates from roll = X and acc. eng. = 0. Ballast .. .. .	161
73	Acceleration of a rigid body .. .. .	162

LIST OF TABLES

<u>Table</u>	<u>Page</u>
2.1 Asymptotic values for non-dimensional RAO's	27
4.1 Ship particulars .. .. .	50
4.2 Calculated responses compared to recorded ..	65
4.3 Equivalent wave spectra for heading 130 <sup>o</sup> and 135 <sup>o</sup> .. .. .	68
4.4 Prediction of responses on heading 90 <sup>o</sup> using equivalent spectra from Table (4.3) ..	71
4.5 Cross-prediction of one response using spectra derived from the other .. .. .	72
5.1 Ship particulars .. .. .	76
5.2 Regression coefficients for comparison between estimated and recorded max values of heights C	101
5.3 Distribution of wind speeds and wind direction for the analysed records .. .. .	134
5.4 Regression analysis for estimated and measured values and between responses .. .. .	147
5.5 Regression between measured responses .. ..	148

## INTRODUCTION

Optimal operation of any ship in heavy weather is governed by consideration of three main factors, safety, economy and comfort. These are not necessarily of opposing nature as safe operation which leads to minimum damage to the ship, cargo and crew is good economy. When consideration of safety, however, leads to unnecessary time loss, by maintaining too low speed or navigating excessive distances, the operation is not the most economic possible. The responsibility for the operation of the ship lies with the captain whose actions are based on experience and judgement of the conditions.

With the increase of ship sizes and speeds has come an increasing interest in shipborne instrumentation which, in heavy weather, would assist captains of such ships in the increasingly difficult decision making concerning the safe operation of the ship. Such instruments may monitor and display various parameters such as motions, accelerations, stresses, etc. which may be difficult for the captain to assess, and on which he may wish to base his decisions. A further obvious development would be an instrument which could also give some guidance on what actions, such as a change of speed or course, would be most favourable under the given circumstances. For such a system it is, however, necessary to have information not only about the ship's response to the sea, but also about the actual sea itself, with respect to wave height, wave period and wave direction.

It is the aspect of deriving information about the sea from a moving ship which has been the objective of the investigation presented in this paper, and it should thus be seen as an exploration into one small but important area of the total complex of operation of ships in heavy weather and associated instrumentation systems.

This paper consists of six chapters and an appendix, of which the first three chapters contain most of the theoretical concept and the next three applications of the theory and discussion of the results.

The first chapter contains a short review of research concerning ships' responses to confused seas in general and presents some recent approaches to shipborne warning and guidance instrumentation systems. Chapter two gives the theoretical background for calculation of ship responses to confused seas, based on superposition of wave spectra and transfer functions.

In chapter three a method is proposed for deriving information about the sea from a moving ship and may be seen as the core on which the following investigations are based. It is described how a response of a ship is used to derive an "equivalent wave spectrum" which may be used for predicting other responses or the effects of a change of the ship's speed and heading.

In chapter four, the method described in chapter three is tested on measurements made on a containership. Comparisons are made between a measured wave spectrum and "equivalent wave spectra" derived from two different ship responses and between recorded and predicted values.

In chapter five the method is tested on recordings from a tanker. It is also described how the recordings have been analysed in two different ways, by spectrum analysis and a simple statistical method.

Chapter six finally, is a discussion of results from the investigations.

A great deal of effort has gone into the design of all the computer programs used for the project. The theory and the various formulae

utilized in the programs are to be found in the text and schematic flow diagrams are included in the appendices. Listings of the programs have, however, been excluded as they would only represent one possible design rather than an optimum solution. Most of the programs were written in Fortran IV and executed on an ICL 1905A computer but BASIC was also used for some programs run on an ICL 2003.

Figures are included as close as possible to the text from which they are referred. Formulae and tables are numbered in such a way that the first digit refers to the chapter number and following the dot is the order number for that chapter. Numbers in square brackets refer to the list of references at the end.

INSTRUMENTATION AS AN AID FOR OPERATION OF SHIPS IN HEAVY WEATHER

In comparison with the rapid progress made in other scientific areas such as aviation, electronics, etc. during the last century, the long traditions and the empirical methods used in ship design have earned naval architecture a reputation of being a conservative science governed by the rule of thumb. The reason for using empirical rules in ship design in spite of the improved methods for calculating stresses and deflections in various constructions, is the difficulty of determining the actual loads and forces caused by the sea which the ship must be designed to withstand.

Full scale measurements have been made in order to establish the load variations the ship's hull is subjected to at sea, but it was the statistical approach, pioneered by St. Denis and Pierson in 1953 [1], which, by outlining a new method for calculation of ship behaviour in irregular waves, sparked off the intense research in hydrodynamics and oceanography which has led to the rapid development of ship design during the last few decades. One of the difficulties in ship design today is, according to Bennet [2], to keep the balance of knowledge within the three steps of all structural design: the determination of the load, the calculation of the response, and the choice of adequate strength, expressed by stress and/or deflection criteria. Introduction of digital computers and refined methods for stress analysis has called for increased knowledge of wave loads and ship responses, and many projects have been carried out in order to verify and improve on the theoretical methods of predicting ships' behaviour at sea, such as [3-16]. Effects of ship speed, wave direction, wave heights, wave periods, angular energy spread etc. have been studied. The research has



led to the distributions of response values having been determined, methods for short-term and long-term predictions developed, etc., but there are still problems waiting to be solved.

There are also arguments put forward claiming the naval architects are too traditional in their approach and methodology, such as the rigid body concept which means that vibrations are treated separately from the motions of the rigid body. A more fundamental approach, which does not make such a distinction but where the ship is treated as a vibrating flexible body, is advocated by Bishop and Price [17-19].

Even if the wave loads and the ship's response to them could be fully determined the ship would, for economic reasons, still be designed with the assumption that it would be handled in a seamanlike manner at sea. This means that the officers are expected to take evasive actions when necessary in order to reduce wave loads in extreme weather conditions. Investigations such as [20-23] have been carried out with the objective of finding operational limits for various types of ships in rough weather, either as evaluations of various design parameters, or as guidelines for safer ship operation. It should be remembered that there are no specific limits below which the safety of the ship is assured as both the loads from the waves and the strength of the ship are statistical variables for which any values are possible, although with different probabilities. What can be achieved by appropriate actions is an increase of the probability of the wave induced loads being less than the strength of the ship.

Out of the many projects of full scale measurement of various ship responses, involving installations of sensors, gauges, processors,

recorders, etc., grew the idea of displaying the measured responses on the navigation bridge as an aid for the officers when judging the severity of the forces acting on the ship. The value of such assistance to the ship operators would be higher for the larger ships on which the punishment the ship receives from the sea may be difficult to appreciate from the bridge. Instrumentation giving this kind of assistance is usually referred to as a "hull-surveillance" or heavy weather warning system. Interest in such systems has been shown by the classification societies and it is possible that some kind of system for monitoring of and warning against wave loads may be required on certain types of ships in the future. As well as warning the captain against dangerous load levels and so reducing the risks of damage, an instrumentation system could also be used to collect records of response values over long periods of time which may be used for assessing the risks of fatigue damage.

Descriptions of various surveillance systems may be found in references [29-34]. The design and number of responses measured vary between the systems but measurement of longitudinal midship stress and vertical acceleration at one or more positions is usually incorporated. The gradual development of a system from a simple unit with analog display and alarms to computer orientated system with guidance facilities has been described in several papers by Lindemann [24-29]. Hoffman and Lewis [34] have made a detailed survey of eight systems which have been used as parts of various research projects and which may be commercially available.

The characteristics of the instruments were evaluated with respect to the following eleven parameters:

responses considered, sensors used, display units, transmission of signals, processing, input-output capabilities, calibration, alarms, guidance data for manoeuvring, reliability and cost. As they found a

OPERATION OF V.L.C.C.'S IN HEAVY WEATHER

BY

Civ.ing Staffan Robertsson

A thesis submitted in partial  
fulfilment of the requirements  
for the Degree of Doctor of  
Philosophy of the C.N.A.A.  
(London).

School of Maritime Studies

Plymouth Polytechnic

Plymouth

Devon. England

Plymouth, April, 1979.

in collaboration with the Esso Petroleum Company Limited and Lloyds  
Register of Shipping.

great variation in the design and capabilities of the systems, Hoffman and Lewis give specifications for a recommended heavy weather damage avoidance system. A summary of their proposal is given below.

Sensors - midship strain gauges, 1 port and 1 starboard, to give indication of the combined effect of the static still water load, the slowly varying wave load and the high frequency dynamic loads.

Accelerometers - 1 vertical and 1 lateral located at critical points, to give indication of the combined wave-induced motions of heave, pitch and roll. Deflection sensors consisting of 1-5 strain gauges located under the forecastle deck to monitor local wave pressures or the effects of water shipped on deck. Display - a self-contained display unit providing information about the current status of various responses displayed on needle gauges with warning and danger levels indicated.

Permanent records of the various responses.

Alarms - Both audio and visual with two levels : warning and danger.

Guidance - Graphical presentation of the variation of responses with sea state, ship speed, and heading relative to the waves. Alternatively, an interactive computer system responding to input information of ship speed, heading etc.

At the time of their investigation they did not find any of the systems conformed to all their criteria, but concluded that the EDO systems [ 33] was most readily adaptable to meet their specifications. It was at the time the only available system incorporating guidance information for the selection of alternative speeds and headings. Since then other systems based on mini computers have become available [ 29, 30, 32]. For comparison, a summary of the features of some recent systems are given here.

"HWDAS, The Heavy Weather Damage Avoidance System" [33].

comprises a port and starboard strain-gauge sensor which measures longitudinal stresses in the hull. The system of midship gauges is aimed at a general indication of the severity of the sea, as well as specific vertical and lateral bending moment responses. Vertical motions such as heave and pitch are represented by an accelerometer at the bow and lateral motions are measured by an accelerometer at the deck side. Slamming or shipping of water are claimed to be "detected and analysed" without description of how this is achieved. Coverage of additional responses may be included, either measured directly or "calculated in a computer". Such "calculations" are results from theoretical calculations, stored in the computer. The software modules give two separate modes of guidance labelled as "the maximum response prediction program" and "the manoeuvring analysis module". It is further claimed that "by inputting the wind speed, relative heading and forward speed, the navigator is able to determine the amount of change necessary in speed and/or heading in order to reduce the response by a required amount". This guidance process is not explicitly described, but it seems likely that the input wind speed is used for determination of a wave spectrum which is used for the predictions.

The "Auto Ship-bridge Motions monitor" [32]

is a system similar to HWDAS and comprises accelerometers for measuring vertical acceleration at the bow as well as rolling and pitching angles. A strain gauge is "employed for assessing wave load". As an option there is a computer based prediction facility which claims to predict "hull motions, including vertical acceleration of the bow" and "anticipated deck wetness". The operator is to set "wave length, wave height, direction, ship speed and ballast conditions by means of

digital switches". The information about the wave system is presumably to be gathered by visual observations.

Norcontrols "WEDAR" is a hull surveillance system as outlined in [ 26]. Monitoring of vertical acceleration of the bow and the port and starboard midship stresses are included. Prediction facilities are not included but a "trend indicator" shows the change of responses with time. In [ 29], Lindemann describes "a second generation system" which "performs global and local surveillance, carries out trend analysis and predictions, watches the roll motion and performs as a tour recorder". Predictions are made by estimation of the wave system from the motion of the ship.

The "Hull Monitoring System (HMS)" described in [ 30] comprises a computer and "computes, analyses and displays draught and trim, stability, hull stress, slamming, cargo lashing force and flooding". The system gives alarms when various predetermined values are exceeded, but any prediction facilities are not included.

It is important to realize that any prediction by an instrumentation system can only be at best as good as the input information about the wave system. The obvious dilemma is the conflict between the advantages to be gained from a guidance system and the great difficulties in obtaining accurate information about the wave system.

At the outset of this project it was felt unsatisfactory to have to rely on visual observations of the sea for any predictions and after consultations with Dr. Goodman and Mr. Taylor of Lloyds Register of Shipping it was decided to investigate a method whereby the ship's motions are utilized to define a wave spectrum. The method which is outlined in [ 35] and will be fully described in chapter 3 was conceived by Rask and the author at Chalmers University of Technology when comparing calculated and measured ships responses and found this to be simplified by utilizing the fact that response periods are affected by the periods of the existing wave system only and not by

the wave height. As visual estimates of the sea with respect to wave height, period, etc. from a moving ship are surprisingly difficult to make, even in good visibility, it would be regarded as an important improvement on the predicting facilities if they could be made superfluous. The periods of the ship's responses as well as their magnitude would be needed and the possibility of predicting unmonitored responses as well as estimates of results of actions in advance were to be investigated. It is interesting, therefore, to note that the same approach has, since this project began, been presented in [ 29 ] and instruments utilizing the method are presently being evaluated in several ships. [ 29 ] is also one of the very few publications which include mention of response periods as well as response values.

The idea of estimating the sea state from the ship's motions appears to have been used in [ 23 ] to estimate the wave height at the time of measurements, although the procedure is not described in that paper.

Even though instruments which monitor and display various responses are of value to the navigators, a system which could also give reliable guidance on how to manoeuvre the ship through an area of bad weather, is believed to be of great importance as a complement to ordinary weather routing where the objective is to minimize the number of encounters with bad weather areas. A captain could then, for instance, consult the system as to when and by how much the speed could be increased after having weathered out a storm, or, facing bad weather, work out in advance whether to avoid it by changing course and maintaining speed or whether to slow down and steer through the bad area. If the true sea state could be successfully detected from the ship's motions this would be of value to the weather routing organisations as improved feedback to their predictions could be obtained.

THEORY

The following investigation of the use of the ship as a wavebuoy is based on a comparison between actual measured motions of the ship travelling in an unknown seaway and theoretically calculated motions in defined wave spectra. This section gives a short review of the long established methods for calculation of a ship's responses to irregular waves which have been employed for this project.

Ship responses in irregular waves

In 1953 the oceanographer W.T. Pierson and the naval architect M. St. Denis presented a famous paper [1] in which they made the assumption that "the sum of the responses of a ship to a number of simple sine waves is equal to the response of the ship to the sum of the waves". This was a novel idea which for the first time outlined a method whereby ships behaviour in, and response to, irregular waves could be calculated. It sparked off intensive research both in the field of naval architecture, for which it was seen as a tool for improved design criteria, and in the field of oceanography in order to supply realistic wave spectra. The concept has been commonly accepted since and is a standard procedure today, see for instance [36-39]. Discrepancies between theory and full scale measurements are generally ascribed to insufficient knowledge about the actual wave spectrum and/or unsatisfactory response amplitude operators (RAO's) which represent the ship's response to the individual sine waves in the wave spectrum.

Wave spectrum

"Modern research on wind-generated waves may be said to have started with the first measurements and analysis of ocean wave spectra in 1948 by Barber and Ursell, to have risen to a considerable peak of



activity in the years around 1960, and then to have steadily declined in quantity, if not in quality, to the present day", quoted from Cartwright [40], who further states:

"Understanding of the mechanisms of wave generation by wind has made great progress since the total inadequacy of some 20 years ago, but the mechanisms are now seen to be so complex that realistic wave forecasting can only be attempted on national funding".

One of the most important contributions to naval architecture from the oceanographers' research is that of describing a seaway by means of a wave spectrum, from which certain statistical parameters such as the significant wave height and the mean period can be deduced. This is based on the assumption that the irregular wave pattern that makes up the sea surface consists of an infinitely large number of regular sinusoidal waves superimposed on each other, each component having its own frequency, amplitude and phase. The surface elevation at one point as a function of time  $S(t)$  can then be expressed:

$$S(t) = \sum_{i=1}^N a_i \cos(\omega_i t + \alpha_i)$$

where  $a_i$  = amplitude for component wave with frequency  $\omega_i$

$\alpha_i$  = phase displacement " " " "  $\omega_i$

and where  $\alpha_i$  is random and evenly distributed over the interval  $0, 2\pi$

The mean value of each component = 0 and the variance =  $\frac{1}{2} a_i^2$ . As

the energy of a gravitational wave is  $E = \frac{1}{2} a^2 \rho g b \lambda$

where  $a$  = wave amplitude

$b$  = breadth of wave

$\lambda$  = wave length

$\rho g$  = specific weight of water

the energy per unit area is proportional to  $\frac{1}{2}a^2$  i.e. the variance. The variance of the function  $S(t)$  is the sum of the variances for all the components, and a diagram of  $\frac{1}{2} a_i^2$  as a function of  $\omega$  gives a representation of the energy distribution over the components making up  $S(t)$ . With the number of components approaching infinity the energy spectrum  $S_w(\omega)$  can be defined as:

$$S_w(\omega) d\omega = \frac{1}{2} a_i^2$$

where  $S_w(\omega)$  is a continuous function so that the total energy of the wave system is  $E = \int_0^{\infty} S_w(\omega) d\omega = \sigma^2$  where  $\sigma^2 =$  variance of the surface elevation.

This means that for a period of time short enough for the wave surface to be regarded as a stationary ergodic random process, usually accepted to be in the order of 20-30 min, the wave system can be represented by such a wave spectrum. Because of factors such as wind speed, duration, fetch and previous weather conditions the wave spectra representing the sea vary from time to time and place to place. For theoretical computational purposes, however, it is practical to use a mathematically defined spectrum which will be representative of a typical seaway. This has been an area for extensive research for the last 30 years and various types of spectra have been proposed [41-48].

The parameters defining the spectrum vary between the proposals but they are generally the wind speed, wave height, wave period or combinations of these.

The wave spectrum used in this project is of Pierson-Moskowitz type [42] and will be referred to as the P-M spectrum. It can be expressed in a general form as:

$$S_w(\omega) = A/\omega^5 e^{-B/\omega^4} \quad (2.1)$$

where  $S_w(\omega)$  is the spectrum ordinate at frequency  $\omega$ .

A and B are constants which are related to the spectrum's moments.

The  $n$ :th moment is defined

$$m_{nw} = \int_0^{\infty} \omega^n S_w(\omega) d\omega$$

and with (2.1)

$$m_{nw} = A/4B \times B^{n/4} \Gamma(1-n/4)$$

where  $\Gamma(t) = \int_0^{\infty} e^{-x} x^{t-1} dx$  is the Gamma function.

From this:

$$m_0 = A/4B, \text{ the area under the spectrum}$$

$$m_2 = A/4 \sqrt{\pi/B}$$

$$m_4 = \infty$$

It can be shown, see for example [38] that for a random process a mean zero up-crossing frequency can be defined from the moments so that

$$\omega_2 = \sqrt{m_2/m_0}$$

and A and B can then be expressed:

$$B = \omega_2^4/\pi$$

$$A = 4m_0 \omega_2^4/\pi$$

Substitution into (2.1) gives

$$S_w(\omega) = \frac{4m_0 \omega_2^4}{\pi \omega^5} e^{-\left(\frac{\omega_2}{\omega}\right)^4/\pi} \quad (2.2)$$

This represents a one-dimensional spectrum describing long crested sea where all wave components travel in the same direction.

In reality, however, the waves usually are shortcrested due to

various wave components travelling in different directions. A spectrum containing information about such directional variation is called two-dimensional and is more complicated to obtain from measurements. As is the case for the shape of the spectrum the directional properties vary from observation to observation [49-53] so that it is practical for theoretical calculations to use some standardized functions which will describe the directional distribution of wave components. Several such functions have been proposed, a summary of which can be found in [54], using the assumption that all frequencies have the same directional distribution and are symmetrical with respect to the main wave direction. This is, of course, not necessarily the case in real seas where for instance newly created windwaves may travel in a direction different to old swell remaining from a previous storm. But unless one is concerned with the situation at a specific location at a certain time a general spread function is useful. Apart from unidirectional sea, i.e. no energy spread, the following two distributions have been used for this project, and will henceforth be referred to as spread function 1 and 2 respectively:

$$f_1(\mu) = 2/\pi \cos^2 \mu \quad -\pi/2 \leq \mu \leq \pi/2 \quad (2.3)$$

$$f_2(\mu) = 1/\pi \cos^2(\mu/2) \quad -\pi \leq \mu \leq \pi \quad (2.4)$$

where  $\mu$  is the angle of a wave component measured from the symmetry axis, i.e. the main wave direction. Both fulfil the necessary condition:

$$\int_{-\gamma}^{\gamma} f(\mu) d\mu = 1 \quad (2.5)$$

where  $\gamma = \pi/2$  and  $\pi$  respectively.

A two dimensional spectrum can then be expressed as

$$S_w(\omega, \mu) = S_w(\omega) f(\mu) \quad (2.6)$$

and the n:th moment

$$m_{nw} = \int_0^{\infty} \int_{-\gamma}^{\gamma} \omega^n S_w(\omega) f(\mu) d\mu d\omega \quad (2.7)$$

### Response amplitude operators

The response amplitude operator (RAO) refers to a ship's response to regular waves at a certain heading, speed and loading conditions. For each wave length the response amplitude has been shown to be approximately proportional to the wave amplitude when not too large, for many types of responses, such as bending moments, motions and acceleration so that the RAO's can be expressed in a non dimensional form with respect to the wave amplitude. For example the RAO's  $Y_P$  and  $Y_R$

pitch  $Y_P = R_P / (2\pi a / \lambda)$

roll  $Y_R = R_R / (2\pi a / \lambda)$

where  $R_P$  and  $R_R$  are the pitch and roll angle amplitudes respectively and obtained in a regular wave with amplitude  $a$  and frequency  $\omega$  and where  $(2\pi a / \lambda)$  is the slope of such a wave. Similarly, for vertical acceleration

$$Y_A = R_A / a\omega^2$$

where  $a\omega^2$  is the vertical acceleration of the wave.

The RAO's may be obtained from model experiments, either by repeated tests in regular waves of varying lengths or by a "transient wave" consisting of several waves generated so as to coincide at a given point. Another alternative is by calculation of a ship's response to regular waves based on hydrodynamic equations describing the

ship's motions [39] . By determining the ship's response to a wide range of wave lengths or frequencies a continuous function  $Y(\omega)$ , often referred to as the "transfer function", may be formed. The function is often given as a function of wavelength,  $\lambda$  to ship length  $L$ ,  $Y(\lambda/L)$ .

The RAO's are dependent on the ship's heading towards the waves, its speed and the loading condition. Keeping the latter two constant the transfer function can be expressed as a function of  $\omega$  and heading  $\beta$

Strip theory is regarded as giving reliable information about the ship's response in head and bow sea whereas quartering and following seas cause difficulties which have not been mastered to the same degree of accuracy. Nevertheless, most available computer programs for strip calculations do give values for headings smaller than  $90^\circ$ , (head sea being  $=180^\circ$ ). The problems encountered when dealing with following seas seem to be due to the awkward frequencies of encounter experienced in these conditions. The frequency of encounter  $\omega_e$  is the relative wave frequency as experienced by a ship which itself is moving. For gravity waves the speed of propagation  $C$  is  $C = g/\omega$  so the frequency of encounter can be expressed:

$$\omega_e = \omega \left( 1 - \frac{U\omega}{g} \cos\beta \right) \quad (2.8)$$

where  $\omega$  = absolute wave frequency

$U$  = speed of the ship

$\beta$  = heading relative to the direction of wave propagation

( $180^\circ$  = opposite direction to the waves)

$g$  = constant of gravity

From this definition it can be seen that for  $90^\circ < \beta \leq 180^\circ$ ,  $\cos \beta$  is negative and thus  $\omega_e$  always positive. However, in conditions where  $0^\circ \leq \beta < 90^\circ$ ,  $\cos \beta$  is positive and  $\omega_e$  can obtain negative as well as positive and zero values depending on the speed  $U$ ; so that:

$$\omega_e > 0 \text{ for } U \cos \beta < g/\omega$$

$$\omega_e = 0 \text{ for } U \cos \beta = g/\omega$$

$$\omega_e < 0 \text{ for } U \cos \beta > g/\omega$$

As can be seen from equation ( 2.8) there is one unique value of  $\omega_e$  for every given value of  $\omega$ . The inverse however is not true, and it can be shown that for  $0^\circ \leq \beta \leq 90^\circ$  and certain combinations of  $U$  and  $\omega$  three different values of  $\omega$  gives the same absolute value of  $\omega_e$ . Two of these are caused by long waves overtaking the ship and the third from a shorter wave being overtaken by the ship. The implications of this were fully described in the paper by St. Denis and Pierson[1] .

#### The principle of linear superposition

It will be assumed that the ship's response amplitude in regular waves is directly proportional to the wave amplitude so that  
response amplitude =  $Y a$

where  $Y$  = response amplitude operator

and  $a$  = amplitude of regular wave

Then for the wave

$$S(t) = a \cos \omega t$$

the response will vary as

$$r(t) = Y a \cos (\omega t + \alpha)$$

where  $\alpha$  = phase difference between the wave and the response signal.

This is only true, however, when the ship is stationary or travelling in a direction perpendicular to the direction of the wave propagation, because the ship is not excited by the absolute wave frequency but by the frequency of encounter. So the response signal is

$$r(t) = Y a \cos (\omega_e t + \alpha)$$

where  $\omega_e = \omega(1 - \frac{U\omega}{g} \cos \beta)$  as before

and  $\alpha$  = the phase between the wave encounter frequency and the response frequency.

Following the assumption of Pierson and St. Denis, the response in irregular waves is the sum of responses to the regular wave components and a response spectrum can be defined in analogy with the wave spectrum:

$$S_R (\omega_e) d\omega_e = \sum_i \frac{1}{2} (a_i Y_i)^2 d\omega_e$$

with the wave spectrum defined as

$$S_w (\omega_e) d\omega_e = \sum_i \frac{1}{2} a_i^2 d\omega_e$$

it follows that

$$S_R (\omega_e) = Y^2 (\omega_e) S_w (\omega_e)$$

The n:th moment is

$$m_{Rn} = \int_0^{\infty} \omega_e^n S_R (\omega_e) d\omega_e = \int_0^{\infty} \omega_e^n Y^2 (\omega_e) S_w (\omega_e) d\omega_e \quad (2.9)$$

The encounter wave spectrum can be found by transformation of the wave spectrum and allowing for the conservation of energy:



$$S_w(\omega_e) d\omega_e = S_w(\omega) d\omega$$

or

$$S_w(\omega_e) = S_w(\omega) / \left| \frac{d\omega_e}{d\omega} \right|$$

where  $\left| \frac{d\omega_e}{d\omega} \right| = 1 - \frac{2U\omega \cos\beta}{g}$  is the Jacobian

so that

$$S_w(\omega_e) = S_w(\omega) / \left( 1 - \frac{2U\omega \cos\beta}{g} \right)$$

From this it can be seen that  $S_w(\omega_e)$  has an infinite value for  $\omega = g/2U \cos \beta$  corresponding to

$$\omega_e = g/4U \cos \beta$$

which makes the evaluation of the integral difficult.

One possible way to overcome this problem can be found in [38] and the approach employed here follows similar lines.

A wave spectrum expressed as a function of  $\omega$  as in (2.2) has a shape when plotted which varies according to the selected value of  $\omega_2$ . A small value of  $\omega_2$  gives a narrow shape with a sharp peak whereas a large value makes it wide and shallow. Numerical integrations of spectra expressed in such a form should thus be made carefully and the increments selected with respect to  $\omega_2$ . For this reason it is an advantage if the spectrum is expressed in a non-dimensional form. Furthermore, it was shown in [55] that if the spectrum is of Pierson Moskowitz type and both the spectrum and the transfer function are functions of logarithmic values, a change of spectrum period results in a linear shift of the spectrum along the abscissa with respect to the transfer function. For example, if the spectrum is a function of  $\ln(\lambda/\lambda_2)$  where

$$\lambda_2 = 2\pi g \frac{m_{ow}}{m_{2w}}$$

and the transfer function of  $\ln (\lambda/L)$  where  $L =$  length of the ship,

then

$$\ln (\lambda/\lambda_2) = \ln (\lambda/L) - \ln (\lambda_2/L)$$

Equation (2.9) can now be expressed:

$$m_{nR} = \int_{-\infty}^{\infty} \omega_e^n Y^2 (\ln \lambda/L) S_w (\ln \lambda/\lambda_2) d \ln (\lambda/\lambda_2) \quad (2.10)$$

$$\text{where } S_w (\ln \lambda/\lambda_2) = S_w (\omega) / \left| \frac{d \ln (\lambda/\lambda_2)}{d\omega} \right|$$

$$\text{which with } \left| \frac{d \ln (\lambda/\lambda_2)}{d\omega} \right| = \left| \frac{d \ln (\omega_2/\omega)^2}{d\omega} \right| = \frac{2}{\omega} \text{ gives}$$

$$S_w (\ln \lambda/\lambda_2) = \frac{\omega}{2} S_w (\omega) \quad (2.11)$$

By using the following relationship for deep water waves:

$$\omega = \sqrt{2\pi g/\lambda}$$

and further

$$\omega_2 = \sqrt{m_2/m_o} = 2\pi/T_2$$

$$T_2 = \sqrt{2\pi\lambda_2/g}$$

so that from

$$\lambda/\lambda_2 = (\omega_2/\omega)^2$$

and by putting

$$X = \ln \lambda/\lambda_2$$

equation (2.11) becomes

$$S (\ln \lambda/\lambda_2) = \frac{2m_o}{\pi} e^{2X} e^{-2X/\pi} \quad (2.12)$$

having a peak at

$$X = \ln \sqrt{\pi}$$

Furthermore

$\omega_e$  can now be rewritten so that

$$\begin{aligned} \omega_e &= \omega \left( 1 - \frac{U\omega}{g} \cos \beta \right) = \sqrt{\frac{2\pi g}{\lambda}} \left( 1 - \frac{U\sqrt{2\pi g/\lambda}}{g} \cos \beta \right) = \\ &= \sqrt{\frac{2\pi g}{\lambda_2}} \sqrt{\frac{\lambda_2}{\lambda}} \left( 1 - \frac{2\pi U}{gT_2} \sqrt{\frac{\lambda_2}{\lambda}} \cos \beta \right) = \\ &= \frac{2\pi}{T_2} \sqrt{\frac{\lambda_2}{\lambda}} \left( 1 - \frac{2\pi U}{gT_2} \sqrt{\frac{\lambda_2}{\lambda}} \cos \beta \right) \end{aligned}$$

Equation ( 2.10) can now be written

$$m_{nR} = \int_{-\infty}^{\infty} \left[ \frac{2\pi}{T_2} \sqrt{\frac{\lambda_2}{\lambda}} \left( 1 - \frac{2\pi U}{gT_2} \sqrt{\frac{\lambda_2}{\lambda}} \cos \beta \right) \right]^n Y^2(\ln \lambda / L) S_w(\ln \lambda / \lambda_2) d \ln(\lambda / \lambda_2)$$

for heading  $\beta$

or with  $x = \ln(\lambda / \lambda_2)$

and  $Z = \ln(\lambda / L) = X + \ln(gT_2^2 / 2\pi L)$

$$m_{nR} = \int_{-\infty}^{\infty} \left( \frac{2\pi}{T_2} \right)^n e^{-nx/2} \left( 1 - \frac{2\pi U}{gT_2} e^{-x/2} \cos \beta \right)^n Y^2(Z) S_w(x) dx$$

As  $(2\pi/T_2)^n$  is a constant finally:

$$\frac{m_{nR}}{(2\pi/T_2)^n} = \int_{-\infty}^{\infty} e^{-nx/2} \left( 1 - \frac{2\pi U}{gT_2} e^{-x/2} \cos \beta \right)^n Y^2(Z) S_w(x) dx \quad (2.13)$$

So far it has been assumed that the sea is unidirectional and the ship is travelling in a direction  $\beta$  relative to the wave direction. As  $Y(Z)$  is the transfer function for this heading, it should strictly be denoted  $Y(Z, \beta)$ .

For shortcrested sea it was assumed in equation ( 2.6 ) that the energy spread is independent of the frequency so that a two dimensional spectrum could be expressed

$$S_w(\omega, \mu) = S_w(\omega) f(\mu)$$

which makes equation (2.13) for short crested sea:

$$\frac{m_{nR}}{(2\pi/T_2)^n} = \int_{-\gamma}^{\gamma} \int_{-\infty}^{\infty} e^{-nx/2} \left( 1 - \frac{2\pi U}{gT_2} e^{-x/2} \cos(\beta+\mu) \right)^n Y^2(Z, \beta+\mu) S_w(x) f(\mu) dx d\mu \quad (2.14)$$

where  $\beta$  = main wave direction

$\mu$  = component wave direction

$\gamma$  = integration limit depending on the spread function used

$x = \ln(\lambda/\lambda_2)$

$Z = \ln(\lambda/L)$

$U$  = ship speed

$T_2$  = mean wave period ( $= 2\pi \sqrt{m_{ow}/m_{2w}}$ )

and  $f(\mu)$  = the energy spread function.

In analogy with the mean wave period  $T_2$  a mean response period  $T_{2R}$  can be defined as:

$$T_{2R} = 2\pi \sqrt{m_{oR}/m_{2R}} \quad (2.15)$$

The broadness of a spectrum is represented by the spectrum width parameter  $\epsilon$  such that:

$$\epsilon = \sqrt{1 - m_2^2 / m_o m_4} \quad (2.16)$$

By putting

$M_{nR}(\beta) = m_{nR} / (2\pi/T_2)^n$  for heading  $\beta$  in equation (2.14) equations (2.15) and (2.16) can be expressed:

$$T_{2R}(\beta) = T_2 \sqrt{M_{oR}(\beta) / M_{2R}(\beta)}$$

$$\epsilon(\beta) = \sqrt{1 - M_{2R}^2(\beta) / M_{oR}(\beta) M_{4R}(\beta)}$$

Practical applications

The expression in equation (2.14) can be numerically evaluated using a computer and the integration performed as a summation according to:

$$M_{nR}(\beta) = \sum_{\mu=-\gamma}^{\gamma} F(\mu) \left[ \sum_{x=c_1}^{c_2} e^{-nx/2} \left( 1 - \frac{2\pi U}{gT_2} e^{-x/2} \cos(\beta+\mu) \right)^n Y^2(Z, \beta+\mu) S_w(x) \Delta x \right] \quad (2.17)$$

where  $F(\mu) = \int_{\frac{\mu-\Delta\mu}{2}}^{\frac{\mu+\Delta\mu}{2}} f(\mu) d\mu = F(\mu+\Delta\mu/2) - F(\mu-\Delta\mu/2)$

and  $c_1, c_2$  represents the range of summation.

For spread function 1:

$$F(\mu) = 1/2\pi (2\mu + \sin 2\mu) , \gamma = \pi/2$$

and for spread function 2:

$$F(\mu) = 1/2\pi (\mu + \sin \mu) , \gamma = \pi$$

If the expression within brackets in equation (2.17) is set to

$N(\beta+\mu)$  the equation becomes:

$$M_{nR}(\beta) = \sum_{\mu=-\gamma}^{\gamma} F(\mu) N(\beta+\mu)$$

and it can be seen that for  $\mu = 0$  and  $F(\mu) = 1$

$$M_{nR}(\beta) = N(\beta)$$

which is the moment for heading  $\beta$  in longcrested sea. It is practical, therefore, to start by calculating  $N(\beta)$  for all  $\beta$  between 0 and  $\pi$  for which there are available transfer functions and then apply the spread function desired. This saves some computations since

$N(\beta+\mu) = N(2\pi-(\beta+\mu))$  due to symmetry between starboard and port.

For this project transfer functions for 13 headings between  $0^\circ$  and  $180^\circ$  have been used so that  $\Delta\mu = \pi/12$ .

The spectrum in (2.2)

$$S_w(\omega) = \frac{4 m_o \omega_2^4}{\pi \omega^5} e^{-\frac{1}{\pi} \left(\frac{\omega_2}{\omega}\right)^4}$$

can be transformed to be a function of  $\ln(\lambda/\lambda_2)$  such that

$$S_w(\ln \lambda/\lambda_2) = S_w(\omega) / \left| \frac{d \ln(\lambda/\lambda_2)}{d\omega} \right|$$

and from

$$\ln(\lambda/\lambda_2) = \ln(\omega_2/\omega)^2$$

$$\text{the Jacobian } \left| \frac{d \ln(\lambda/\lambda_2)}{d\omega} \right| = \frac{2}{\omega}$$

so that

$$S_w(\ln \lambda/\lambda_2) = \frac{2 m_o}{\pi} \left(\frac{\omega_2}{\omega}\right)^4 e^{-\frac{1}{\pi} \left(\frac{\omega_2}{\omega}\right)^4}$$

and by putting

$$x = \ln(\lambda/\lambda_2) = \ln(\omega_2/\omega)^2$$

$$S_w(x) = \frac{2m_o}{\pi} e^{2x} \frac{-1}{\pi} (e^{2x}) = \frac{2m_o}{\pi} e^{2x-1} \frac{e^{2x}}{\pi} \quad (2.18)$$

The area under the spectrum  $m_o$  is usually related to the significant waveheight, the mean of the highest one third of the waves, so that

$$H_{1/3} = 4 \sqrt{m_o}$$

If, however,  $m_o$  in (2.18) is set at one ( $m_o = 1$ ) then the response

value can be directly related to the wave system in such a way that

a response value on a certain probability level corresponds to a

wave height on the same probability level. In this respect the

response values have been referred to the significant waveheight and are

hence to be taken as significant response/significant waveheight.

It should be noted that as "waveheight" is double amplitude, trough to crest, the response value is also double amplitude.

The summation over  $x$  should be made so that an appropriate range of the spectrum is covered and wavelengths of interest are included. The spectrum decays slowly for negative  $x$  values and much more rapidly for positive, which makes the negative summation limit awkward to decide on. It was decided, however, that a summation over  $x = -4$  to  $2$  with an increment of  $0.1$  would be satisfactory. This gives

$$m_0 = 0.999903, \quad T_2 = 1.0055, \quad \epsilon = 0.8034$$

Extension of the range by 33% to  $x = -6$  to  $2$  would give  $m_0 = 0.999998$ ,  $T_2 = 1.0008$ ,  $\epsilon = 0.8676$  which is an improvement of  $0.01\%$ ,  $0.47\%$  and  $8\%$  respectively. The exact values are  $m_0 = 1$ ,  $T_2 = 1$  and  $\epsilon = 1$ .

The width parameter  $\epsilon$  shows the biggest improvement of  $8\%$  but the use of  $\epsilon$  is restricted to a correction factor for the significant response value in  $\sqrt{1 - \epsilon^2}/2$  which improves by  $3\%$ . The relatively small gain in accuracy was not judged to justify a  $33\%$  increase in computer time.

The range of wavelengths covered by  $x = -4$  to  $2$  are, for example,

$$\lambda = 0.26\text{m} - 104\text{m} \text{ for } T_2 = 3 \text{ sec}$$

$$\text{and } \lambda = 11.4\text{m} - 4615\text{m} \text{ for } T_2 = 20 \text{ sec.}$$

where the peak of the spectrum is at  $25\text{m}$  and  $1107\text{m}$  respectively.

The RAO's or transfer functions were provided for  $\lambda/L = 0.05$  to 2.55 with an increment of 0.05 for the tanker and  $\lambda/L = 0.1$  to 5.1 with increment of 0.1 for the containership. In Figure (1) can be seen the relative range of spectrum and the transfer functions for the tanker for some mean wave periods. It is clear that if the summation over the range of the spectrum is constant, the transfer functions must be extrapolated outside the range for which they are given.

Nordenström [54] has given asymptotic functions for various transfer functions in a non-dimensional form and shown the implications of this when calculating short and long term response values. A similar approach which was easily included into the computer program has been used for this project. The responses which were calculated are listed in Table (2.1) together with their asymptotic values for small and large  $\lambda/L$  values.

TABLE 2.1

Asymptotic values for non-dimensional RAO's

Response	Non-dimensional form	small $\lambda/L$	large $\lambda/L$
Pitch	$P/(2\pi a/\lambda)$	0	$ \cos \beta $
Roll	$R/(2\pi a/\lambda)$	0	$ \cos(\pi - \beta) $
Vertical acceleration	$A/(a\omega^2)$	0	1*
Relative motion	$RM/a$	1	0

\* It should be noted here that the vertical acceleration is that of the encounter wave so that  $a\omega^2 = a(\omega - U\omega^2 \cos \beta/g)^2$  when evaluating the actual value.



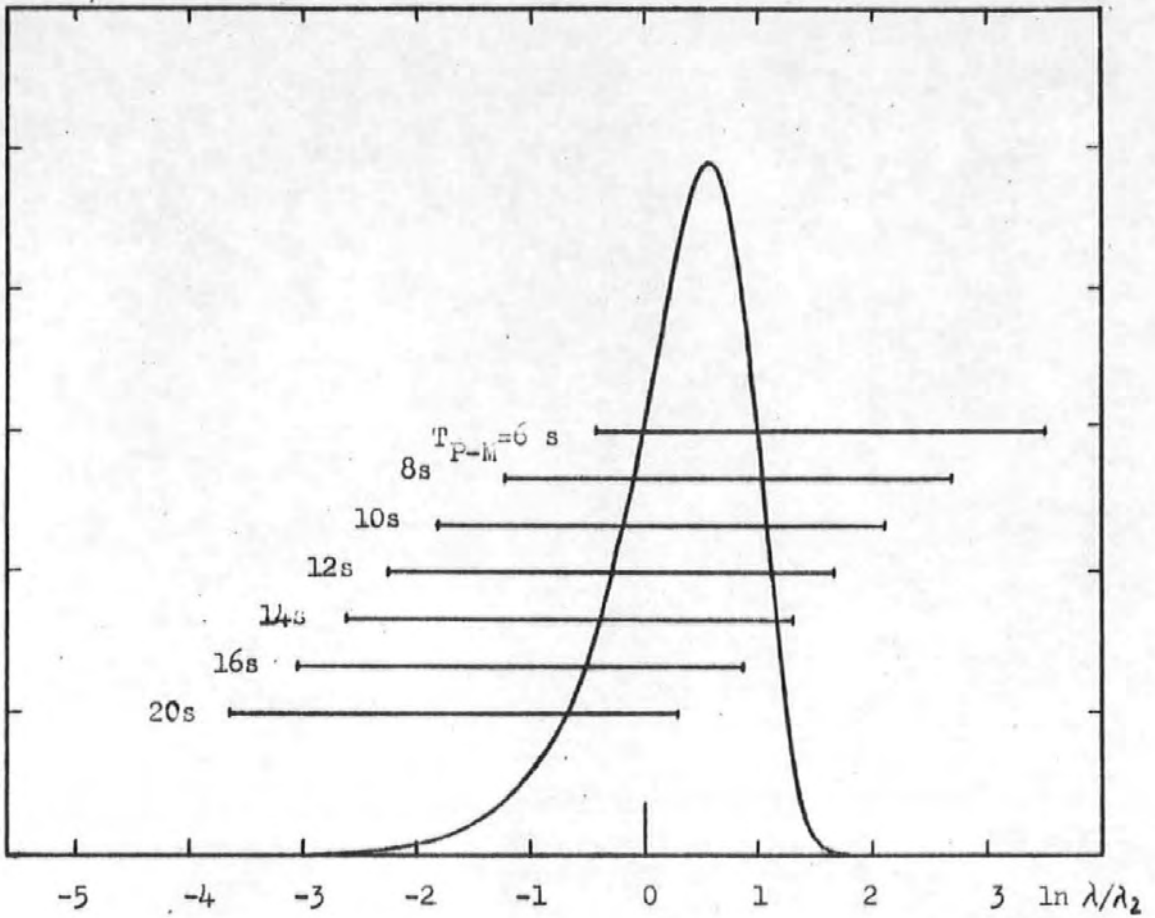


Fig. 1

The relative range of wave spectrum and transfer functions for different wave periods and  $\lambda/L = 0.05$  to 2.55.

In order to avoid too much of a 'jump' between the last available RAO value and the asymptotic value, a regression line was formed from the last three RAO values and used as an extension of the transfer function for large  $\lambda/L$  values until the asymptotic value was reached. The regression line was of the form:

$$Y = a x^b$$

$$\text{where } b = \frac{\sum(\ln x_i)(\ln y_i) - (\sum \ln x_i)(\sum \ln y_i) / n}{\sum(\ln x_i)^2 - (\sum \ln x_i)^2 / n}$$

$$a = \exp \left[ \frac{\sum \ln y_i}{n} - b \frac{\sum \ln x_i}{n} \right]$$

$$n = 3$$

$x_i = \lambda/L$  for the last three RAO values and

$y_i =$  the last three RAO values

The effect of this is schematically illustrated in Figure 2.

#### Significant values and expected max values

The many recordings of wave conditions at sea have revealed that the surface elevation at one point as a function of time  $S(t)$  closely follows the Normal or Gaussian distribution. The same distribution can usually be applied for many response variations with time, exceptions being for example, vertical bending moments where sagging moments tend to be larger than hogging. For most engineering purposes however, it is of interest to know the distribution of maxima rather than the elevation in order to predict wave heights or response amplitudes that can be expected. Short term distributions and the max values that can be expected within 20-30 minutes are of interest to

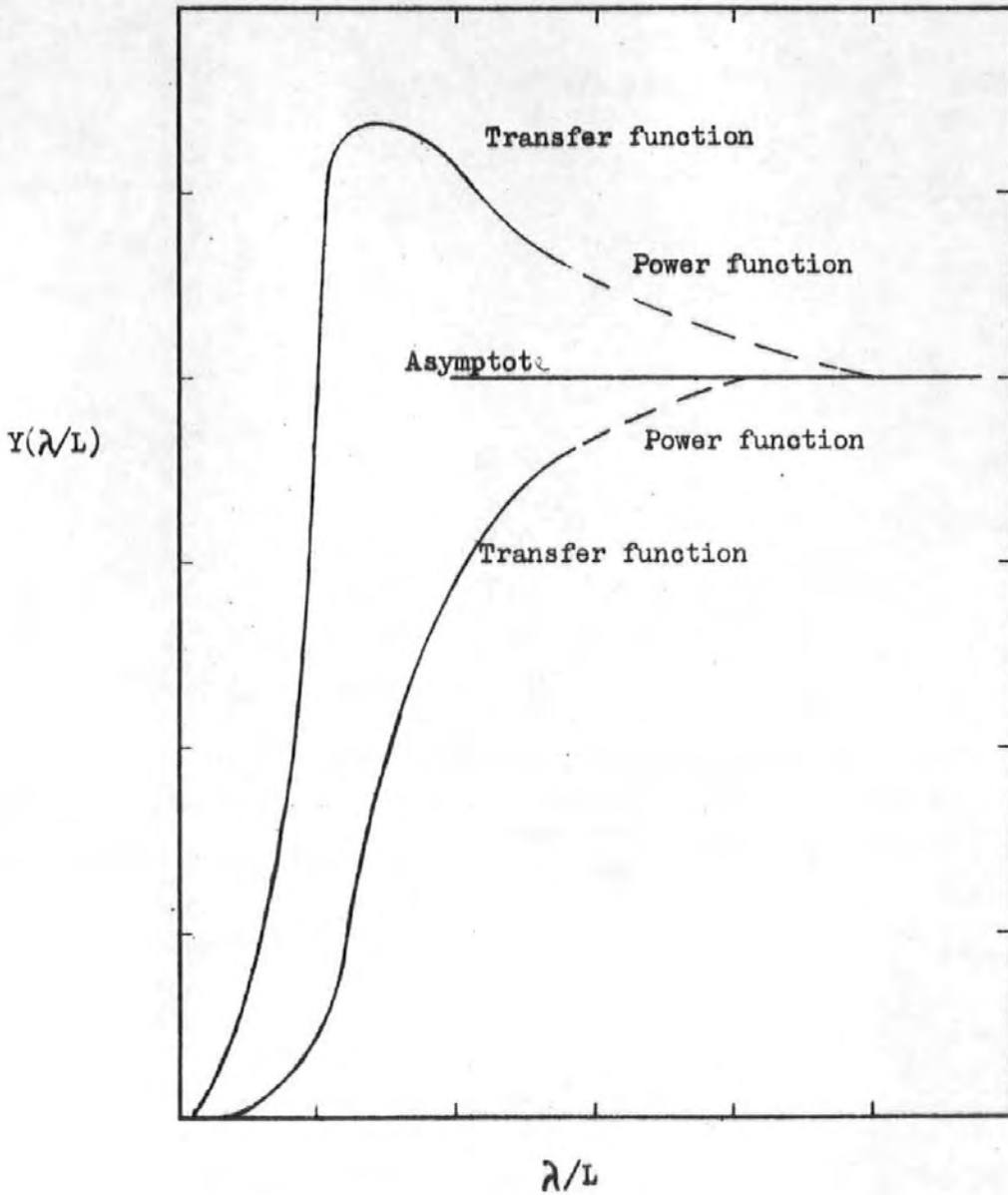


Fig. 2

Bridging of the gap between the transfer function and the asymptote by a power function.

the captain when manoeuvring his ship in a storm, whereas long term distributions of maxima, in the order of 20 years, are of interest to the designer of ships and other structures exposed to wave loads. In this project the short term situations only will be considered.

Several investigations have dealt with the distribution of such short term maxima in order to find a mathematical expression which closely fits measured maxima. Andrew and Price [56] have for instance shown how a generalised gamma function can be successfully applied for this purpose, when the distribution is known, and extrapolation beyond recorded values can be made with some confidence. The method, is, however, cumbersome and it is an advantage if a distribution can be used which can more easily be defined from the process.

Based on a work by Rice [57], Cartwright and Longuet-Higgins [58] have shown how the distribution of maxima can be estimated from the moments of a Gaussian process spectrum. The following expression was obtained:

$$f(\xi) = \frac{\epsilon e^{-\xi^2/2m_0} \epsilon^2}{\sqrt{m_0} \sqrt{2\pi}} + \frac{\xi \sqrt{1-\epsilon^2}}{m_0} e^{-\xi^2/2m_0} \left[ \frac{1}{2} + \frac{1}{\sqrt{2\pi}} \int_0^{\xi/\epsilon} \frac{1-\epsilon^2}{m_0} e^{-x^2/2} dx \right] \quad (2.19)$$

where  $\xi$  is a local maximum with respect to the mean level and can be negative as well as positive.

$$\int_0^Z e^{-x^2/2} dx = \begin{cases} 0 & \text{for } Z = 0 \quad (\epsilon = 1) \\ \sqrt{2\pi} / 2 & \text{for } Z = \infty \quad (\epsilon = 0) \end{cases}$$

$m_0$  = the area under spectrum

and  $\epsilon = \sqrt{1 - m_2^2/m_0 m_4}$  the spectrum width parameter so that  $0 \leq \epsilon \leq 1$ .

When the process is narrow so that  $\epsilon \rightarrow 0$  it can be seen from (2.19) that

$$f(\xi) = \frac{\xi e^{-\xi^2/2m_0}}{m_0} \quad \xi > 0$$

which is the Rayleigh distribution.

For a wide spectrum on the other hand, so that  $\epsilon \rightarrow 1$

$$f(\xi) = \frac{e^{-\xi^2/2m_0}}{\sqrt{m_0} \sqrt{2\pi}}$$

which is the Gaussian or Normal distribution.

The shape of  $f(\xi)$  in (2.19) which is gradually changing from the Rayleigh distribution to the Gaussian for increasing  $\epsilon$ , can be found in [58]. It is often assumed that the response spectrum is narrow enough to allow  $\epsilon = 0$  when the probability of a maximum exceeding a value  $\xi_m$  can be found from the Rayleigh distribution as:

$$\begin{aligned} P(\xi > \xi_m) &= 1 - P(\xi \leq \xi_m) = 1 - (1 - e^{-\xi_m^2/2m_0}) = \\ &= e^{-\xi_m^2/2m_0} \end{aligned} \quad (2.20)$$

The often used significant value is defined as the mean of the highest one third of the maxima so that

$$P(\xi > \xi_{1/3}) = 1/3$$

and evaluation of the mean of the highest one third  $\bar{\xi}_{1/3}$

$$\bar{\xi}_{1/3} = 3 \int_{\xi_{1/3}}^{\infty} \frac{\xi^2}{m_0} e^{-\xi^2/2m_0} d\xi$$

yields

$$\bar{\xi}_{1/3} = 2 \sqrt{m_0}$$

In this report significant values refer to double amplitude so that the significant response value  $R_{1/3}$  is:

$$R_{1/3} = 4 \sqrt{m_0}$$

The mean square value  $\bar{\xi}^2$  is defined as  $\bar{\xi}^2 = \int_{-\infty}^{\infty} \xi^2 f(\xi) d\xi$

which for the Rayleigh distribution gives

$$\overline{\xi^2} = 2 m_0$$

$$\text{or } \xi_{1/3} = \sqrt{2 \overline{\xi^2}}$$

For equation (2.19) ref [58] has shown

$$\overline{\xi^2} = m_0 (2 - \epsilon^2)$$

so that

$$\xi_{1/3} = 2 \sqrt{m_0} \sqrt{1 - \epsilon^2/2}$$

and the response value

$$R_{1/3} = 4 \sqrt{m_0} \sqrt{1 - \epsilon^2/2}$$

### Shipping of green water

Some of the hazards to a ship operating in rough seas, such as shipping of green water and slamming, can be related to the relative motion between the bow of the ship and the sea surface. Slamming is normally defined as an event where the bottom of the ship after an emergence re-enters the water at a velocity relative to the surface exceeding a predetermined value, the so called threshold velocity. Such an impact can cause local damage to the plating as well as overall stresses of high magnitude, the so called whipping stresses. Slamming is normally not experienced by large tankers with big draughts but due to their size and full form damage to the shell plating above the water line due to impacts with the waves may be sustained. This is usually referred to as bow flare slamming and has been subject to several investigations [59-62].

Such damage has been reported to be inflicted even under conditions when the pitching and heaving of the ship are negligible when it appears to be caused by waves breaking on to the bow [59] making it a design problem rather than an operational one.

In conditions when the ship is pitching and heaving, and thus contributing to the relative motion, the danger of impact damage is increased and shipping of green water may also be experienced. Such situations on the other hand, may be improved by correct manoeuvring of the ship. Shipping of green water is understood to be an event where the relative motion amplitude is greater than the local freeboard so that the waves come on to the deck and the static and dynamic forces from the water masses can cause severe damage to the structure and deck fittings. Increasing probability of shipping green water would indicate an increasing risk of damaging the ship.

If the relative motion is known, the probability of, or risk for, shipping of green water may be calculated from the following:

Let  $F$  = the local freeboard

$r$  = relative motion amplitude.

$m_{or} = \sigma_r^2$  the variance of relative motion.

Assume the maxima of the relative motion variation is Rayleigh distributed. Then:

$$f(r) = \frac{r}{m_{or}} e^{-r^2/2m_{or}}$$

so that the probability of shipping green water, i.e. the probability of an amplitude being larger than the freeboard  $r > F$

$$P(r > F) = 1 - P(r \leq F) = e^{-F^2/2m_{or}} \quad (2.21)$$

Response values in this report are generally expressed as significant response in double amplitude so that for relative motion

$$R_r 1/3 = 4 \sqrt{m_{or}}$$

With this substituted, (2.21) becomes:

$$P(r > F) = e^{-8F^2/R_r^2 1/3}$$

The probability can also be expressed as the relative frequency of the event such that

$$\frac{f_s}{f_r} = P(r > F) = e^{-8F^2/R_r^2 1/3}$$

where  $f_s$  = the mean frequency of shipping of water

$f_r$  = the mean frequency of the relative motion

If  $f_r$  or the mean period of the relative motion is known, the mean time between the events  $T_s$  is then

$$T_s = T_R e^{8F^2/R_r^2 1/3}$$

where  $T_R = 2\pi \sqrt{m_{or}/m_{2r}}$  may be predicted from another response or evaluated by direct measurements.



Shipping of green water may be seen as sequence of events, with a mean frequency of occurrence =  $fs$ , which is likely to follow some distribution in time. Ochi [37] has shown good agreement between the distribution in time of slamming events and the Poisson distribution. It seems reasonable to assume, as the same statistical conditions of the events are fulfilled, that the sequence of shipping water follows the same distribution so that

$$P(N = K) = \frac{\lambda^K e^{-\lambda}}{K!}$$

where  $N$  = number of occurrences of the event during a specified time  $T$

$K$  = integer

$\lambda$  = mean number of occurrences of the event in time  $T$ , so that

$$\lambda = c T$$

and  $c$  = mean frequency of occurrence

With  $c = fs$ , the probability of at least one event occurring within the time  $T = T_s$ , the average time, can be found as

$$P(N > 0) = 1 - P(N = 0) = 1 - e^{-\lambda}$$

where  $\lambda = fs T_s = 1$

and  $P(N > 0) = 1 - e^{-1} \approx 0.63$

Thus the probability of experiencing at least one shipping of green water within the time  $T_s$  is about 63%, where  $T_s$  is the mean period from

$$T_s = Tr e^{8F^2/R} 1/3$$

WAVE SPECTRUM DERIVED FROM THE MOTIONS OF A SHIP

The methods for predicting ships' behaviour in irregular waves have been subject to a lot of research and development since the paper by Pierson and St. Denis [1] was presented and it is generally accepted today that for a known seaway many ship responses can be confidently predicted by superposition of transfer functions and wave spectra. The method is used both for short term predictions, i.e. assessing a ship's performance in a particular seaway, and for long term predictions in order to estimate the maximum wave loads and responses that can be expected during a ship's service life. For such purposes, actual measured wave spectra or wave spectra of a standardized form may be used.

Comparisons between predicted values and values measured onboard call for the wave spectrum at the time of measurement to be known, but obtaining it is difficult and often costly, especially a two-dimensional spectrum. One method used is launching of wave buoys from which the information is transmitted either by cables, in which case the ship must be stopped [8] or by radio, in which case the buoy is not always retrieved [14].

Another is the measurement of the relative motion between the ship and the sea surface by radar or sonar and after the ship motion components are subtracted from the recording a one dimensional spectrum may be obtained. The method is relatively new and few results have been published [15,17, 63] For recordings of wave height, the Tucker wave recorder [64] has been extensively used, especially on weatherships, but seems to be less reliable for measurements on moving ships. Attempts to use the ship itself as a wave buoy have also been reported [65] but any results of this are not known to have been published.

### Equivalent wave spectra

It has already been mentioned that it is of importance to know the wave spectrum when comparing full scale measurements and theoretical predictions. Another context, in which this is important, is for shipborne warning instrumentations with prediction and guidance ability. If, in a period of heavy weather and severe ship motions, an instrument is consulted about what action should be taken in order to ease the situation, the wave spectrum must be known. As there is no known simple way of obtaining the wave spectrum from a moving ship an alternative approach has been investigated in this project.

Instead of deriving the true wave spectrum at any instant of time, the ship's responses are used to derive a wave spectrum of standardized shape which is defined by its significant wave height and mean wave period, and which would cause the same ship motions as the actual one. The two parameter spectra used is of Pierson-Moskowitz type and referred to as the "equivalent" wave spectrum.

The concept is based on the fact that with a very few exceptions, response periods calculated for a spectrum of P-M type are monotonous functions of the mean wave period and independent of the wave height. The procedure for deriving the equivalent wave spectrum is illustrated in figure 3. Let figure 3, a, c, e represent the actual case so that in:

a -  $S_w(x)$  is the actual wave spectrum with a mean wave period

$$T_w = 2\pi \sqrt{m_{ow}/m_{2w}} \quad \text{and spectrum area } m_{ow}$$

c -  $Y(x)$  is a response transfer function for the actual speed and heading

e -  $S_R(x)$  is the measured corresponding response spectrum with the mean response period  $T_R = 2\pi \sqrt{m_{oR}/m_{2R}}$  and area  $m_{oR}$

Figures 3 b, d, f, g illustrate the theoretical calculations so that in:

b -  $S_T(x)$  is the theoretically defined two parameter spectra, each with the same area  $m_{OT}$  but different mean periods  $T_T$

d -  $Y(x)$  is the same as in c

f -  $S_{RT}$  are the theoretical response spectra such that

$S_{RT}(x) = S_T(x) Y^2(x)$ , each with an area  $m_{ORT}$  and a mean response period  $T_{RT}$

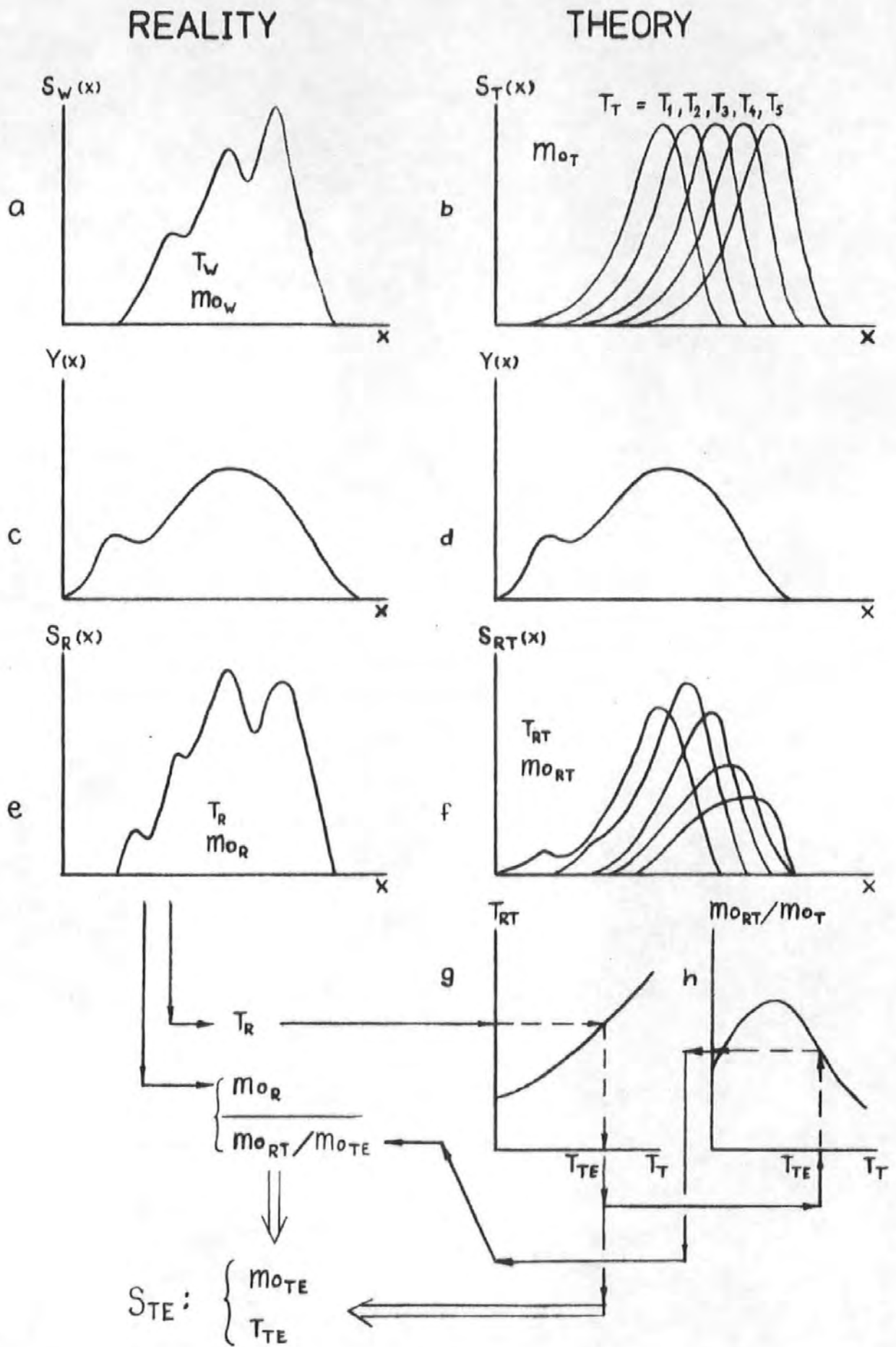
g - the mean response periods  $T_{RT}$  plotted as a function of the mean wave period  $T_T$

h - ratio of response spectrum area and wave spectrum area  $m_{ORT}/m_{OT}$  as a measure of response value per unit wave height, plotted as a function of the mean wave period  $T_T$

As the response period is independent of wave height, the recorded period  $T_R$  may be used to identify the mean wave period of the "equivalent" wave spectrum  $T_{TE}$  which would cause the same response period as the actual one, as illustrated in figure 3 g. The response value per unit wave height is usually not a monotonous function of wave period, see 3 h, but having identified the period  $T_{TE}$  the theoretical value of  $m_{ORT}/m_{OTE}$  can be found. Finally, division of the recorded response  $m_{OR}$  by  $m_{ORT}/m_{OTE}$  yields the area  $m_{OTE}$  and hence the wave height of the equivalent spectrum.

In this way an equivalent wave spectrum, of a theoretically defined shape, with a mean wave period  $T_{TE}$  and wave height  $\sqrt{m_{OTE}}$  which would cause the ship to respond with the same magnitude and period as the actual wave spectrum, may be found. It should be remembered though that the objective is not to obtain the true wave spectrum but merely

Fig. 3 Derivation of the equivalent spectrum.



a substitute which may be used for estimating the effect of a change of course and heading. Utilized in an instrumentation system this means that a spectrum derived in this way from a response, say pitch, at a certain speed and heading may be used by the system to estimate the pitch response which would be experienced should the captain decide to alter the course and/or the speed. Prior to any action he could thus evaluate the respective advantages of various options open to him.

As different responses are sensitive to different wave components in the wave system it is likely that the equivalent wave spectrum obtained from each response will be different, unless the actual wave spectrum is of the same form as the equivalent. In spite of this, it would be of interest to know whether a spectrum derived from one response could be used for estimation of another, here called "cross-prediction", as this would make it possible to reduce the number of responses which would have to be monitored by the instrumentation system. It seems likely that such cross-predictions could be made between closely correlated responses as they react similarly to the sea, but the question is how accurately it could be made between uncorrelated responses.

The success of the method of using an equivalent spectrum for predicting purposes is likely to be affected by how accurately the heading towards the waves can be estimated, the angular energy spread in the wave system and the accuracy of the transfer functions.

As the P-M spectrum describes a fully developed sea, the described method may be expected to be more accurate for heavy weather conditions.

## CHAPTER 4

### INVESTIGATION I. CONTAINERSHIP

#### Introduction

In order to apply the previously described method of using the ship as a "wave buoy" it is necessary to have information about the ship's motions in a seaway for both magnitude and period. Although several full-scale recordings on various ships have been made by research organisations over the last thirty years, the published results usually contain information about response magnitudes only, leaving out the periods. It is also necessary to know the ship's response to known wave spectra as predicted by theoretical calculations.

The kind co-operation of Lloyds Register of Shipping made available this type of information for full-scale measurements on a containership. A full description of this full-scale trial, which was a joint project between Lloyds Register of Shipping and the Swedish Ship Research Foundation, can be found in reference [ 8, 9, 10]. Even though this 36,000 tonnes, 28 knot containership is not a VLCC it presents many other important problems with respect to operation in heavy weather due to its high speed and deck cargo and is likely to benefit at least as much as a VLCC from a reliable warning instrumentation. Because the actual wave spectrum was recorded during measurement an opportunity was found to compare the "equivalent spectrum" with the true one and hence to evaluate the ship's ability to act as a "wave buoy".

Figure (4 ) shows the manoeuvres carried out during a set of measurements and it is the recordings from leg 7 which have been subject to some detailed analysis here.

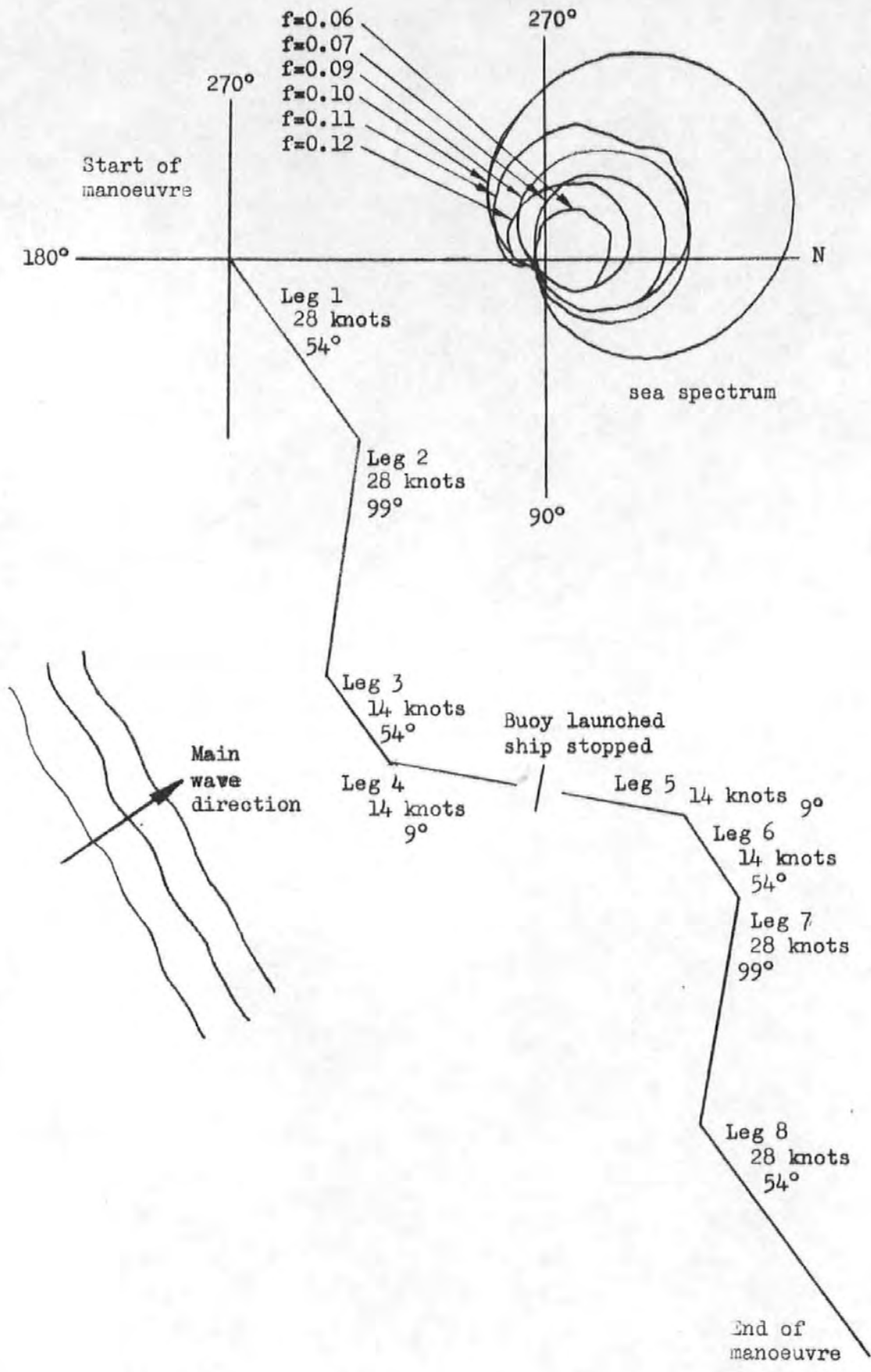


Fig. 4.

Measurement manoeuvre. From ref. [8].



The results will be commented on at the end of the chapter.

### Wave data

The seaway was measured by a pitch-roll buoy sensing vertical acceleration and two components of wave slope. Analysis of such a recording provided estimates of the directional characteristics of the waves as well as the uni-directional wave spectrum.

In Figure ( 5 ) the measured uni-directional spectrum is plotted together with a spectrum of Pierson-Moskowitz type with the same area and mean wave period, so that for both:

Significant wave height :  $H_{1/3} = 3.26\text{m}$

Mean wave period :  $T_2 = 7.77\text{s}$

The agreement between the shape of the two spectra appears reasonable.

The directional properties of the spectrum can be seen in Figure (4) for the wave components containing most energy. It is evident that the angular energy spread with respect to the main wave direction is similar for the various components. The mean wave direction for components of 0.1 Hz, representing the spectrum peak, is  $329^\circ\text{T}$  whereas a weighted mean for the wave system gives  $324^\circ\text{T}$ . With the ship steering  $99^\circ\text{T}$  the mean wave directions relative to the ship are  $130^\circ$  and  $135^\circ$  respectively when head sea is defined as  $180^\circ$ .

In Figure ( 6 ) the directional distributions of the three most energy rich components are plotted together with the two theoretical spread functions, and it can be seen that spread function 2

$$f_2(\mu) = 1/\pi \cdot \cos^2(\mu/2)$$

closely follows the recorded distribution.

Judging from figures ( 5 ) and ( 6 ) it appears that a spectrum of P-M type with the angular spread function  $f_2$  gives a representative

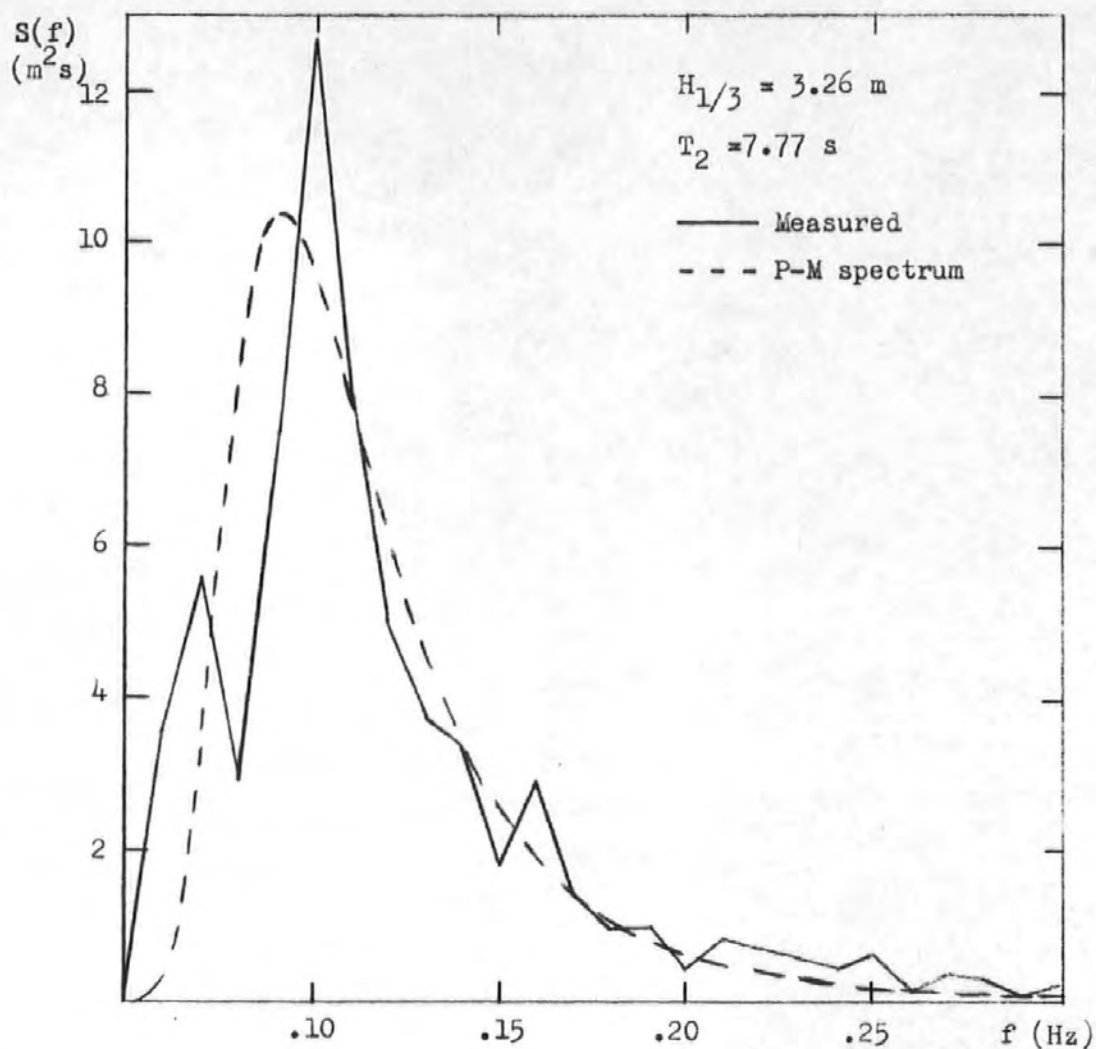


Fig. 5

Comparison of the recorded spectrum and a spectrum of Pierson-Moskowitz type with the same  $H_{1/3}$  and  $T_2$ .

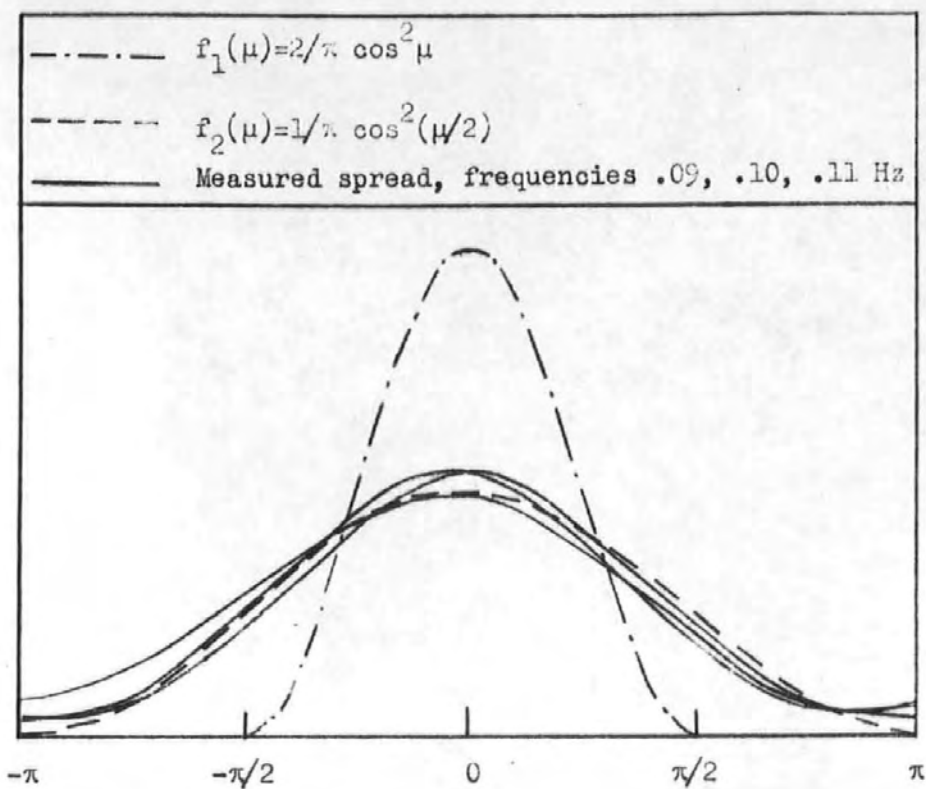


Fig. 6

Comparison of measured angular energy spread and theoretical spread functions.

picture of the actual sea state.

### Measured responses

Spectral analysis, using a Fast Fourier Transform method, of the digitised response signals had been carried out by Lloyds Register and results in the form of tabulated spectrum ordinates and the moments  $m_0 - m_6$  as a function of frequency, were available for this investigation. The response spectra for pitch and vertical acceleration at F.P. together with  $m_0$  and  $T_2$  are shown in figures ( 7 ) and ( 8 ) respectively.

Significant response values and mean response periods were calculated and found to be:

Pitch motion :

$$P_{1/3} = 4 \sqrt{m_0} = 2.01^{\circ}$$

$$T_P = 2\pi \sqrt{m_0/m_2} = 7.88s$$

Vertical acceleration at the forward perpendicular:

$$A_{1/3} = 4 \sqrt{m_0} = 0.21g = 2.02 \text{ m/s}^2$$

$$T_A = 2\pi \sqrt{m_0/m_2} = 6.90s$$

No adjustment to the significant values due to spectrum width was applied here following the approach of reference [9].

Information of this type enabling the response periods to be calculated was not available for any of the other legs in figure ( 4 ).

### Response calculations

Calculations of response values and response periods for the containership were carried out in accordance with the method described in the theory section. For this purpose the transfer functions for pitch and vertical acceleration at the F.P. were available in a tabulated form for the following conditions:

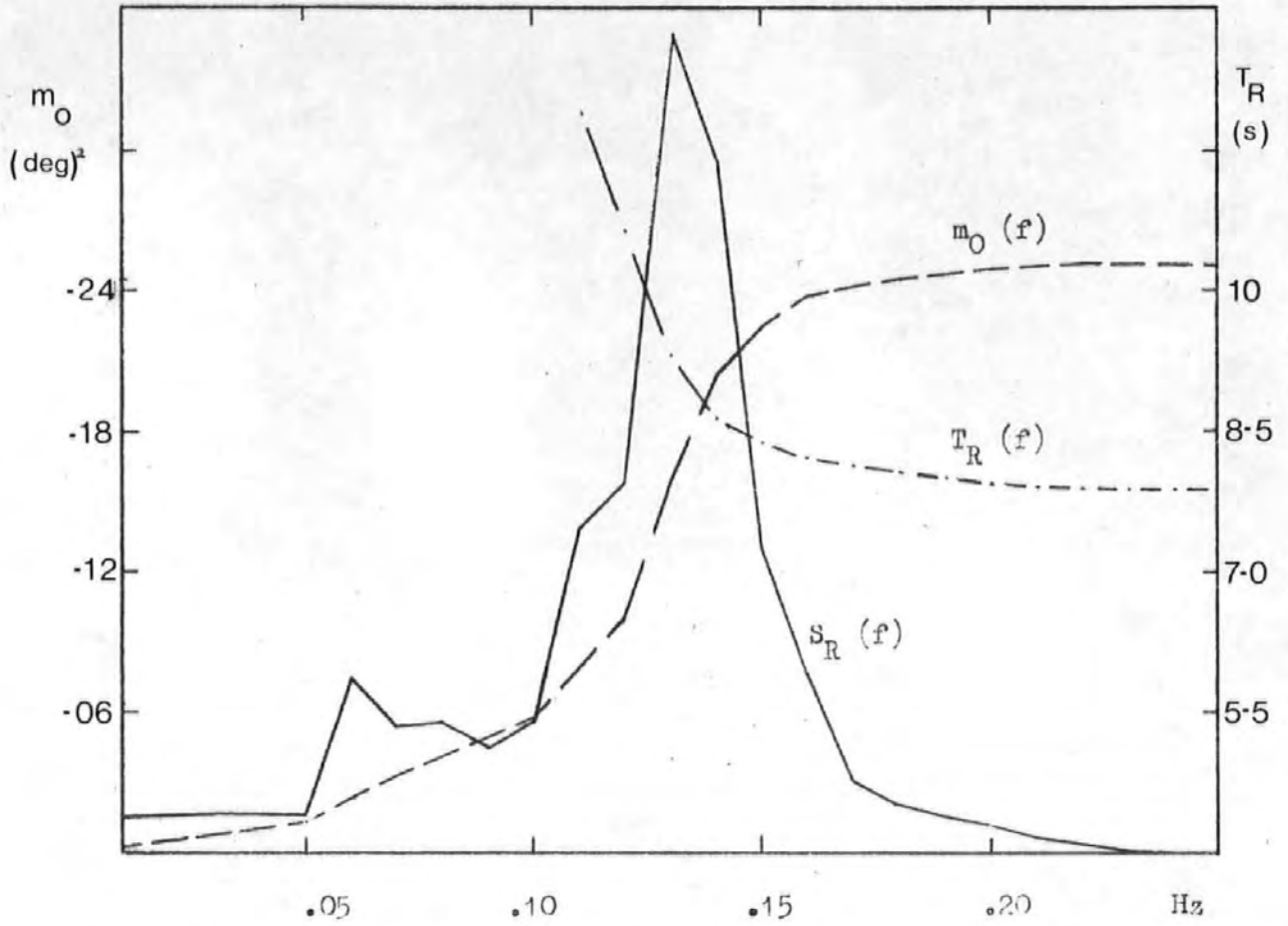


Fig. 7

Recorded response spectrum for pitch  $S_R(f)$ , and spectrum area  $m_O$  and mean response period  $T_R$  as functions of frequency.

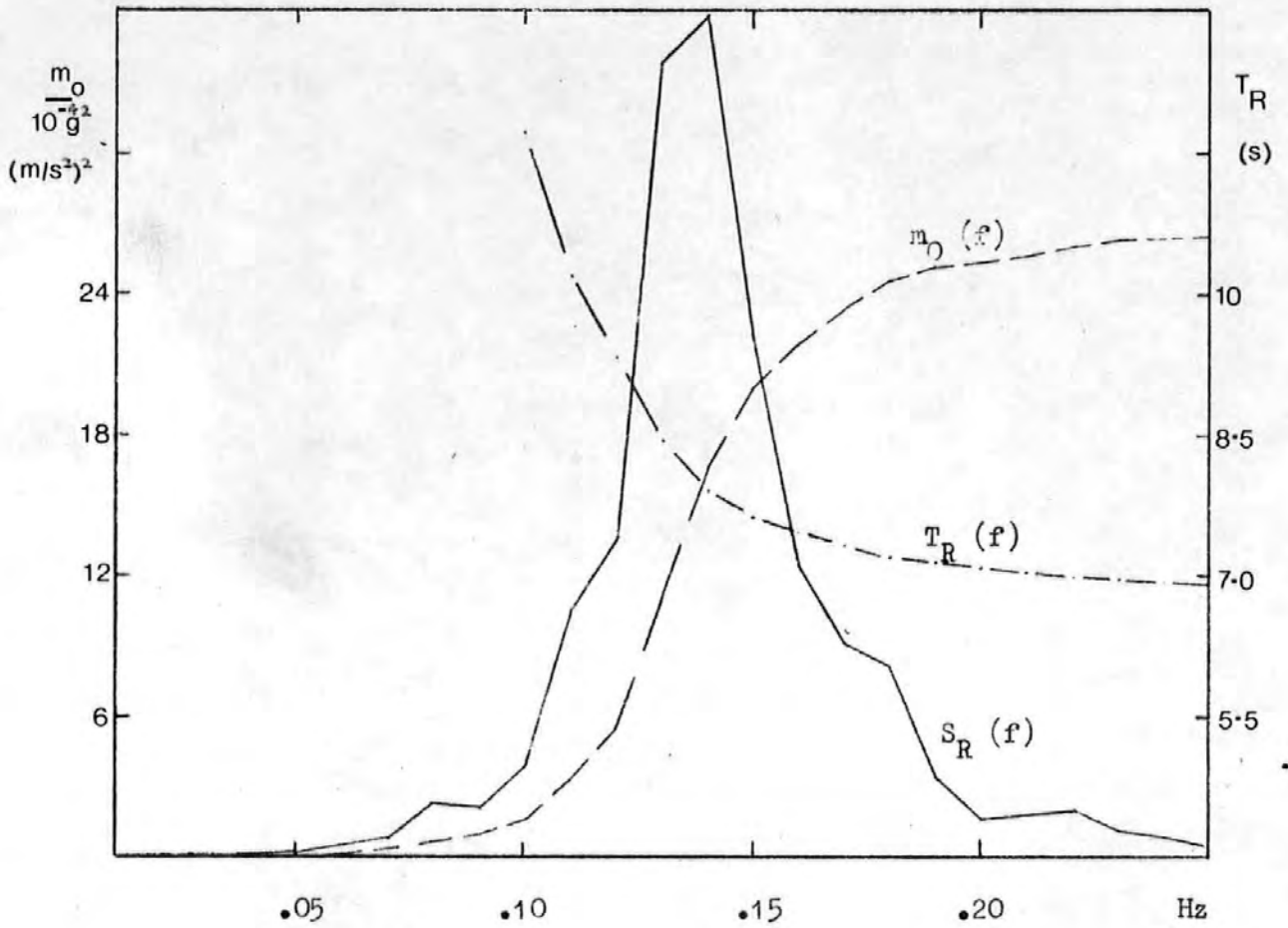


Fig. 8.

Recorded response spectrum for vertical acceleration at the F.P.

$S_R(f)$ , and spectrum area  $m_0$  and mean response period  $T_R$  as functions of frequency.

Speed : 28 knots corresponding to Froudenumber

$F_n$  : 0.287

$\lambda/L = 0.1$  to  $5.1$  with increment of  $0.1$

Headings :  $0^\circ$  to  $180^\circ$  with increment of  $15^\circ$

The ship particulars are listed in table (4.1). It has a bulbous bow and a transom stern and the accommodation deckhouse is situated one third of the ship's length from stern. The draught on the trial was 9.1 m.

TABLE (4.1)

Ship particulars	
Length Oa	275.27m
Length bp	257.60m
Breadth moulded	32.21m
Depth moulded	23.90m
Draught on trials	9.10m
Block coefficient	0.58
Deadweight loaded	35000 tonnes
Displacement loaded	58446 tonnes
Service power	75000 bhp
Service speed	26 knots

Some results from the calculations of response values and periods for various mean wave periods are plotted in figures (9) - (20).

Response in uni-directional sea can be calculated only for headings for which the transfer function is available whereas response for any heading in short-crested sea can be evaluated when an energy spread function is applied. This is schematically shown in figure (21).

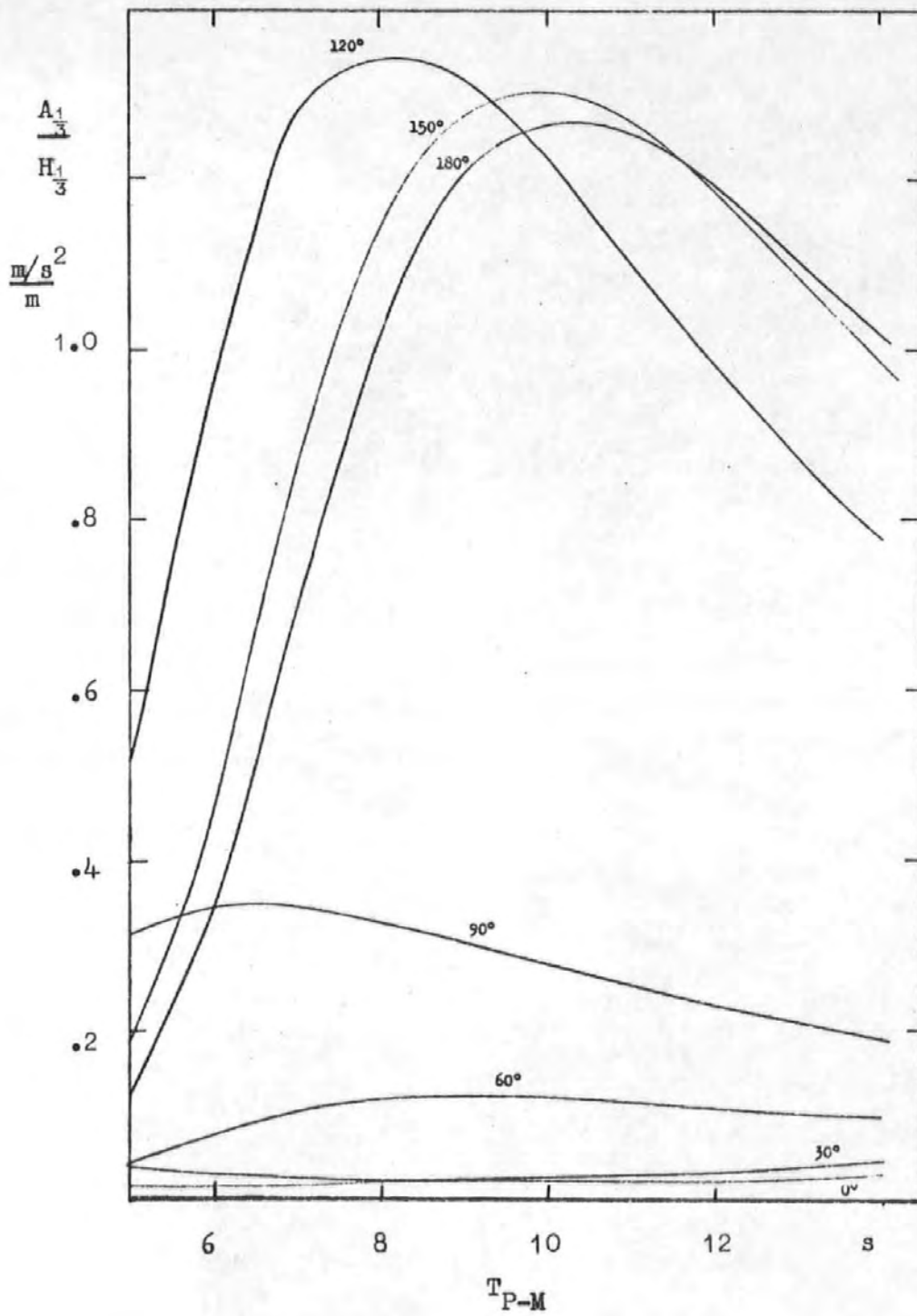


Fig. 9

Vertical acceleration at the F.P. for different headings without spread.



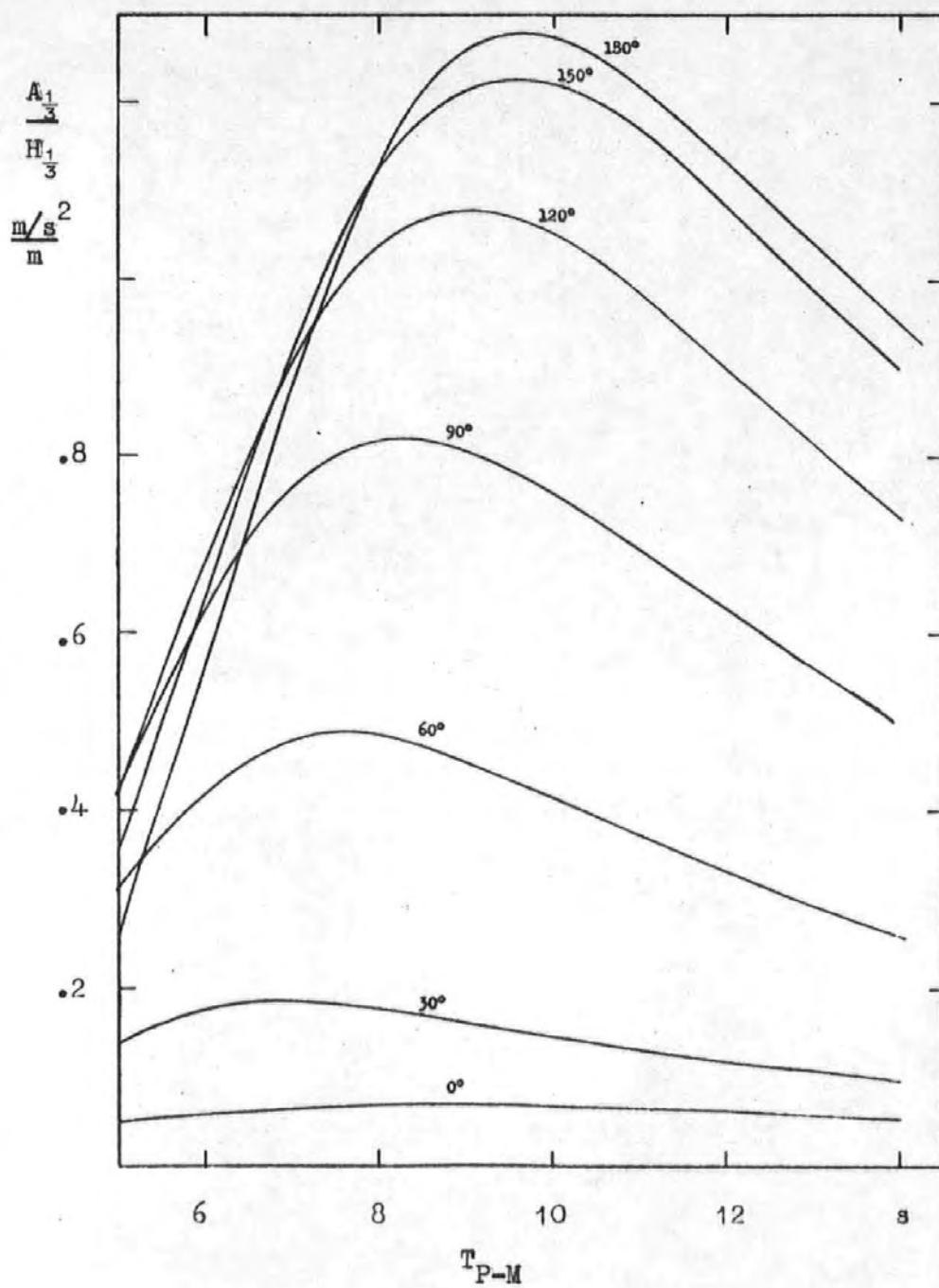


Fig. 10

Vertical acceleration at the F.P. for different headings spread function 1.

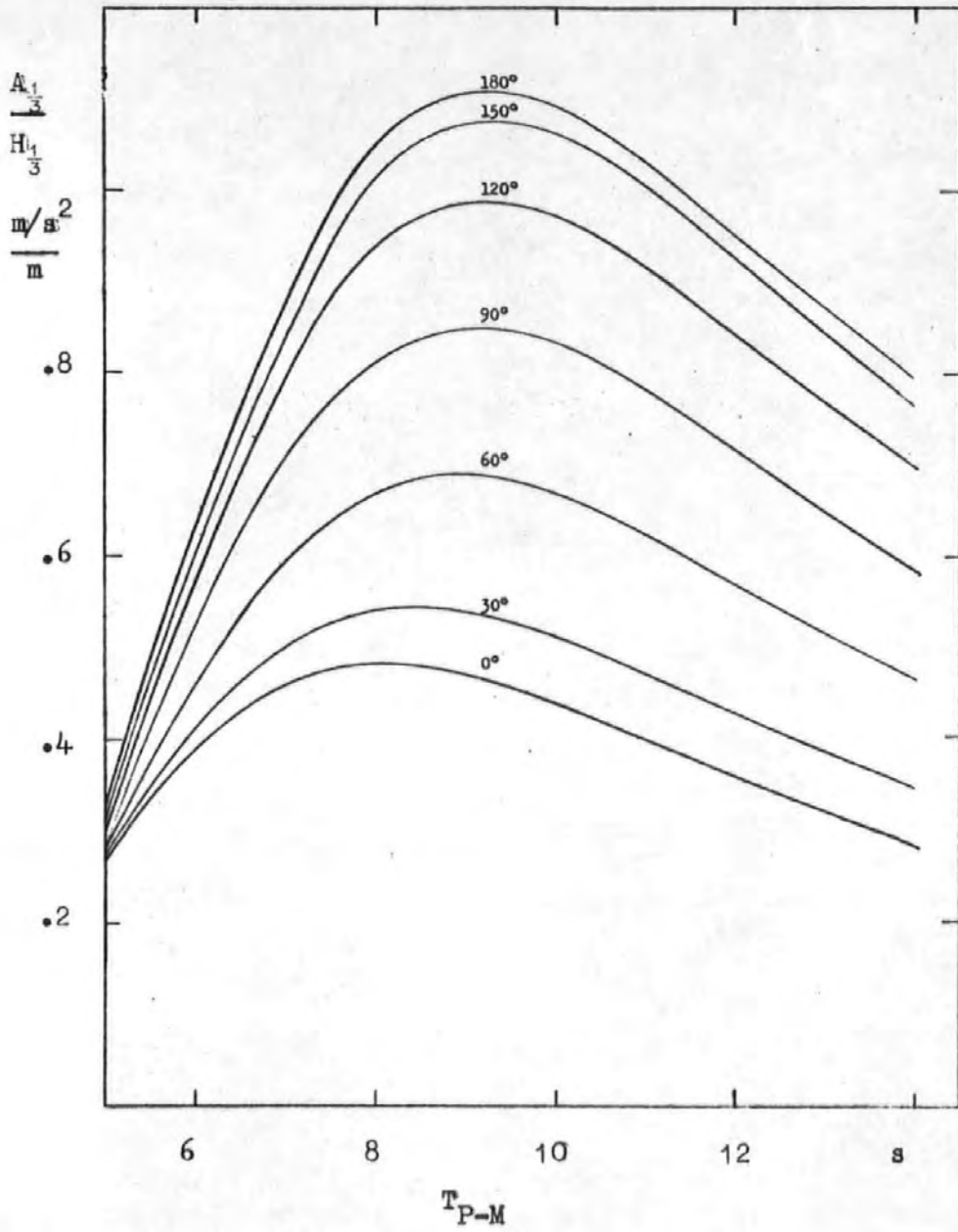


Fig. 11

Vertical acceleration at the F.P. for different headings spread function 2.

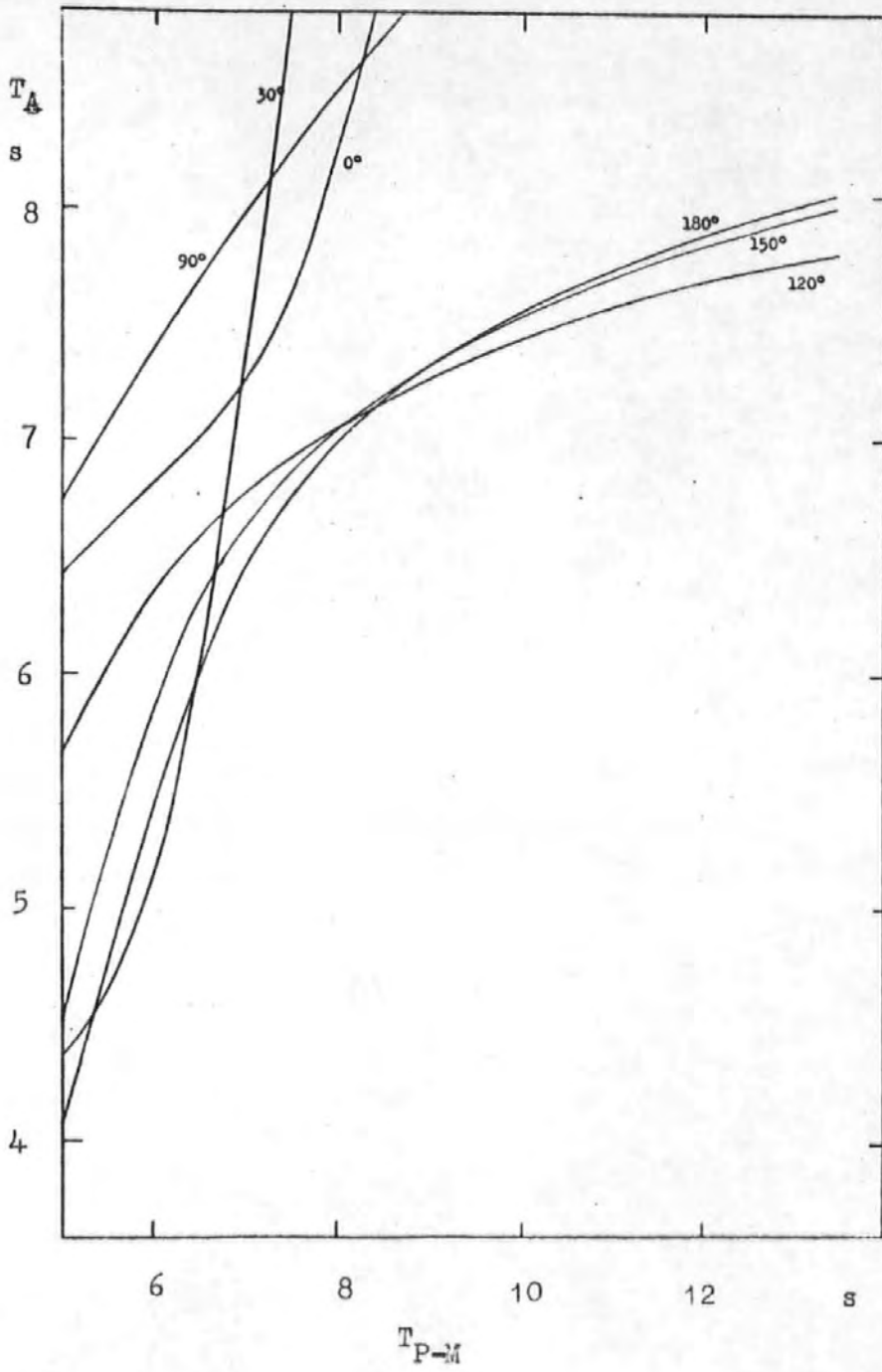


Fig. 12

Acceleration period for various headings without spread.

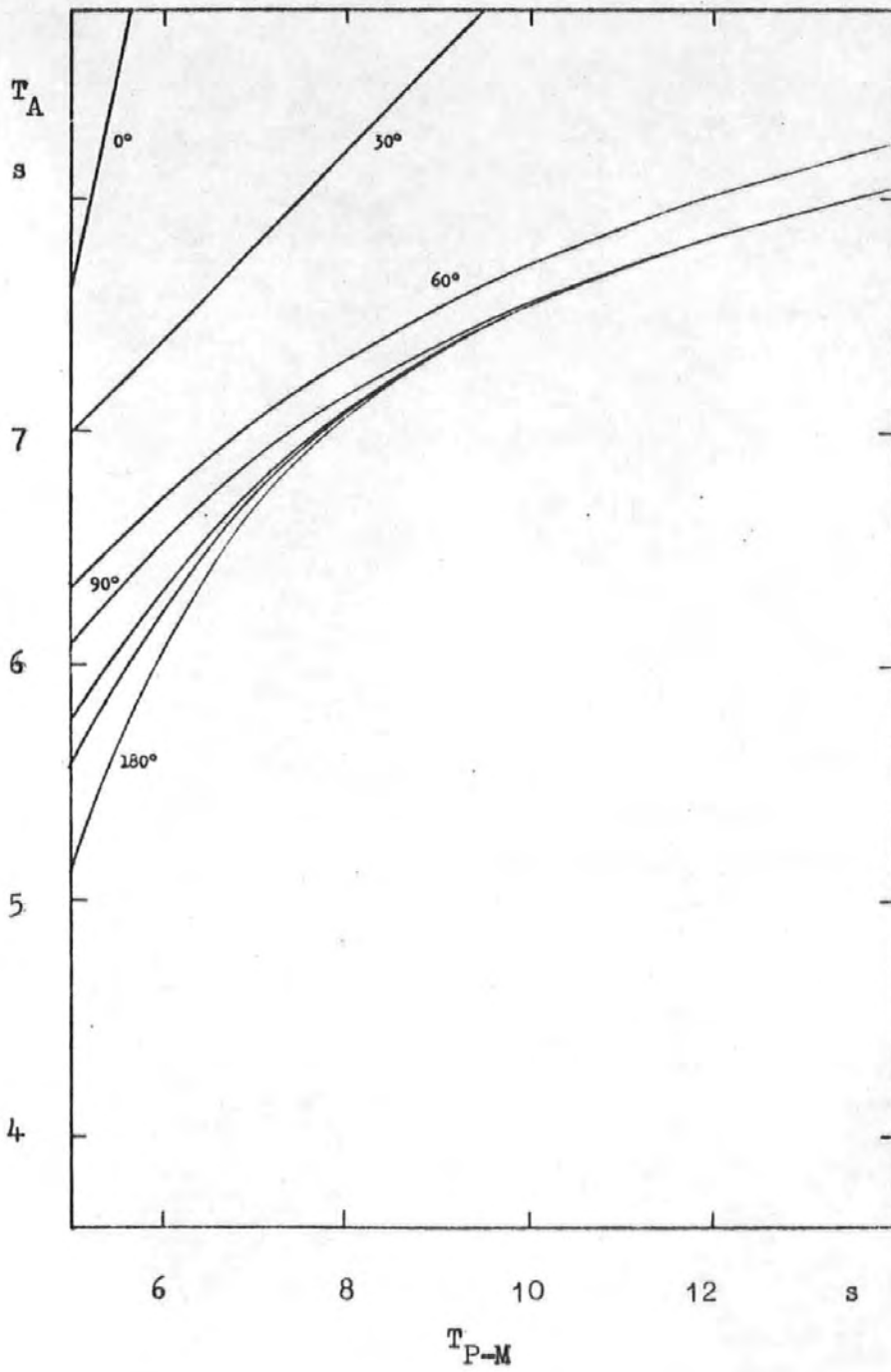


Fig. 13

Acceleration period for various headings spread function 1.

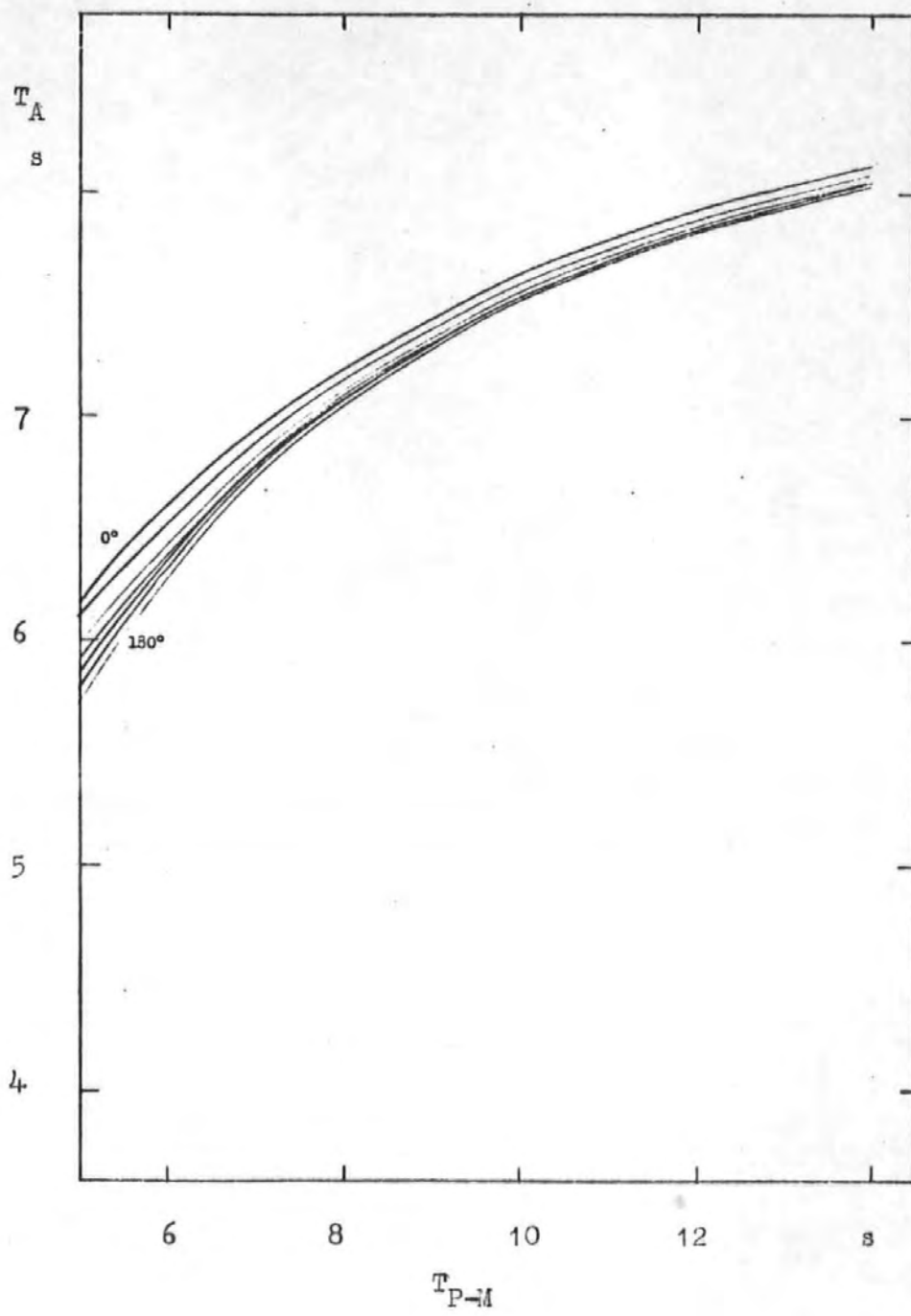


Fig. 14

Acceleration period for various headings spread function 2.

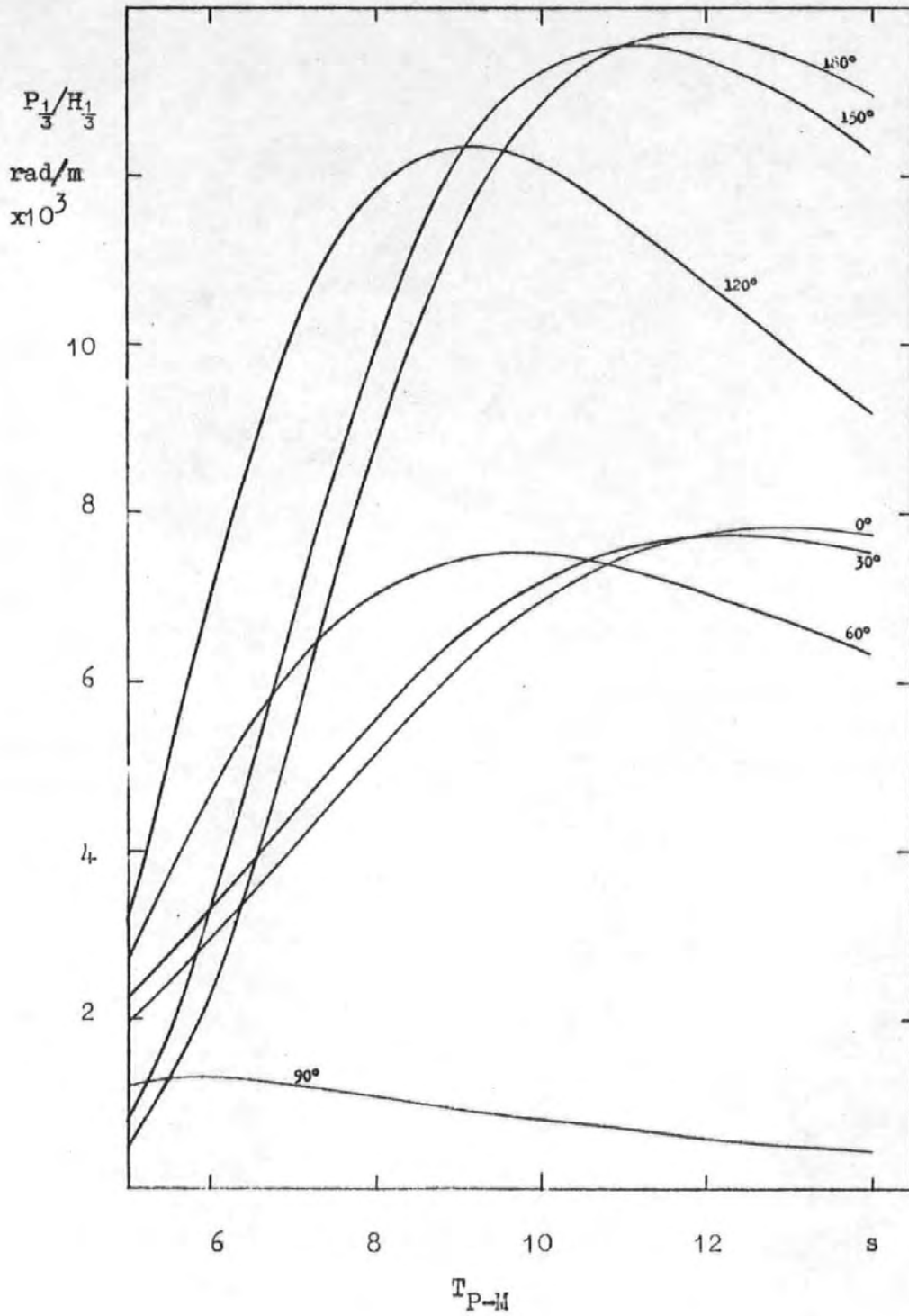


Fig. 15

Pitch angle for various headings without spread.

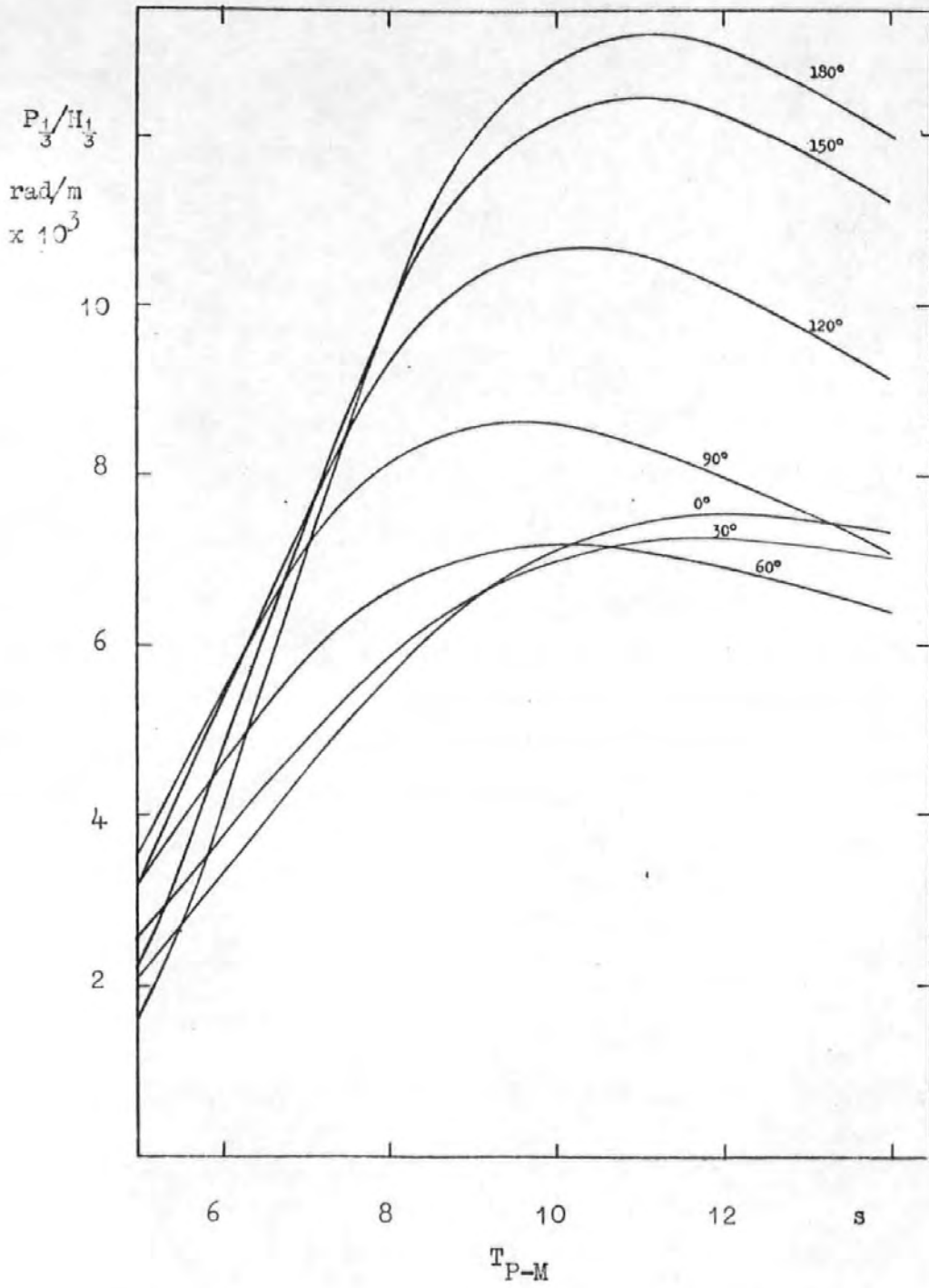


Fig. 16

Pitch angle for various headings with spread function 1.

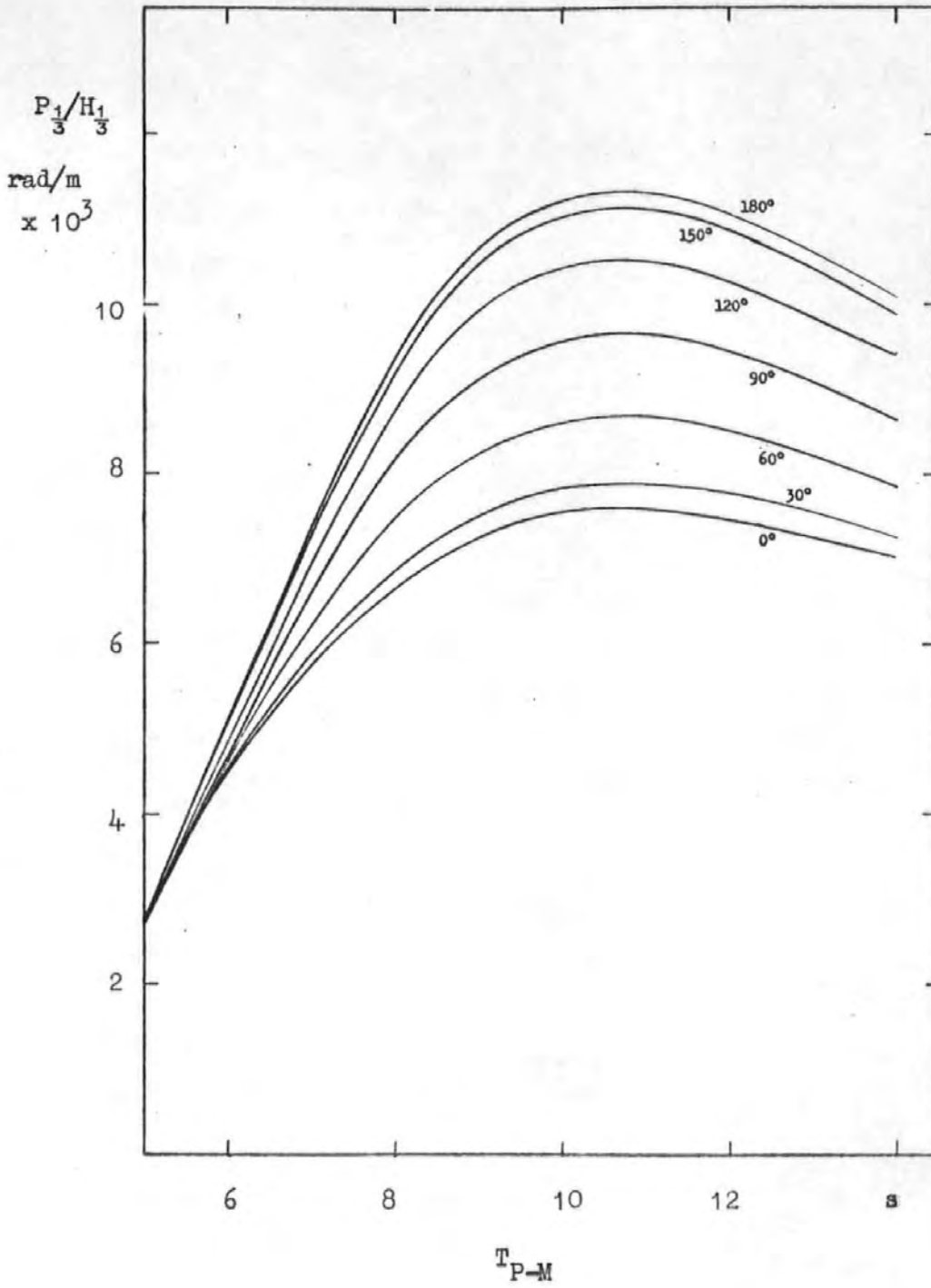


Fig. 17

Pitch angle for various headings with spread function 2.



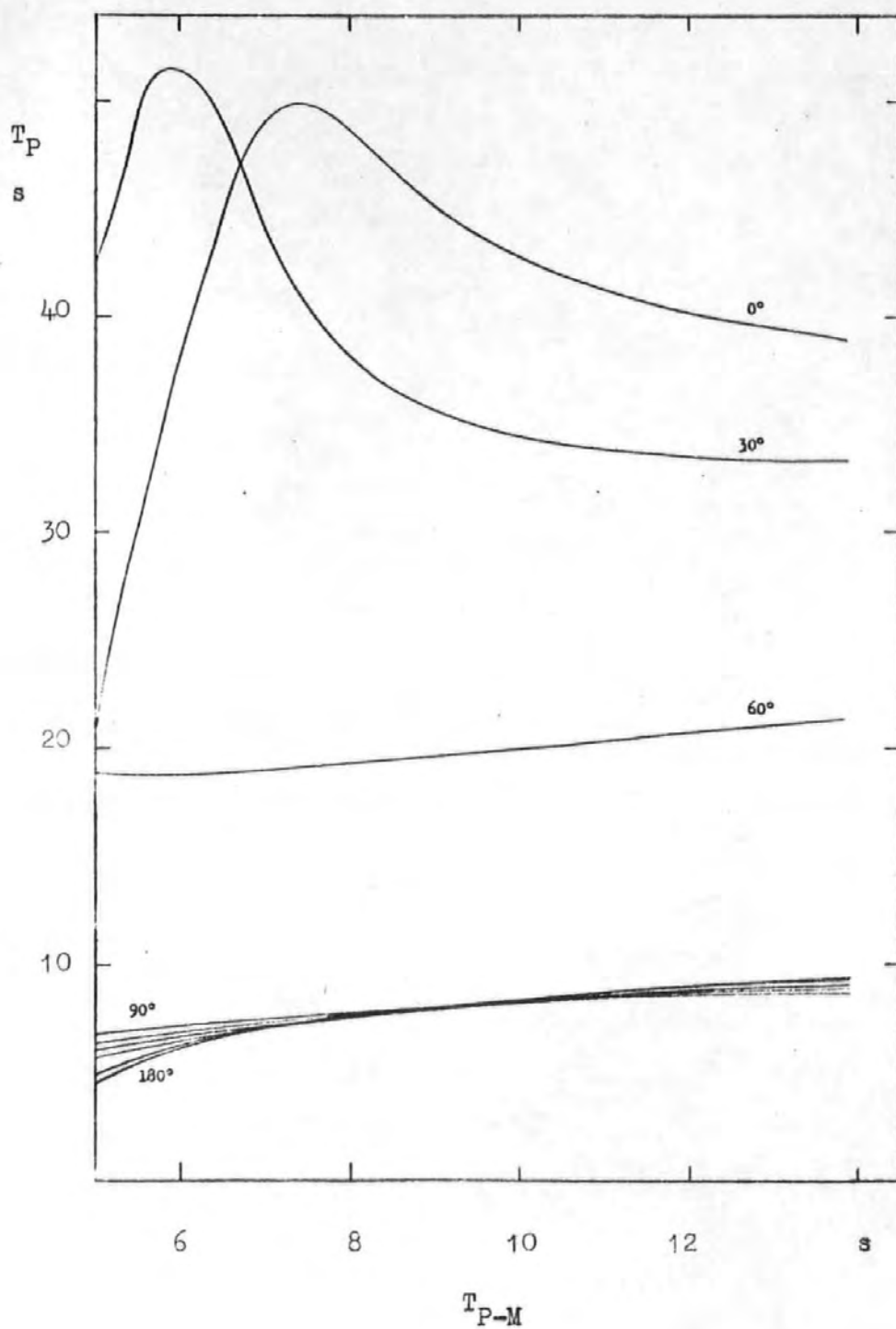


Fig. 18

Pitch periods for various headings without spread.

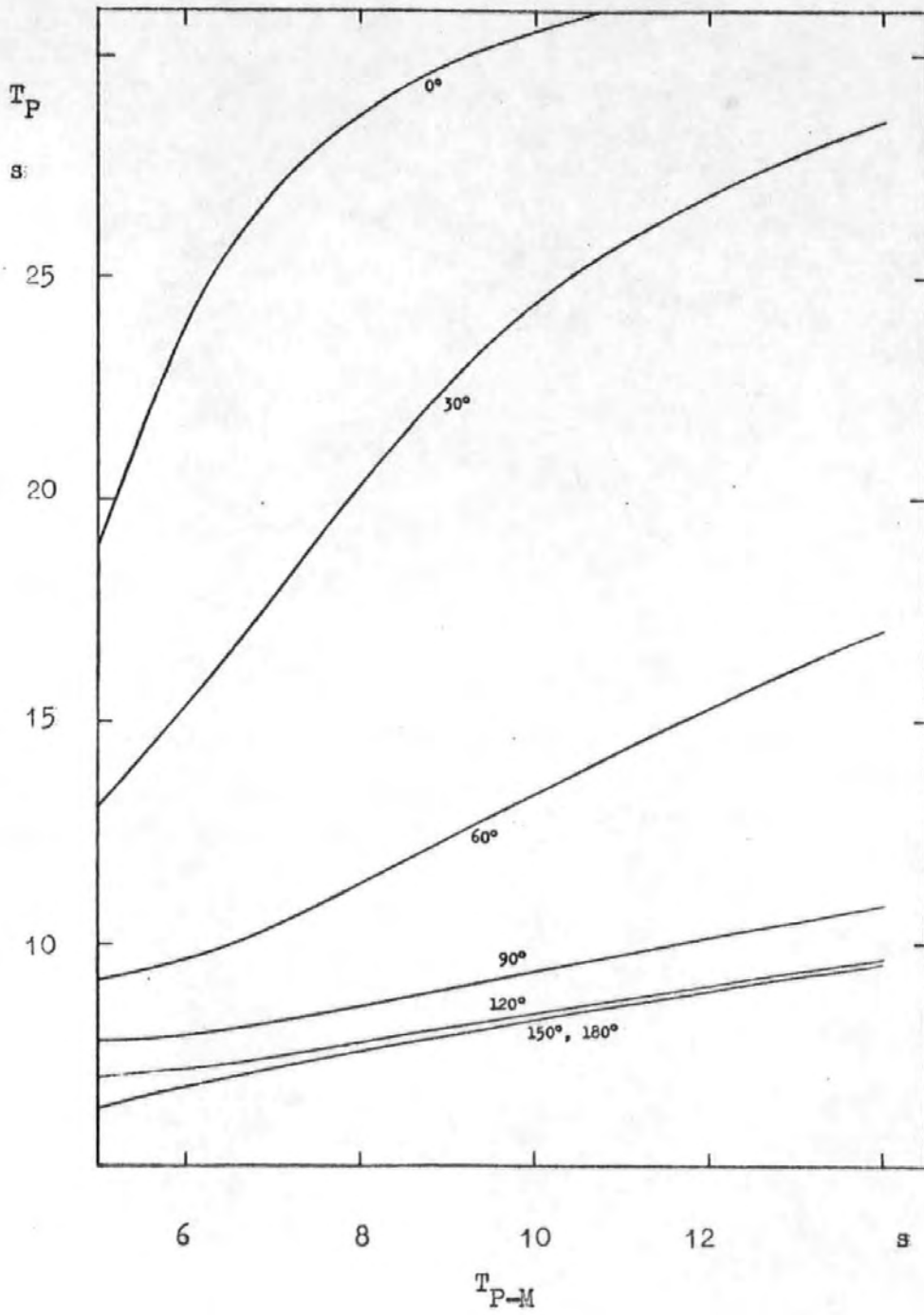


Fig. 19

Pitch periods for various headings with spread function 1.

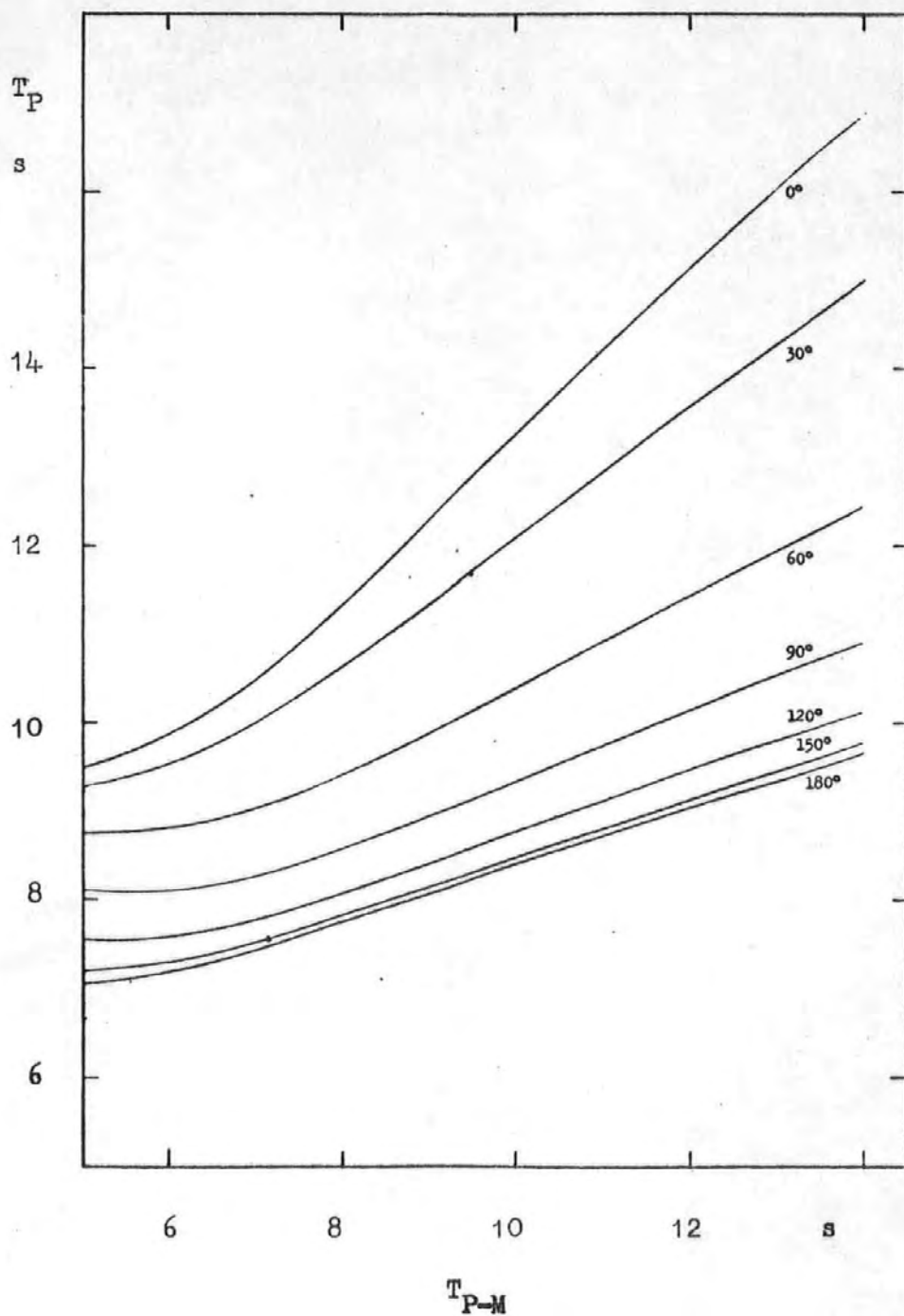


Fig. 20

Pitch periods for various headings with spread function 2.

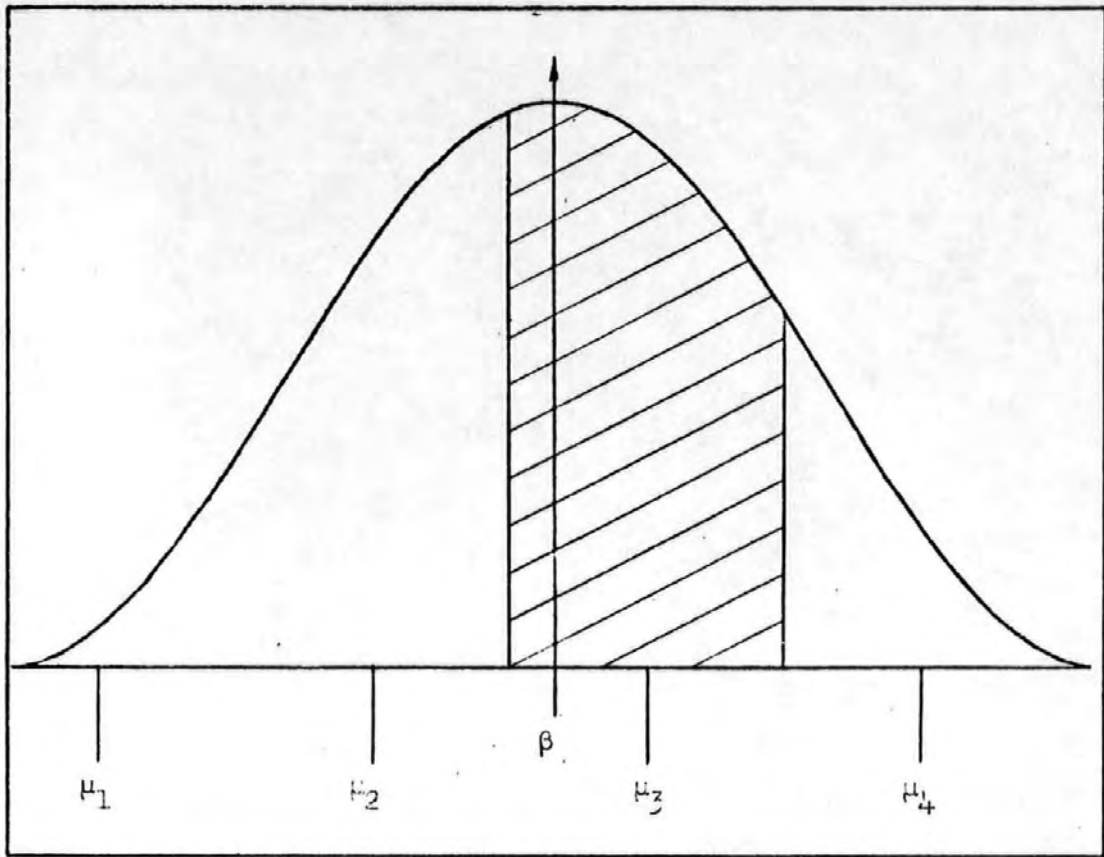


Fig. 21

Allocation of weight to the transfer function for headings  $\mu_3$  (shaded) when calculating response in heading  $\beta$ .

where the shaded area represents relative proportion or weight allocated to the unidirectional response for heading  $\mu_3$  when applying the spread function.  $\mu_1$ ,  $\mu_2$  etc. represented headings for which RAO's are available, and  $\beta$  the heading for which the response is wanted. In this case where RAO's are known for headings only  $15^\circ$  apart this is not of significant importance but it nevertheless made it possible to evaluate the response at heading  $130^\circ$ , corresponding to that of the spectrum peak frequency.

The computer program was not designed so that spectra of arbitrary shape could be used, which would have been necessary had the aim been to investigate any discrepancies in response spectra in order to improve on the transfer functions. Instead, all theoretical responses have been calculated for spectra of P-M type since the object was to test the idea of using an equivalent spectrum. Listed in Table ( 4.2 ) below are the results for headings  $130^\circ$  and  $135^\circ$  obtained for such a spectrum with a significant wave height  $H_{1/3} = 3.26\text{m}$  and a mean period  $T_2 = 7.77\text{s}$ . Values are double amplitude.

TABLE (4.2 )

Calculated responses compared to recorded

Heading	Spread	Acc. F.P. (m/s <sup>2</sup> )		Pitch (degrees)	
		Significant value	Response period	Significant value	Response period
135	-	4.05	6.98	2.00	7.45
135	fnc 1	3.49	7.05	1.73	7.54
135	fnc 2	3.10	6.99	1.61	7.86
130	fnc 1	3.45	6.99	1.72	7.58
130	fnc 2	3.05	6.99	1.60	7.90
Recorded values :		2.02	6.90	2.01	7.88

$$\text{fnc 1} = \frac{2}{\pi} \cos^2 \mu \quad -\pi/2 \leq \mu \leq \pi/2$$

$$\text{fnc 2} = \frac{1}{\pi} \cos^2 (\mu/2) \quad -\pi \leq \mu \leq \pi$$

### Derivation of equivalent wave spectra

What is labelled as an equivalent wave spectrum is a spectrum of P-M type which when applied to the transfer functions gives a response value and a response period equal to those caused by the actual sea. So from the measured values of the two parameters, significant value and mean response period, it is possible to find the equivalent wave spectrum.

The first step is to find the mean spectrum period which corresponds to the known response period. As the mean response period is defined as

$$T_R = 2\pi \sqrt{m_{OR}/m_{2R}}$$

$$\text{where } m_{OR} = \int_0^{\infty} S_R(\omega) d\omega$$

$$\text{and } m_{2R} = \int_0^{\infty} \omega^2 S_R(\omega) d\omega$$

the period is independent of the magnitude of the response and hence the wave height. The only condition that must be fulfilled is that  $T_R$  is a monotonous increasing or decreasing function of  $T_{P-M}$  the mean wave period in the P-M spectrum. A large slope, i.e. a high dependency of  $T_T$  upon  $T_{P-M}$  is an advantage as error in the estimation of  $T_R$  has less effect on the estimated value of  $T_{P-M}$ . This step is illustrated in figure (22). From figure (18) it can be seen that this procedure is not applicable for pitch in unidirectional sea for headings  $0^\circ$  and  $30^\circ$  as there are two values of  $T_{P-M}$  which result in the same  $T_R$ . It is uncertain how limiting this is with respect to an eventual instrumentation based on this technique, but it can be seen from figures (19) and (20) that when a spread function is applied the condition of monotony is fulfilled. It is also a generally held view that transfer functions as derived from

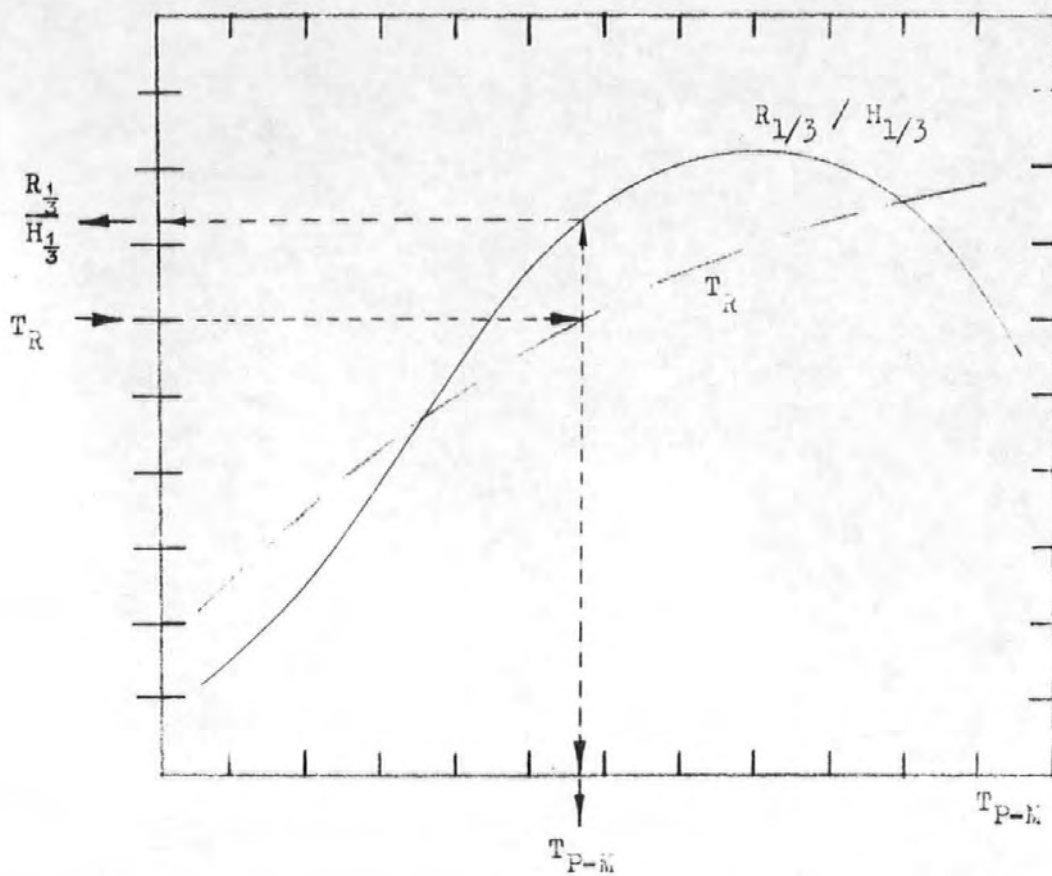


Fig. 22

The principle of how known values of  $T_R$  and  $R_{1/3}$  are used to determine  $T_{P-M}$  and  $H_{1/3}$ .



strip theory are somewhat less reliable for following and quartering seas which affect response calculations for these headings. Using a spread function of some kind is also justified by the fact that the sea waves are generally short-crested.

Having determined the wave period, the corresponding significant response value per unit significant waveheight is found and finally a division of the measured value by the theoretical yields the significant waveheight of the equivalent wave spectrum. See figure (22 ).

In Table (4.3 ) the equivalent wave spectra derived by this method for headings  $130^\circ$  and  $135^\circ$  are listed.

TABLE (4.3 )

Equivalent wave spectra for heading  $130^\circ$  and  $135^\circ$

Heading	Spread	Acceleration F.P.		Pitch	
		H 1/3(m)	T <sub>P-M</sub> (s)	H 1/3(m)	T <sub>P-M</sub> (s)
$135^\circ$	-	1.70	7.53	2.79	8.87
$135^\circ$	fnc 1	1.96	7.52	3.27	8.75
$135^\circ$	fnc 2	2.23	7.48	4.02	7.83
$130^\circ$	fnc 1	1.99	7.49	3.37	8.65
$130^\circ$	fnc 2	2.26	7.47	4.18	7.69
Recorded value		H 1/3 = 3.26m	T <sub>2</sub> = 7.77s		

In practice the actual heading or main relative wave direction is difficult to estimate and in order to find the effects of a misjudgement of the heading, the equivalent spectra were derived for various other headings as well. The results are plotted in figure (23 ).

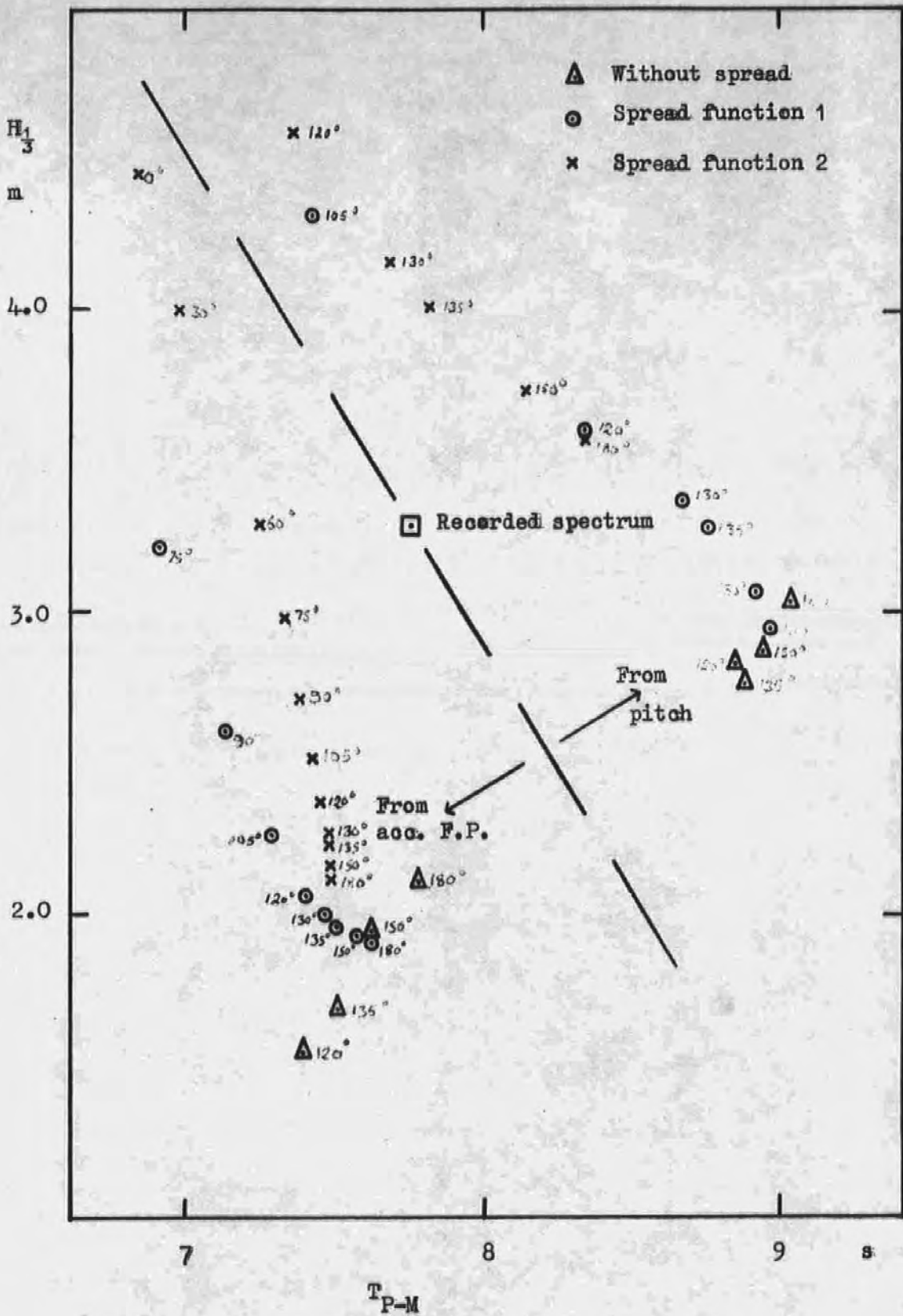


Fig. 23

Spectra derived from acceleration and pitch responses.

### The use of the equivalent spectrum for predictions

As can be seen from figure ( 23 ) none of the equivalent spectra obtained has both of the parameters height and period coinciding with those of the measured spectrum. Whether this is due to the difference in shape between the actual spectrum and that of the P-M spectrum or whether it is due to erroneous transfer functions, is difficult to conclude. It may be a mixture of the two reasons. The important point however, is not whether the ship may be used as a wave buoy in the sense that it would give the true spectrum, but whether the derived equivalent spectrum can be employed for predicting the response that would be experienced after a change of course and/or speed.

The response values, but not periods, for vertical acceleration at the forward perpendicular and pitch were available for leg 8 in figure ( 4 ) which corresponds to a heading of  $90^{\circ}$ . (Corresponding values were available for other legs as well, but the theoretical calculations were carried out only for a speed of 28 knots). Table (4.4) was compiled by using the equivalent spectra listed in Table (4.3) to estimate the response in heading  $90^{\circ}$ , in such a way that a spectrum obtained from pitch assuming spread function 1 was used to predict pitch in  $90^{\circ}$  also with spread function 1 and so on.

TABLE (4.4 )

Prediction of responses on heading 90° using equivalent spectra  
from Table (4.3 )

For acceleration at F.P.

From heading	H 1/3	T <sub>P-M</sub>	Spread	Significant value	Response period
135°	1.70	7.53	-	0.57	8.28
135°	1.96	7.52	fnc 1	1.56	7.00
135°	2.23	7.48	fnc 2	1.69	6.93
130°	1.99	7.49	fnc 1	1.58	6.99
130°	2.26	7.47	fnc 2	1.71	6.93
Equivalent to recorded	3.26	7.77	-	1.09	8.40
	"	"	fnc 1	2.64	7.07
	"	"	fnc 2	2.58	7.02
Recorded acceleration 90°				1.78 m/s <sup>2</sup>	-

For pitch

135°	2.79	8.87	-	0.15	7.97
135°	3.27	8.75	fnc 1	1.59	8.87
135°	4.02	7.83	fnc 2	1.82	8.51
130°	3.37	8.65	fnc 1	1.64	8.83
130°	4.18	7.69	fnc 2	1.84	8.47
Equivalent to recorded	3.26	7.77	-	0.21	7.72
	"	"	fnc 1	1.49	8.49
	"	"	fnc 2	1.46	8.49
Recorded pitch 90°				1.27°	-

A test of the possibility of making cross predictions was also made, i.e. from the equivalent spectra derived from pitch the value of vertical acceleration was estimated for the same heading. These results are listed in Table ( 4.5 ).

TABLE ( 4.5 )

Cross-prediction of one response using the spectra derived from the other

From Acc. F.P.				Predicted values of pitch	
Heading	H 1/3	T <sub>P-M</sub>	Spread	Sign. Value	Resp. period
135°	1.70	7.53	-	.98	7.35
135°	1.96	7.52	fnc 1	.98	7.45
135°	2.23	7.48	fnc 2	1.03	7.77
130°	1.99	7.49	fnc 1	.99	7.49
130°	2.26	7.47	fnc 2	1.04	7.81
Recorded values of pitch				2.01°	7.88s
From pitch				Predicted values of Acc. F.P.	
135°	2.79	8.87	-	3.75	7.27
135°	3.27	8.75	fnc 1	3.78	7.24
135°	4.02	7.83	fnc 2	3.85	7.01
130°	3.37	8.65	fnc 1	3.80	7.22
130°	4.18	7.69	fnc 2	3.87	6.97
Recorded values of acc. F.P.				2.02 m/s <sup>2</sup>	6.90s

## Conclusions

It is not possible to draw any far-reaching conclusions from this example alone, but a few points are worth mentioning.

The recorded spectrum is in good agreement with the P-M spectrum but a sharper peak as well as a swell component are noticeable and the calculated responses differ somewhat from those recorded as can be seen in Table (4.2). Response periods are in good agreement whereas acceleration values are over-estimated and pitch values slightly underestimated. For  $90^{\circ}$  heading both acceleration and pitch are over-estimated as shown in Table (4.4).

From Table (4.3) and figure (23) may be concluded that the equivalent wave spectra as defined from the ship's motions are different from the actual one and that a difference in the estimated wave direction has a marked effect. How large the discrepancies would be, had the true wave spectrum had a shape completely different from that of the P-M type, is not possible to assess from this example, but it seems reasonable to assume that they would increase.

What is particularly interesting is the remarkable consistency in the predicted values in Table (4.5) even though the parameters of the spectra used are quite different. The predicted response value is not right but the errors are almost constant and the response periods are in good agreement.

Judging from the results in Table (4.4) the predicted value would not have improved had the parameters of the equivalent spectra been the same as the recorded.

The overall accuracy of the prediction procedure is acceptable but any far reaching conclusions about the method's general tendency to over or under estimate responses cannot be made from this example alone.

The correct parameters of the actual wave spectrum were not obtained

from either pitch or acceleration and whether the parameters may be obtained from a combination of equivalent spectra from different responses is uncertain. As an example, it may be seen from Table (4.3) that the mean of the values derived from acceleration and pitch with spread function 2 in heading  $135^{\circ}$  gives  $H_{1/3} = 3.13\text{m}$  and  $T_{P-M} = 7.66\text{s}$  which is close to the actual one. But if this tendency as well as the constant errors in the cross-prediction are consistent can only be assessed by further investigations of the same type. Only then, if ever, could the appropriate correlation factors be established.

INVESTIGATION II . TANKER

Introduction

The recordings of ship motions, ship speed, wind speed, etc. used for this analysis were made by the British Ship Research Association on board a 250,000 tDW tanker during a return journey Europe-Persian Gulf in the summer of 1972.

Recordings were made every 12 hours for about 20 minutes regardless of the weather situation, but no special recording manoeuvres were carried out and no wave measurements were made.

The records were produced by a data logger which sensed and digitized the output from various sensors, producing a time record consisting of circa 1200 values for each sensor.

The recordings available for the containership, as described in a previous chapter, were used in an attempt to estimate one response from the spectrum deduced from another, but no firm conclusions could be drawn from that single sample. For this analysis on the other hand, several recordings were available and the aim was to find out how reliably such cross-predictions can be made. 42 records from the ballast voyage and 47 from the laden voyage were analysed, but not all could be used for cross-prediction purposes as will be explained later.

As there are 12 hours between each measurement it was not possible to investigate the method to predict the effect of a change of course as was employed for the containership.



A different investigation by B.S.R.A. of these records is described in reference [66].

DATA

Table 5.1

---

	<u>Ship particulars</u>	
	Loaded	Ballast
Lpp	330.71m	330.71m
B	51.82m	51.82m
D	25.60m	25.60m
d	19.58m	6.02m
$\Delta$	284,700 tonnes	76,700 tonnes
$C_B$	0.828	0.765
Service speed	16 knots	

---

The ship has a bulbous bow, the accommodation deckhouse and bridge structure is situated at the aft end.

For this investigation the following nine signals were used, all of which were digitized once a second:

1. Ship speed, from the ship's own instruments
2. Course, from the ship's own instruments
3. Relative wind speed, from a cup type anemometer driving a tachogenerator
4. Relative wind direction, from a wind vane driving a potentiometer. Together with the anemometer positioned high up a mast on the superstructure to minimize interference by the superstructure.
5. Pitch angle

6. Roll angle
7. Heave acceleration. The gyroscopes and the heave accelerometer were positioned in the engine room close to the centre line. This "heave" acceleration is thus a combination of heave acceleration and pitch acceleration and will be referred to as "acc. eng." meaning vertical acceleration in the engine room.
8. Rudder angle, from the ship's own instruments.
9. Thrust, from a thrustmeter.

The appropriate units for these signals were yielded by a calibration function such that

$$Y = A (V + B)$$

where V is the "raw" digital value

A and B constants

and Y the value in dimensional form.

For all signals the mean value and the variance were calculated.

The three responses, pitch, roll and acc. eng. were to be used for the cross-prediction method and thus had to be analysed with respect to response periods as well as response values.

#### Analysis methods

It was decided to subject the signals representing pitch, roll and acc. eng. to two different methods of analysis which would yield the desired parameters  $R_{1/3}$  and  $T_R$  in two different ways for comparison.

One method was spectral analysis of the records which gave the moments of the spectra, from which response values, response periods and broadness were calculated, and a plot of the spectra.

The other method can be regarded as a computerized "manual" method where maxima, zero-crossings, etc. were registered as the signals were analysed. This method, henceforth referred to as the "manual method", gave apart from  $R_{1/3}$ ,  $T_R$  and  $\epsilon$  plots of maxima and height distributions compared to the Rayleigh distribution.

Prior to these analyses the signals were transformed to a zero-mean level. In order to avoid errors due to instrumental zero-drift, this was done in a way described in [67] that the mean values of the first and last one third of the points were calculated, and a line passing through the mean values at one sixth from the beginning and end was the zero line. Another possibility which has been used by other authors is to take the regression line from all the points as zero line. An example of the three signals is shown in Figure (24 ).

A few records were selected at random in order to check whether the assumption that the ordinates were Normal distributed was reasonable. This was done simply by visual inspection and the agreement was found to be satisfactory. Fig. 25. See Figures (25 - 27)

#### The manual method

The first step for this method was to cut off the ends of the signal in such a way that the first and last positive values preceded by a negative value, i.e. positive slope, were made the starting point and the end point respectively, thus forming a signal with an exact number of cycles.

Three values at a time were studied so that if  $X(i)$  denotes the  $i$ :th value of the time series forming the signal, then maxima, minimum and zero up-crossings were registered according to the following definitions:

RECORDING ON ESSO NORTH VIRGIA

RECORD NO: 33 DATE: 1972-5-25

RECORDED TIME SIGNAL IN MACHINE UNITS

X = PITCH

• = ROLL

o = HEAVE

o = TWO VALUES IN SAME PLACE

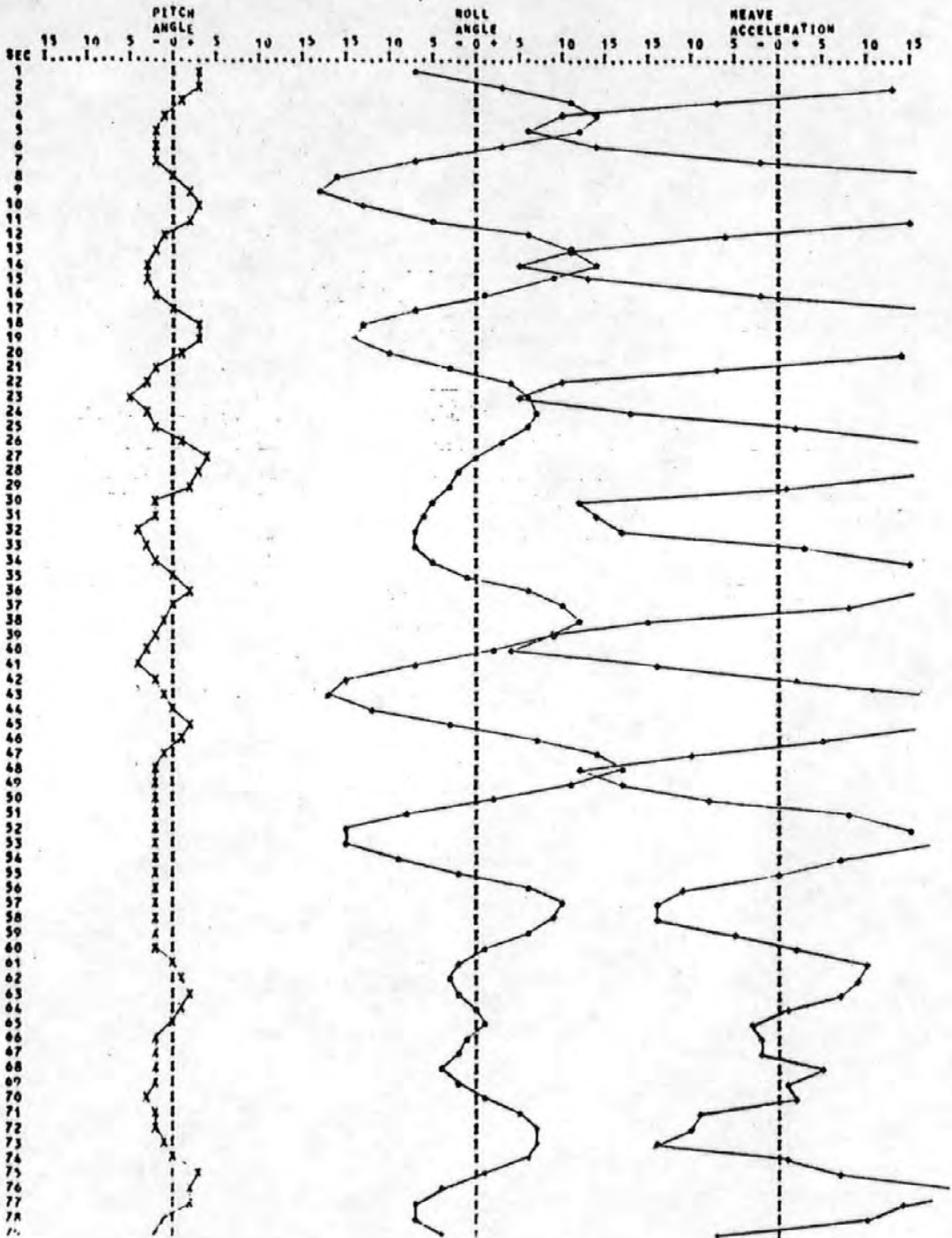


Fig. 24

Examples of the digitized response signals.

RECORD NO: 33 DATE: 1972- 5-25

NORMAL DISTRIBUTION COMPARED TO THE DISTRIBUTION OF PITCH ANGLE

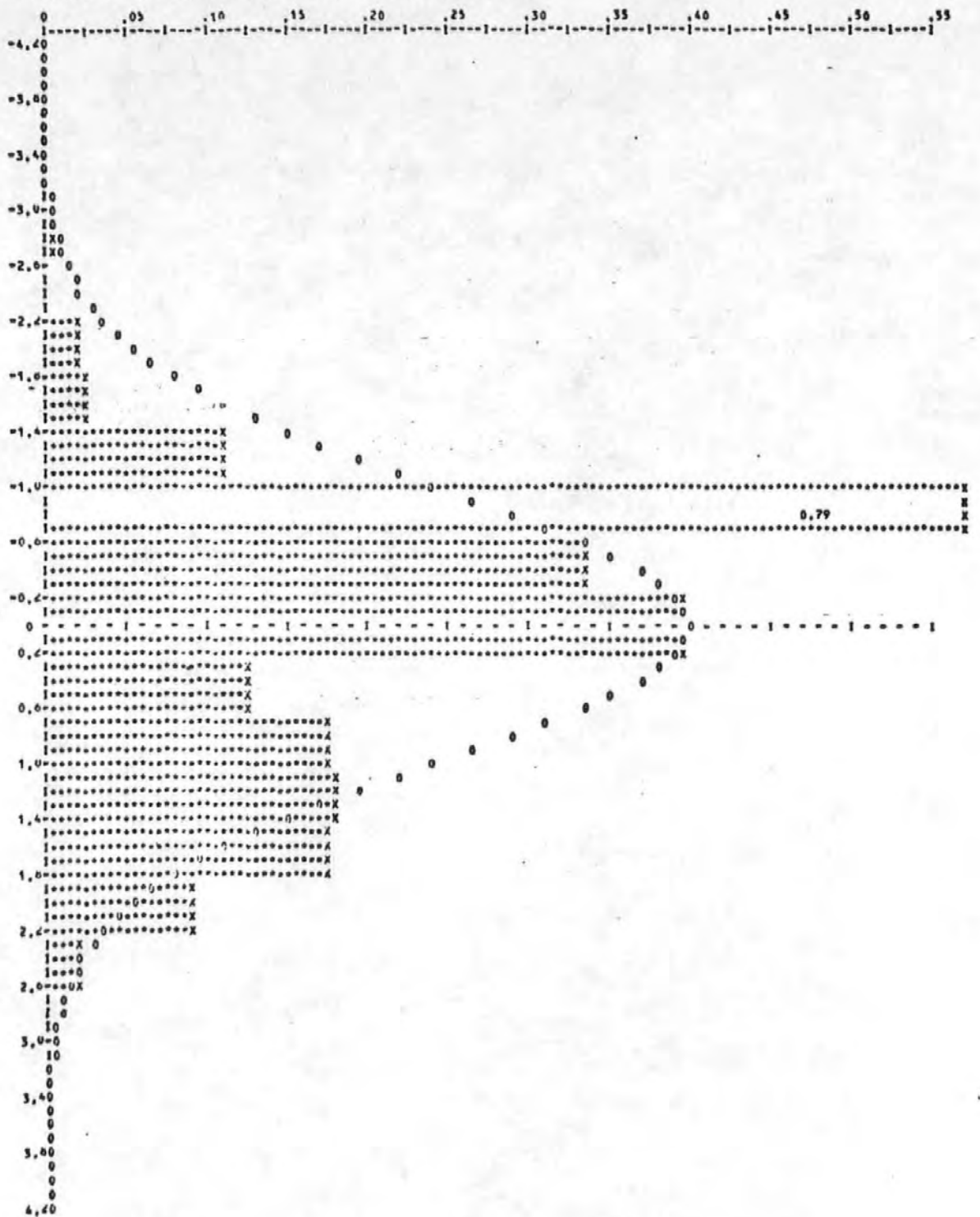


Fig. 25

Pitch signal compared to the Normal distribution.

RECORD NO: 33 DATE: 1972- 5-25

NORMAL DISTRIBUTION COMPARED TO THE DISTRIBUTION OF ROLL ANGLE

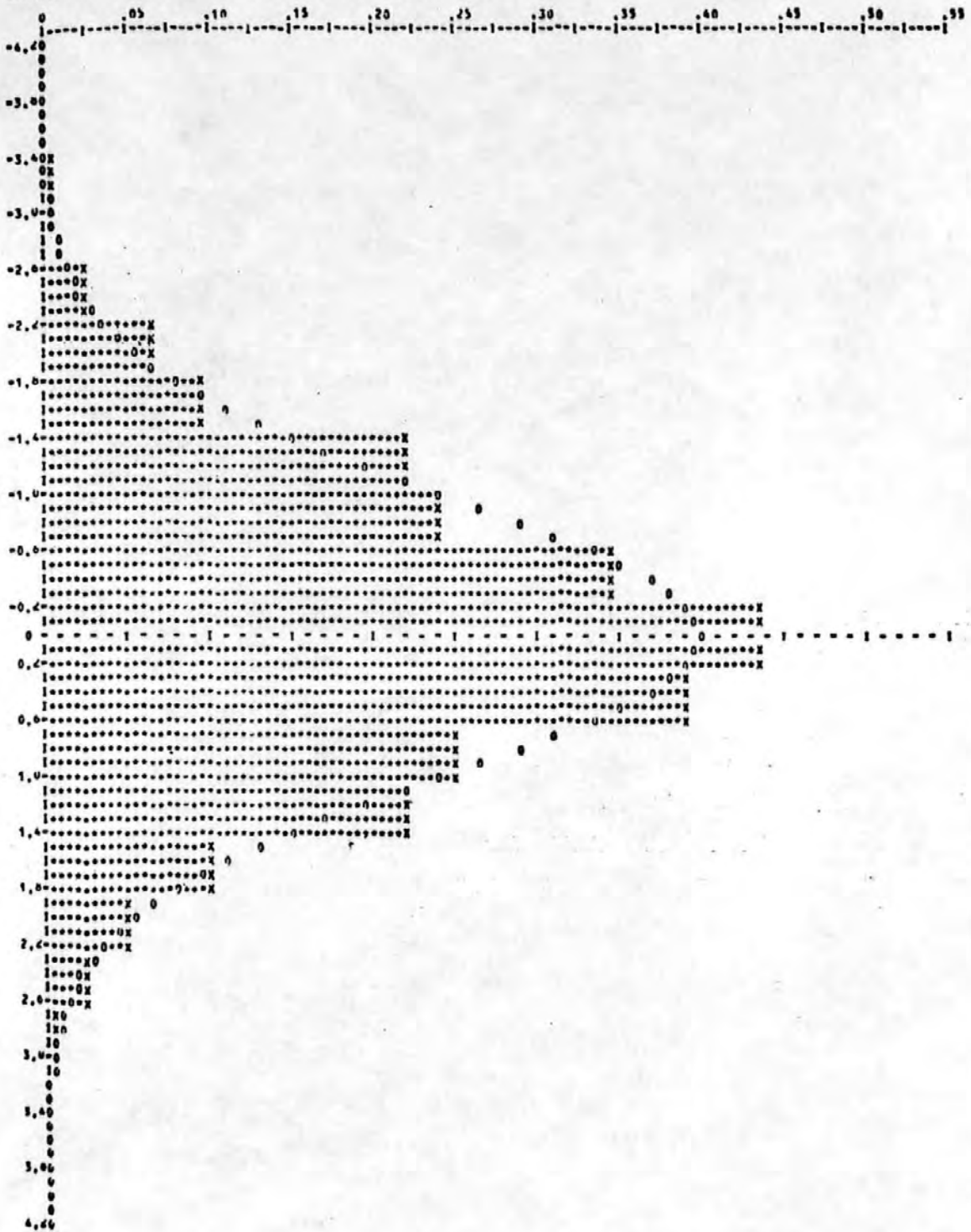


Fig. 26

Roll signal compared to the Normal distribution.

RECORD NO: 33      DATE: 1972-5-23

NORMAL DISTRIBUTION COMPARED TO THE DISTRIBUTION OF HEAVE ACCEL

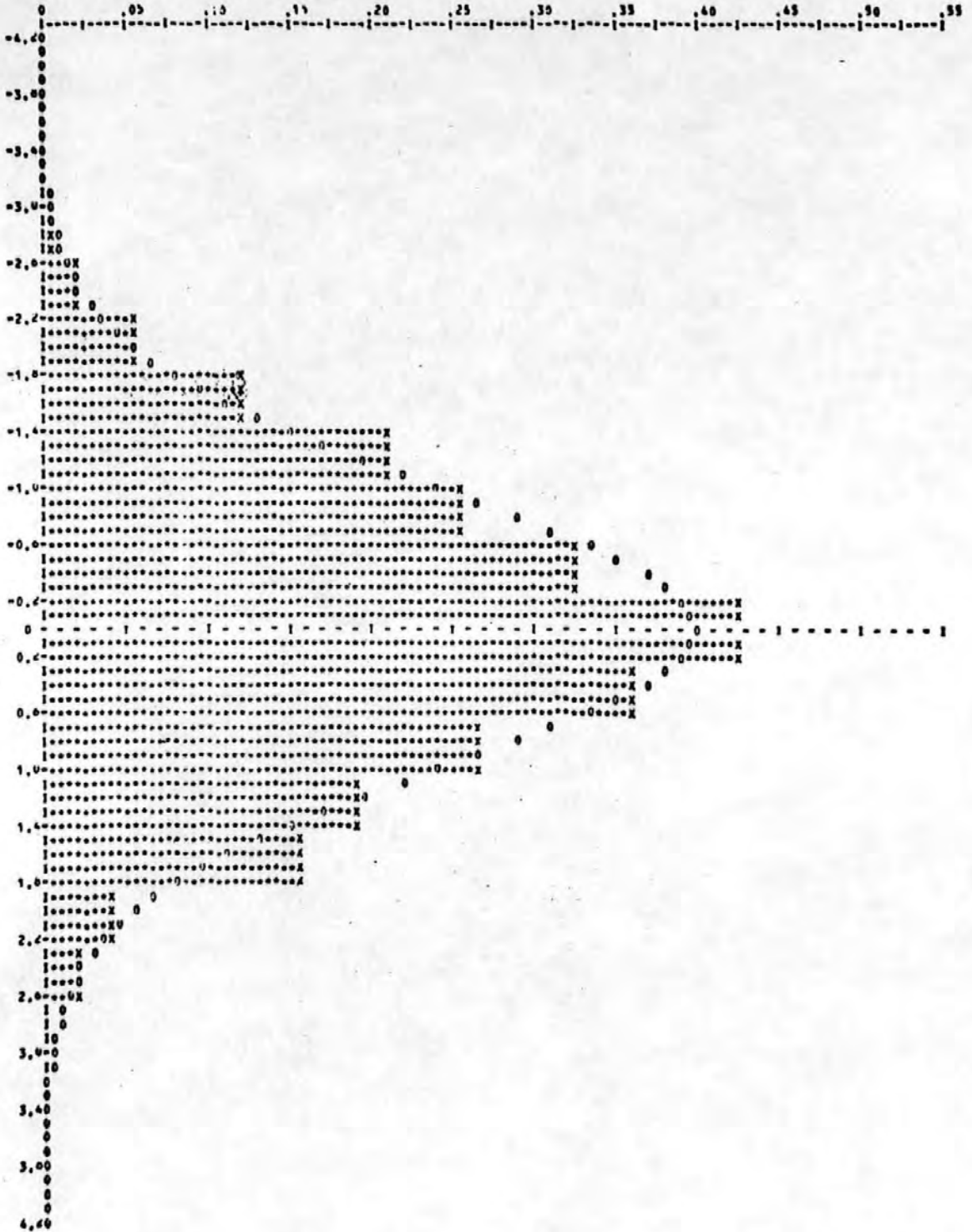


Fig. 27

Acc. eng. signal compared to the Normal distribution.

Fig. 28  
Example of output from the "manual method".

RECORD NO: 33      DATE: 1972- 5-25      PITCH ANGLE      DEGREES

NO OF POINTS: 1267    ZERO UP-CROSSINGS: 130    MAX VALUES POS AND NEG: 140    HEIGHTS: 258

T2 PERIOD: 9.74 (ST.DEV.: 2.63)      BAND WIDTH: 0.515

VARIABLE	VALUE	SIGNIFICANT RESPONSE VALUE	SPREAD ADJUSTED RESPONSE VALUE
VARIANCE:	4.056E-02	8.055E-01	7.502E-01
MEAN SQUARE OF MAXIMA:	0.306E-02	4.152E-01	7.592E-01
MEAN SQUARE OF AMPLITUDES:	6.803E-02	7.377E-01	6.871E-01
MEAN SQUARE OF HEIGHTS:	2.587E-01	7.193E-01	6.699E-01

LARGEST MAX: 6.851E-01      SMALLEST MIN: -6.328E-01      LARGEST HEIGHT: 1.125E 00  
MACHINE UNITS: 6.96E 00      -6.42E 00      1.14E 01

EXPECTED MAX VALUES FROM:	AMPLITUDES	HEIGHTS
SQRT(MSU*LN(N)):	6.407E-01	1.199E 00
ADJUSTED FOR WIDTH:	6.636E-01	1.245E 00
SQRT(VAR*2*LN(POINTS)):	7.612E-01	1.522E 00

DISTRIBUTION OF ZERO UP-CROSSINGS:

SEC	FRQ	%	SEC	FRQ	%	SEC	FRQ	%	SEC	FRQ	%	SEC	FRQ	%
1	0	0.00	7	10	7.69	13	4	3.08	19	1	0.77	25	0	0.00
2	1	0.77	8	14	10.77	14	2	1.54	20	0	0.00	26	1	0.77
3	2	1.54	9	34	26.15	15	0	0.00	21	0	0.00	27	0	0.00
4	0	0.00	10	39	30.00	16	0	0.00	22	0	0.00	28	0	0.00
5	1	0.77	11	11	8.46	17	3	2.31	23	0	0.00	29	0	0.00
6	2	1.54	12	4	3.08	18	1	0.77	24	0	0.00	30	0	0.00

MAXIMA:

MEAN OF HIGHEST 1/3: 4.111E-01  
DIVIDED BY SQRT(MEAN SQUARE/2): 2.017E 00

HEIGHTS:

MEAN OF HIGHEST 1/3: 6.923E-01  
DIVIDED BY SQRT(MEAN SQUARE/2): 1.926E 00



$X(i)$  is a maximum if  $X(i-1) < X(i) \geq X(i+1)$

$X(i)$  is a minimum if  $X(i-1) > X(i) \leq X(i+1)$

a zero up-crossing occurred if  $X(i) \geq 0$  and  $X(i-1) < 0$ .

This means that even though the continuous signal could have values exceeding  $X(i)$ , the digitized value closest to the peak,  $X(i)$  was taken to be the maximum and no attempt was made to fit a curve to the points in order to approximate the true maximum. With a sampling interval of one second and typical zero crossing periods for the signal of ten seconds, this is not expected to introduce any significant errors.

The number of negative maxima were also counted as well as the largest maximum and smallest minimum between zero crossings. An example of the results obtained by this method is shown in Figure (28).

#### Mean response period

The period of one cycle was recorded as the number of intervals between two values larger than or equal to zero preceded by negative values. Thus, as the sampling interval was one second, each cycle would be given periods in integer values of seconds only. A better approximation of the actual period could have been achieved by interpolation between the negative and positive value. This would not make any difference to the calculated mean response period, but would have some effect on the standard deviation of the period. Mean response period was found by

$$T_R = \frac{1}{N} \sum_{n=1}^N T_n$$

and the standard deviation from

$$\sigma = \frac{\sum_{n=1}^N T_n^2 - \left( \sum_{n=1}^N T_n \right)^2 / N}{N(N-1)}$$

where  $T_n$  = period for cycle  $n$

and  $N$  = total number of cycles

The reason for calculating the standard deviation of the periods was to get a general idea of how "regular" the irregular signal was with respect to periods and the accuracy in  $\sigma$  calculated in this way was considered adequate for this purpose. The distribution of periods was also calculated and tabulated. The theoretical distribution of intervals between zero crossings is, however, very complicated, see for example [38] and no comparison between measured and theoretical periods was made.

#### Estimation of the spectrum width parameter $\epsilon$

The parameter  $\epsilon$  is a measure of the width of the spectrum and is defined in terms of the spectrum's moments as

$$\epsilon^2 = 1 - m_2^2 / m_0 m_4$$

When the spectrum is not calculated and therefore, the moments  $m_2$  and  $m_4$  not known Cartwright and Longuet-Higgins [58] have shown how the parameter  $\epsilon$  can be estimated from the ratio of negative maxima and the total number of maxima over a long time interval. The following relationship was derived:

$$\epsilon^2 = 1 - (1-2r)^2$$

where  $r = \frac{\text{number of negative maxima}}{\text{total number of maxima}}$

The width parameter  $\epsilon$  was estimated in this way.

### Response values

In Chapter 2 it was shown how the significant response values could be found from

$$R_{1/3} = 4 \sqrt{m_0} \sqrt{1 - \epsilon^2/2}$$

where  $m_0$  was the area under spectrum. But the area  $m_0$  is also the variance of the irregular signals ordinate. So in this case the variance  $\sigma_x^2$  of all the points forming the signal was calculated and the significant response value found from

$$R_{1/3} = 4 \sqrt{\sigma_x^2} \sqrt{1 - \epsilon^2/2}$$

### Comparison to the Rayleigh distribution

It was earlier shown that the distribution of maxima for a Gaussian process follows the Rayleigh distribution when the process is narrow, i.e.  $\epsilon = 0$ .

The probability density function for a Rayleigh distributed variable  $X$  can be expressed as

$$f(X) = \frac{2X}{R} e^{-\frac{X^2}{R}}$$

where  $R$  is a parameter.

When comparing a sample of  $N X_i$  to the theoretical distribution it can be shown [37] by the maximum likelihood method that the most efficient estimator  $R_e$  of the parameter  $R$  is:

$$R_e = \frac{\sum X_i^2}{N} = \overline{X^2}$$

where  $\overline{X^2}$  is the mean square value of  $X$ .

$R_e$  is random variable which has the gamma probability distribution and ref[37] recommends  $N > 120$  for the estimation. For samples in the order of  $N > 30$  the confidence limits of  $R$  increase and can be determined from the Normal probability distribution, so that

$$\left( \frac{R_e}{\frac{U_{\alpha/2}}{\sqrt{N}} - 1} \right) < R < \left( \frac{R_e}{\frac{U_{\alpha/2}}{\sqrt{N}} + 1} \right)$$

where  $U_{\alpha/2}$  = critical value of the normal distribution for a given  $\alpha$ .

The significant value, defined as the mean of the highest one third of the  $X$ -values can be found as follows. Let  $a$  be the lower limit of the one third highest values so that

$$P(X > a) = 1 - F(a) = 1/3$$

where  $F(X) = 1 - e^{-X^2/R}$  is the cumulative probability function of  $f(X)$ .

Then

$$e^{-a^2/R} = 1/3$$

giving

$$a = \sqrt{R \ln 3}$$

The mean of the values larger than or equal to  $a$  can be found by the moment about the origin so that

$$\begin{aligned} X_{1/3} &= 3 \int_a^{\infty} X f(X) dX = 3 \int_a^{\infty} 2X^2/R e^{-X^2/R} dX = \\ &= 3 \left\{ a e^{-a^2/R} + \sqrt{\pi R} (1 - \phi(\sqrt{2a/R})) \right\} \end{aligned}$$

$$\text{where } \Phi(\sqrt{2a/R}) = \frac{1}{2\pi} \int_{-\infty}^{\sqrt{2a/R}} e^{-u^2/2} du$$

is the cumulative Gaussian probability function.

Substitution of a gives

$$X_{1/3} = \sqrt{R} (\sqrt{\ln 3} + 3 \sqrt{\pi} (1 - \Phi(\sqrt{2 \ln 3})) = 1.4158 \sqrt{R}$$

for convenience often approximated to

$$X_{1/3} \approx \sqrt{2R} = \sqrt{2} \bar{X}$$

and the ratio

$$\frac{X_{1/3}}{\sqrt{X^2/2}} = 2$$

For programming purposes, the comparison between the distribution of the variable and the Rayleigh distribution is simplified by using a normalized Rayleigh function which is accomplished by putting

$$y = X/\sqrt{X^2/2}$$

and so that

$$f(y) = f(x) \left| \frac{dx}{dy} \right|$$

which gives

$$f(y) = y e^{-y^2/2}$$

This function was plotted together with the histogram of the variable.

The histogram was formed by dividing all values by  $\sqrt{X^2/2}$  sorting in ascending order and counting the number of occurrences in each interval  $\Delta y$ .

Each bar  $f(y_i)$  is thus given a height of

$$f(y_i) = M(y_i)/N\Delta y$$

where  $M(y_i)$  = number of values in the interval  $y_i \pm \Delta y/2$  and  $N$  =

total number of values.

The actual mean of the highest one third was also calculated by

$$y_{1/3} = \frac{1}{N-2N/3} \sum_{i=2N/3}^N y_i \quad (5.1)$$

which for agreement with the Rayleigh distribution should give

$$y_{1/3} \approx 2$$

The following three variables were tested for agreement:

- a) maxima, as the distance from the mean level to a maximum (can be negative)
- b) heights, as the distance between a maximum and the following minimum or a minimum and the following maximum
- c) heights, as the distance from the largest/smallest maximum/minimum between zero crossings and the mean of the smallest/largest preceding and proceeding minima/maxima between zero crossings.

The program was designed to plot the histogram with a  $\Delta y = 0.2$  which worked well for heights as from b) and c). For maxima however, and especially for the pitch signal,  $\Delta y$  should have been given a larger value as the largest pitch amplitude usually was less than 10 quantization levels of the digitized signal. Therefore, although the nondimensional value of significant maxima was near 2 the histogram showed little resemblance to the Rayleigh distribution as seen from Figures (29-31). An improvement would probably have been obtained by the inclusion of minima reflected in the zeroline.

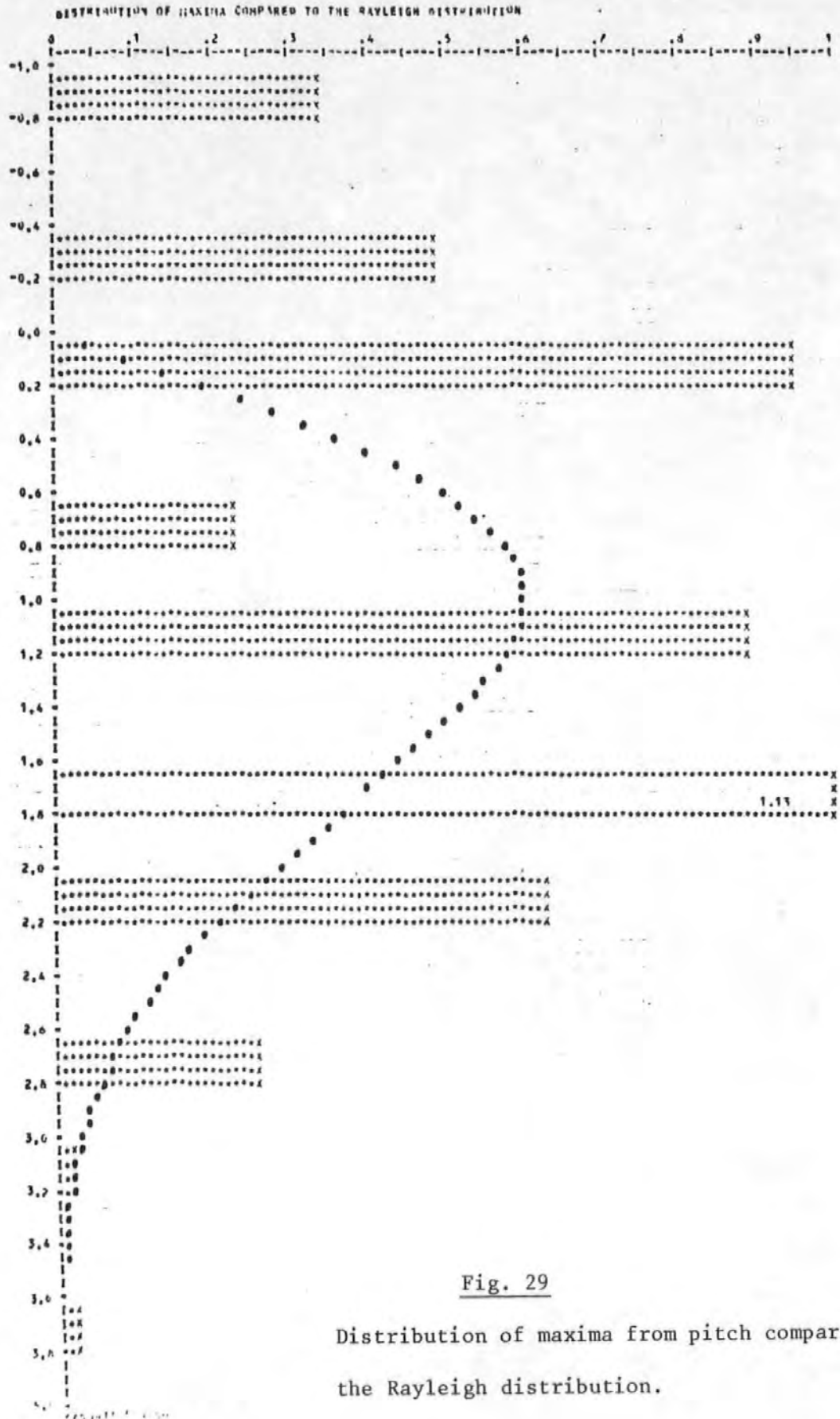


Fig. 29

Distribution of maxima from pitch compared to the Rayleigh distribution.

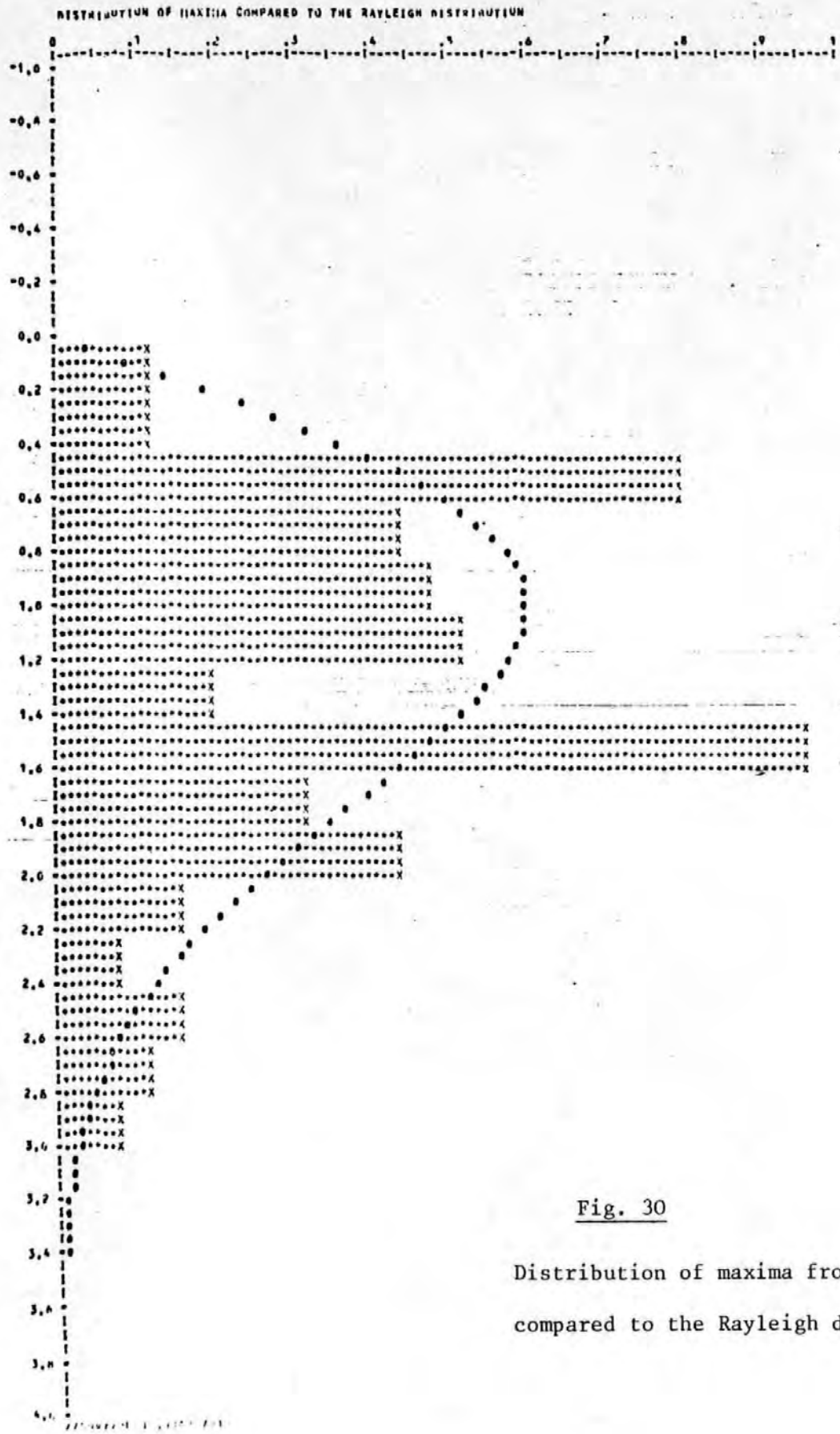


Fig. 30

Distribution of maxima from roll compared to the Rayleigh distribution.





Fig. 31

Distribution of maxima from acc. eng. compared to the Rayleigh distribution.

No statistical test was carried out on the distributions but visual inspection suggested that heights as defined in c) gave slightly better agreement than heights defined in b). Figures (32 - 34) give examples of distributions of heights as in c). The significant value  $R_{1/3}$  of heights as from

$$R_{1/3} = y_{1/3} \sqrt{\overline{h^2}/2}$$

where  $\overline{h^2}$  = mean square of heights as defined in c) and  $y_{1/3}$  = the non-dimensional significant value as from equation ( 5.1 ) will henceforth be referred to as the "measured significant value" and was compared to the significant values calculated by the spectrum analysis and the manual method.

#### Expected max values

The largest value of heights as defined under c) on page 89 was registered and compared to the theoretically calculated largest value.

Let the variable X be distributed according to the Rayleigh distribution so that

$$f(X) = \frac{2X}{R} e^{-X^2/R}$$

where R = mean square of X.

The probability that any one value of X exceeds a preset value  $X_m$  is

$$P (X > X_m) = 1 - P (X \leq X_m) = 1 - F(X_m)$$

$$\text{where } F(X) = 1 - e^{-X^2/R}$$

is the cumulative probability function. From a population of N values, let  $X_m$  be the value with the probability 1/N to be exceeded, so that:

$$P (X > X_m) = 1/N$$

then

$$1 - F(X_m) = e^{-X_m^2/R} = 1/N$$

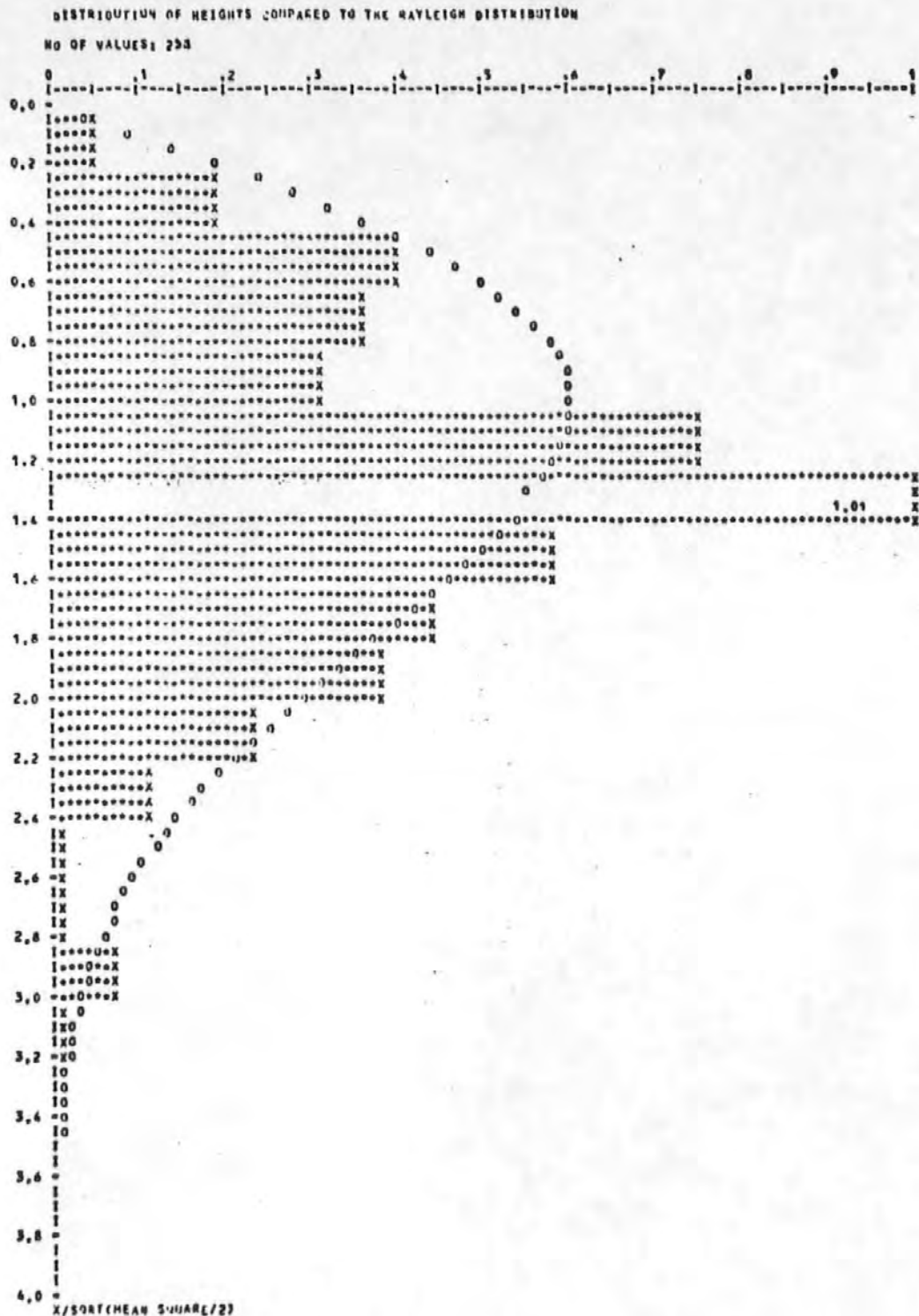


Fig. 32

Distribution of heights from pitch compared to the Rayleigh distribution.

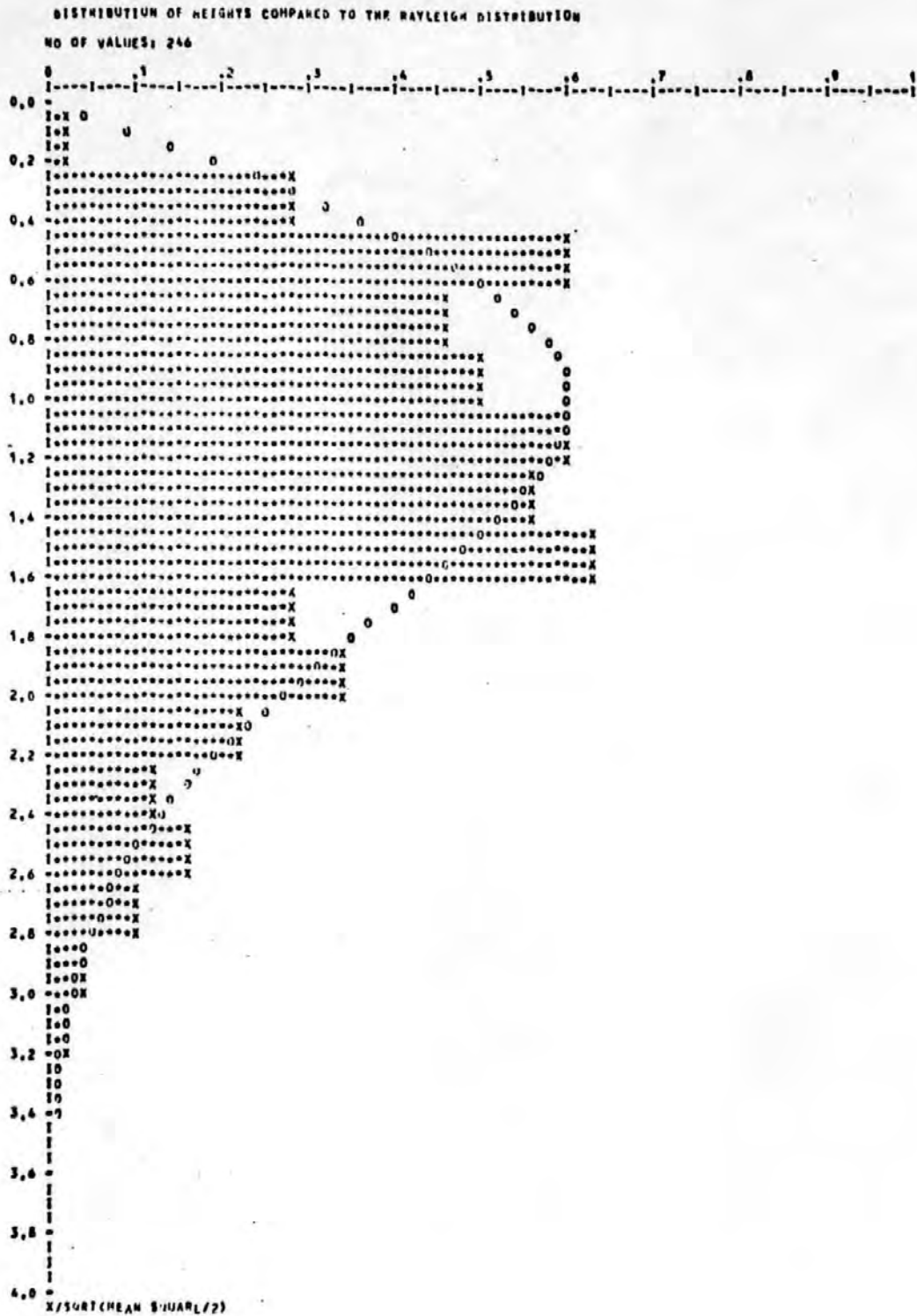


Fig. 33

Distribution of heights from roll compared to the Rayleigh distribution.

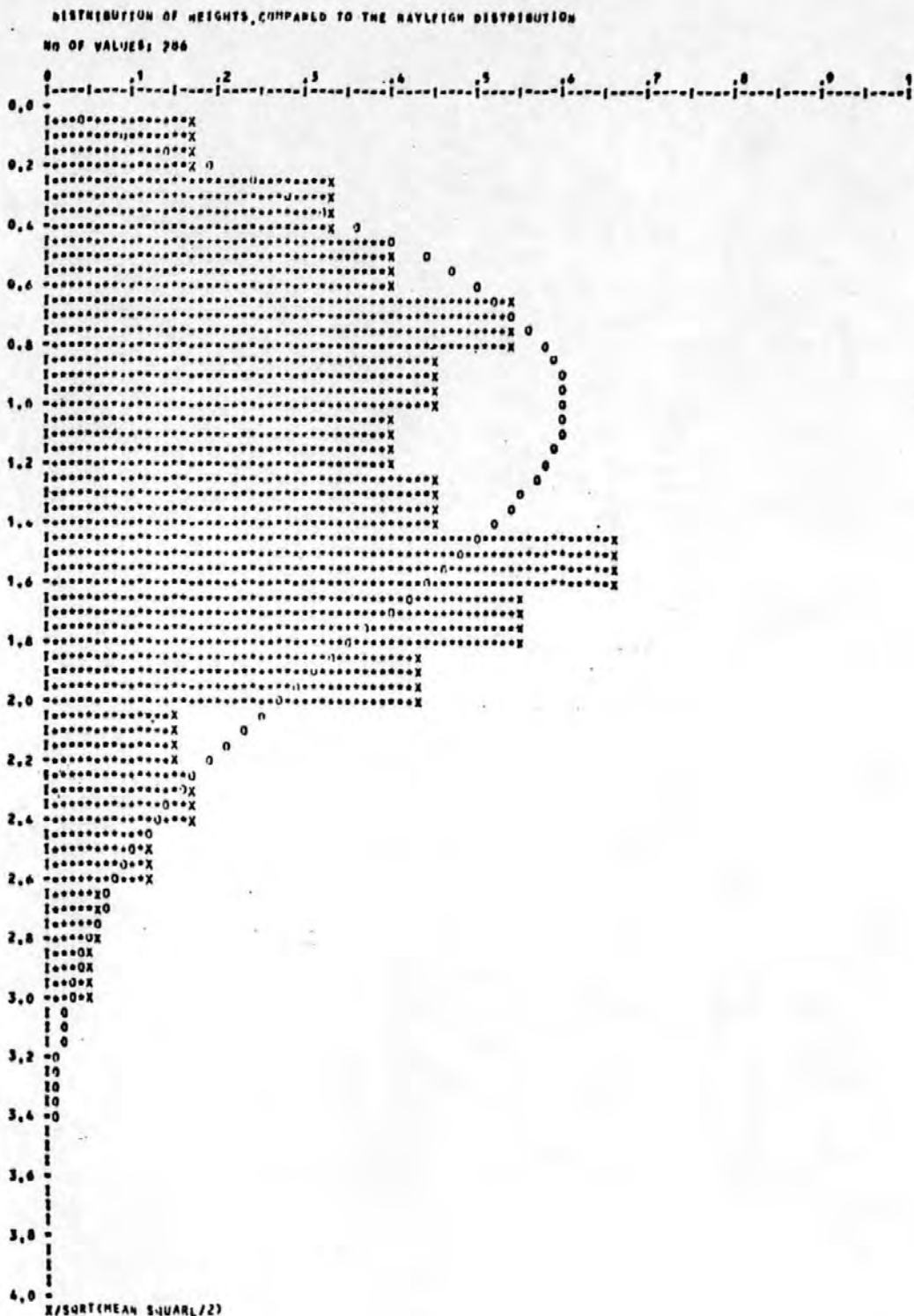


Fig. 34

Distribution of heights from acc. eng. compared to the Rayleigh distribution.

from which

$$X_m = \sqrt{R \ln N}$$

It can be shown [37] that this is the most probable largest value in a sample of  $N$ . The distribution of extremes is, however, skew so that the probability of an extreme value  $X_e$  exceeding a value  $a$  is given by

$$P(X_e > a) = 1 - (1 - e^{-a^2/R})^N$$

which for  $a = \sqrt{R \ln N}$  gives

$$P(X_e > X_m) = 1 - (1 - e^{-\ln N})^N$$

and for large  $N$

$$P(X_e > X_m) = \lim_{N \rightarrow \infty} 1 - (1 - \frac{1}{N})^N = 1 - e^{-1} = 0.63$$

The most probable max value  $X_m$  can thus be expected to be exceeded with probability 0.63. On average the extreme value from a sample of  $N$  will be larger than  $X_m$ , and Longuet-Higgins [68] has given an asymptotic value for this mean value of extremes, i.e. the expected extreme value:

$$X_e = \sqrt{R} \left( \sqrt{\ln N} + \gamma/2 \sqrt{\ln N} \right) \quad (5.2)$$

where  $\gamma = 0.5772 \dots$  Euler's constant.

For processes which are not narrow and the distribution of maxima deviates from the Rayleigh distribution, the more the broader the process, the above formula has been revised in [58] for values of  $\epsilon < 1$  and can be expressed

$$X_e = \sqrt{R} \left[ (\ln(N \sqrt{1-\epsilon^2}))^{\frac{1}{2}} + \gamma/2 (\ln(N \sqrt{1-\epsilon^2}))^{-\frac{1}{2}} \right] \quad (5.3)$$

The largest expected height has been estimated according to this formula and compared to the largest registered heights. Figures (35-37) show plots of the registered values versus estimated values, for the

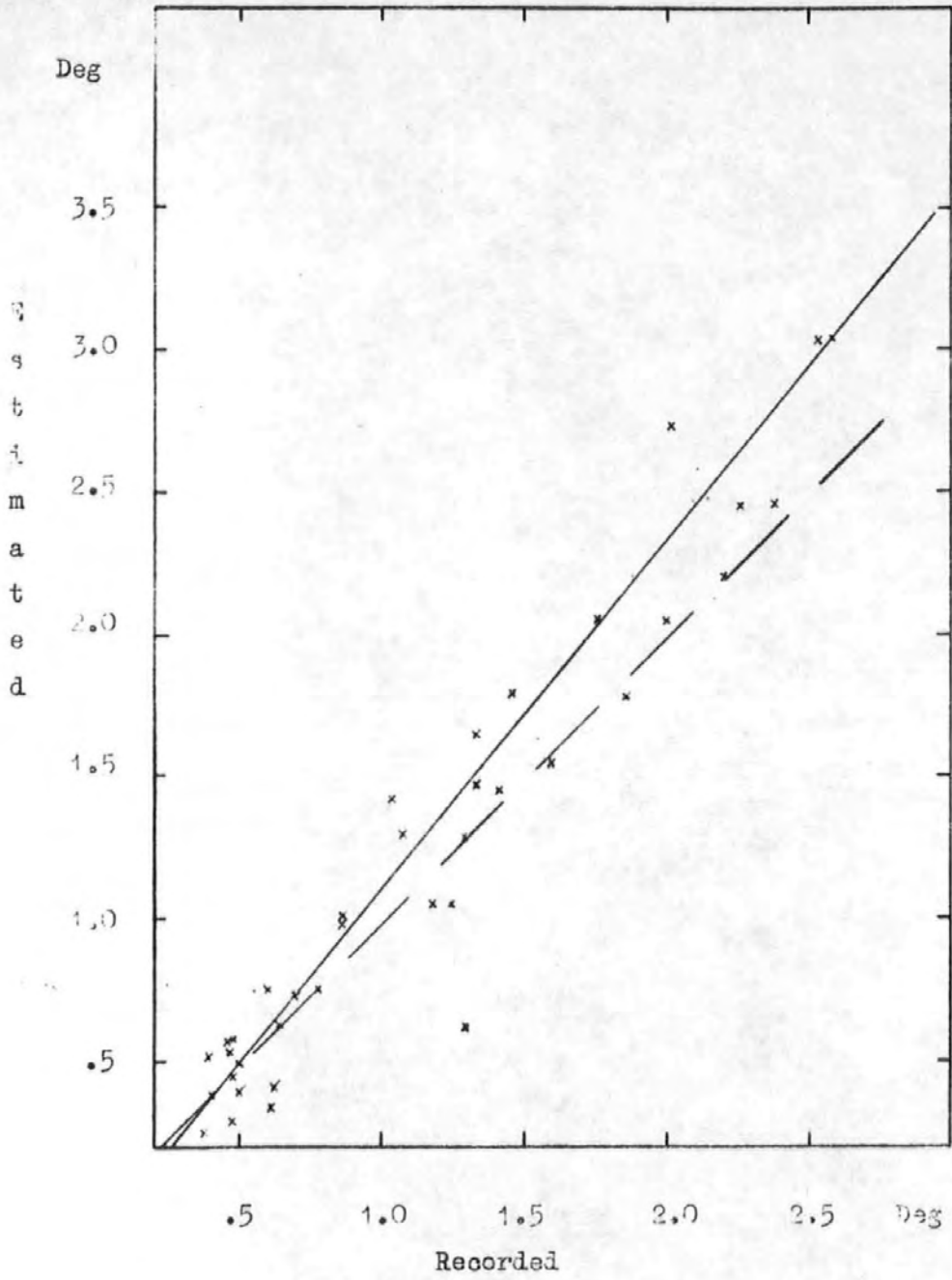


Fig. 35

Estimated versus recorded max values for pitch. Regression line solid, ideal relationship broken line.



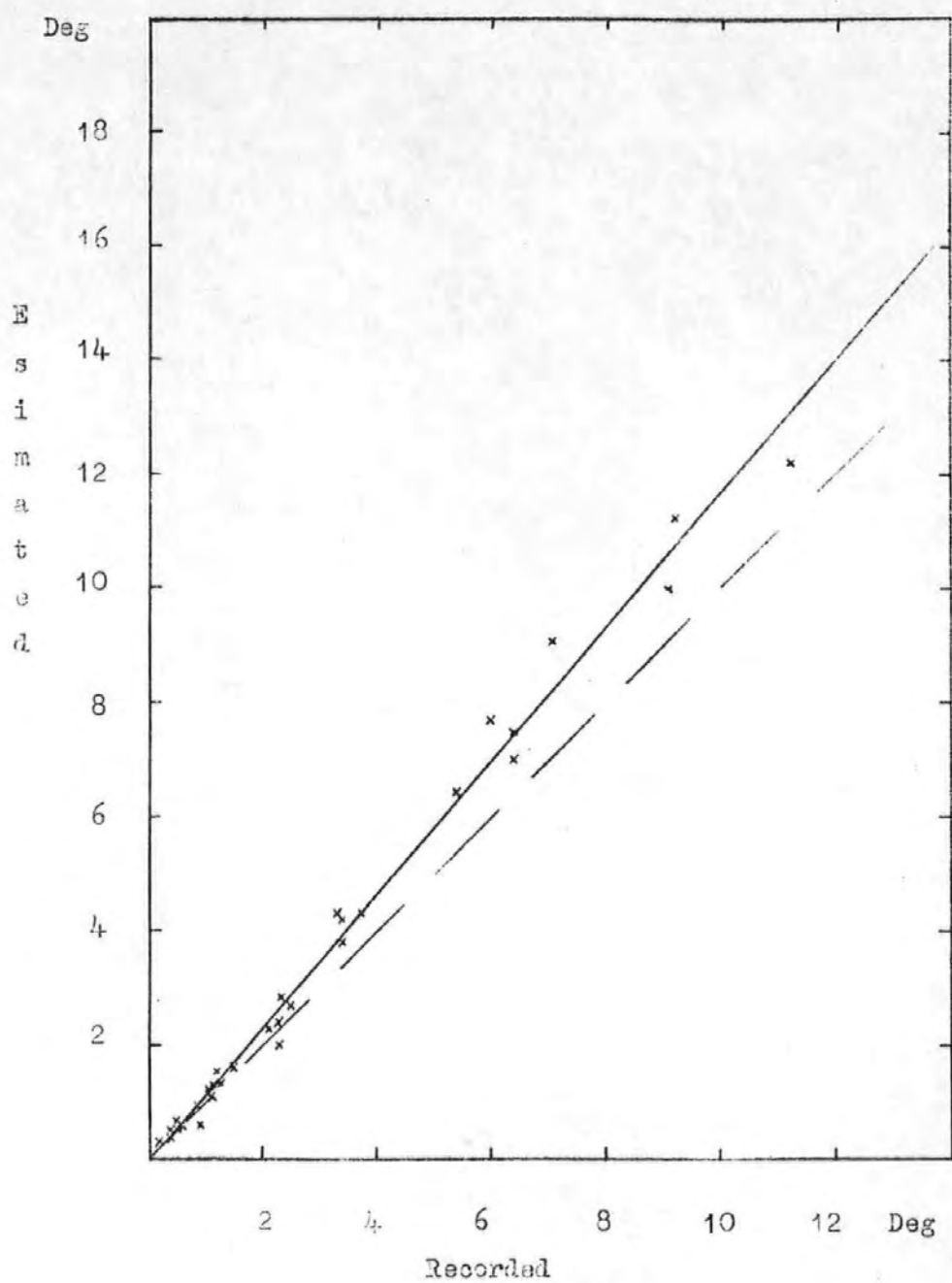


Fig. 36.

Estimated versus recorded max values for roll. Regression line solid, ideal relationship broken line.



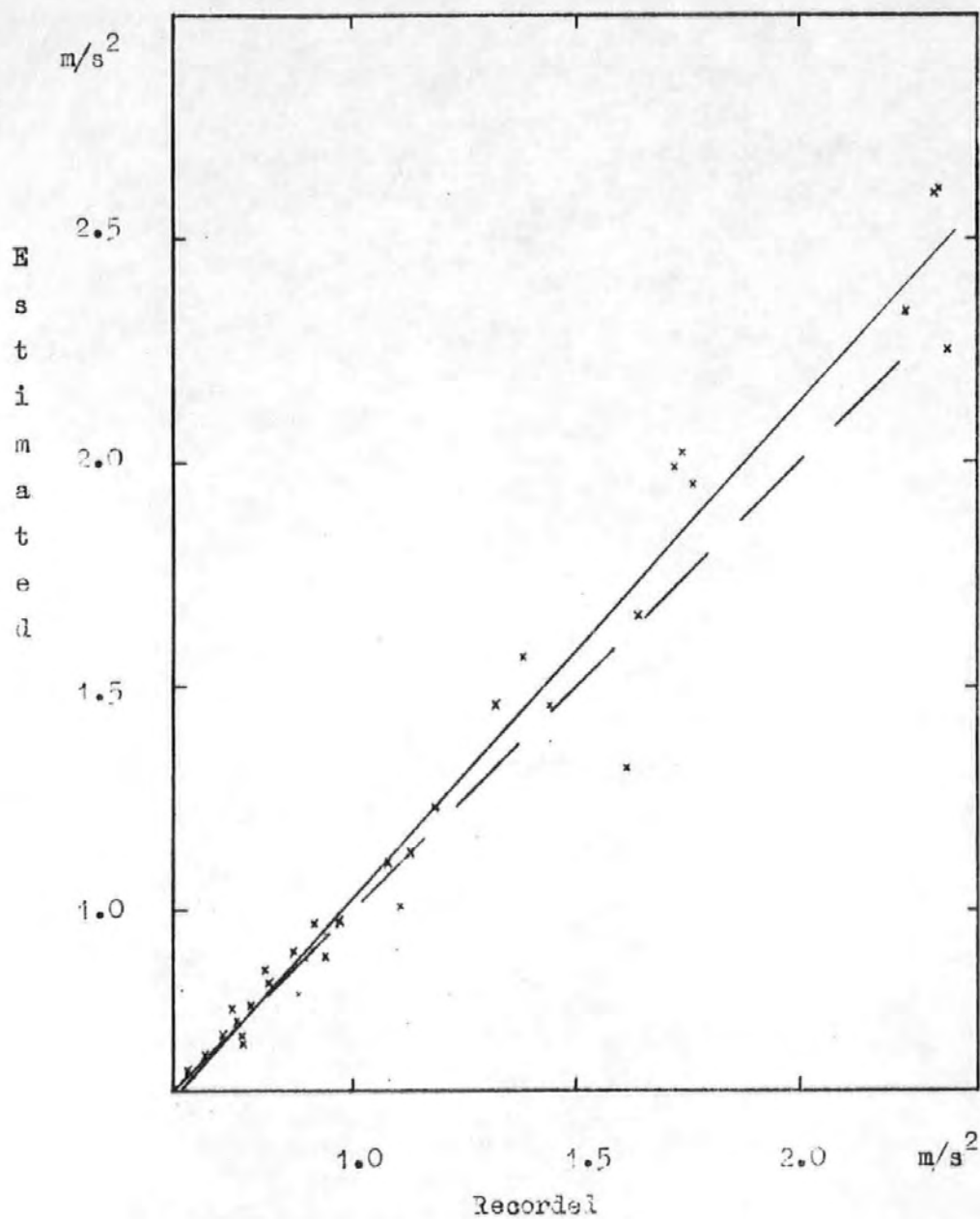


Fig. 37

Estimated versus recorded max values for acc. eng. Regression line solid, ideal relationship broken line.

laden condition.

In the figures the broken line represents a perfect relationship and the solid line is the regression line for the points. Agreement between registered and estimated max values are reasonable although it can be seen from Table 5.2 that the values estimated from the formula (5.3) are generally slightly larger than the recorded, with the exception of pitch values from the ballast journey.

The results may be summarized by the coefficients A and B of the regression lines such that

$$\text{Estimated value} = A \{ \text{Recorded value} \} + B$$

and the coefficient of determination  $r^2$

defined as

$$r^2 = \frac{[\Sigma xy - \Sigma x \Sigma y / N]^2}{[\Sigma x^2 - (\Sigma x)^2 / N][\Sigma y^2 - (\Sigma y)^2 / N]}$$

where N = the number of values

N = 38 for laden voyage and 41 for ballast.

TABLE 5.2

Regression coefficients for comparison between estimated and recorded max values of heights C (defined on page 39 )

$$\text{Estimated} = A \times \text{Rec.} + B$$

	Full Load			Ballast		
	Pitch	Roll	Acc. Eng.	Pitch	Roll	Acc. Eng.
A	1.15	1.16	1.11	0.99	1.08	1.02
B	-0.10	-0.04	-0.03	0.06	0.05	-0.00
$r^2$	.93	.99	.97	0.79	0.96	0.96
Largest Recorded Value	2.59 <sup>o</sup>	11.23 <sup>o</sup>	1.83m/s <sup>2</sup>	1.38 <sup>o</sup>	9.53 <sup>o</sup>	1.77m/s <sup>2</sup>

## Spectrum analysis of the response signals

The recorded variations in time of the responses are assumed to be realisations of stationary ergodic processes. Spectral density functions as defined in chapter two, for these realisations have been derived from the estimated auto-correlation functions, see [38, 69, 70, 71].

### Autocorrelation function

For a realisation of a random process  $r(t)$  the mean of the product at times  $t_1$  and  $t_2$  is called the autocorrelation function and is defined:

$$R(t_1, t_2) = E \left[ r(t_1) r(t_2) \right]$$

It is a measure of the correlation between two values spaced  $v = t_2 - t_1$  apart. Some properties may be established for the autocorrelation function when the random process, of which  $r(t)$  is a realisation, can be assumed to be stationary and ergodic. A process is said to be stationary if none of the statistical properties of the process change with time. It is ergodic if each realisation of the process has the same statistical properties as any other realisation at a fixed time or if the expectations are equal to the corresponding temporal averages taken along a single realisation. An ergodic process must thus be stationary, but the reverse need not be true. For the autocorrelation function of an ergodic process then

$$R(t_1, t_2) = R(t_1 + t, t_2 + t) \quad \text{for all } t,$$

and in particular

$$R(0, t_2 - t_1) = R(v) \quad v = t_2 - t_1$$

Furthermore,

$$R(v) = E \left[ r(t) r(t + v) \right] = E \left[ r(t - v) r(t) \right] = R(-v)$$

so that  $R(v)$  is a real and even function of  $v$ .

From the inequality

$$E \left[ (r(o) \pm r(v))^2 \right] \geq 0$$

it follows

$$2 R(o) \pm 2 R(v) \geq 0$$

so that

$$R(o) \geq R(v)$$

and generally

$$R(v) \rightarrow 0 \text{ for } v \rightarrow \infty$$

So, the autocorrelation function has a maximum for  $v = 0$  at the value

$$R(o) = E \left[ r^2(t) \right] = \text{VAR} \left[ r(t) \right] = \sigma_r^2$$

#### The Fourier Transform and random processes

Consider a function which, as opposed to a realisation of a random process, is periodic with period  $T$  but not simple harmonic. Such a function may be expressed in form of a Fourier series such that

$$u(t) = a_0/2 + \sum_{n=1}^{\infty} (a_n \cos \omega_n t + b_n \sin \omega_n t) \quad (5.4)$$

$$\text{where } a_n = 2/T \int_{-T/2}^{T/2} u(s) \cos \omega_n s \, ds$$

$$b_n = 2/T \int_{-T/2}^{T/2} u(s) \sin \omega_n s \, ds$$

$$\text{and } \omega_n = 2n\pi/T$$

both  $t$  and  $s$  refer to time.

Substitution of  $a_n$  and  $b_n$  into (5.4) and adopting the complex notation so that

$$a_n \cos \omega_n t + b_n \sin \omega_n t = g_n e^{i\omega_n t} + \overline{g_n} e^{-i\omega_n t}$$

where  $g_n = 1/2 (a_n - ib_n)$

and its complex conjugate  $\overline{g_n} = 1/2 (a_n + ib_n)$

The following expression can be derived

$$u(t) = \sum_{n=-\infty}^{\infty} e^{i\omega_n t} \frac{1}{T} \int_{-T/2}^{T/2} u(s) e^{-i\omega_n s} ds = \sum_{n=-\infty}^{\infty} g_n e^{i\omega_n t}$$

$$( 5.5 )$$

where  $g_n = \frac{1}{T} \int_{-T/2}^{T/2} u(s) e^{-i\omega_n s} ds$

is referred to as the Fourier transform of the periodic function.

With the autocorrelation of the periodic function given by

$$R(v) = \frac{1}{T} \int_{-T/2}^{T/2} u(t) u(t+v) dv$$

this can be expressed in terms of the Fourier transform coefficients

as

$$R(v) = \frac{1}{T} \int_{-T/2}^{T/2} u(t) \sum_{n=-\infty}^{\infty} g_n e^{i\omega_n(t+v)} dt$$

or after rearrangement

$$\begin{aligned}
 R(v) &= \sum_{n=-\infty}^{\infty} g_n e^{i\omega_n v} \frac{1}{T} \int_{-T/2}^{T/2} u(t) e^{i\omega_n t} dt = \\
 &= \sum_{n=-\infty}^{\infty} g_n e^{i\omega_n v} \overline{g_n} = \sum_{n=-\infty}^{\infty} |g_n|^2 e^{i\omega_n v} = \\
 &= \sum_{n=-\infty}^{\infty} F_n e^{i\omega_n v}
 \end{aligned}$$

where  $F_n = |g_n|^2$  is the two sided spectral density function. The autocorrelation function  $R(v)$  and the spectral density function  $F_n$  form a Fourier transform pair so that:

$$\begin{aligned}
 R(v) &= \sum_{n=-\infty}^{\infty} F_n e^{i\omega_n v} \\
 F_n &= \frac{1}{T} \int_{-T/2}^{T/2} R(v) e^{-i\omega_n v} dv \quad (5.6)
 \end{aligned}$$

An aperiodic, non-periodic function such as a realisation of a random process can only be expressed as a Fourier series if the period of the series tends to infinity. Allowing for this, equation (5.5) can be rewritten so that for  $T \rightarrow \infty$ ,  $\omega_n$  becomes the continuous angular frequency  $\omega$  and  $\lim_{T \rightarrow \infty} 1/T = d\omega/2\pi$ , the expression becomes:

$$u(t) = \frac{1}{2\pi} \int_{-\infty}^{\infty} e^{i\omega t} d\omega \int_{-\infty}^{\infty} u(s) e^{-i\omega s} ds =$$

$$\int_{-\infty}^{\infty} G(\omega) e^{i\omega t} d\omega \quad (5.7)$$

$$\text{where } G(\omega) = \frac{1}{2\pi} \int_{-\infty}^{\infty} u(s) e^{-i\omega s} ds$$

And similar to the derivation of (5.6) the Fourier transform pair of the autocorrelation function and the two sided spectral density function can be formed

$$R(v) = \int_{-\infty}^{\infty} F(\omega) e^{i\omega v} d\omega$$

$$F(\omega) = \frac{1}{2\pi} \int_{-\infty}^{\infty} R(v) e^{-i\omega v} dv \quad (5.8)$$

Two conditions regarding  $u(t)$  must however, be fulfilled in order to make equation (5.7) valid. These are:

$$\int_{-\infty}^{\infty} |u(t)| dt \text{ must exist and}$$

$$\int_{-\infty}^{\infty} u^2(t) dt \text{ be finite.}$$

A realisation of a random process  $r(t)$  does not meet these conditions so that the spectrum cannot be calculated from the autocorrelation function straight away. Instead an approximation of spectrum may be obtained from an estimate of the autocorrelation function from a truncated realisation. Thus by defining

$$r(t) = \begin{cases} r(t) & \text{in the interval } [0, T] \\ 0 & \text{otherwise} \end{cases}$$

the autocorrelation function for this interval can be found from

$$R^T(v) = \frac{1}{T} \int_0^{T-|v|} r(t) r(t+v) dt \quad |v| \leq T \quad (5.9)$$

$$\text{and } R^T(v) = 0 \quad |v| > T$$

The expected value of this is

$$\begin{aligned} E[R^T(v)] &= E\left[\frac{1}{T} \int_0^{T-|v|} r(t) r(t+v) dt\right] = \\ &= \frac{1}{T} \int_0^{T-|v|} R(v) dt = \begin{cases} R(v) \left(1 - \frac{|v|}{T}\right) & |v| \leq T \\ 0 & |v| > T \end{cases} \end{aligned}$$

The error introduced by using  $1/T$  instead of  $1/(T-|v|)$  is small when  $T \gg |v|$  and the estimate using  $1/T$  does usually have a smaller least square error than that derived by using  $1/(T-|v|)$  apart from being an advantage for computational purposes.

From the estimated correlation function the one sided spectral density function, autospectrum,  $S(\omega)$  defined as

$$S(\omega) = 2F(\omega) \quad \omega \geq 0$$

can be estimated in accordance with (5.8):



$$\begin{aligned}
E \left[ S^T(\omega) \right] &= E \left[ \frac{1}{\pi} \int_{-T/2}^{T/2} R^T(v) e^{-i\omega v} dv \right] = \\
&= \frac{1}{\pi} \int_{-T/2}^{T/2} E \left[ R^T(v) e^{-i\omega v} \right] dv = \\
&= \frac{1}{\pi} \int_{-T/2}^{T/2} R(v) \left( 1 - \frac{|v|}{T} \right) e^{-i\omega v} dv \quad (5.10)
\end{aligned}$$

where  $S^T(\omega)$  is the estimate of  $S(\omega)$  from an interval of length  $T$ , and so that

$$\lim_{T \rightarrow \infty} E \left[ S^T(\omega) \right] = \frac{1}{\pi} \int_{-\infty}^{\infty} R(v) e^{-i\omega v} dv = S(\omega)$$

By putting

$$w(v) = \begin{cases} 1 - |v|/T & |v| \leq T \\ 0 & |v| > T \end{cases}$$

equation (5.10) can be expressed

$$E \left[ S^T(\omega) \right] = \frac{1}{\pi} \int_{-\infty}^{\infty} R(v) w(v) e^{-i\omega v} dv \quad (5.11)$$

where  $w(v)$  is called the lag window through which  $R(v)$  is viewed.

The Fourier transform of  $w(v)$ , called the spectral window, is

$$W(\Omega) = \frac{T}{2\pi} \left( \frac{\sin \Omega T/2}{\Omega T/2} \right)^2 \quad (5.12)$$

equation (5.11) can now be expressed

$$E \left[ S^T(\omega) \right] \approx S(\omega) \int_{-\infty}^{\infty} W(\Omega) d\Omega = S(\omega) \quad \text{for large } T.$$

The variance of the estimate is, however, large compared to the estimated value. An improvement has been shown to be obtained by dividing the realisation into parts, of length  $M$  evaluating  $S^M(\omega)$  for each part and forming the mean of all  $S^M(\omega)$ . Such a mean is called the smoothed estimate of  $S(\omega)$  and will be denoted  $\overline{S^T}(\omega)$ .

This method can be shown to have the same effect as substituting  $T$  in equation (5.12) by  $M$  so that

$$W(\Omega) = \frac{M}{2\pi} \left( \frac{\sin \Omega M/2}{\Omega M/2} \right)^2$$

which is called Barlett's window.

There are several proposed spectral windows for various applications and a general expression for the smoothed spectrum estimate is

$$\overline{S^T}(\omega) = \frac{1}{\pi} \int_{-\infty}^{\infty} w(v) R^T(v) e^{-i\omega v} dv$$

Since the autocorrelation is a real and even function it follows finally:

$$\overline{S^T}(\omega) = \frac{1}{\pi} \int_{-\infty}^{\infty} w(v) R^T(v) \cos \omega v dv \quad (5.13)$$

### Application

The numerical evaluations of these formulas have been made for responses where the continuous signal  $r(t)$  was sampled at intervals  $\Delta t$  and thus forming a series of  $N$  values  $X_i$   $i = 1, 2, 3, \dots, N$  so that

$$T = N\Delta t$$

where  $T$  is the total length of the realisation. The following discrete versions of the previous formulas has been used.

For the auto-correlation function according to (5.9)

$$R^T(k) = \frac{1}{N} \sum_{i=1}^{N-k} X_i X_{i+k} \quad K = 0, 1, 2 \dots M-1$$

where M is the number of lags.

The spectrum ordinates according to (5.13) were found from

$$\overline{S^T}(\omega_i) = \frac{\Delta t}{\pi} \left[ R^T(0) + 2 \sum_{K=1}^{M-1} R^T(K) w(K) \cos(\omega_i K t) \right] \quad (5.14)$$

where  $\omega_i = \frac{\pi}{\Delta t} \frac{i}{N_S}$   $i = 0, 1, 2 \dots N_S$

so that the total frequency interval  $[0, \pi/\Delta t]$  was divided into parts so that the ordinates for  $N_S + 1$  values of  $\omega$  were obtained.

The lag window proposed by Tuckey (Hanning) was selected so that:

$$w(K) = \frac{1}{2} \left[ 1 + \cos\left(\frac{\pi K}{M}\right) \right]$$

For the signals analysed here  $\Delta t$  was 1 second and  $N_S$  was put to 157 giving spectrum ordinates with a spacing of  $\omega = 0.02$ . The moments of the spectrum according to

$$m_n = \int_0^{\infty} \omega^n S(\omega) d\omega$$

were calculated from

$$m_n = \sum_{i=0}^c \omega_i^n S(\omega_i) \Delta\omega \quad (5.15)$$

where  $\Delta\omega = 0.02$

and  $c =$  a truncation value.

As the analysed response signals, pitch angle, roll angle and vertical acceleration in the engine room can be regarded as relatively narrow-

banded processes, possibly with the exception of acceleration, it was considered justifiable to truncate the high frequency tail of spectrum at a frequency  $\omega = \omega_c$ . This would seem reasonable even for vertical acceleration as this signal might contain frequencies caused by vibration and the results of the spectrum analysis were to be compared to calculated values of vertical acceleration, due to a combination of pitch and heave only. Thus the information lost by excluding any high frequency tails was not considered as being of importance to this investigation. A reasonable check on how much was lost could also be made by comparing the area under spectrum  $m_0$  from equation (5.15) and the value of  $R^T(0)$  as both represent the variance  $\sigma^2$  of the process, bearing in mind that  $\overline{S^T}$  is an estimate of the true spectrum. The ratio  $m_0/R^T(0)$  gave in this way an indication of the area under spectrum lost by the truncation. Reference [72] has investigated the effects of the truncation frequency for broad banded wave spectra of Pierson-Moskowitz type and given a lower limit of three times the frequency of spectrum's max for mean periods  $\geq 7$  seconds. The following truncation frequency  $\omega_c$  was used:

$$\omega_c = \omega_i \text{ for } \overline{S^T}(\omega_i) \leq \overline{S^T} \text{ max}/200 \quad \omega_i > 1$$

$$\omega_c = \omega_i \text{ for } \omega_i = 3\omega_i(\overline{S^T} \text{ max}) \quad \omega_i > 1$$

These are also similar to those used by Loukakis [5].

From the moments the mean response period  $T_R$  was found by

$$T_R = 2\pi \sqrt{m_0/m_2} \quad (5.16)$$

the significant response value adjusted for the spectrum width from

$$R_{1/3} = 4 \sqrt{m_0} (1 - \epsilon^2/2) \quad (5.17)$$

where

$$\epsilon = \sqrt{1 - m_2^2 / m_0 m_4} \quad ( 5.18 )$$

The effects on the moments from a truncation is larger for higher moments so that  $m_4$  is more reduced than  $m_0$ , and the spectrum width will be smaller. As the width parameter is used in ( 5.17 ) the significant value is affected by this. However, the correction factor which is

$$\sqrt{1 - \epsilon^2/2} = \begin{cases} 1 & \text{for } \epsilon = 0 \\ \sqrt{1/2} \approx 0.707 & \text{for } \epsilon = 1 \end{cases}$$

was not believed to change dramatically because of the truncation.

For the value of M, the lag number, Marks [70] has recommended 30-60 as being satisfactory for most seakeeping events. 60 lags were also used by Loukakis [5].

In order to test the method of analysis and the effects of some different M values a test signal X(t) was produced from

$$X(t) = \sum_{i=1}^N a_i \cos (\omega_i t + \alpha_i)$$

where  $\alpha_i$  is a phase angle evenly distributed between 0,  $2\pi$  and randomly selected

$a_i$  = the ordinates of the components and selected from a predetermined spectrum.

N = the number of components used to form the signal, here put = 30. Figure (38) shows the outcome of this test, and as predicted a higher value of M gives a better representation of the peaks but can also generate false peaks. It was decided that M = 60 would give a representative picture of the spectrum as well as keeping computer time at a reasonable level. Figures (39-41) are examples of output from the analysis of response signals by the spectral analysis program.

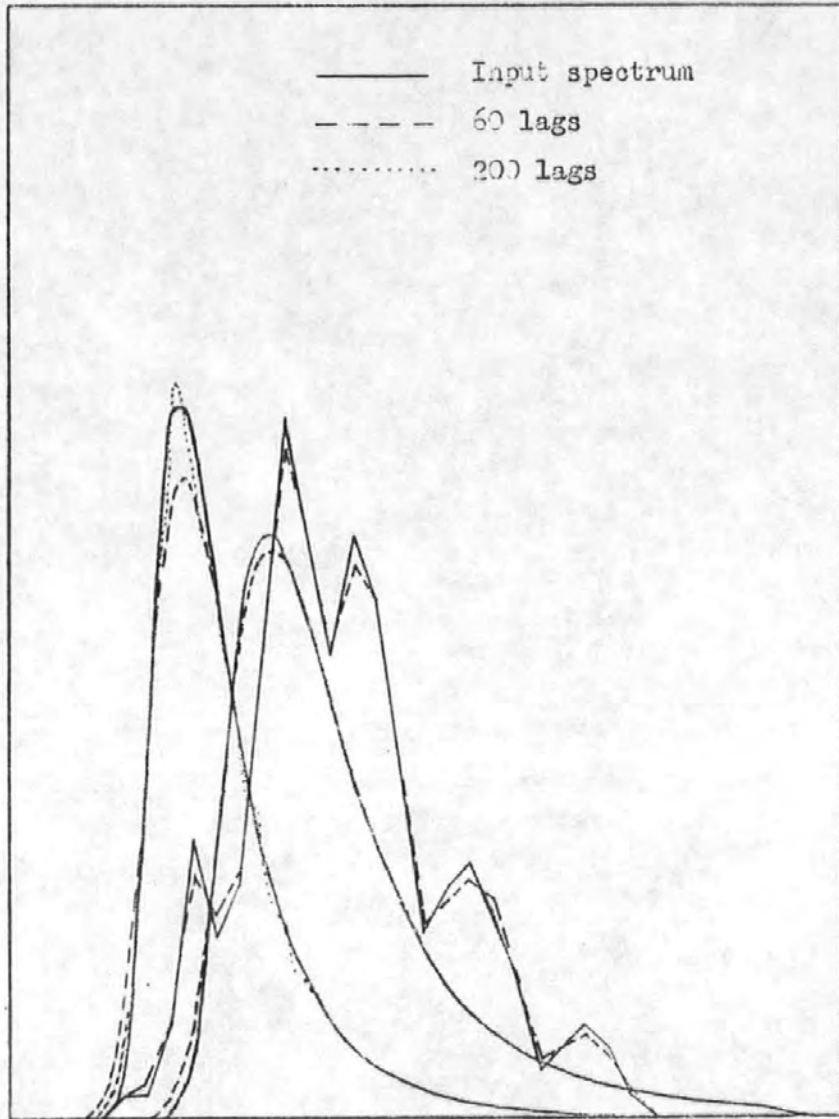


Fig. 38

Comparison between input spectra and corresponding spectra divided by different lag values.

Fig. 39  
 Example of response spectrum of pitch.

RESPONSE SPECTRUM FOR PITCH ANGLE  
 RECORD NO: 35      DATE: 1972- 5-25  
 LENGTH OF RECORDING: 21.33 MINUTES  
 R(1): 4.0511E-02      PERCENT OF SPECTRUM AREA COVERED: 99.2  
 MOMENTS OF SPECTRUM:  
 M0= 4.0190E-04    M1= 2.2231E-02    M2= 1.4661E-02    M3= 9.9822E-03    M4= 6.9504E-03  
 SIGNIFICANT VALUE: 8.018E-01 DEGREES      SIGN VALUE ADJUSTED FOR WIDTH: 7.542E-01 DEGREES  
 T2-PERIOD: 10.402 SEC    CREST PERIOD: 9.125 SEC    WIDTH: 0.480

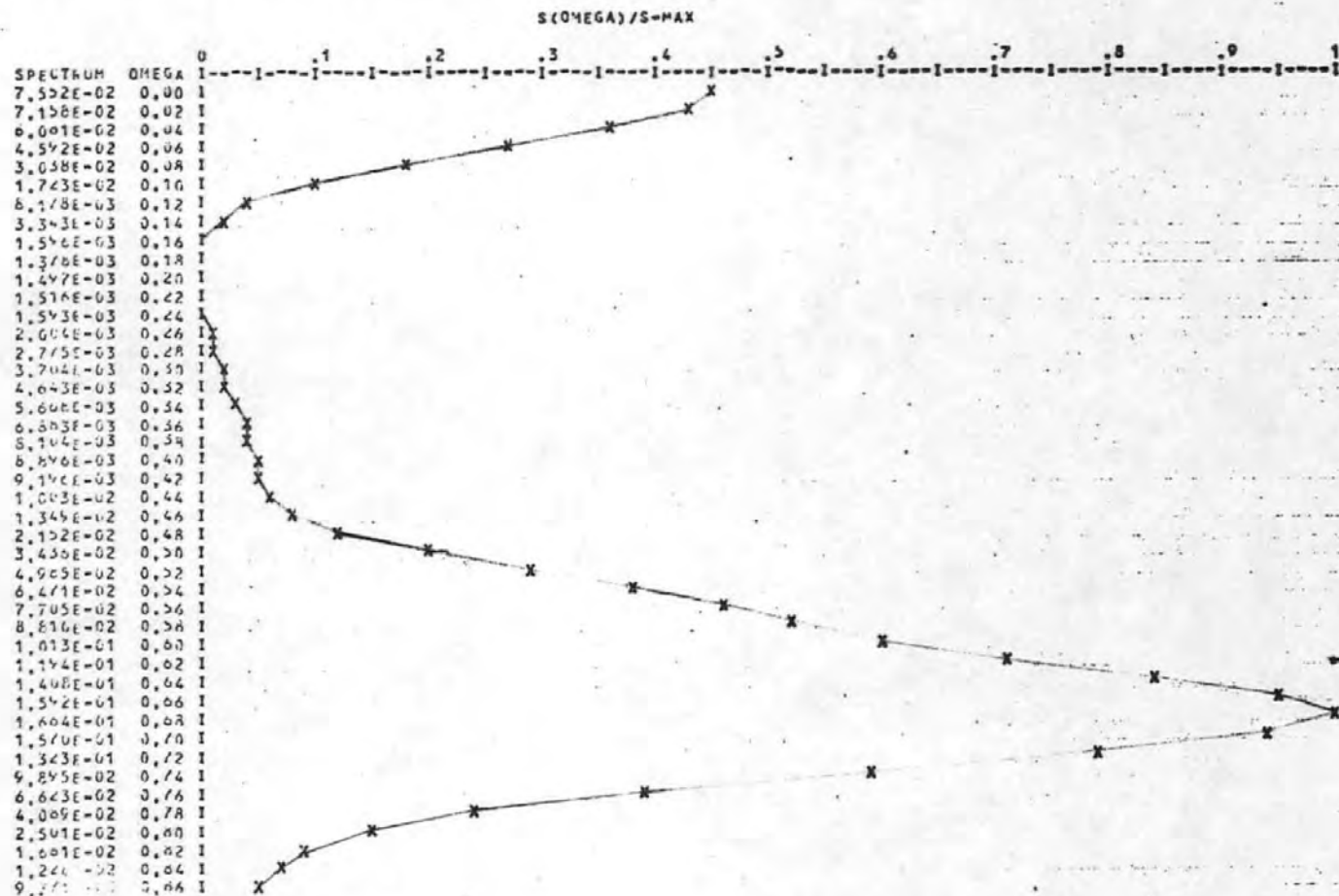


Fig. 40  
 Example of response spectrum of roll.

RESPONSE SPECTRUM FOR ROLL ANGLE

RECORD NO: 33      DATE: 1972- 5-25  
 LENGTH OF RECORDING: 21.33 MINUTES  
 R(1): 2.3768E 00      PERCENT OF SPECTRUM AREA COVERED: 100.0  
 MOMENTS OF SPECTRUM:  
 M0= 2.3757E 00    M1= 1.4373E 00    M2= 8.8030E-01    M3= 5.4453E-01    M4= 3.4016E-01  
 SIGNIFICANT VALUE: 6.165E 00 DEGREES      SIGN VALUE ADJUSTED FOR WIDTH: 6.102E 00 DEGREES  
 T2-PERIOD: 10.322 SEC    CREST PERIOD: 10.108 SEC    WIDTH: 0.203

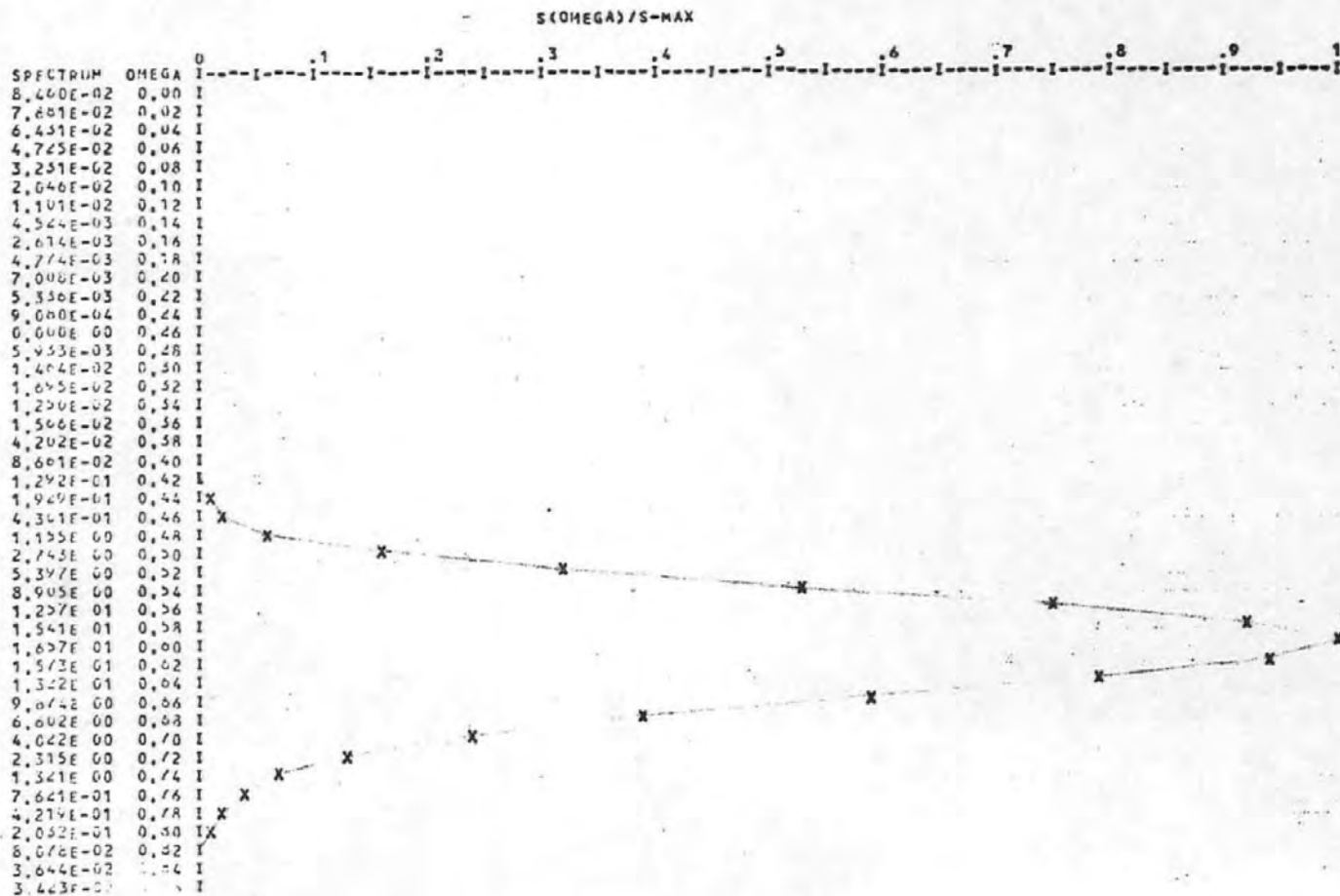
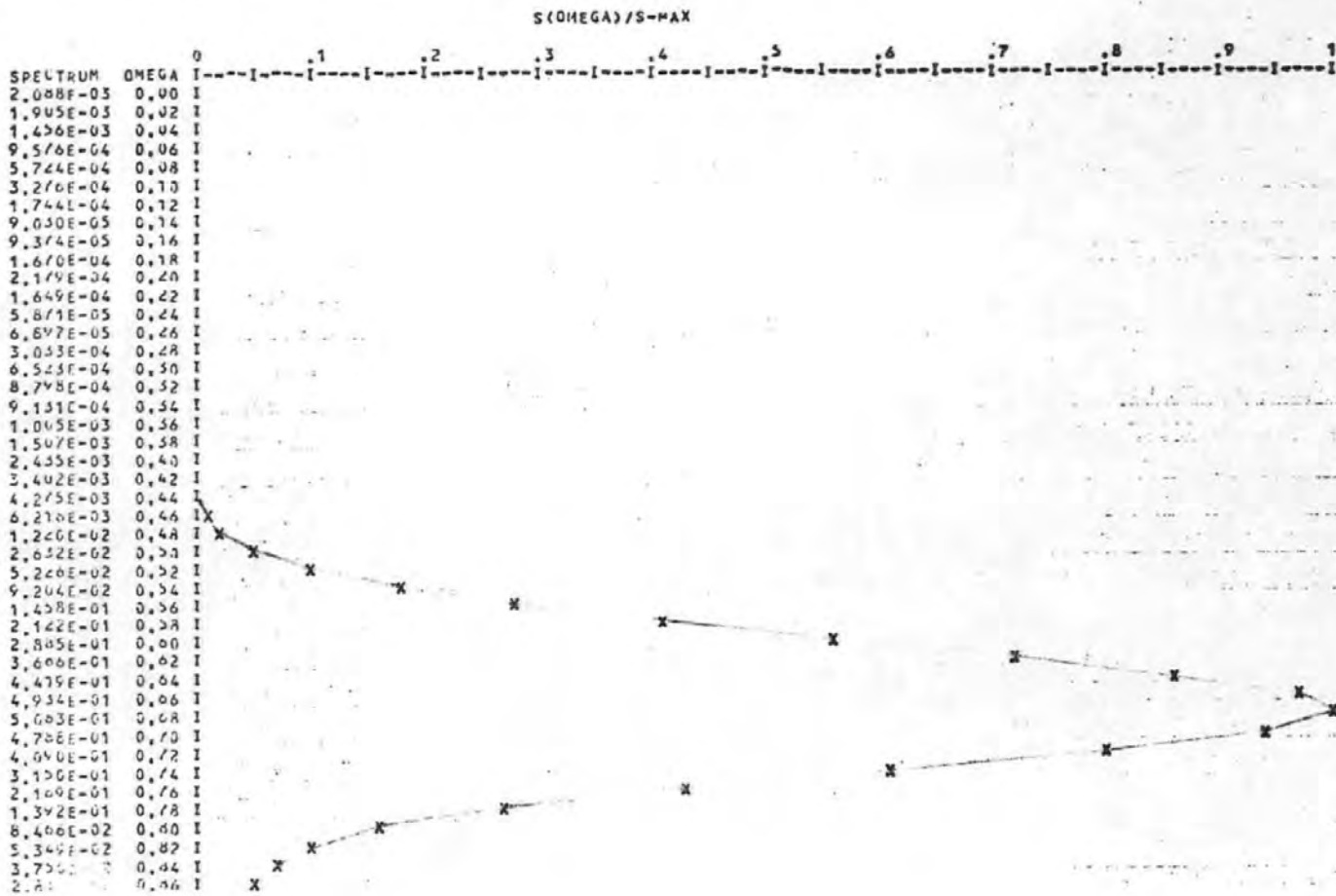




Fig. 41  
 Example of response spectrum of acc. eng.

RESPONSE SPECTRUM FOR HEAVE ACCEL

RECORD NO: 35      DATE: 1972-5-25  
 LENGTH OF RECORDING: 21.33 MINUTES  
 R(1): 9.1340E-02      PERCENT OF SPECTRUM AREA COVERED: 98.8  
 MOMENTS OF SPECTRUM:  
 M0= 9.0202E-02    M1= 6.0777E-02    M2= 4.1567E-02    M3= 2.8812E-02    M4= 2.0240E-02  
 SIGNIFICANT VALUE: 1.201E 00 M/SEC+2      SIGN VALUE ADJUSTED FOR WIDTH: 1.185E 00 M/SEC+2  
 T2-PERIOD: 9.256 SEC      CREST PERIOD: 9.004 SEC      WIDTH: 0.231



Comparison of results from the spectral analysis and the "manual method"

The mean of the largest one third recorded heights has been compared to the significant values estimated from the two methods of analysis. The recorded heights are according to definition c) page 89 the mean of the distance from the largest peak between zero-crossings to the preceding and following smallest minimum between zero-crossings. It could be argued that a comparison should instead have been made between significant single amplitudes, measured and recorded, as the theoretical distribution has been derived for maxima rather than heights [58]. Many of the analysed records were, however, from conditions where the motions of the ship were small resulting in a low ratio of amplitude to quantization level, say in the order 3-5 for pitch angle. By using the heights that ratio is doubled and thus improves accuracy. It is also common to relate responses to significant waveheight which is double amplitude and it is logical then to let the significant response also be double amplitude. Loukakis [5] has also found good relationship between heights defined as above, and theoretical estimates.

In Figures (42-47) the recorded significant values versus estimated are plotted for the two methods of analysis from the laden voyage.

Crosses represent values estimated from

$$R_{1/3} = 4 \sqrt{m_0} \quad \text{for the spectrum analysis and}$$

$$R_{1/3} = 4 \sqrt{\sigma^2} \quad \text{for the manual method}$$

whereas circles were obtained by including the adjustment for spread such that

$$R_{1/3} = 4 \sqrt{m_0} \sqrt{1 - \epsilon^2/2} \quad \text{and}$$

$$R_{1/3} = 4 \sqrt{\sigma^2} \sqrt{1 - \epsilon^2/2} \text{ respectively}$$

In figures (39) and (40) the broken line with dots is the regression line for the crosses, the solid line for the circles and the broken line represents the perfect relationship. The regression lines are not shown in figures (44-47) as they are very close to the perfect line. The reasons for the slight difference in response values obtained from the two methods without adjustments for spectrum width are due partly to the signal being shortened by cutting the ends before applying the manual method, and partly to  $m_0$  being calculated from the area under the truncated spectrum rather than from the variance.

The mean response periods obtained from the spectral analysis method as

$$T_R = 2 \pi \sqrt{m_0/m_2}$$

have been compared to those obtained by the manual method. In figures (48-50) the results from the laden voyage are plotted, and it can be seen that there are some discrepancies between the periods obtained from the two methods. This is an interesting and important result. As the mean spectrum period in the equivalent wave spectrum is determined by the measured response period as described in Chapter 3 it is important to get as accurate an estimate as possible of the response period. In figures (51-53) the calculated response periods for wave spectra of P-M type are plotted, solid lines, together with the significant response values per metre significant wave height, broken lines for laden condition and 14 knots, a speed which corresponds to most of the records. A comparison of the measured and calculated response periods reveals

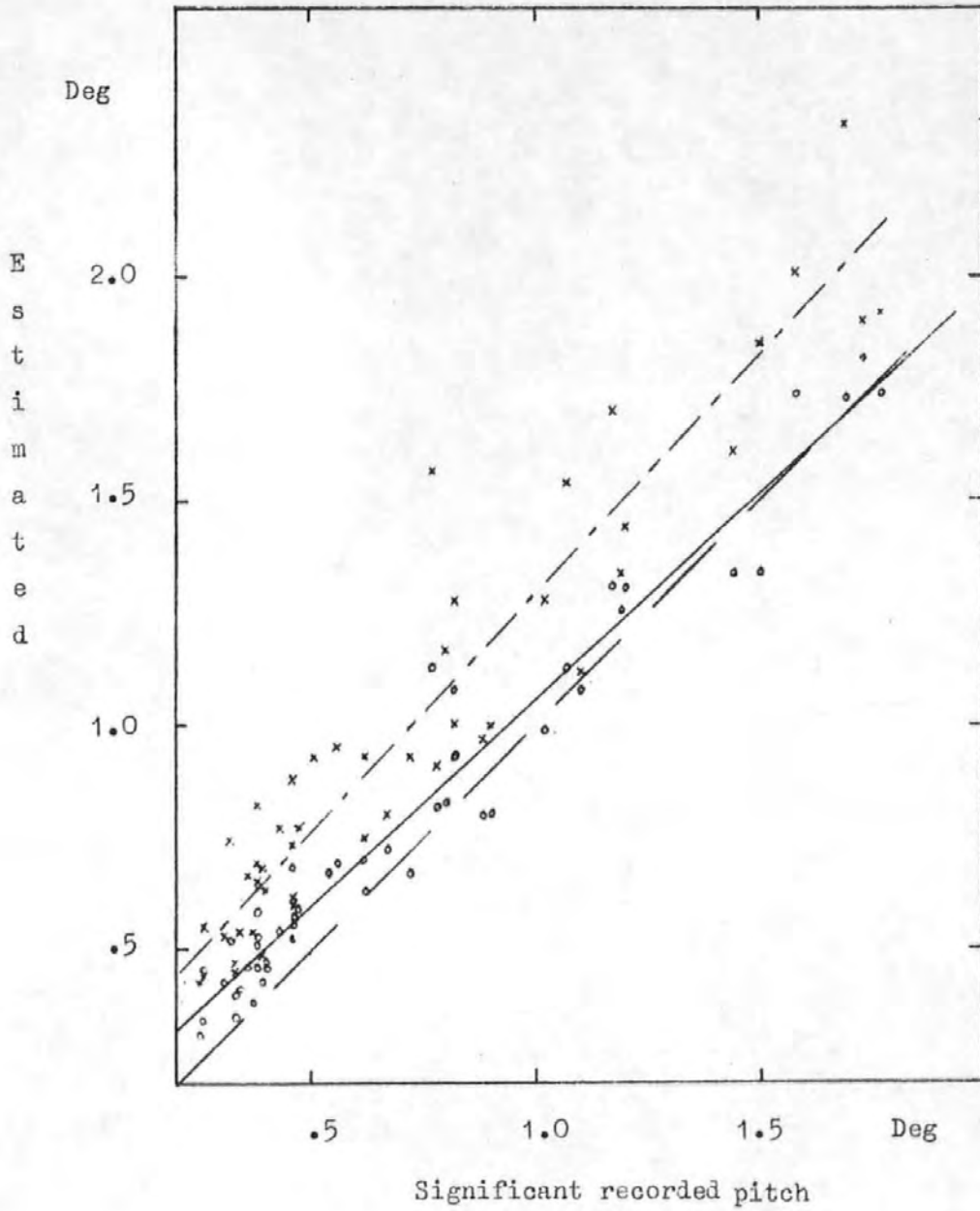


Fig. 42

Recorded significant pitch versus estimated from the manual method with regression lines X = without, O = with adjustment for spread.

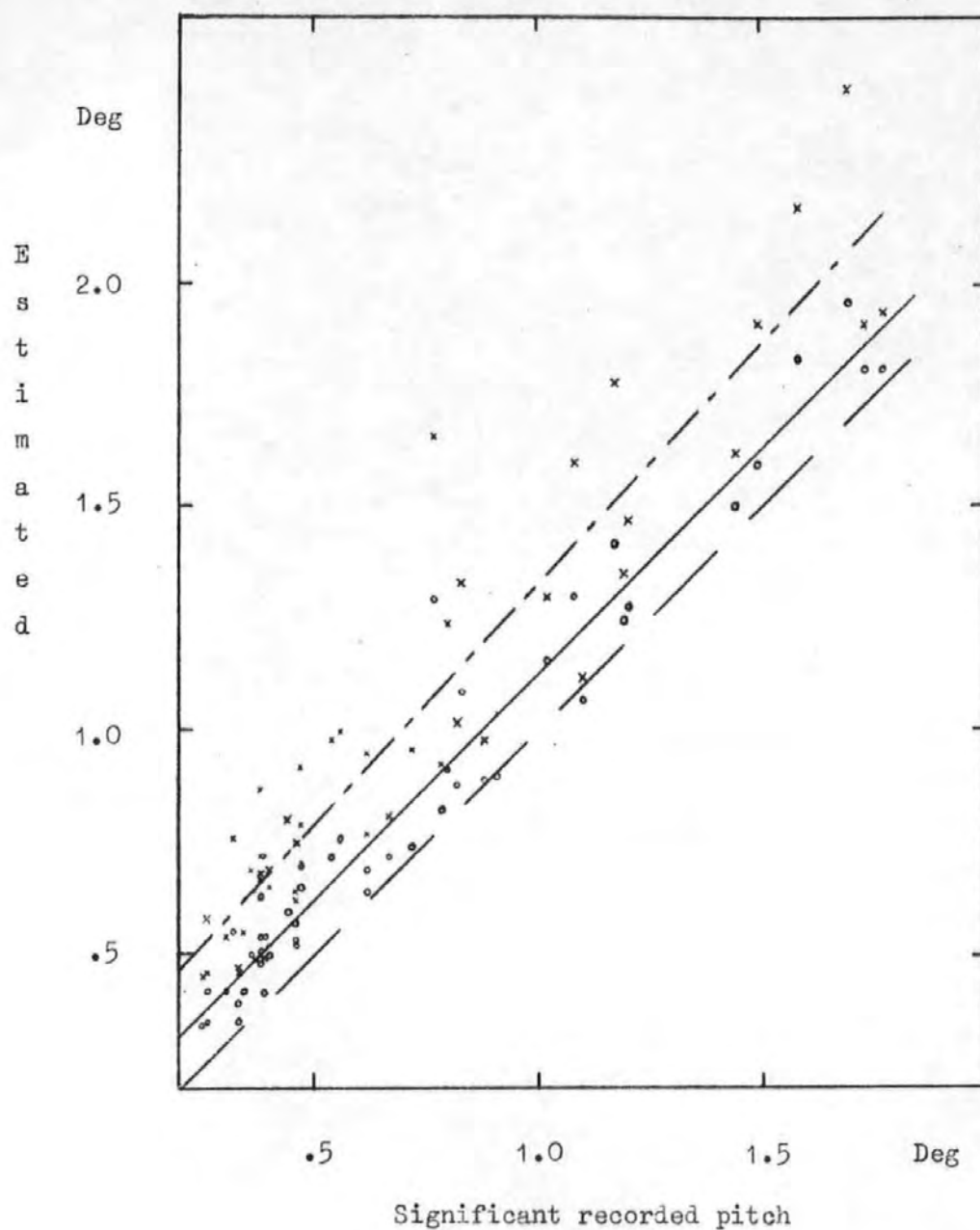


Fig. 43

Recorded significant pitch versus estimated from the spectrum method, with regression lines X = without, O = with adjustment for spread.

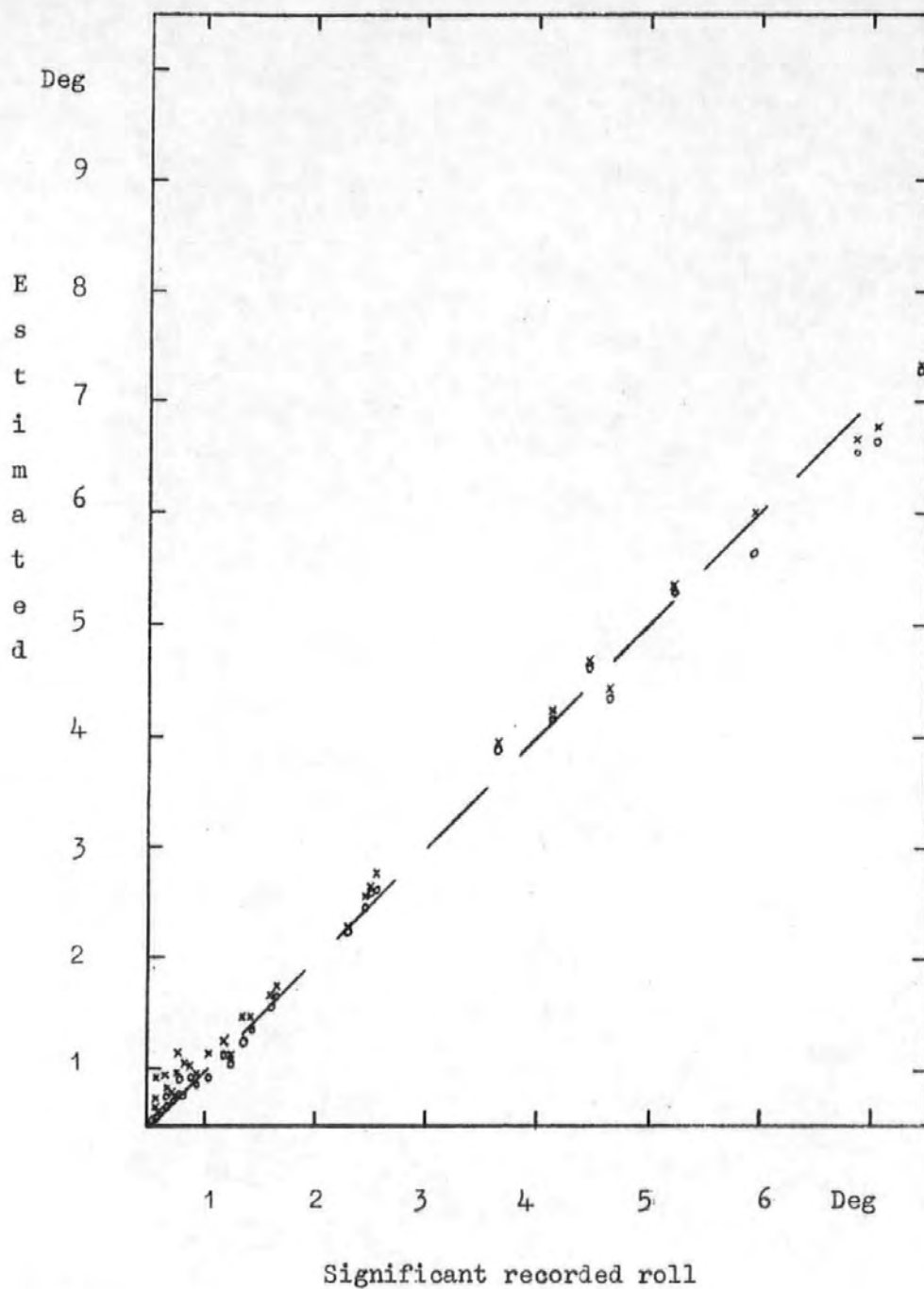


Fig. 44

Recorded significant roll versus estimated from the manual method

X = without, O = with adjustment for spread.

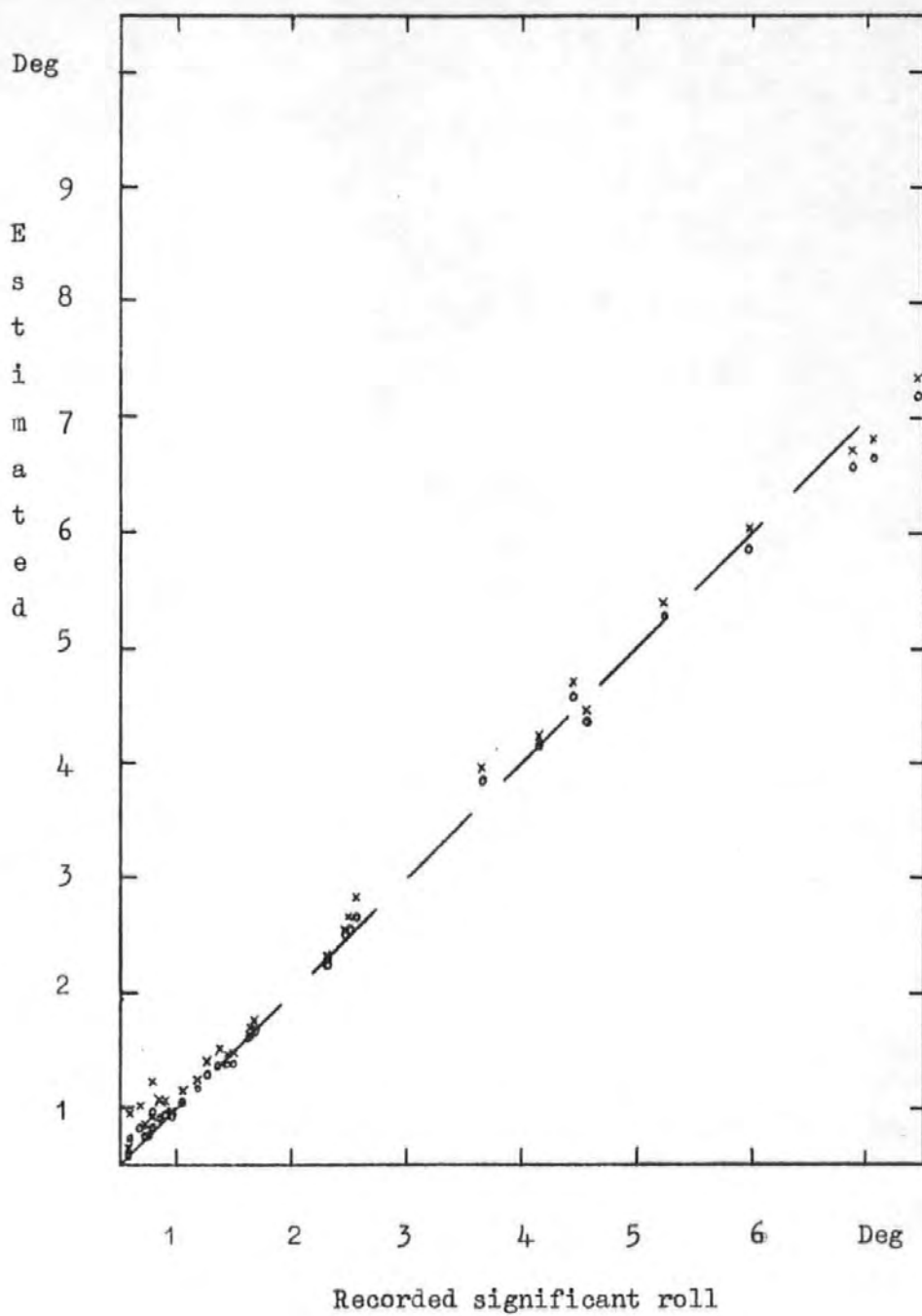


Fig. 45

Recorded significant roll versus estimated from the spectrum method

X = without, O = with adjustment for spread.

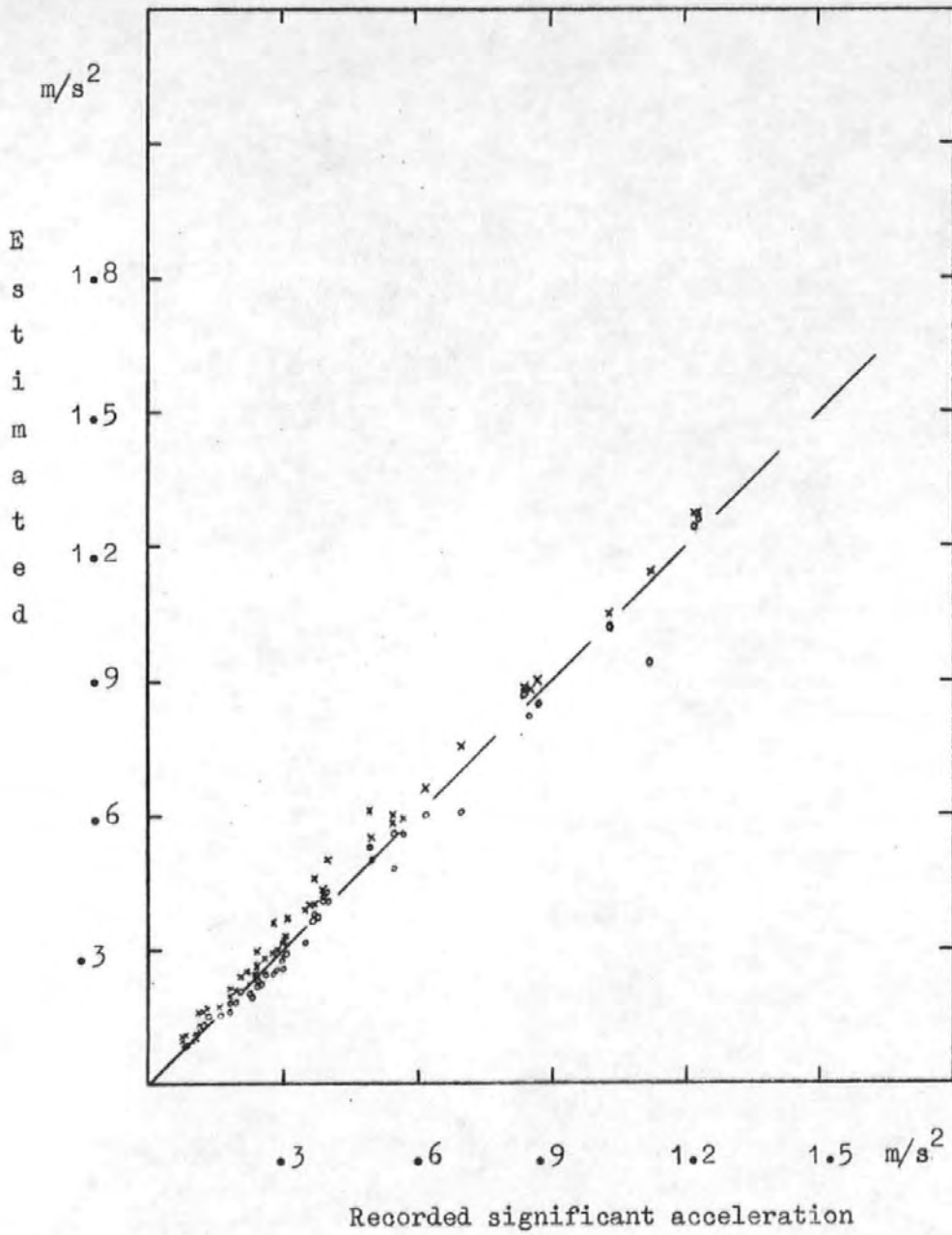


Fig. 46

Recorded significant acc. eng. versus estimated from the manual method

X = without, O = with adjustment for spread.



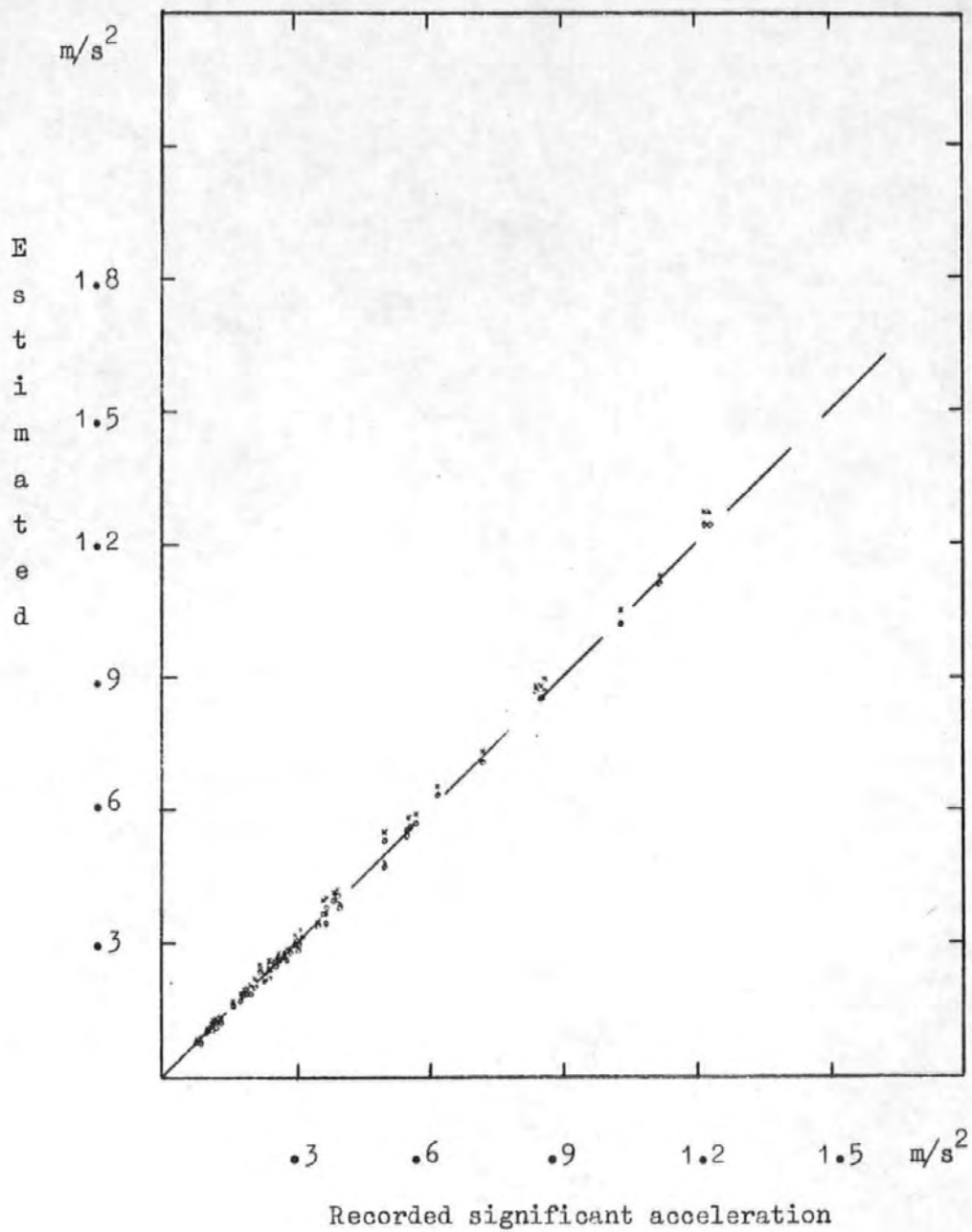


Fig. 47

Recorded significant acc. eng. versus estimated from the spectrum method

X = without, O = with adjustment for spread.

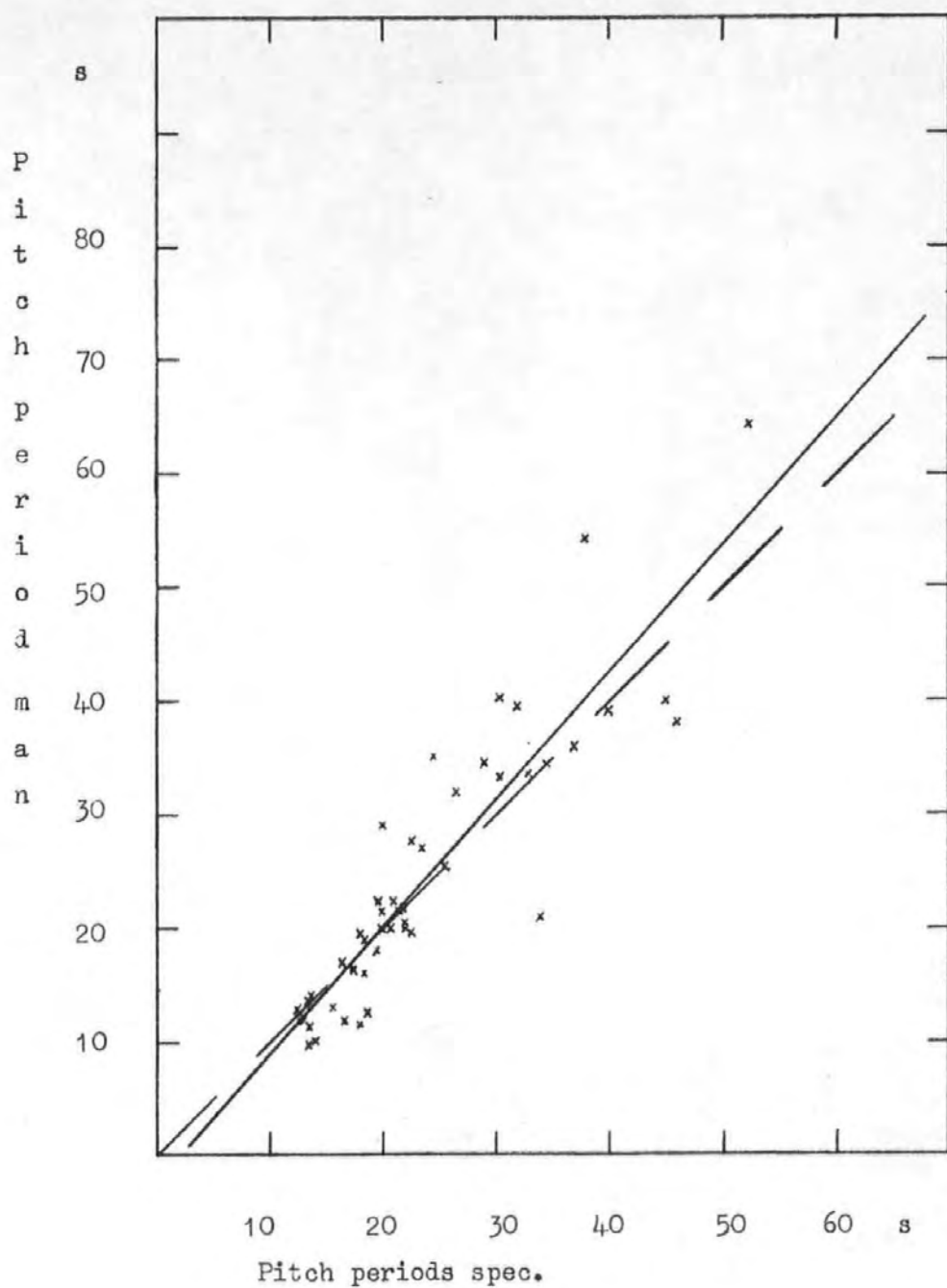


Fig. 48

Pitch periods obtained from spectrum analysis versus manual method with regression line.

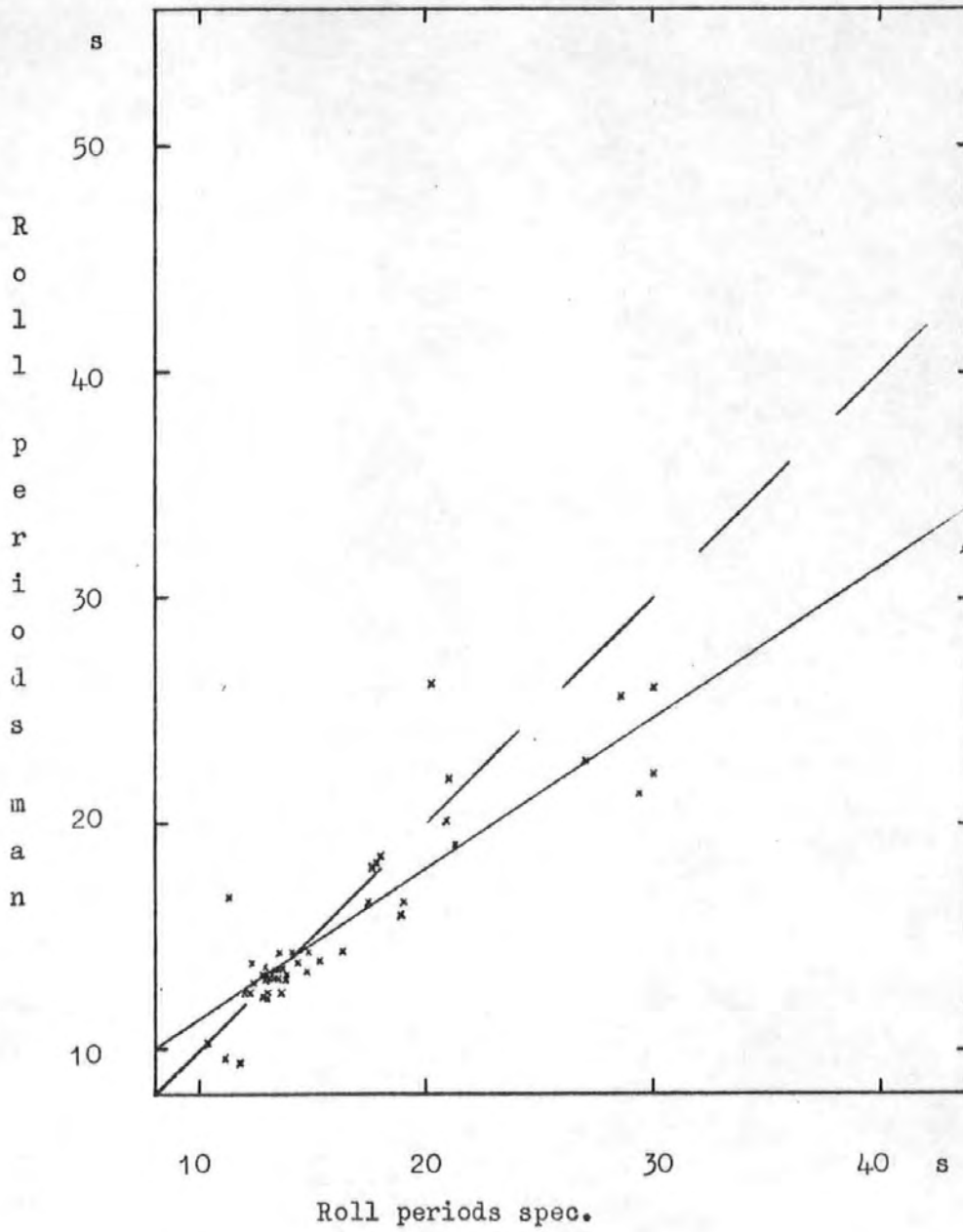


Fig. 49

Roll periods obtained from spectrum analysis versus manual method with regression line.

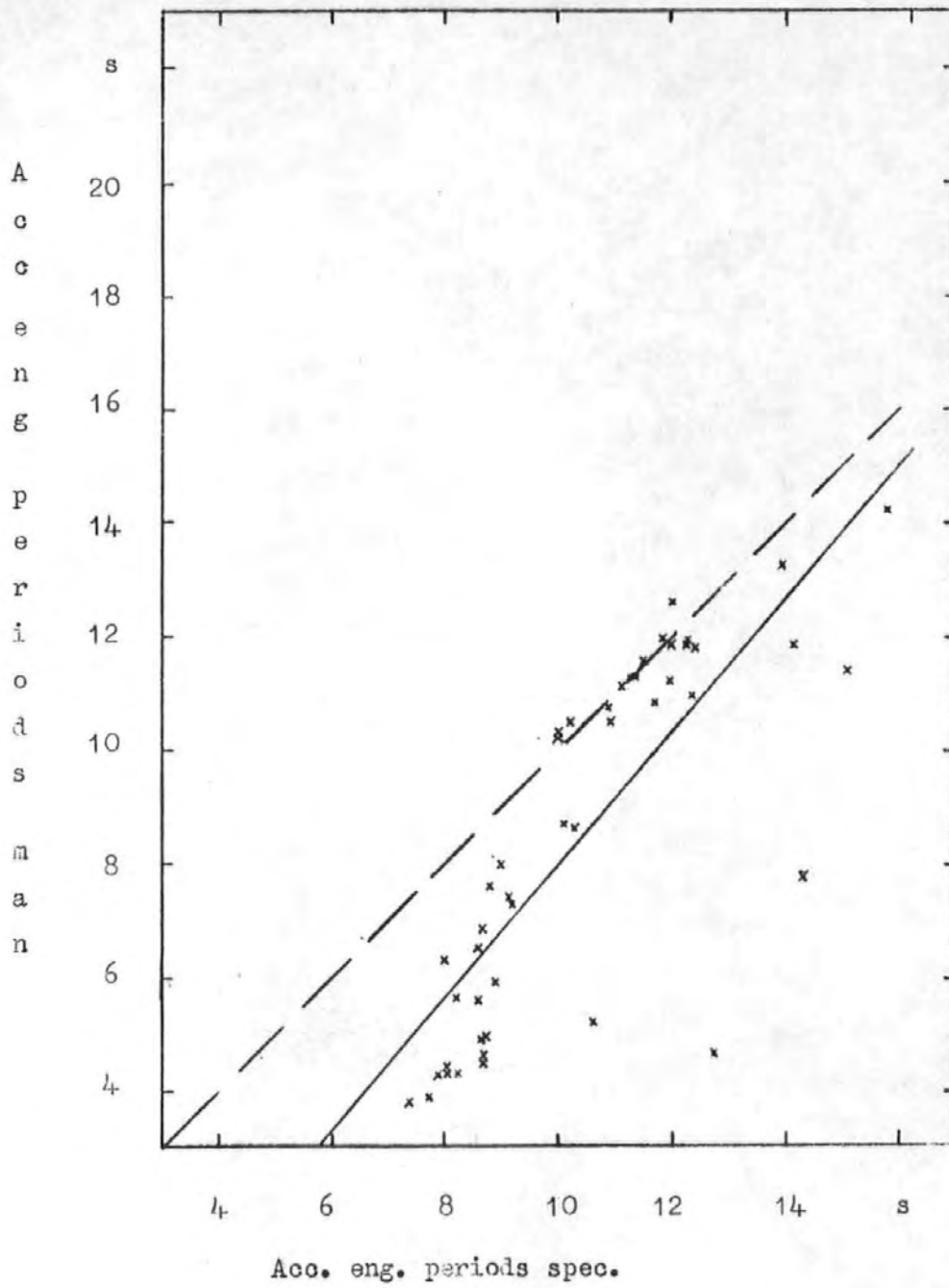


Fig. 50

Acc. eng. periods obtained from spectrum analysis versus manual method with regression line.

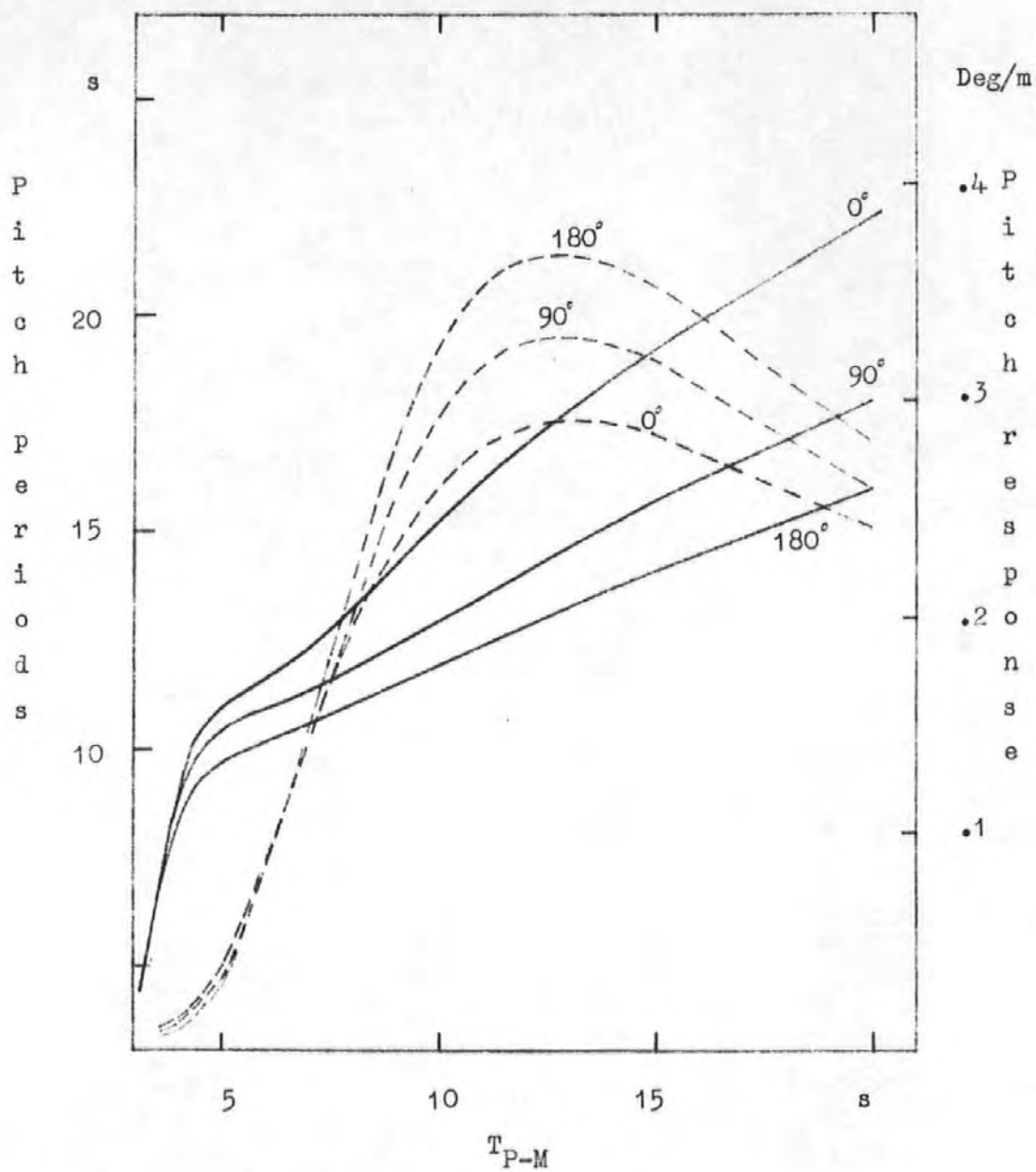


Fig. 51

Pitch responses, broken lines and pitch periods, solid lines for full load, 14 knots and spread function 2.

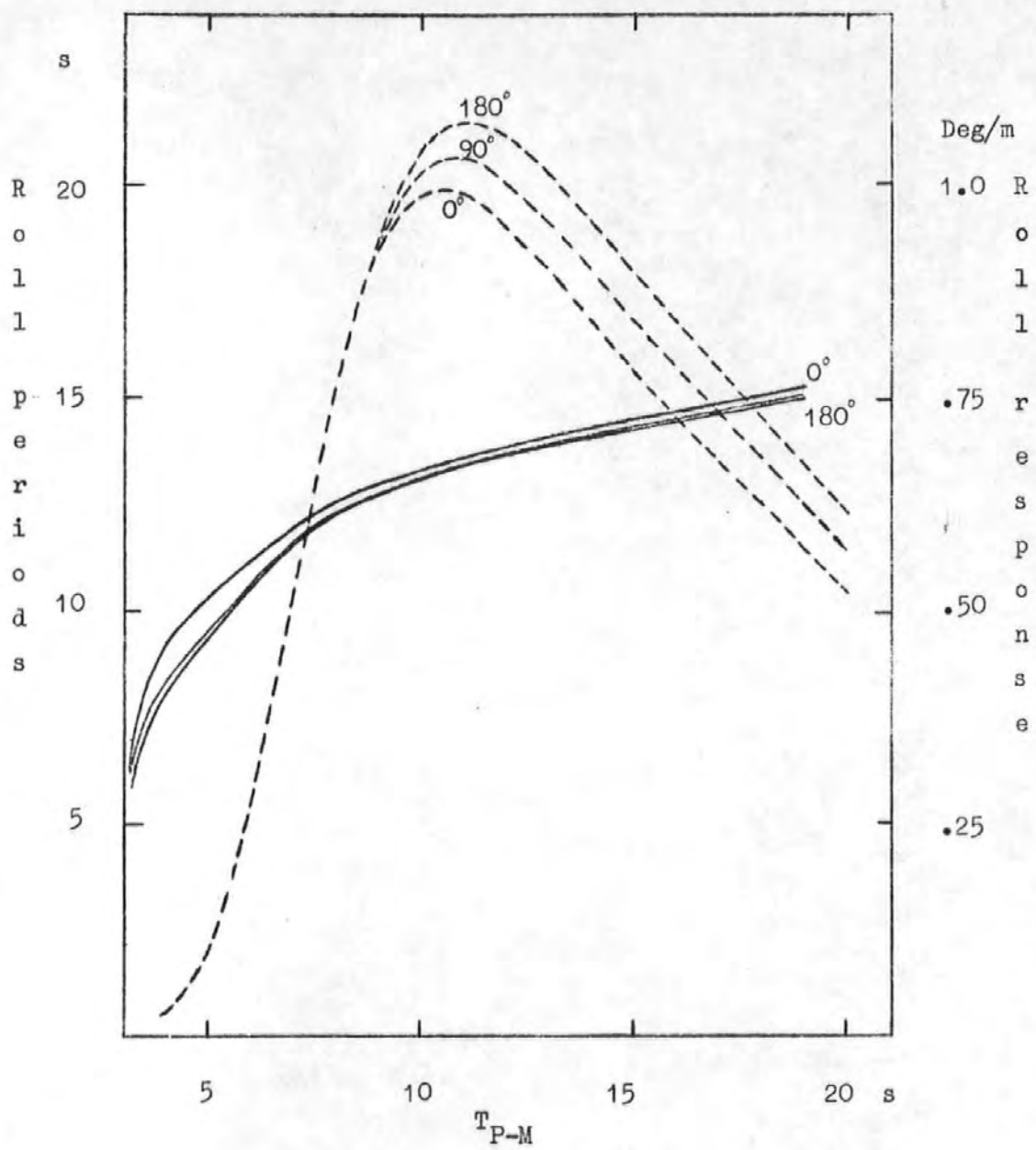


Fig. 52

Roll responses, broken lines, and roll periods, solid lines, for full load, 14 knots and spread function 2.

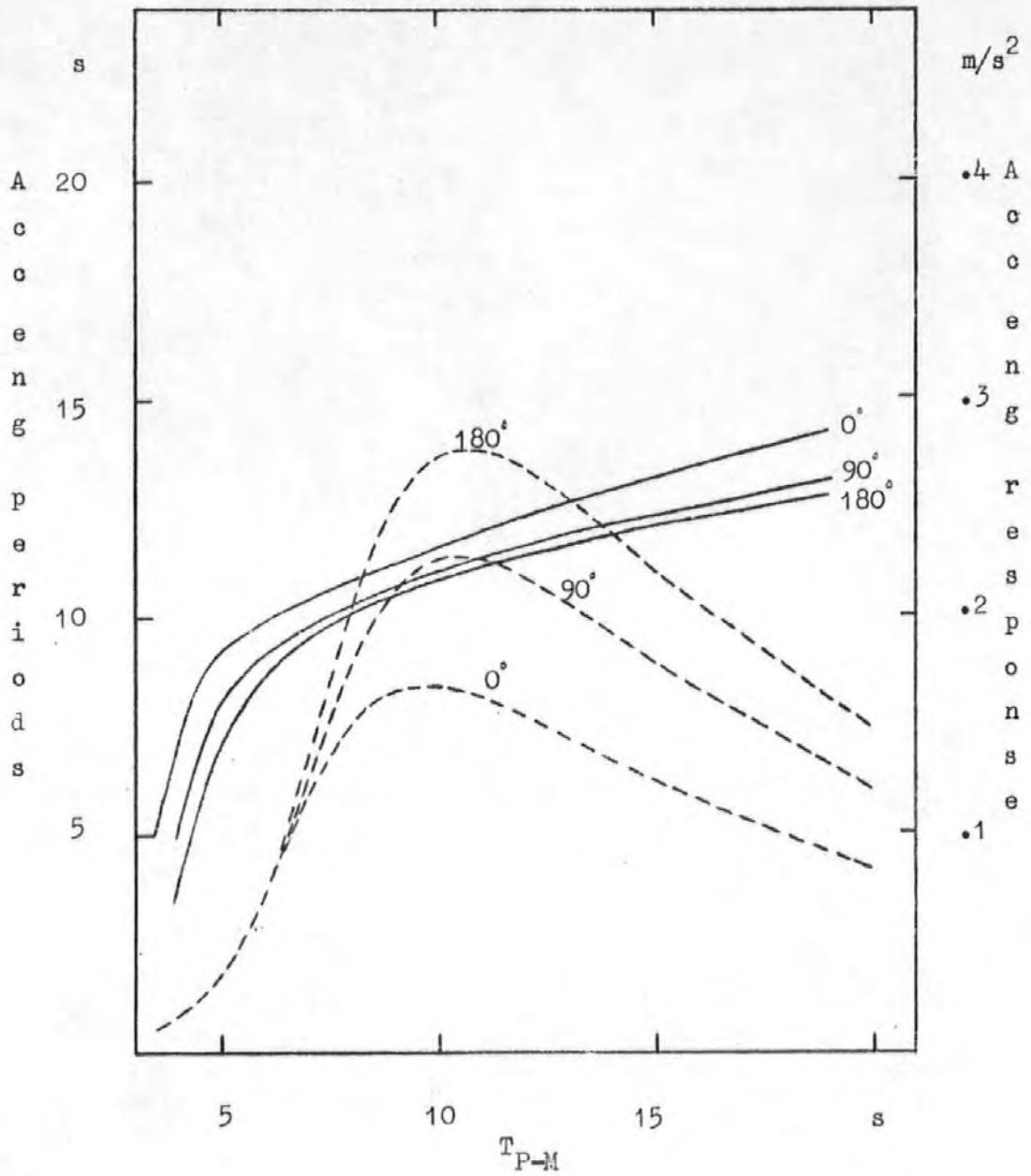


Fig. 53

Acc. eng. responses, broken lines, and acc. eng. periods, solid lines, for full load. 14 knots and spread function 2.

that some of the measured periods are outside the range of the theoretical values. For the pitch signal some very long periods were registered, surprisingly enough for head sea, but in most of these cases the amplitude of signal was small. An inspection of the signal shows that it mainly consists of values remaining constant at one or two quantization levels for a long time interrupted by the occasional zero-crossing. The "manual" method of analysis of such a signal gives a long mean period with large standard deviation, whereas the spectrum analysis results in most of the spectrum area close to  $\omega = 0$ . It is doubtful whether such a signal should be regarded as a registration of the pitch response or just small fluctuations in the instrumentation system. It is also difficult to explain periods of 40-50 seconds. For roll there were also some long periods registered and much the same arguments as for pitch can be used to explain this. Within the range of the theoretical periods the agreement between the two methods was good. For the signal of vertical acceleration in the engine room two features stand out. Firstly, some four or five values are estimated very differently by the two methods. But, here again, those are from records with very small amplitude and may be disregarded. Secondly, it can be seen that in the range of 10-14 seconds the agreement between the two methods is good, whereas for periods less than 10 the spectrum analysis method gives estimates of periods which are longer than that of the "manual" method. This is probably due to contributions of vibrations to the signal causing zero-crossing periods of 2-3 seconds to be registered by the manual method. By the truncation of the high frequency tail of the response spectrum these components are eliminated



by the spectrum method. Use of digital filtering of the signal before analysis would probably have given closer agreement for signals of short periods. As the theoretical calculations of response periods do not take vibrations into account, it was felt justifiable to take the results obtained from the spectrum method as being the most representative of the response periods. Hence the following investigation of cross predictions has been made with the results obtained from the spectrum analysis method.

#### Estimation of one response from another

The values of significant response and response periods obtained from the spectrum analysis of the records were used to determine the equivalent wave spectrum of Pierson-Moskowitz type as outlined in Chapter 3. Thus, the response period was used to find the mean wave period  $T_{P-M}$  of the wave spectrum and from the significant response value the significant wave height  $H_{1/3}$  was calculated.

The parameters affecting the theoretical calculations are the loading conditions, ship speed, wave direction and directional spread. In order to compare the theoretical results with the recorded the same parameters must be determined for the recordings. Of these, the loading condition is known and ship speed found from the ship's instruments, leaving wave direction and spread to be estimated, as no wave data was recorded by the instrumentation.

#### Wave direction and spread

Visual observations of the sea with respect to wave height, period and direction were made by the crew and recorded on a log-sheet. The instrumentation operated automatically and recorded for about twenty minutes every twelve hours. Every second recording was made at night and no corresponding visual observations were made for these.

For this investigation only the wave direction was of interest.

Because half the number of recordings were without visual observations and it was of interest to try an approach not using visual data, the wave direction was instead estimated from the measured wind direction. The mean values from the recorded ship speed, relative wind direction and relative wind speed were thus combined to give mean absolute wind direction and speed. It was then simply assumed that the wave direction was the same as the wind direction, even though this may not always be true in reality. Light varying winds may, for example, exist, together with heavy swell from a previous storm or fresh strong winds may build up over a wavefield travelling in another direction. This simplified definition of wave direction may thus have introduced errors of unknown quantity. Comparison with the observed wave directions did, however, generally give a good agreement, even though examples were found for which the "defined" following sea was observed as head sea. Which one of these is correct is impossible to say, but it is well known that it can be difficult for an observer on a moving ship to distinguish between following sea and head sea when the sea is moderate and no breakers are present. The wind speeds and wind directions for the analysed records are tabulated below. The directions are grouped into 7 classes with intervals of  $30^{\circ}$  and so that direction 1 is following wind,  $\pm 15^{\circ}$  and direction 7 is head wind,  $165^{\circ} - 195^{\circ}$ .

Table 5.3

Distribution of wind speeds and wind directions for the analysed records

1 = following wind

7 = head wind

Direction

7	1								
6									1 <sup>(3)</sup>
5						1 <sup>(2)</sup>			
4		1							
3				1					
2		4	7 <sup>(1)</sup>	4	1				
1									

FULL

LOAD

Ship

Speed:

12 knots

7			3	1	1	1			
6			1	5	2	1			
5		1							
4			1						
3			1 <sup>(4)</sup>						
2			1 <sup>(4)</sup>	2 <sup>(4)</sup>					
1		1 <sup>(4)</sup>		1 <sup>(4)</sup>					

BALLAST

Ship

Speed:

14 knots

Wind  
Speed

0    5    10    15    20    25    30    35    40 knots

(1) Ship speed in one case 10 knots

(2) Ship speed : 9 knots

(3) Ship speed: 7 knots

(4) Ship speed: 16 knots

As seen from the table the predominant wind direction was following for the laden voyage and head for the ballast voyage. In order to minimize the errors which may have been introduced by assuming the wave direction being the same as that of the wind, the directional spread has been assumed to be according to spread function 2, i.e. the widest spread.

The ratios of the measured pitch and roll values were also calculated in the hope of using these as indication of the wave direction, high values indicating head or following sea and low values beam sea. This attempt was, however, not fruitful as the theoretically calculated values are dependent on the mean wave period, which in turn only can be determined when the heading is known.

Thus, the results described in the following have been obtained using spread function 2 and assuming wind and wave directions to be the same.

#### Wave height and period of the equivalent spectrum

For each record the three responses - pitch motion, roll motion and vertical acceleration in the engine room were compared with respect to significant value and period to the theoretically calculated values and the two parameters significant wave height  $H_{1/3}$  and mean wave period  $T_{P-M}$  for the equivalent spectrum were determined. It was not expected that the three responses would yield the same wave spectrum as their receptance to various wave components are different. None of the spectra defined by the responses in this way should be assumed to be the true spectrum at the time of the recording, but merely equivalent spectra of Pierson-Moskowitz type and nothing but theoretical substitutes. The actual wave spectrum may, naturally, be very different in shape to that of the P-M type. Figures (54-57) show the significant wave heights and mean periods derived from the

three responses. They are plotted for comparison in such a way that values obtained from pitch are along the X-axis and those from roll and acc. eng. along the y-axis.

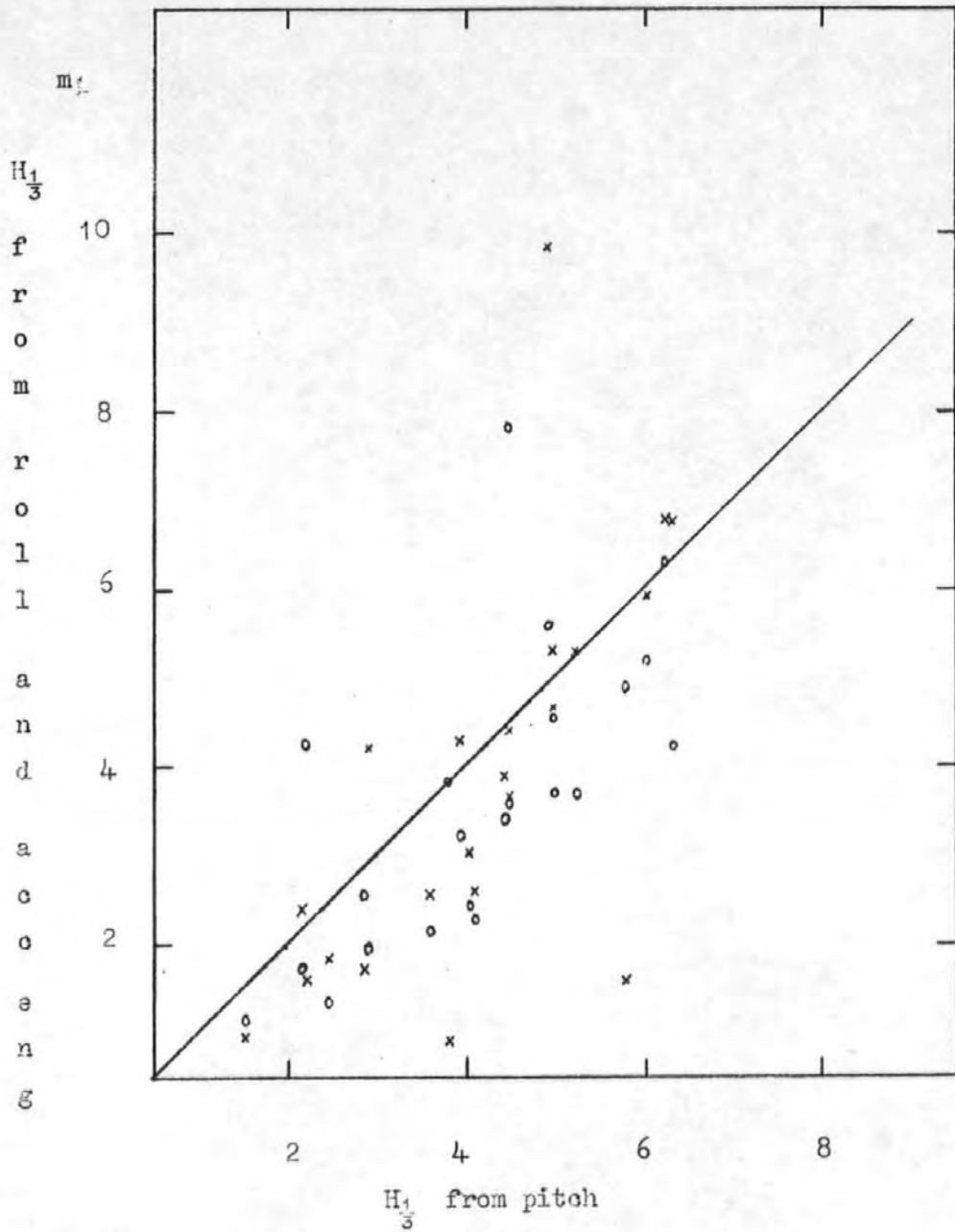


Fig. 54

Significant wave heights of the equivalent spectra obtained from pitch versus heights from roll = X and acc. eng. = 0. Full load.

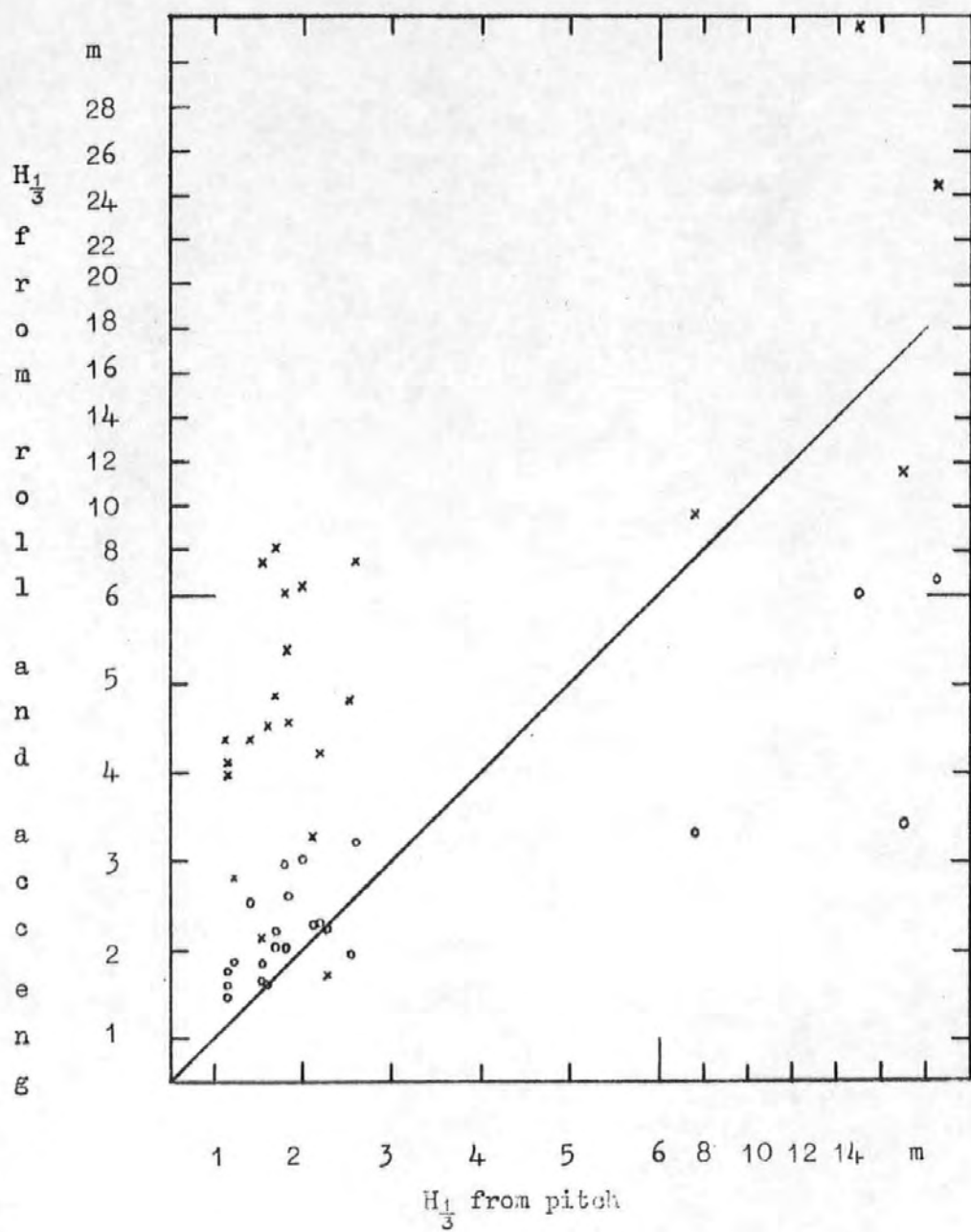


Fig. 55

Significant wave heights of the equivalent spectra obtained from pitch versus heights from roll = X and acc. eng. = 0 Ballast.

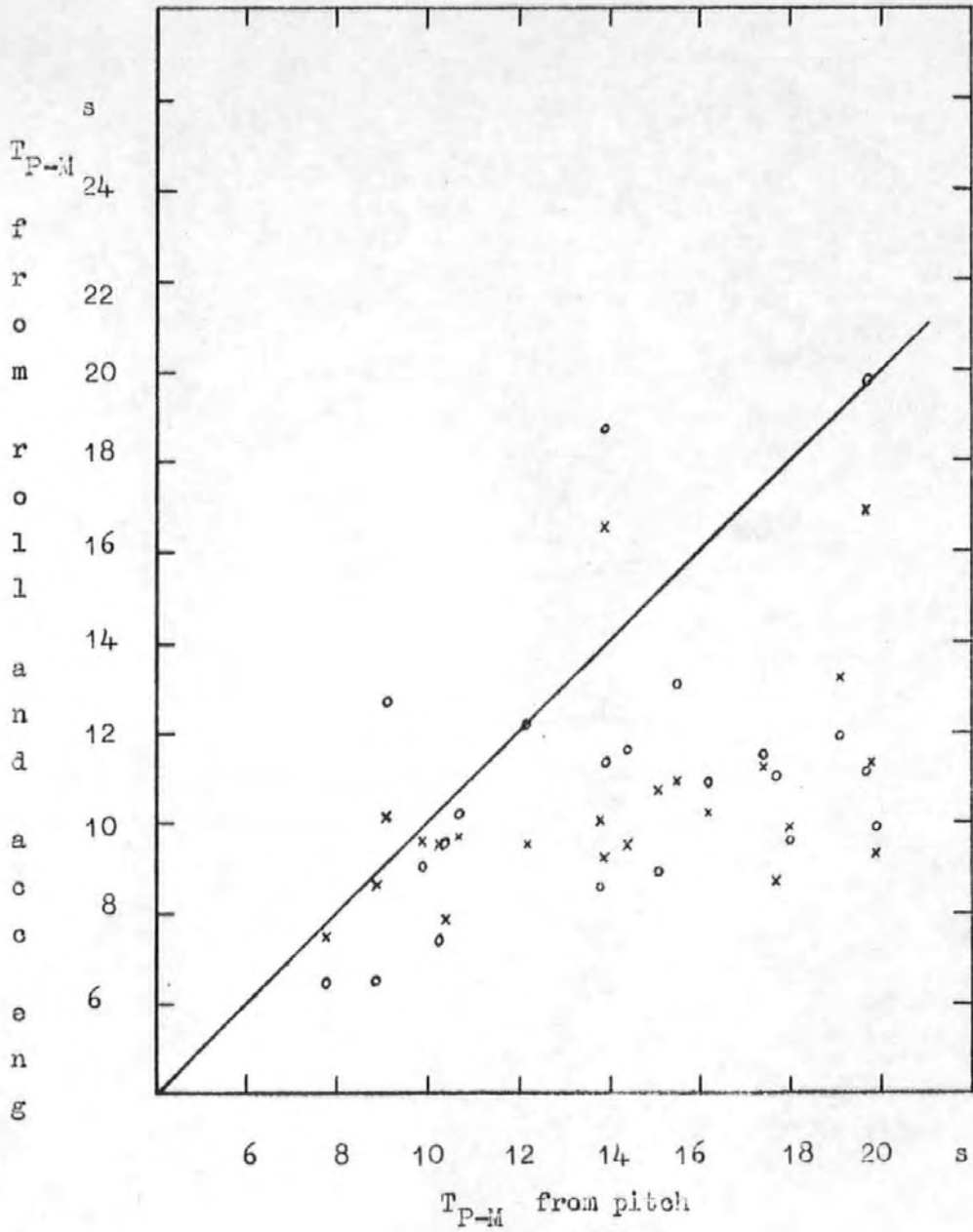


Fig. 56

Mean wave periods of the equivalent wave spectrum obtained from pitch versus periods from roll = X and acc. eng. = 0. Full load.



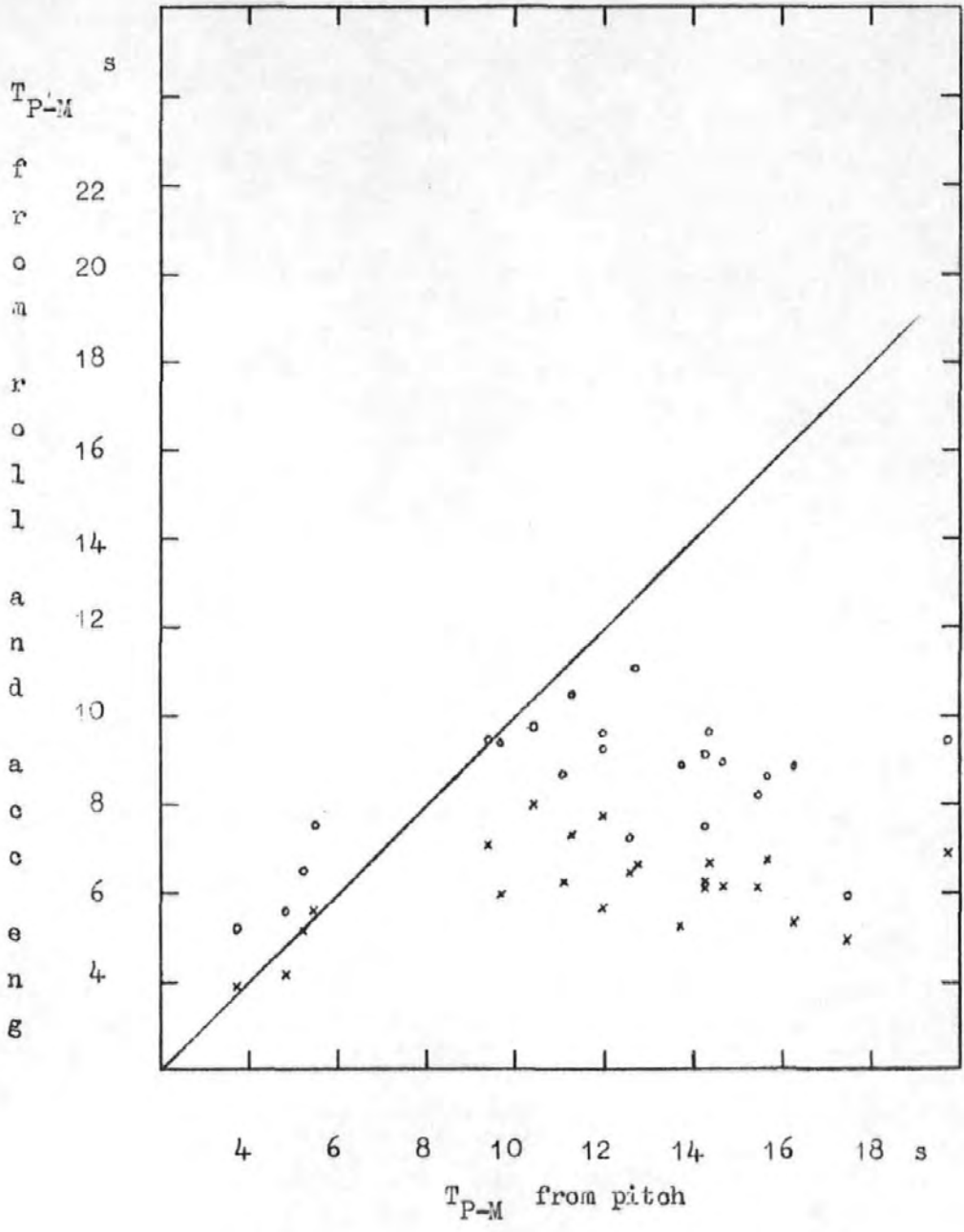


Fig. 57

Mean wave periods of the equivalent wave spectrum obtained from pitch versus periods from roll = X and acc. eng. = O. Ballast.

### Sensitivity to response periods in estimating wave heights

From figures (51-53) it can be seen that the slope of the curves representing response periods are levelling out to a relatively small value after the initial rise. For parts of the area where the slope is small, the slope of the curves representing significant response value per unit significant wave height is large. This has the effect that a small error in the measured mean response period, i.e. a small difference on the vertical scale, has a relatively larger effect on the horizontal scale, affecting the two parameters which are to be estimated, i.e. the mean spectrum period and the response value. The wave height of the equivalent wave spectrum is derived by division of the measured value by the value from the graph, so that

$$H_{1/3} = R_M / R_T$$

where  $R_M$  = measured response

and  $R_T$  = theoretical response value per unit wave height

As the significant wave height derived in this way is inversely proportional to  $R_T$  it will be affected by differences in  $R_T$ .

This is illustrated graphically in figures (58-60) in such a way that for any response period, along the horizontal axis, the effect in metres per second difference error, in the measured response period, per unit response value, can be found at the vertical axis. Hence the vertical scale is denoted

$$\Delta m / \Delta T_R R_{1/3}$$

where  $\Delta T_R$  = error in measured response period

$R_{1/3}$  = measured significant response value

and  $\Delta m$  = difference in wave height

For example, assume measured significant pitch angle is  $2^\circ$  and mean pitch period is 13 seconds in following sea. Then from figure (58):  
 $\Delta m / \Delta T_p P_{1/3} = 0.8$  for  $T_p = 13$  seconds so that the difference in the estimated wave height is  $\Delta m = 0.8 \times 2 = 1.6\text{m}$  per second deviation in the recorded response period.

It can be seen from the figures that for response periods for pitch and roll less than about 12 seconds, the estimated wave height becomes uncertain, whereas no such obvious lower limit is found for acceleration. In fact, none of the analysed records had to be discarded due to critically small response periods.

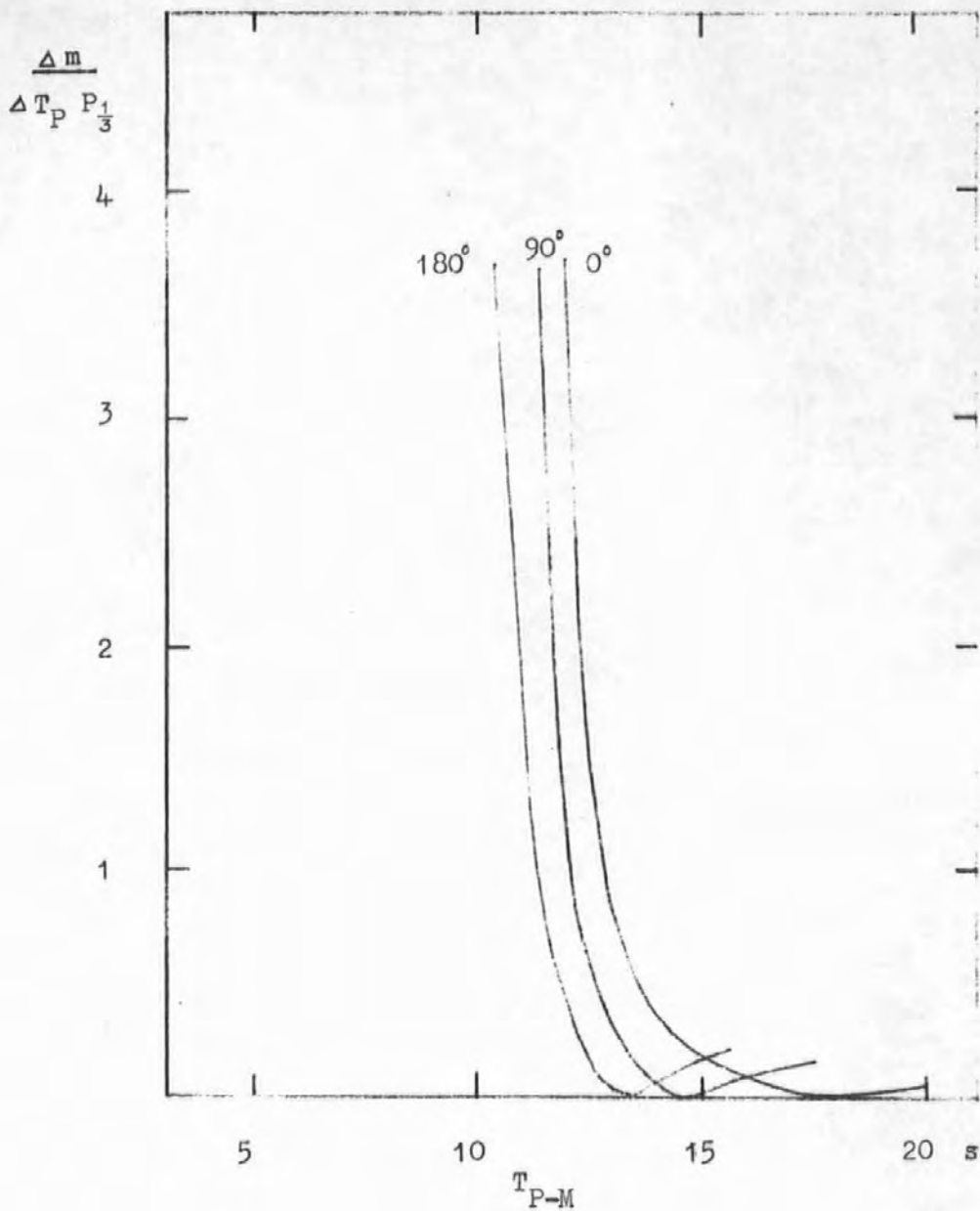


Fig. 58

Sensitivity of pitch to errors in the recorded pitch period. Full load 14 knots.

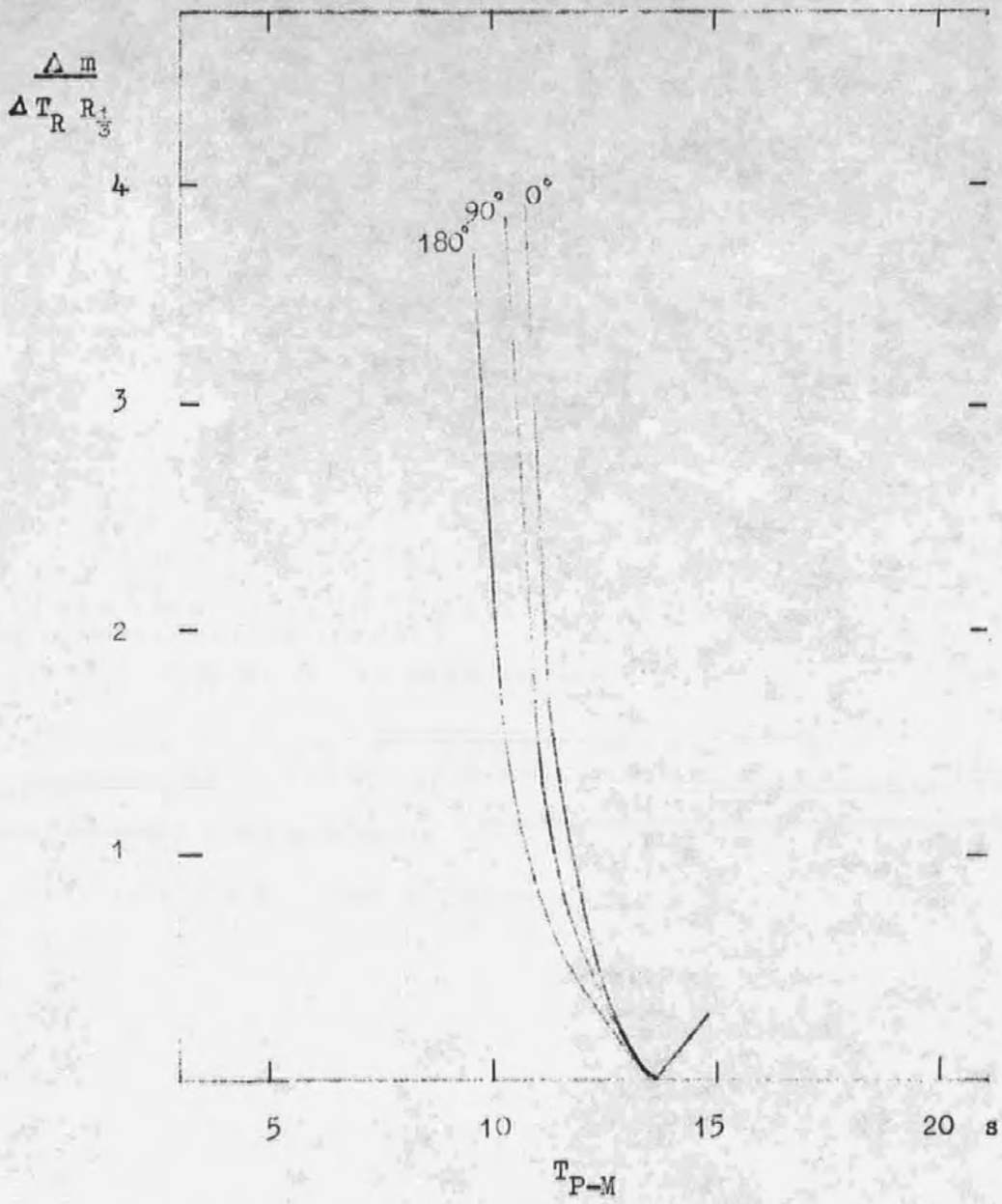


Fig. 59

Sensitivity of roll to errors in the recorded roll period. Full load, 14 knots.

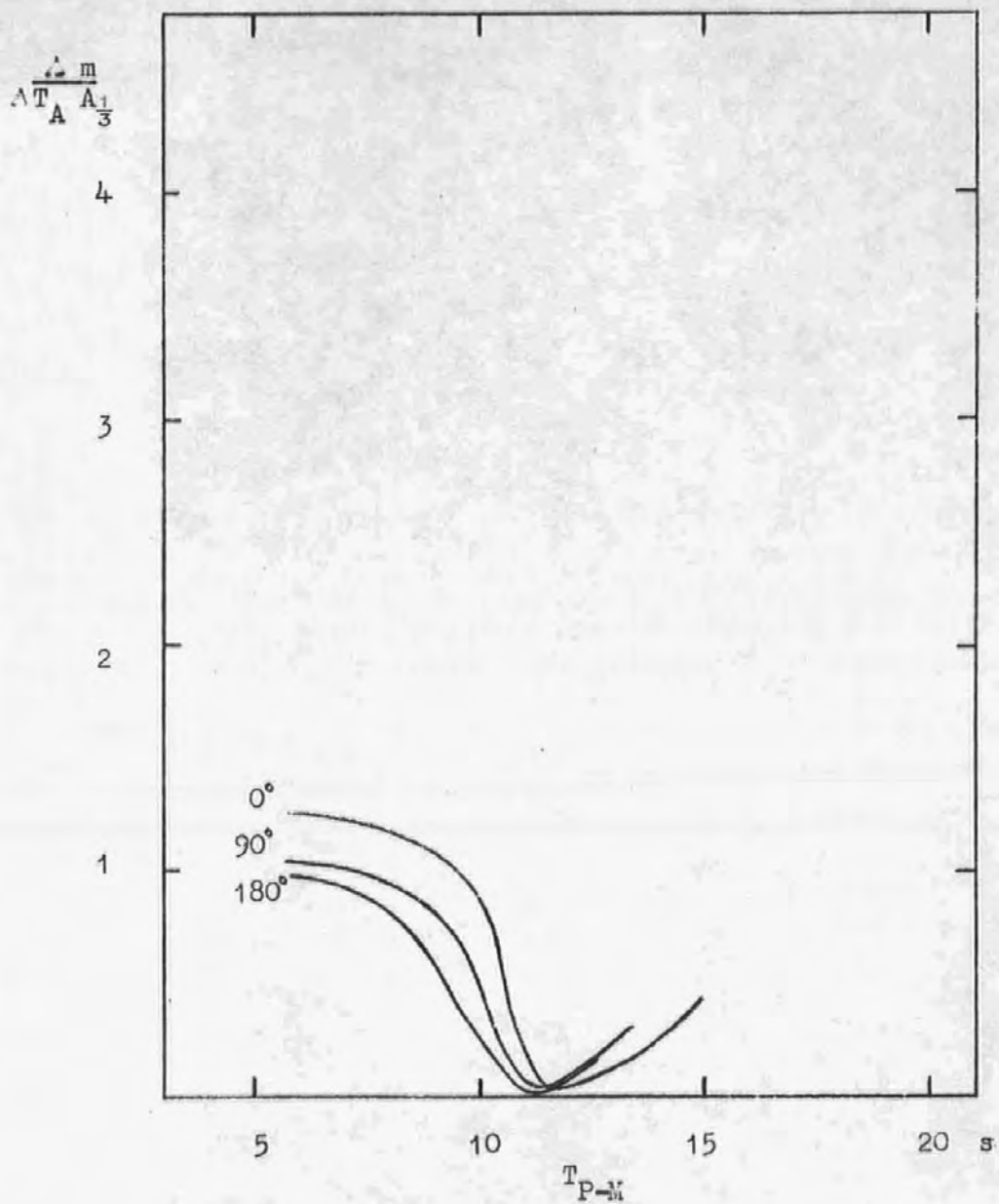


Fig. 60

Sensitivity of acc. eng. to errors in the recorded acc. eng. period.

Full load, 14 knots.

### Comparison of measured and predicted values

The measured significant response value for any one response was compared to those predicted from each of the other two responses. For example, the equivalent spectra derived from the roll motion was used to estimate the pitch motion in such a wave spectrum. The estimated values were then compared to the measured value. In figures (61-66) these comparisons are plotted with the measured quantity along the X-axis and the two estimated values along the y-axis. The values are from all headings and speeds as listed in Table 5.3 . In all figures the solid lines are the regression line and the associated 95% confidence lines for the crosses, and the broken lines are the corresponding for the circles. Even though the measured quantity is along the horizontal axis it was used as the dependent variable for the regression analysis. The horizontal distance between the regression line and the lines representing the 95% confidence limits are  $\pm 2$  x the standard error of estimates  $S_e$ . The regression lines, coefficients of determination and standard error of estimates for figures (61-66) are listed in Table 5.4 below. It can be seen that predictions between pitch and acc. eng. are generally more reliable than any estimate of roll. This is probably due to the fact that vertical acceleration and pitch motion are closer correlated than the roll motion and any of the other responses. The generally rather wide confidence bands, and especially for predictions between uncorrelated responses, raises the question of whether the method provides an improvement on the values which may be intuitively expected from the overall motion of the ship. In other words, when the angular spread of energy in the wave system is large, which has here been assumed to be the case, then one would expect a high value for one response to be associated with high

values for the others, i.e. a high correlation between different responses. In order to evaluate this assumption the correlations between the measured responses were calculated and regression analysis applied. The results from this are also included in the Table 5.5 below.

TABLE 5.4

Regression analysis for estimated and measured values

Regression line : Measured value = a Estimated + b

Coefficient of determination :  $r^2$

Standard error of estimate :  $S_e = sy \sqrt{1 - r^2}$

Measured response	Estimated from	a	b	$r^2$	$S_e$	Loading condition
Pitch	Roll	.835	-.003	.504	.370	Full
"	"	1.512	-.296	.350	.335	Ballast
"	Acc.eng.	.720	-.044	.745	.188	Full
"	" "	1.278	-.157	.725	.128	Ballast
Roll	Pitch	.453	1.723	.404	1.163	Full
"	"	.268	1.205	.343	.508	Ballast
"	Acc.eng.	.612	.987	.710	.825	Full
"	" "	.507	1.105	.504	.689	Ballast
Acc.eng.	Pitch	.861	.096	.876	.113	Full
" "	"	1.123	-.142	.760	.153	Ballast
" "	Roll	.927	.093	.574	.278	Full
" "	"	2.423	-.506	.806	.288	Ballast



TABLE 5.5

 $y = ax + b$  Regression between measured responses

Independent variable, y	Dependent variable, x	a	b	$r^2$	$S_e$	Loading condition
Roll	Pitch	3.273	-.748	.474	1.540	Full
"	"	5.234	-.792	.383	1.077	Ballast
Acc.eng.	"	.609	-.130	.614	.216	Full
" "	"	1.198	-.139	.641	.145	Ballast
" "	Roll	.118	.224	.520	.241	Full
" "	"	.158	.199	.796	.109	Ballast

From the tables it can be seen that the correlation, tabulated as coefficient of determination  $r^2$ , is generally higher between estimated and predicted values than between measured responses. The rather surprising exception is the correlation between pitch and roll, which means that the method of using equivalent wave spectrum is not an improvement compared to estimating one response from just the magnitude of the other. Figures 67 and 68 illustrate two examples, one good and one poor, of estimation by using the regression line from the method of equivalent wave spectrum, crosses, and the equation from the regression of the measured quantities, circles. The solid line represents perfect relationship and the broken lines the 95% confidence band for the crosses. The difference in accuracy between the two methods appears to be insignificant.

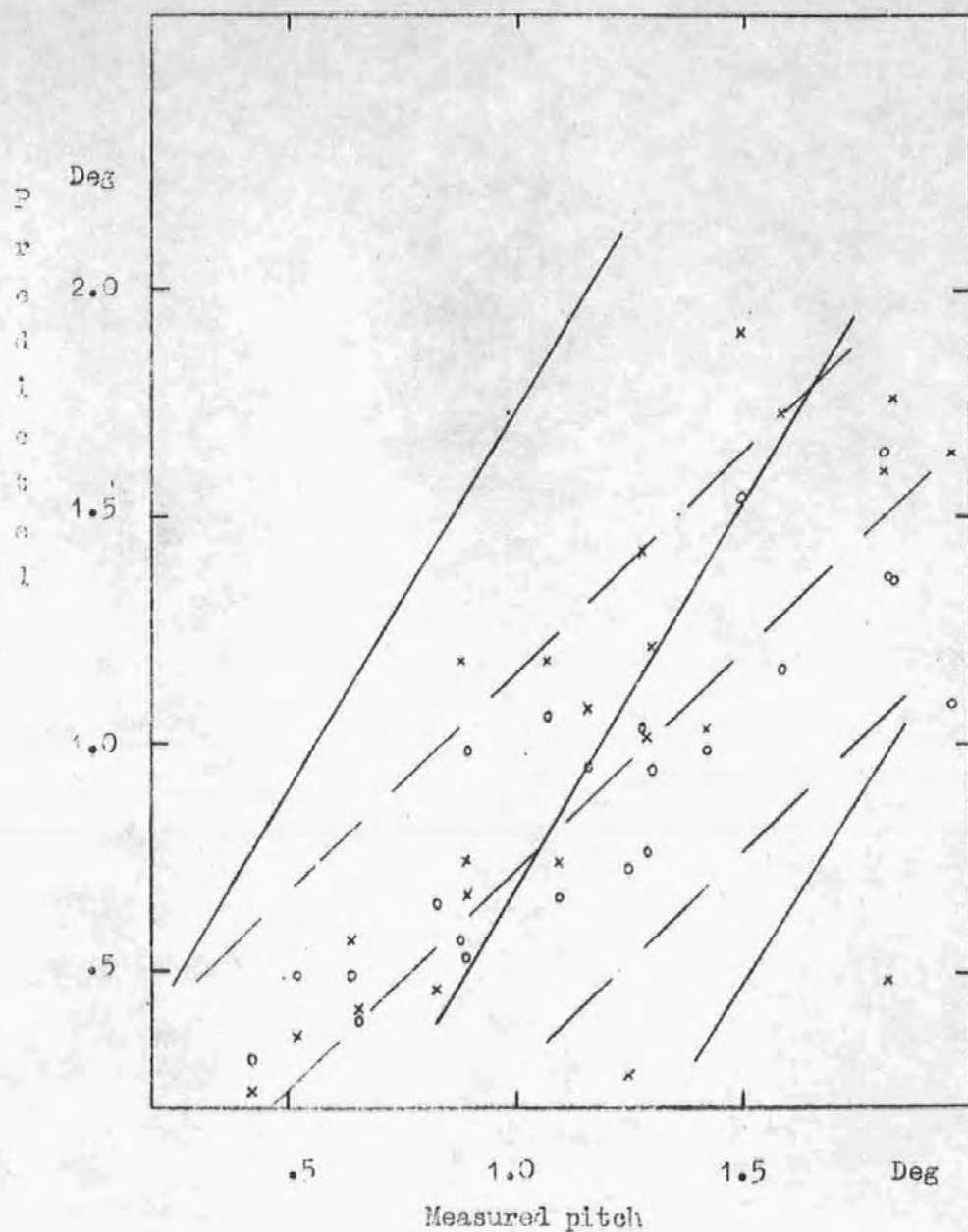


Fig. 61

Measured pitch versus predicted from roll = X and from acc. eng. = 0,  
and regression lines. Full load.

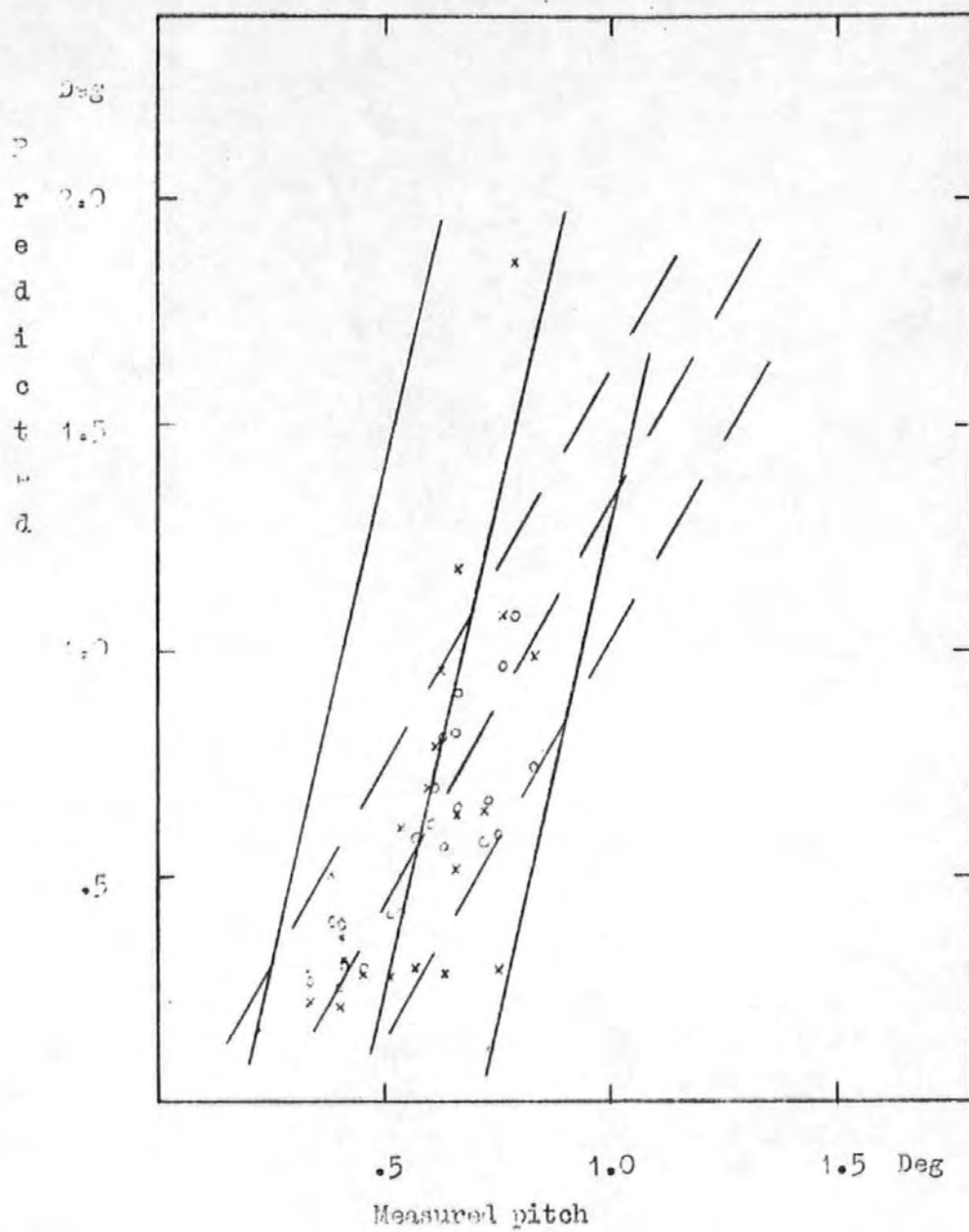


Fig. 62

Measured pitch versus predicted from roll = X and from acc. eng. = 0, and regression lines. Ballast.

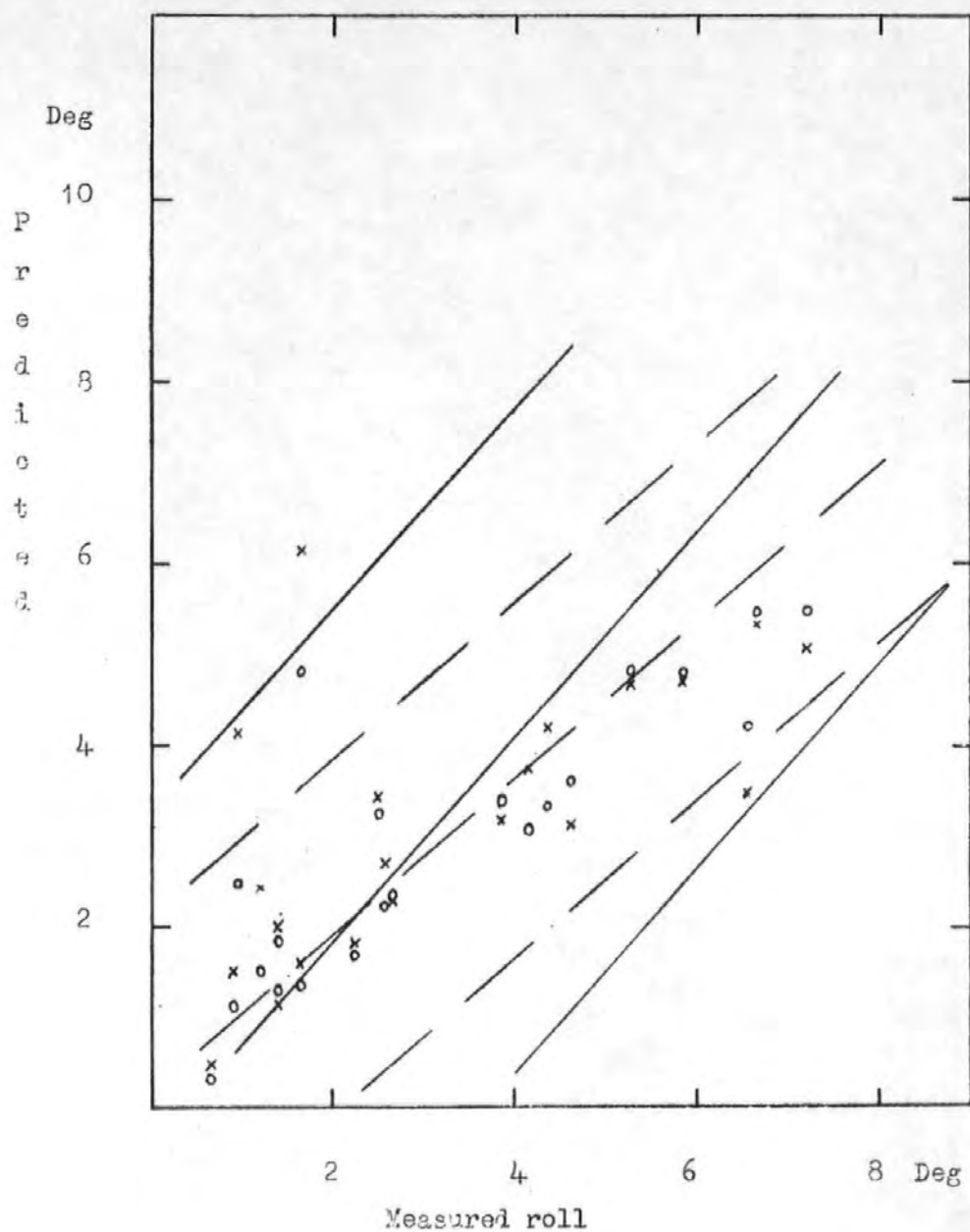


Fig. 63

Measured roll versus predicted from pitch = X and acc. eng. = 0, and regression lines. Full load.

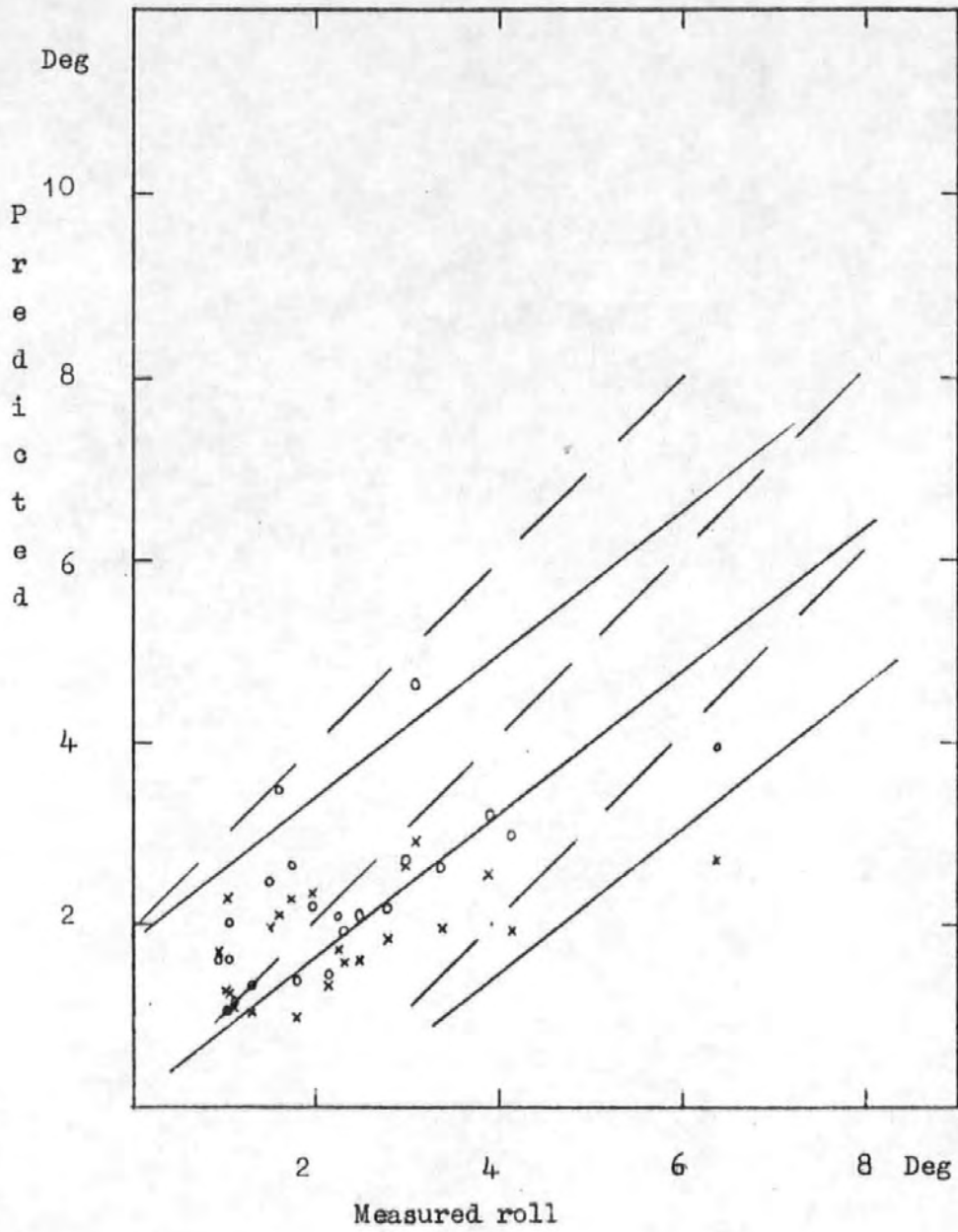


Fig. 64

Measured roll versus predicted from pitch = X and acc. eng. = 0, and regression lines. Ballast.

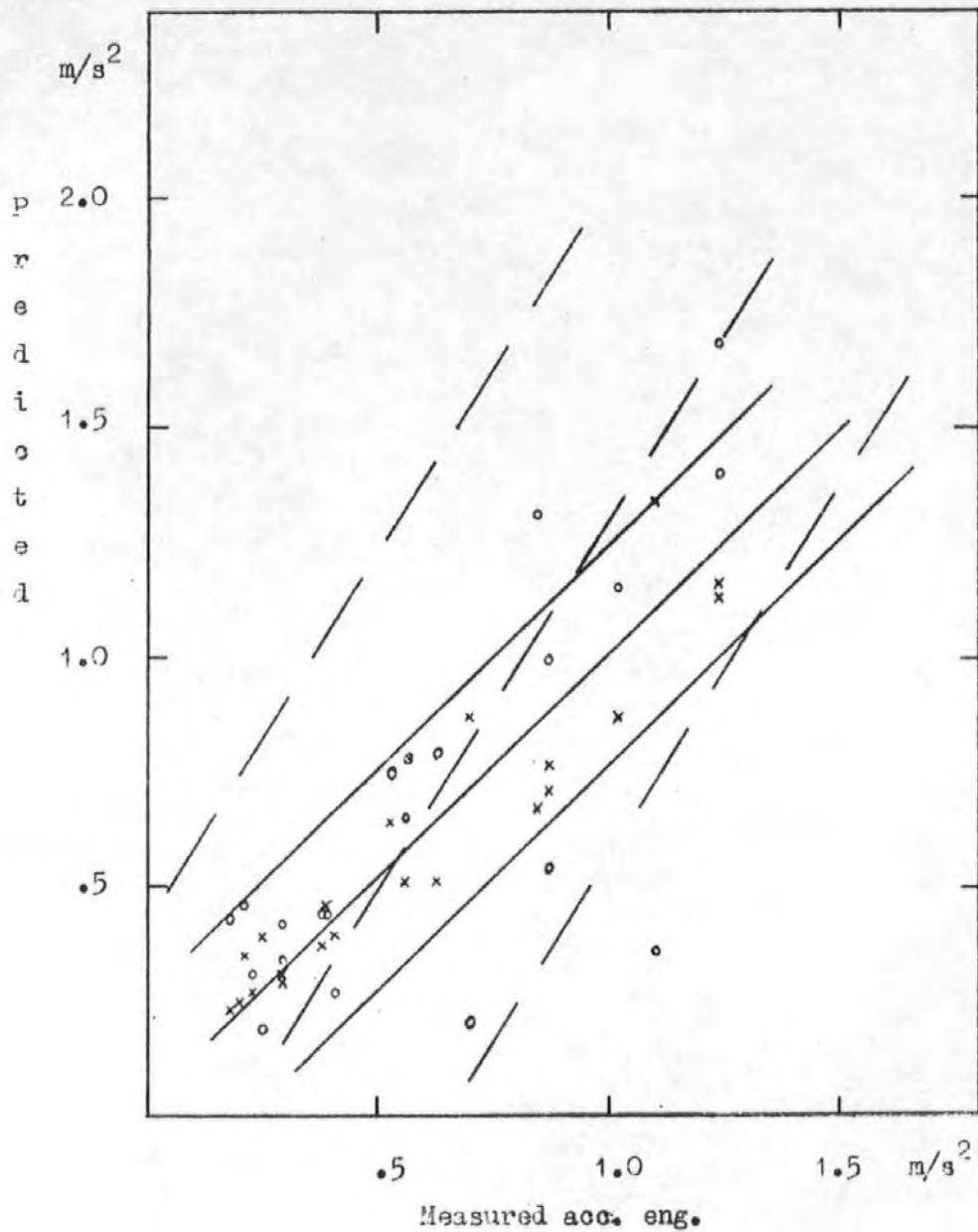


Fig. 65

Measured acc. eng. versus predicted from pitch = X and roll = 0 and regression lines. Full load.

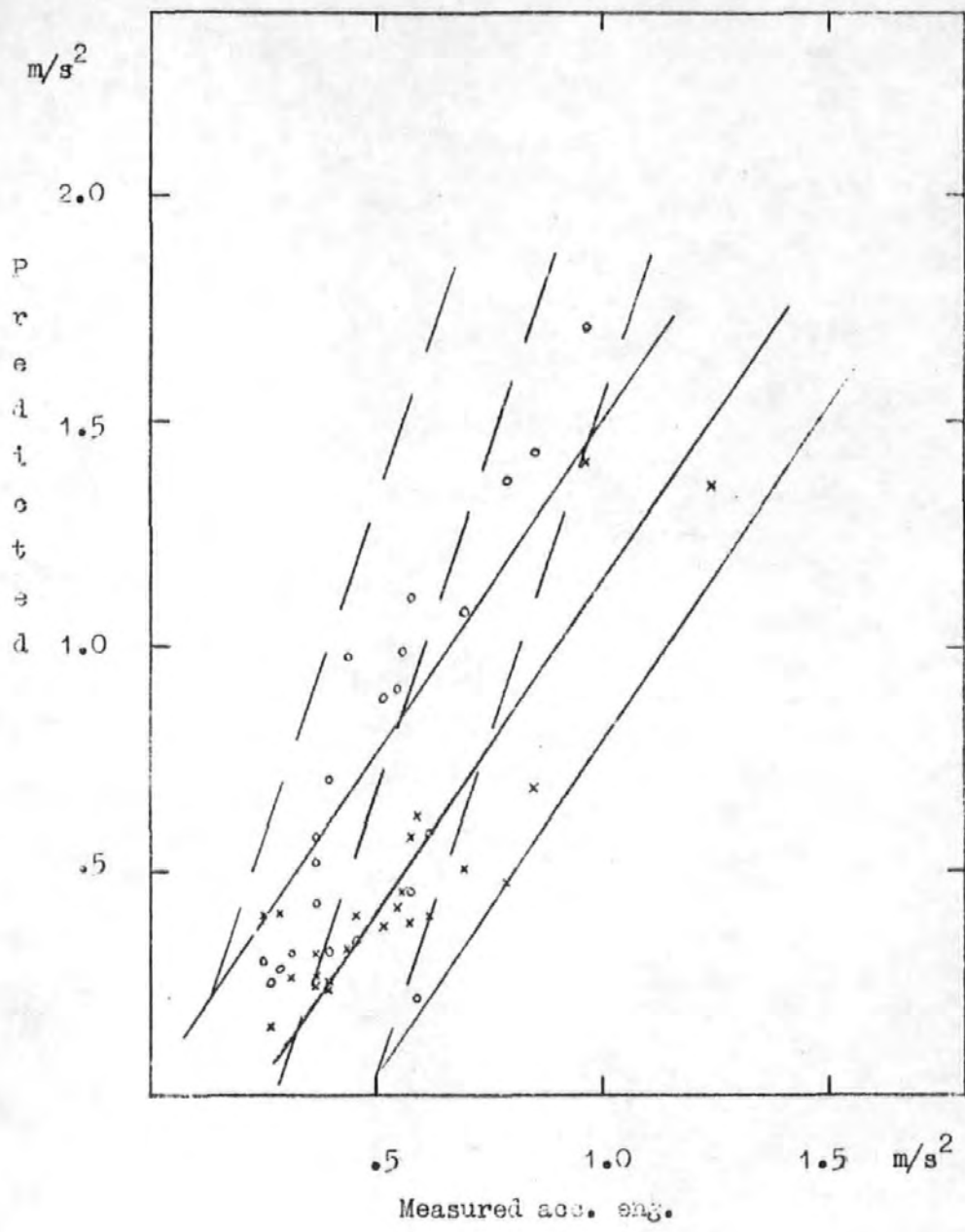


Fig. 66

Measured acc. eng. versus predicted from pitch = X and roll = 0, and regression lines. Full load.

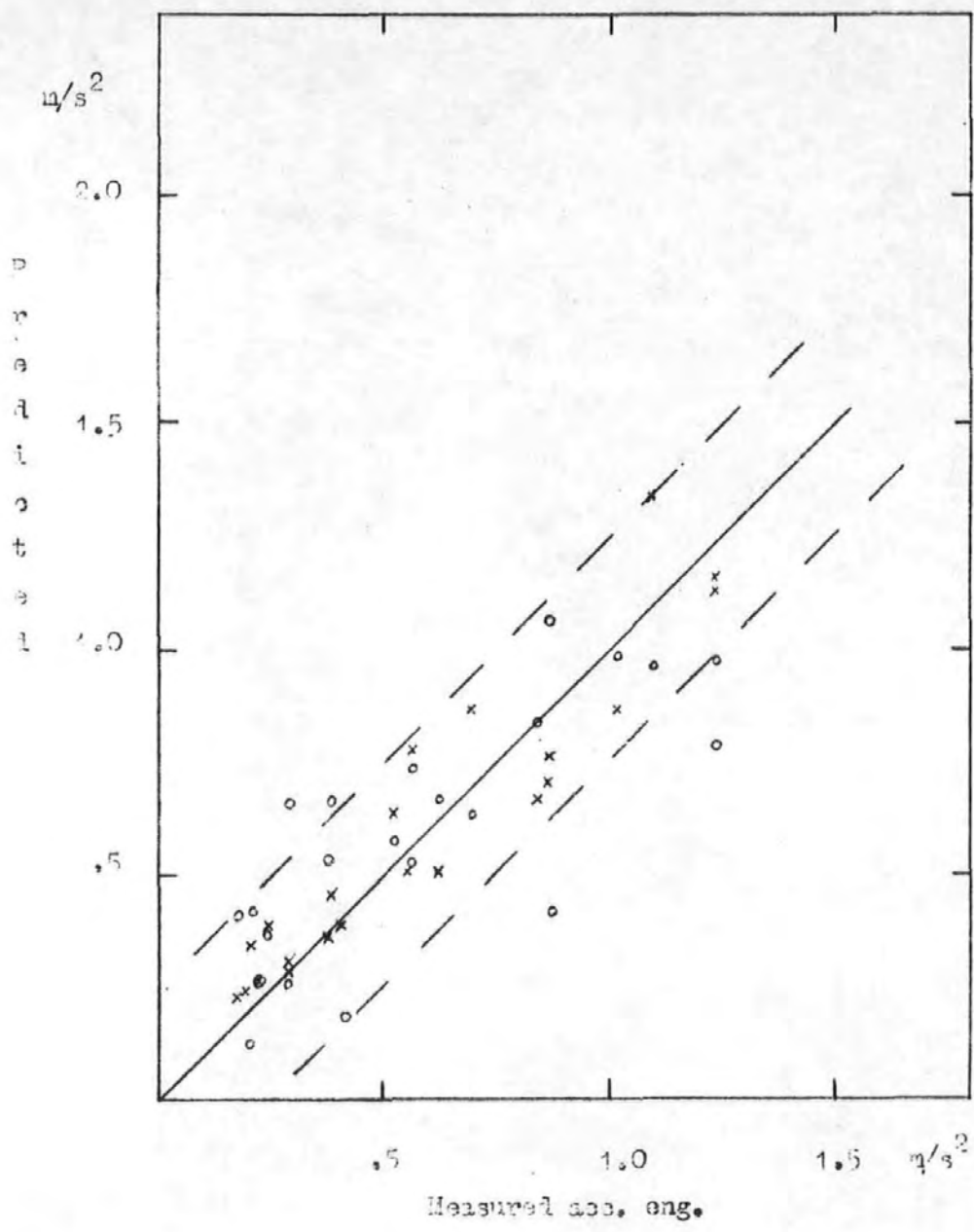


Fig. 67

Measured acc. eng. versus predicted by equivalent spectrum = X and by correlation to pitch = 0. Full load.



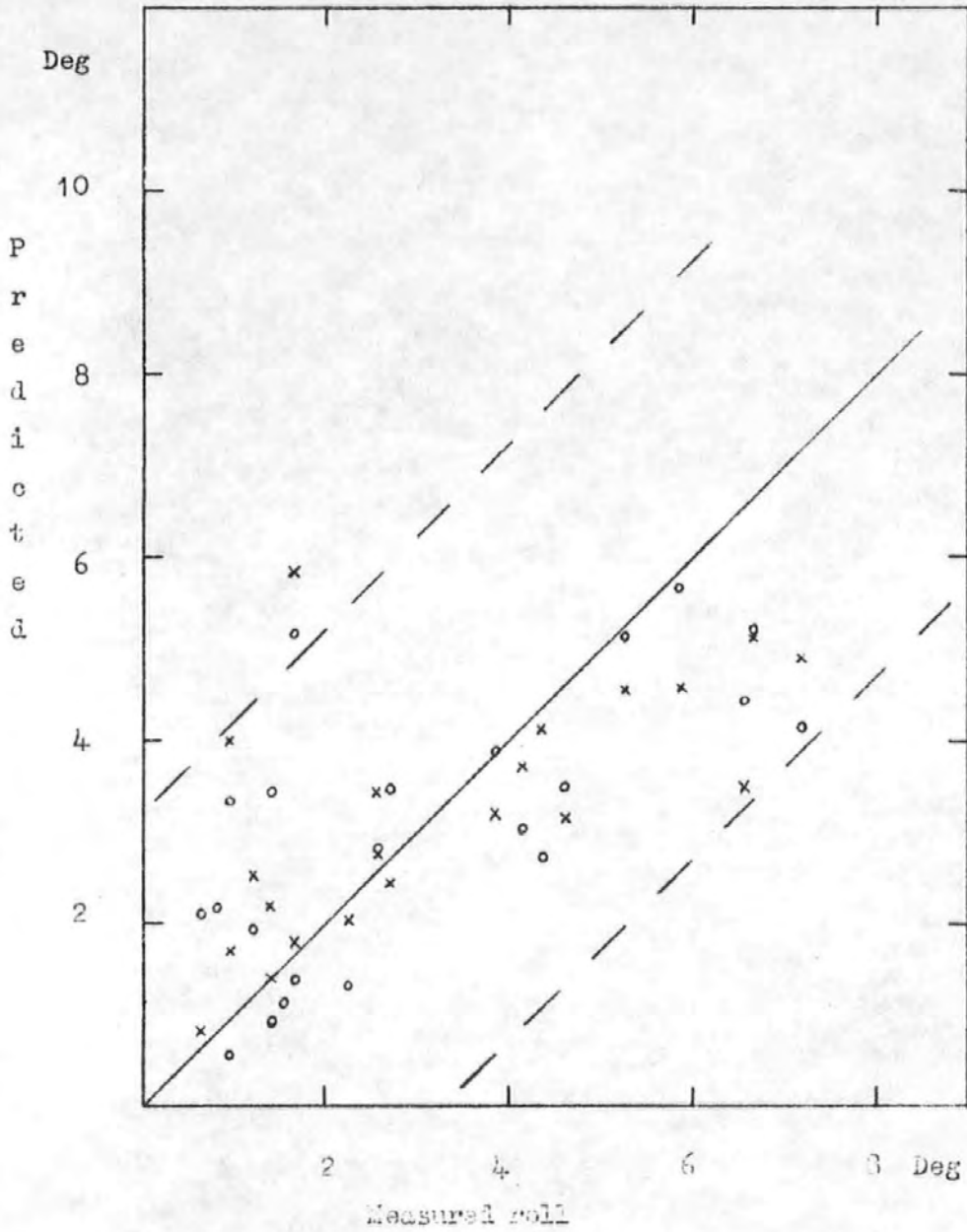


Fig. 68

Measured roll versus predicted by equivalent spectrum = X and by correlation to pitch = O. Full load.

### Prediction of relative motion at the F.P.

The relative motion between the bow and the sea surface was not recorded, so the values estimated from the equivalent wave spectra, obtained from the three responses pitch, roll and acceleration in the engine room, can only be compared relatively without any absolute quantification. The results of estimated relative motion are presented in figures 69 and 70 in such a way that the values obtained from pitch are along the horizontal axis and the corresponding values obtained from roll and acc. eng. are plotted along the vertical axis as crosses and circles respectively. For prediction of relative motion, the response period, i.e. relative motion period, is of interest if the results are to be used for calculating the probability of shipping water, and the results of these are presented in the same way in figures 71 and 72. The only conclusions that can be drawn are that the results from the three responses agree better for the laden condition than from the ballast condition but the differences are rather large in both cases.

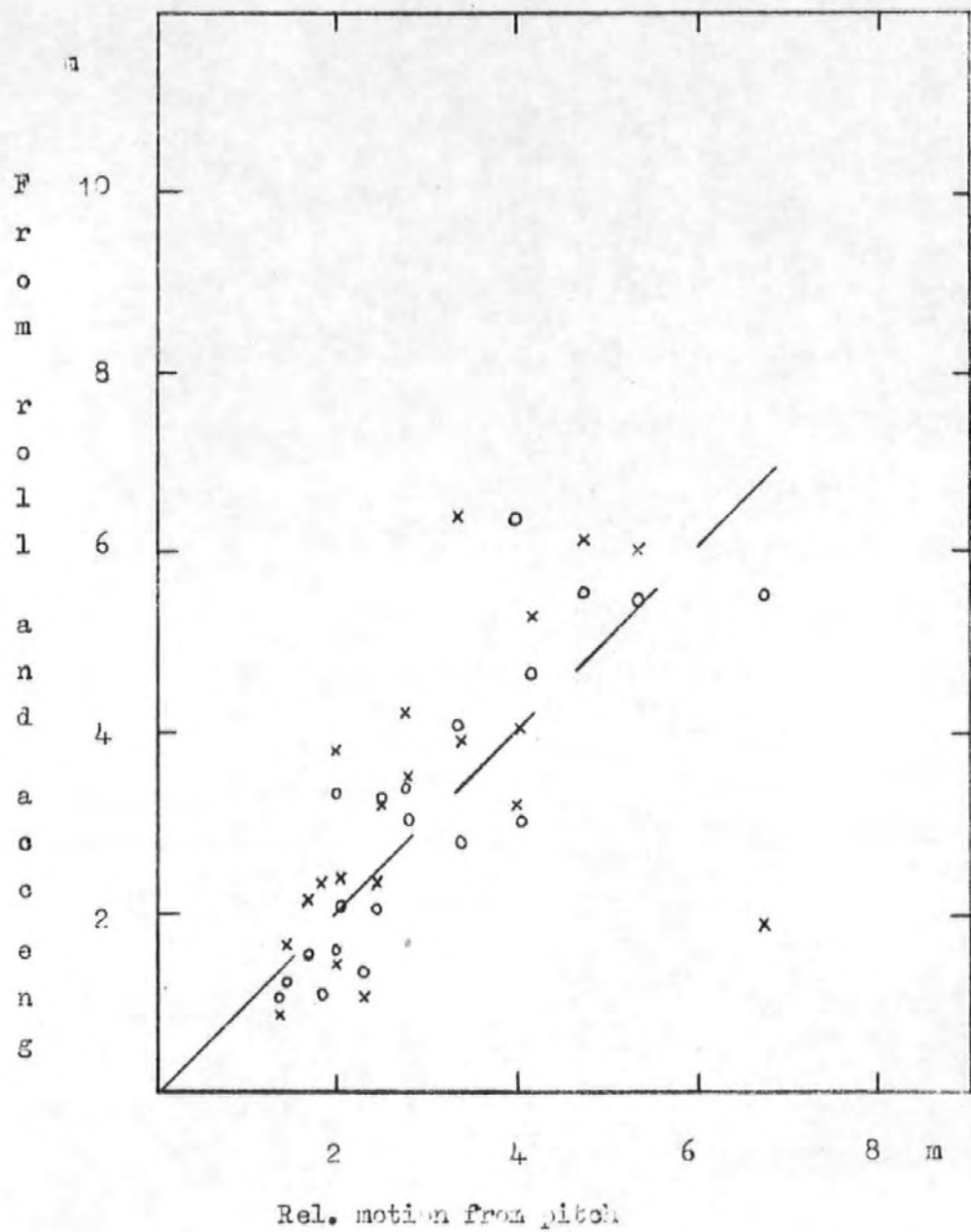


Fig. 69

Relative motion estimated from pitch versus estimates from roll = X and acc. eng. = 0. Full load.

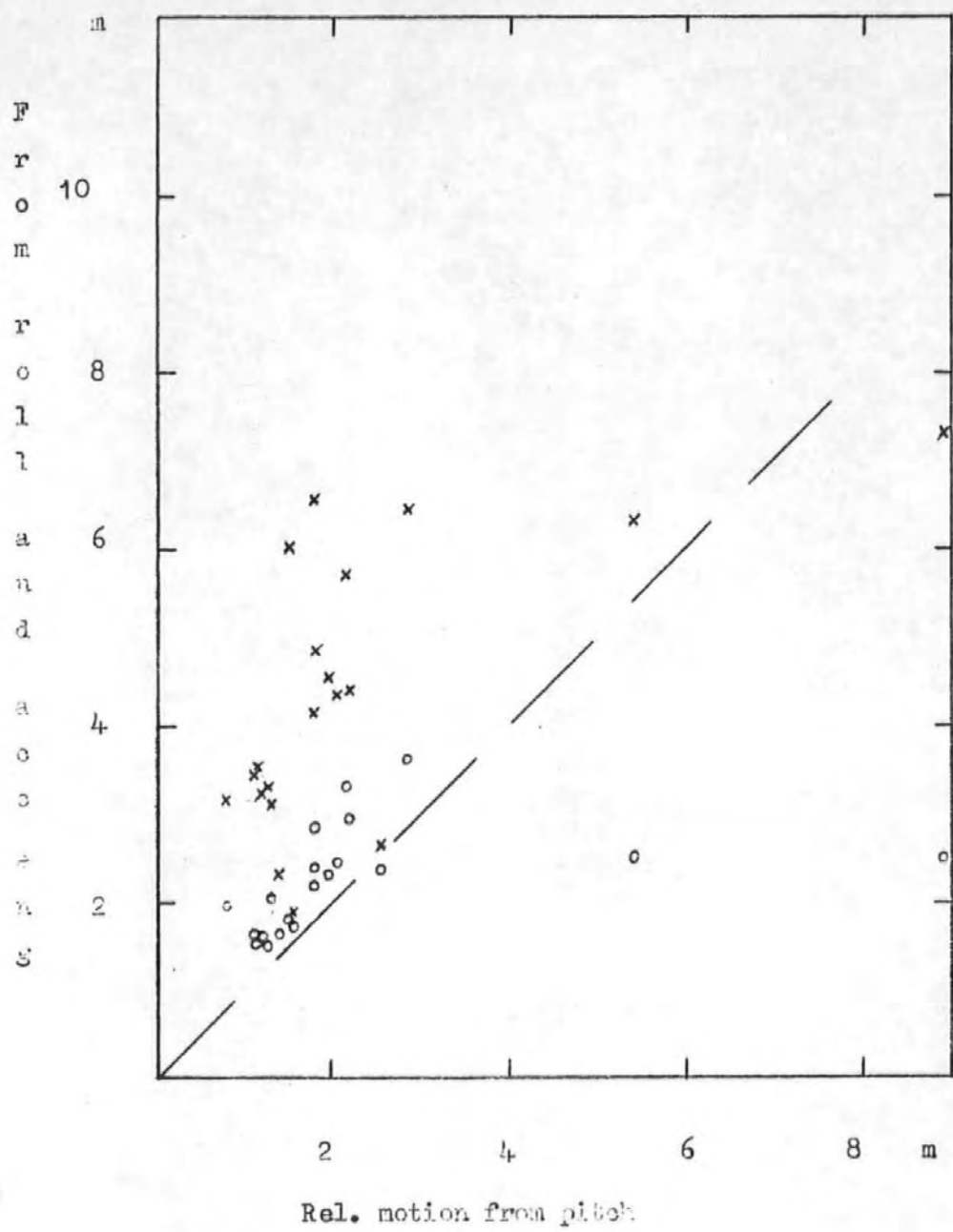


Fig. 70

Relative motion estimated from pitch versus estimates from roll = X and acc. eng. = 0. Ballast.

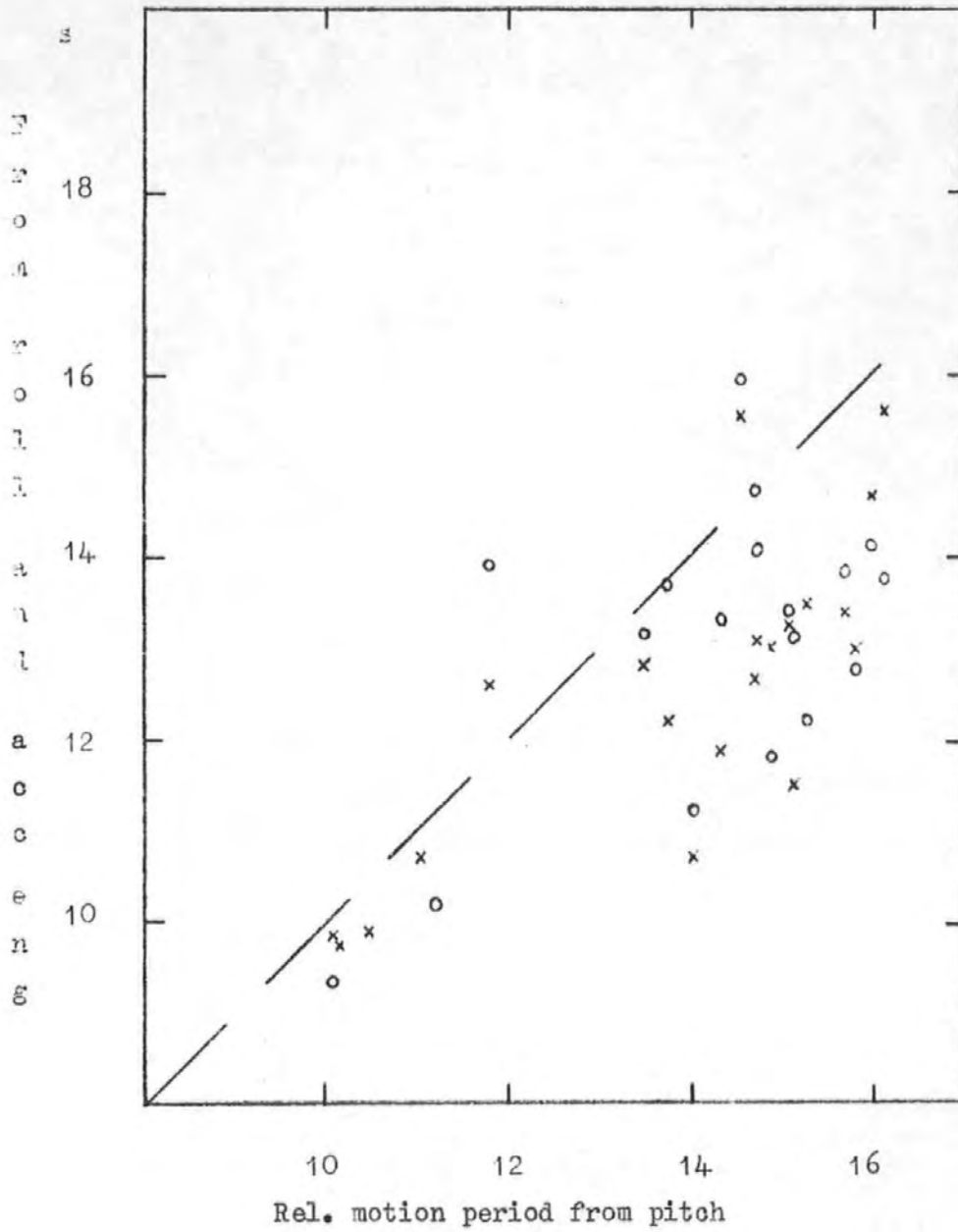


Fig. 71

Relative motion period estimated from pitch versus estimates from roll = X and acc. eng. = 0. Full load.

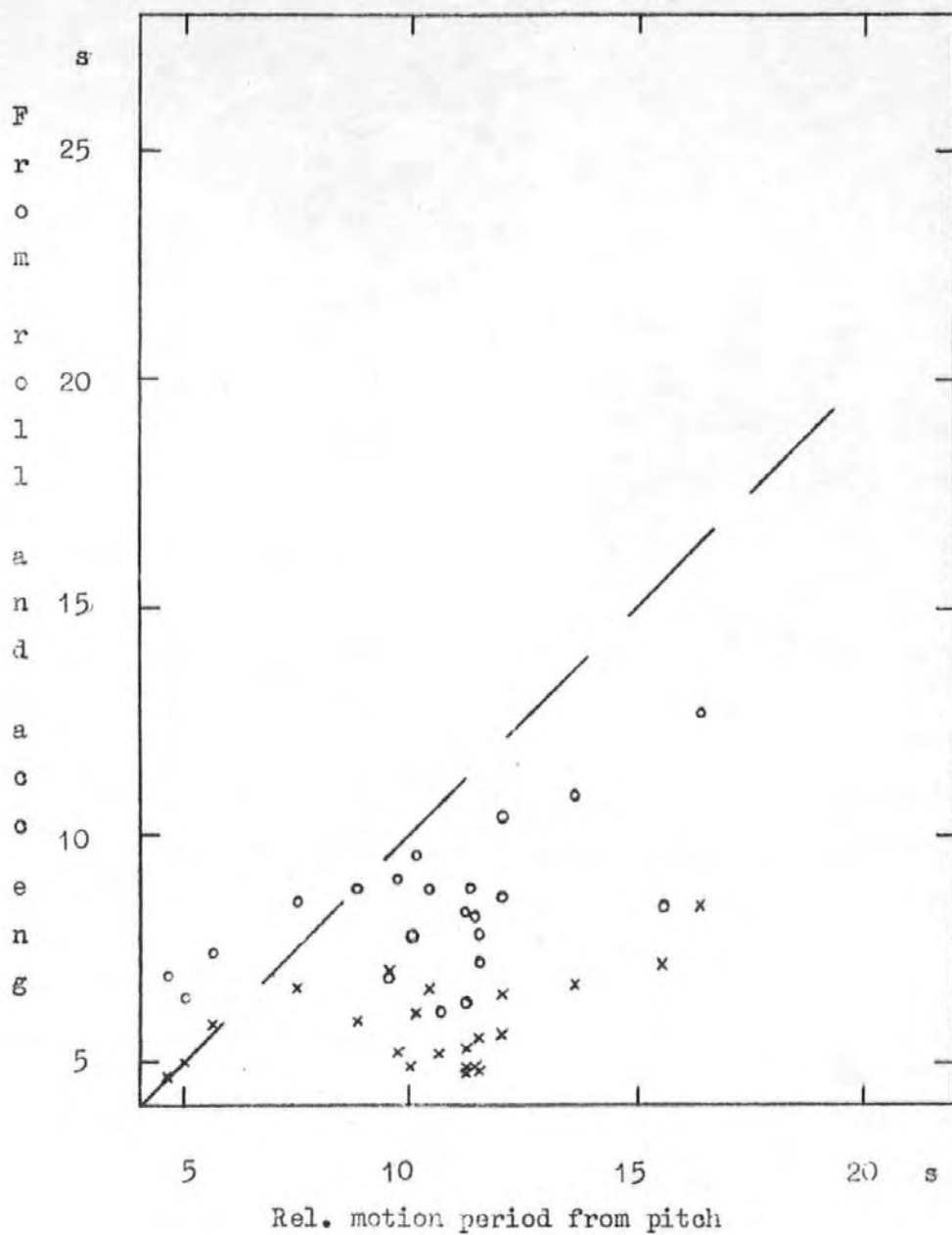


Fig. 72

Relative motion period estimated from pitch versus estimates from roll = X and acc. eng. = 0. Ballast.

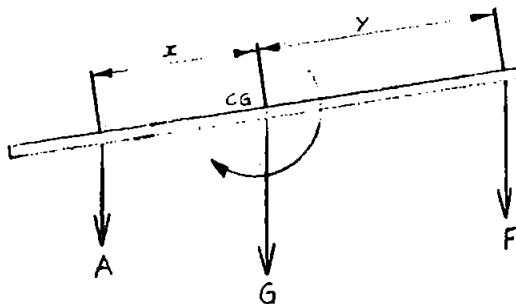
### Acceleration at the F.P.

It was shown in an earlier chapter how the probability of shipping water over the bow could be calculated from the relative motion between the bow and the sea surface. So, if the relative motion could easily be monitored, the probability of shipping water could be displayed by an instrument on the navigation bridge. The direct measurement of the relative motion is, however, difficult and most of the available instrumentation systems rely on the monitoring of the vertical acceleration of the bow as an indication of the severity of the bow motion and the probability of damaging this part. Measuring the bow acceleration is relatively simple, but a reduction in cost and simple installation of an instrumentation system could be achieved if all sensors could be located in the deckhouse and various responses such as the bow acceleration could be deduced from them.

The following is a description of an approach which was tried in an attempt to deduce the vertical acceleration at the forward perpendicular from the recorded signals of pitch and acceleration in the engine room and assuming the ship was behaving as a rigid body.

The situation of a rigid body at an instant of time may be described by the vertical acceleration of the centre of gravity  $G$  and an angular acceleration  $\ddot{P}$  as in the diagram below.

Fig. 73 Acceleration of a rigid body.



The acceleration at the distances  $x$  and  $y$  from the centre of gravity is:

$$A = C - \ddot{P}x$$

$$F = G + \ddot{P}y$$

Combination of the two gives:

$$F = A + \ddot{P}(x + y)$$

So with  $A$  being the vertical acceleration in the engine room,  $\ddot{P}$  the pitch acceleration and  $(x + y)$  the distance between the engine room and the F.P., the vertical acceleration  $F$  at the F.P. can be found.

The available recordings include the vertical acceleration  $A$  but the pitch motion  $P$  rather than the pitch acceleration  $\ddot{P}$ , so the second derivative of the pitch signal must be obtained before the addition can take place. As the signal is no longer continuous but represented by a set of data points the differentiation cannot take place straight away. A possible approach would be to use a curve fitting method for a part of the signal at a time and evaluate the second derivative for each part. The simplest way is to fit three points at a time to a polynomial of the second degree for which the second derivative is a constant and easily calculated. In this case, if  $X_{i-1}$ ,  $X_i$ ,  $X_{i+1}$  denote three ordinates of the original signal, then the second derivative  $\ddot{X}$  is:

$$\ddot{X}_i = X_{i-1} - 2X_i + X_{i+1}$$

Although easy to handle, this method is sensitive to small changes of slope of the signal and tends to give an unrealistically jerky signal with very short period as a result. A smoother result can be obtained in the following way:  $X_{i-1}$ ,  $X_i$ ,  $X_{i+1}$  be ordinates of the motion signal and let the velocity at instant  $i$  be:



$$\dot{x}_i = \left[ (x_{i+1} - x_i) + (x_i - x_{i-1}) \right] / 2$$

and the acceleration at instant  $i$  :

$$\ddot{x}_i = \left[ (\dot{x}_{i+1} - \dot{x}_i) + (\dot{x}_i - \dot{x}_{i-1}) \right] / 2$$

After substitution the acceleration becomes:

$$\ddot{x}_i = \left[ (x_{i-2} - 2x_i + x_{i+2}) \right] / 4$$

Let  $m_{0s}$ ,  $m_{2s}$ ,  $m_{4s}$ ,  $m_{6s}$  be the zeroth, second, fourth and sixth moments of the motion spectrum, and  $m_{0v}$ ,  $m_{2v}$ ,  $m_{4v}$ ,  $m_{0a}$ ,  $m_{2a}$  be the moments of the velocity spectrum and acceleration spectrum respectively. The mean zero-crossing period for the motion signal is

$$T_{2s} = 2\pi \sqrt{m_{0s}/m_{2s}}$$

The period between crests  $T_{4s}$  is depending on the width of the spectrum

so that

$$T_{4s} = T_{2s} \sqrt{1 - \epsilon_s^2}$$

or with

$$\epsilon_s^2 = 1 - m_{2s}^2 / m_{0s} m_{4s}$$

$$T_{4s} = 2\pi \sqrt{m_{2s}/m_{4s}}$$

But the crest period of the motion is the same as the mean period of the velocity since the velocity changes sign between each peak of the motion signal, so

$$T_{2v} = T_{4s}$$

For the same reason, the mean acceleration period is

$$T_{2a} = T_{4v}$$

Furthermore, the moments are related so that

$$m_{0v} = m_{2s}$$

$$m_{2v} = m_{4s}$$

$$m_{oa} = m_{2v}$$

Combination of these yields

$$m_{4s} = m_{oa} \quad (5.19)$$

$$T_{2a} = 2\pi \sqrt{m_{4s}/m_{6s}} = 2\pi \sqrt{m_{oa}/m_{2a}} \quad (5.20)$$

So by calculating  $m_{4s}$  and  $m_{6s}$ , the fourth and sixth moments of the motion spectrum and  $m_{oa}$  and  $m_{2a}$ , the zeroth and second moments of the acceleration spectrum, it is possible to check the method of differentiation.

After several attempts the method had to be abandoned and considered unsuccessful. Even though the actual acceleration was not included amongst the recorded responses and hence not available for comparison, the values derived by this method were generally unrealistic. It was possible to satisfy the conditions in (5.19) and (5.20) for individual records by introduction of various correction factors, but these could not be applied to any other record.

Integration of a digitized signal of this type is generally regarded more reliable than a differentiation, and another contributing factor to the poor results was the actual shape of the pitch motion signal. As mentioned earlier this signal had a very small amplitude and consisted of several consecutive values of the same magnitude and was not suitable for differentiation.

## Conclusions

The digitized signals of the three ship responses - pitching, rolling and vertical acceleration in the engine room, were generally Gaussian with the exception of pitch signals with small amplitudes, fig. 25. Two methods of analysis were used to estimate the two parameters significant response value and mean response period. The two methods were found to give similar response values and the agreement with the recorded response values were found to improve when the correction factor related to the broadness of the signals was applied.

Comparison of maxima and heights of the signals to the Rayleigh distribution was made by visual inspection of plots of histograms and the theoretical distribution as well as the recorded and theoretical significant values. Good agreement was found for the distribution of heights and the plot of the Rayleigh distribution, whereas the distribution of maxima, which included negative values, did not compare as favourably, partly due to too small class sizes being chosen for the histograms. Both maxima and heights did, however, give good agreement with the theoretical significant values. The importance of careful selection of sensitivity of the recording sensors relative to the magnitude of the signal for this type of investigation was emphasized by the analysis of the signal representing pitch. The low sensitivity for this response resulted in the recorded range consisting of few values which increases the quantization error introduced by the digitizing of the continuous signal. As several recordings were made during light weather conditions some cases were found where the recorded pitch signal ranged between  $\pm 2$  units, and the histograms of these signals did, of course, not agree well with the Rayleigh

distribution. The mean response periods estimated by the two methods also showed relatively larger discrepancies for such light weather conditions. From records containing larger response values, the response periods agreed well, but a filtering of vibration contributions to the acceleration signal prior to analysis would probably have improved the comparison for this response.

Response values and response periods from the three signals were used to derive the two parameters, significant wave height and mean wave period, for the equivalent wave spectrum. As expected, the spectra derived from the three responses for each record were different with respect to wave height and wave period. Each type of response reacting differently to the existing wave system and the derived spectra representing each response's receptance to the wave system. The possibility of applying a spectrum which was derived from one response for estimation of another response was investigated. The results showed reasonable agreements between estimated and measured values for predictions of pitch from acc. eng. and vice versa, but poor agreement for estimation of roll from pitch. Estimations of pitch and acc. eng. using this technique were slightly better than estimates based on the correlation of the two responses, whereas the opposite was the case for estimates of roll. The possibility of using a spectrum defined from one response for estimating the same response after a change of course or heading, was not possible as records were taken at twelve hour intervals.

The two important parameters when defining an equivalent wave spectrum the wave direction and energy spread, could not be established effectively from the relative magnitude of pitch and roll, instead,

the somewhat weak assumption that wind and wave direction coincided, was made. In order to minimize errors introduced by this assumption, the energy spread was assumed to be wide. A more stringent analysis of the validity of the method, of using an equivalent wave spectrum could have been made had the actual wave system been known. But as this is not the case in reality, it was of interest to find out how limiting a factor this was.

Other factors which may have affected the investigation unfavourably were the facts that the ballast journey contained records of generally small response values, increasing the relative errors of quantization and the laden voyage contained records of mainly following waves, for which the theoretical calculations of ship responses are regarded as less reliable.

## CHAPTER 6

### DISCUSSION OF RESULTS

#### Derivation of the equivalent wave spectrum

One of the main objectives with this project was to investigate the possibility of using the ship itself as "wave buoy" in the sense that a theoretically defined spectrum of Pierson-Moskowitz type could be derived from the motion of the ship. If successful, a method would have been found which would render the unreliable visual estimates of the wave system unnecessary and the prediction facility of an instrumentation system would be improved. It was clearly stated that the correct values of wave height and mean wave period were not necessarily to be expected from the procedure, but merely two parameters as a substitute for the actual wave system, which could be used in the prediction process. The fact that the actual directional wave system was recorded during the measurement manoeuvres for the container-ship, made it possible to compare the actual wave spectrum to the equivalent spectrum obtained by the method described in Chapter 3.

The actual wave system showed remarkable agreement with a spectrum of P-M type and the angular energy distribution, which was consistent for different wave components, was almost identical to the theoretical spread function 2. Because of the similarities between the actual wave system and that used for the theoretical calculations, a very good agreement was expected between the values obtained by the equivalent spectrum method and the actual values. It was, however, found that neither the spectrum obtained from pitch nor from acceleration at the F.P. was the same as the recorded spectrum. The reasons for the discrepancies are not fully understood but contributing factors may be the small difference in the shape of the measured spectrum and the P-M spectrum, the fact that the analysed response recordings were made some

time after the wave measurements and a slight change of wave spectrum could have occurred in the meantime. Some inaccuracies may also be present in the transfer functions and the extrapolation technique used, and examination of the hydrodynamic theory involved in the strip theory is also recommended by Taylor [8]. What was clearly shown was the effect of misjudgement of the wave direction and the energy spread, see Fig. (23). For example, a range of  $60^{\circ}$  heading gave a difference in waveheight and wave period of circa 1m (31%) respective 1 sec. (14%) for pitch and .25m (11%) respective .4 sec (6%) for acceleration at the bow, using spread function 2. The errors in the estimated waveheight and periods with correctly judged heading and spread were .93m (29%) respective .07 sec (1%) for pitch and 1m (31%) respective 0.31 sec (4%) for acceleration at the bow.

The spectra obtained from the responses of the tanker could not be compared to the true spectra as they were not recorded, and, therefore, could not be quantified, but the discrepancies between the spectra obtained from different responses were again evident. It would have been of interest to know how well the actual mean wave direction agreed with the one assumed from the wind direction.

As the equivalent wave spectrum obtained from the motions of the containership was found to be different from the true spectrum even when the latter was close to a P-M spectrum, it emphasizes the fact that the derived parameters of wave height and wave period should not be taken as being those of the actual wave system.

#### Using the equivalent spectrum for predictions

The question of whether the equivalent wave spectra, however different

from the true one, could be used for predicting the effect of a change of course or for predicting one response from another was investigated. In the case of the containership it was not possible to draw any far-reaching conclusions as there was only one sample available for the investigation. The predictions of responses in a heading of  $90^{\circ}$  using the spectra obtained in  $130^{\circ}$  and  $135^{\circ}$  were incorrect but the errors were small for acceleration,  $1.70\text{m/s}^2$  against recorded  $1.78\text{m/s}^2$  and reasonable for pitch,  $1.83^{\circ}$  against recorded  $1.27^{\circ}$ . Errors in such predictions are acceptable if their magnitudes are consistent and known, but establishment of any correction factors would require several examples of the type investigated. The same argument goes for the attempt to predict one response from another for the containership. It was here, however, interesting to find that the response values predicted from various different wave spectra were very similar. This would indicate that even though the wave direction or energy spread are incorrectly estimated, errors in the predicted value would be the same. Again, this could not be generalised, however, with only one example available.

For the investigation of the recordings from the tanker only the approach of predicting one response from the equivalent spectrum obtained from another could be employed. The actual wave spectra were not measured so the wave direction was assumed to coincide with the wind direction and the energy spread assumed wide. Comparison of predicted and recorded values were made in the form of regression and correlation analysis. The results were acceptable for predictions between pitch and acceleration in the engine room whereas predictions involving roll were poor. Correlation analysis revealed as expected, that pitch and acc. eng. are



closer correlated than roll and either of the other two. It was, in fact, shown that the prediction method using the equivalent wave spectrum was only marginally better than that obtained by just considering the correlation between the responses.

It appears, therefore, that the substitution of an unknown spectrum by a Pierson-Moskowitz spectrum is not always acceptable as uncorrelated responses are sensitive to different components of the wave system. It is, for example, possible to have a situation where the ship is travelling in an almost unidirectional beam swell of a wave length which is causing large roll angles but a very small pitch response. With a translation of the swell into a P-M spectrum, based on the large roll motions, the prediction of the pitch angle would give too large values. Using the spectrum for predicting the roll in another speed, or heading, however, is likely to lead to smaller errors even though the assumed energy spread is of importance. It was hoped that the relative magnitude of the responses which, in this, would be large, could be used to detect the wave direction. But as the ratio is affected by the actual wave system it proved difficult to compare to ratios obtained theoretically by using P-M spectra.

As both the ships investigated are large and hence sensitive to long swell it could be argued that some sort of "swell-spectrum" would be more useful than the P-M spectrum representing fully developed sea. Possibly this would make it possible to handle those situations where the measured response period was too long for the P-M spectrum to be used, but as pointed out earlier, these records contained response values too low to be reliable, or of interest anyway. A correct estimate of the wave direction and energy spread is probably a more important

factor than the choice of spectrum shape.

#### Wave direction and energy spread

Any real solution to the important problem of estimating the heading and spread has not been found from this investigation. It is obviously of great importance to know the heading in order to evaluate the consequences of a change of course and the amount of energy spread affects the relative effect of a course alteration. For the investigation of the tanker the wind direction was assumed to coincide with the wave direction and the spread assumed to be large in order to minimize errors caused by these assumptions. The accuracy of the assumed wave direction could not be evaluated as the actual direction was not known. Arguably the wave direction could be visually estimated with some confidence, but the method would be limited by light and visibility conditions. Neither visual observations nor the use of the wind direction for estimation of the wave direction seem satisfactory and the development of another reliable method would be valuable.

It is possible that the most practical and useful guidance to the operators could be in the form of charts describing the relative effects of speed and course on various responses in general, but it still demands the correct estimation of the wave direction. Not only is it important to know the relative heading, but it is also necessary to know whether the sea comes from starboard or port. Other investigations have reported noticeable differences in longitudinal stresses measured on the port and starboard side of the deck, but whether there is a consistency with respect to the wave direction so that the difference could be used for detecting the heading, is not known.

### Prediction of relative motion

As the relative motion was not measured the predicted values could only be compared relative to each other. The accuracy with which the relative motion and hence the probability of shipping green water, can be estimated from another response is, judging from the presented results, dependent on how closely correlated they are. The most reliable method would be to measure the relative motion at the bow directly, but this is, unfortunately, very difficult. Attempts have been made by measuring the pressure fluctuations below the water level, but the components of dynamic pressure makes it difficult to relate it to the relative motion. Any simple and reliable method has not been reported, but methods such as using sonars, as used on some hydrofoils to measure the height above the water level seem possible. Some success in using wave height radars and inverted fathometers has also been reported, although the objective has been the more difficult task of deducing the wave spectrum rather than just the relative motion.

### The manual method versus spectrum analysis

Two methods were used for analysis of the digitized time records. The spectrum analysis provided the shape of the response spectrum and various moments of the spectrum. The manual method gave comparisons between distributions of amplitudes and heights of the response signal and the Rayleigh distribution. Both methods gave significant response value and mean response period. Some important aspects are worth noting in this context. The response values obtained from the two methods agreed very well but the same could not be said for the response periods, a fact which was perhaps not given enough attention during the investigation. It was argued that the periods obtained by the spectrum analysis, where

the high frequency contributions were truncated, were more realistic than those obtained from the manual method. The somewhat disconcerting factor to be considered is the sensitivity to measured response periods of the estimation of the mean wave period in the equivalent spectrum. Due to the low slope of the curve of response periods as a function of wave periods, a small difference in the measured response value results in a large difference in the estimated wave period. By different truncation conditions of the response spectrum and by introducing various filtering methods of the signal, the "measured" mean response period is affected and some decision on which is the correct value must be made. A further investigation of this aspect would be of value.

The importance of appropriate sensitivity by the sensors was illustrated by the difficulties encountered in the analysis of the pitch signal from the tanker. The small amplitudes relative to the steps in the digitizer, quantization levels, made comparisons of amplitudes to the Rayleigh distribution impossible, caused a significant area of the response spectrum to occur at frequencies close to zero and made differentiation of the signal in an attempt to derive the acceleration at F.P. impossible.

#### Final conclusions

The merits and usefulness of instrumentation systems which monitor various responses and give alarms when certain preset values are exceeded have been reported elsewhere and have not been questioned in this report. The preset alarm levels obviously have to be carefully determined and adjustments of these levels according to service experience is important. It is, however, felt that any predictions or recommendations

made by any system should be regarded with caution, remembering that they are at the best only as good as the information about the wave system which is input to the system, whether it is obtained by visual observation from the wind speed or from the motion of the ship.

The approach investigated here of using wave parameters which are defined from the motion of the ship for predicting purposes has not conclusively been shown to be successful. Because the actual wave systems were not known for the tanker recordings the effects of the assumed headings and spreads could not be evaluated. The assumption made in Chapter 3 that the reliability of the method would increase with the severity of the weather could not be verified, and further full scale trials for this purpose would have to be made. The complexity of wave systems with so many possible combinations of wave heights, wave periods and energy spreads makes the possibility of substituting the actual wave system by a theoretically defined system seem rather restricted. In some cases, when the actual wave system is similar to the theoretical, it ought to work well, but it seems likely that advice based on the assumption often can be misleading. It ought to be pointed out, however, that in none of the investigated cases were the predicted values completely out of range but the general accuracy was not too impressive.

The fact that theories exist which allow short term responses in known wave systems to be calculated with some confidence, does, of course, make the idea of using a shipborne computer for real time calculations attractive. It does, however, seem that the importance of actual wave data is easily forgotten. Perhaps the most important parameter is the relative wave direction and further research in pursuit of methods for automatically detecting this is strongly recommended.

It may finally be concluded from this investigation that:

- the parameters wave height and wave period in an equivalent wave spectrum derived from the motions of the ship should not be regarded as true estimates of the actual sea.
- care should be taken if the equivalent spectrum is used for predicting one response from another, as the reliability of the procedure is dependent on the correlation between the two responses.
- the possibility of predicting the effect on a response from a change in course could not be conclusively evaluated from the single example available.
- the estimated spectra and any predictions from them are highly dependent on the estimated wave direction and the assumed energy spread.
- for prediction of relative motion and hence shipping of water from another response, the latter should be a response which is closely correlated to the relative motion.

## REFERENCES

1. St. Denis, M. "On the motions of ships in confused seas".  
Pierson, W.J. Trans. SNAME Vol. 64, 1953.
2. Bennet, R. "Survey on criteria and requirements for structural design". International symposium on the dynamics of marine vehicles and structures in waves.  
IMECHE 1974. Paper 1.
3. Bennet, R. "Stress and motion measurements on ships at sea".  
The Swedish Shipbuilding Research Foundation.  
Report No. 13, 1958.
4. Bennet, R.,  
Iverson, A.,  
Nordenström, N. "Results from full scale measurements and predictions of wave bending moments acting on ships". The Swedish Shipbuilding Research Foundation. Report No. 32, 1962.
5. Loukakis, T.A. "Experimental and theoretical determination of wave form and ship response extremes". Dept. of Naval Arch. and Marine Eng. Massachusetts Inst. of Tech. Report No. 69-7, 1970.
6. Planeix, J.M. "Wave loads - a correlation between calculations and measurements at sea". Int. Shipbuilding Progress. Vol. 19, No. 216, Aug. 1972.
7. Beukelman, W.  
Buitenhek, M. "Full scale measurements and predicted seakeeping performance of the containership 'Atlantic Crown'".  
Shipbuilding Laboratory, Delft, The Netherlands.  
Report 338-P, 1975.
8. Taylor, K.V. "Full-scale dynamic measurements on M.V. Nihon".  
Development Unit, Lloyds Register of Shipping.  
Report No. 54, 1975.

9. Taylor, K.V.,                   "Full-scale static and dynamic measurements on  
Lundgren, J.                   M.V. Nihon. Comparison of measured motions,  
pressures and stresses with calculated response  
data". The Naval Architect. No. 2, March, 1976.
10. Lundgren, J.,                "Ships with large hatch openings". The Swedish  
Taylor, K.V.                   Ship Research Foundation. Report 111, 1975.
11.                                "Full-scale measurement of wave loads and structural  
response of large ore carriers". The Shipbuilding  
Research Association of Japan. Report No. 81, 1976.
12. Chataignier, P.            "Ship motion and sea loads analysis on seven  
different ships". Association Technique Maritime  
et Aéronautique. Paris, 1976.
13.                                "Further analysis of slamming data from S.S.  
Wolverine State". Teledyn Materials Research,  
Mass. Project 1434, 1972.
14. Tanaka, K.,                "Measurements on the seakeeping quality of high  
Mizoguchi, S.                speed container ships in a seaway". IHI Engineering  
Review. Vol. 8, No. 3, Sept. 1975.
15. Fain, R.A.                   "Design and installation of a ship response  
instrumentation system aboard the SL-7 class  
containership S.S. Sea-Land McLean". U.S. Coast  
Guard. Technical report SSC-238, 1973.
16. Boentgen, R.R.,            "First season results from ship response  
Fain, R.A.,                    instrumentation aboard the SL-7 class  
Wheaton, J.W.                containership S.S. Sea-Land McLean in North Atlantic  
service". U.S. Coast Guard, SSC-264, 1976.
17. Bishop, R.E.D.,            "On the structural dynamics of ship hulls in  
Price, W.G.,                   waves". RINA, 1973.  
Taylor, E.R.



18. Bishop, R.E.D.,        "Ship strength as a problem of structural  
Price, W.G.                dynamics". The Naval Architect. April, 1975.
19. Bishop, R.E.D.,        "Wave-induced response of a flexible ship".  
Price, W.G.,                Int. Shipbuilding Progress. Vol. 24, No. 278,  
Tam, P.K.Y.                 Oct. 1977.
20. Aertssen, G.            "Labouring of ships in rough seas with special  
emphasis on the fast ship". Diamond Jubilee  
SNAME, 1968.
21. Aertssen, G.            "Ship behaviour in extreme and quasi-extreme  
seas". Association Technique Maritime et  
Aéronautique, Paris, 1976.
22. Tani, H.                "Tentative manual of ship handling in rough  
seas". Symposium on ship handling. Netherlands  
ship model basin, Wageningen. Publication No.  
451, Nov. 1973.
23. Lloyd, A.R.J.M.,        "Criteria for ship speed in rough weather".  
Andrew, R.N.                18th American Towing Tank Conference, Maryland.  
Aug. 1977.
24. Lindemann, K.           "Hull surveillance for improved ship handling in  
rough weather". Det Norske Veritas, Report No.  
74-54-S, 1974.
25. Lindemann, K.           "The development of a hull surveillance system".  
The Million Ton Carrier. Proceedings of the  
Super Ocean Carrier Conference, SOCCO. New York,  
1974.
26. Lindemann, K.,        "A system for ship handling in rough weather".  
Nordenström, N.            Proceedings, Fourth ship control systems symposium,  
Den Helder, Oct. 1975.

27. Lindemann, K. "Possible warning conditions and systems for ship handling in rough weather". Ship operation automation II, North Holland publishing company, Vol. 5, 1976.
28. Lindemann, K. "The navigator, ship handling in rough weather and hull surveillance systems". Conference on 'Human factors in the design and operation of ships'. Gothenburg, Feb. 1977.
29. Lindemann, K. "Hull surveillance system, a brief introduction to a second generation system". SO3-project. Det Norske Veritas.
30. Dickey, R.L.,  
De Long, R.C.,  
Gregov, Z. "A hull monitoring system for safe and economic operations". Ship operation automation II, North Holland publishing company, Vol. 5, 1976.
31. Taylor, K.V. "Hull surveillance : Tomorrow's technique". Lloyds Register of Shipping. 100A1, Jan. 1978.
32. "Auto Ship-bridge, Motions monitor". Mitsui Shipbuilding & Engineering Co. Ltd., Japan.
33. "Heavy Weather Damage Avoidance". EDO marine systems, U.S.A. 1974.
34. Hoffman, D.,  
Lewis, E.V. "Heavy weather damage warning systems". NMRC-KP-143. Maritime administration, Washington D.C. 1975.
35. Rask, I.,  
Robertsson, S. "A warning instrument for avoiding damages to ships in heavy weather, theory and suggestions for development". Examination thesis (in Swedish) Chalmers University of Technology, 1975.

36. Bennet, R. "A method to determine the response of ships in irregular waves". Chalmers University of Technology Division of Ship Design, Gothenburg, Sept. 1966.
37. Ochi, M.K., Bolton, W.E. "Statistics for prediction of ship performance in a seaway". Int. Shipbuild. Prog. 1973.
38. Price, W.G., Bishop, R.E.D. "Probabilistic theory of ship dynamics". Chapman and Hall, London, 1974.
39. Salveson, N., Tuck, E.O., Faltisen, O. "Ship motions and sea loads". Trans. SNAME, 1970.
40. Cartwright, D.E. "The science of sea waves after 25 years". International symposium on the dynamics of marine vehicles and structures in waves". IMECHE, 1974.
41. Darbyshire, J. "An investigation of storm waves in the North Atlantic Ocean". Proceedings Royal Society, A 230, 1955.
42. Pierson, W.J., Moskowitz, L. "A proposed spectral form for fully developed wind seas based on the similarity theory of S.A. Kitaigorodskii". Journal of Geophysical Research, Vol. 69, 1964.
43. Darbyshire, J. "The one-dimensional wave spectrum in the Atlantic Ocean and in coastal waters". Ocean Wave Spectra. (Prentice-Hall, Inc.) 1963.
44. Ewing, J.A. "The use of the JONSWAP spectrum with given values of significant wave height and average period". Institute of Oceanographic Sciences, 1975.

45. Chryssostomidis, C., Oakes, M.C. "Selection of wave spectra for use in ship design". Int. Symp. on ocean wave measurements and analysis. American Soc. of Civil Eng. Vol. II, 1974.
46. Hoffman, D. "Analysis of wave records and application to design". Int. Symp. on ocean wave measurements and analysis. American Soc. of Civil Eng. Vol. II, 1974.
47. Scott, J.R. "A sea spectrum for model tests and long term ship predictions". Journal of Ship Research, Dec. 1965.
48. Ferdinande, V. "On the representation of normalised wave spectra from multi-element arrays". Journal of Marine Research, Vol. 35, No. 3, Aug. 1977.
49. Cote, L.J. et al "The directional spectrum of a wind generated sea as determined from data obtained by the Stereo Wave Observation Project". New York University Meteorological Papers, Vol. 6, No. 2, 1960.
50. Oakley, Jr, O.H. "Directional wave spectra measurement and analysis". Seakeeping Symposium, Webb Inst. of Naval Arch. Nov. 1973.
51. Cartwright, D.E., Smith, N.D. "Buoy techniques for obtaining directional wave spectra". Buoy Technology (Marine Techn. Soc. Washington) 1964.
52. Regier, L.A., Davis, R.E. "Observations of the power and directional spectrum of ocean surface waves". Journal of Marine Research. Vol. 35, No. 3, Aug. 1977.

53. Regier, L.A., "Methods for estimating directional wave spectra  
Davis, E.D. from multi-element arrays". Journal of Marine  
Research, Vol. 35, No. 3, Aug. 1977.
54. Nordenström, N. "Methods for predicting long term distributions  
of wave loads and probability of failure for  
ships". Report No. 71-2-S. Det Norske Veritas,  
1972.
55. Lewis, E.V., "Lecture notes on ship motions in irregular  
Bennet, R. seas". Webb Inst. of Naval Arch. 1963.
56. Andrew, R.N., "Applications of generalised gamma functions in  
Price, W.G. ship dynamics". RINA, 1978.
57. Rice, S.O. "Mathematical analysis of random noise". Bell  
System Technical Journal, Vol. 23, 1944 and Vol.  
24, 1945.
58. Cartwright, D.E., "The statistical distribution of the maxima of  
Longuett- a random function". Proc. Royal Society, London,  
Higgins, M.S. Series A, Vol. 237, 1956.
59. Suhara, T. "Bow flare damages of large full ships due to  
wave impact (Analysis and design standard)".  
Int. Shipbuilding Progress, 1976.
60. Hagiwara, K., "Study on wave impact load on ship bow".  
Yuhara, T. Mitsubishi Heavy Industries Ltd. Technical Review,  
June, 1975.
61. Janzén, S., "Hull damage in large ships". Lloyds Register  
Nilsson, O. of Shipping, 1973.
62. Yuhara, T. "Fundamental study of wave impact loads on ship  
bow (3rd report)". Journal of the Soc. of  
Naval Arch. of Japan. Vol. 137, Part 6, June, 1975.

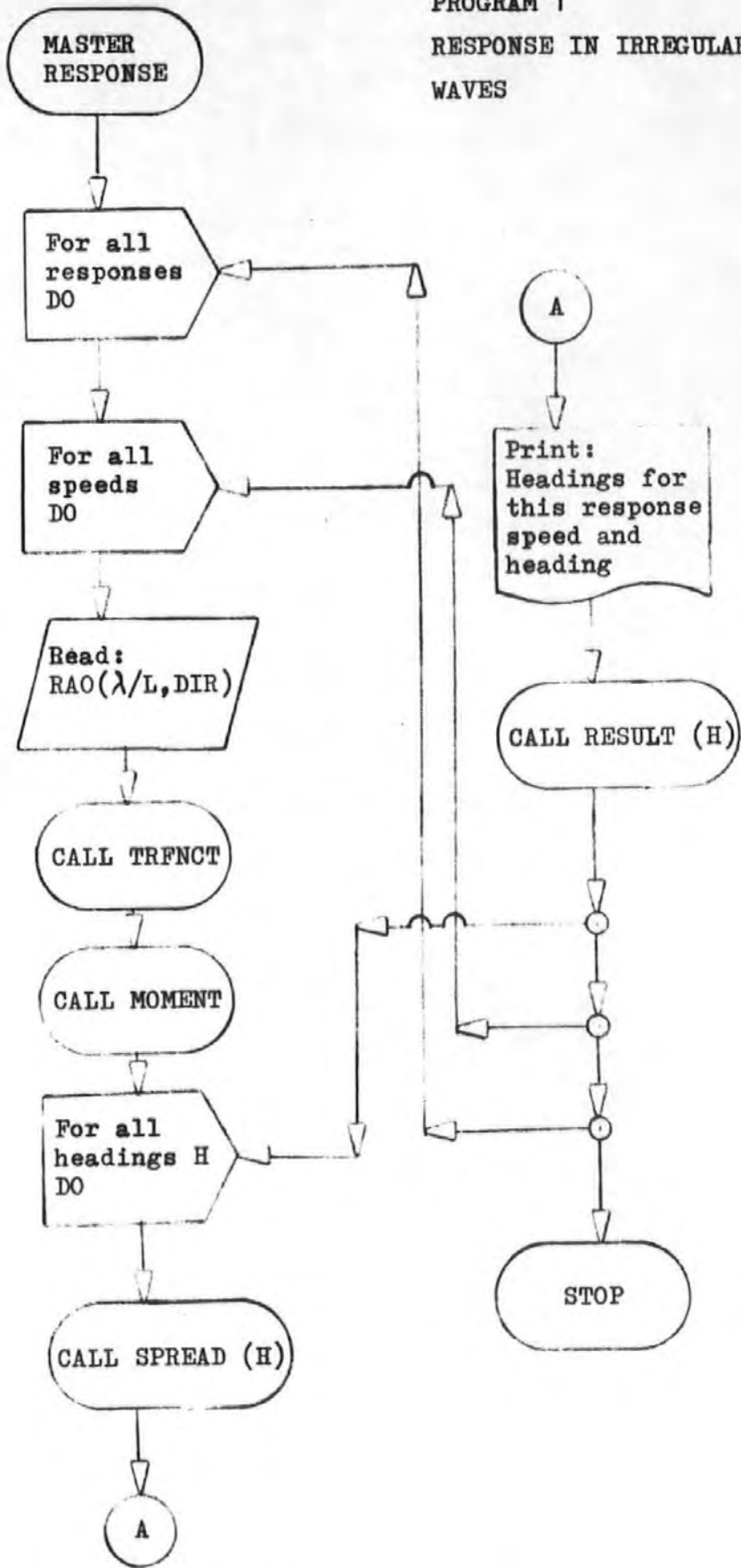
63. Hammond, D.L.,  
Craig, K.J. "System description of a shipboard wave height radar". E.O. Hulburt Center for Space Research, Naval Research Laboratory, Washington D.C. 1973.
64. Tucker, M.J. "A shipborne wave recorder". Inst. of Naval Arch. March 21st, 1956.
65. Söding, H. "Arbeitsbericht des Sonderforschungsbereichs 98". Schiffstechnik und Schiffbau, 1975.
66. Ward, G.,  
Katory, M. "Data on midship bending stresses from four ships". International symposium on the dynamics of marine vehicles and structures in waves. IMECHE, 1974.
67. Newland, D.E. "Random vibrations and spectral analysis". Longman, 1975.
68. Longuet-  
Higgins, M.S. "On the statistical distribution of the heights of sea waves". Journal of Marine Research, Vol. 11, No. 3, 1952.
69. Jansson, Å.A.V. "Undersökning av Fartygs Sjöegenskaper Medelst Frekvensanalys av Fartygsrörelser I Naturliga Vågdr". Rapport Nr. 52, Inst. för Skeppshydromekanik, Chalmers Univ. of Techn. Nov. 1973.
70. Marko, W. "The application of spectral analysis and statistics to seakeeping". SNAME Technical and research bulletin No. 1-24, 1963.
71. Dalzell, S.M. "The mathematics of random processes". Lecture notes, Plymouth Polytechnic, 1974.
72. Bishop, R.E.D.,  
Price, W.G. "On the truncation of spectra". Int. Shipb. Prog. Vol. 25, No. 281, Jan. 1978.

## APPENDIX

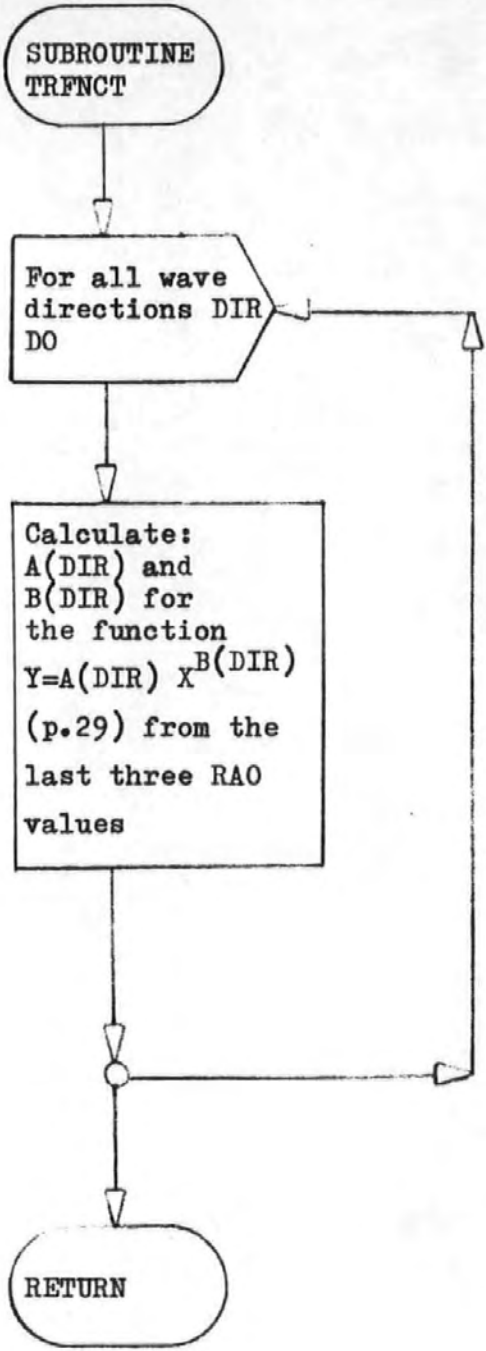
Here will be described in a summarized form the content of the two main computer programs used for this project. Only the logical steps will be described and the formulae used are to be found in the appropriate chapters.

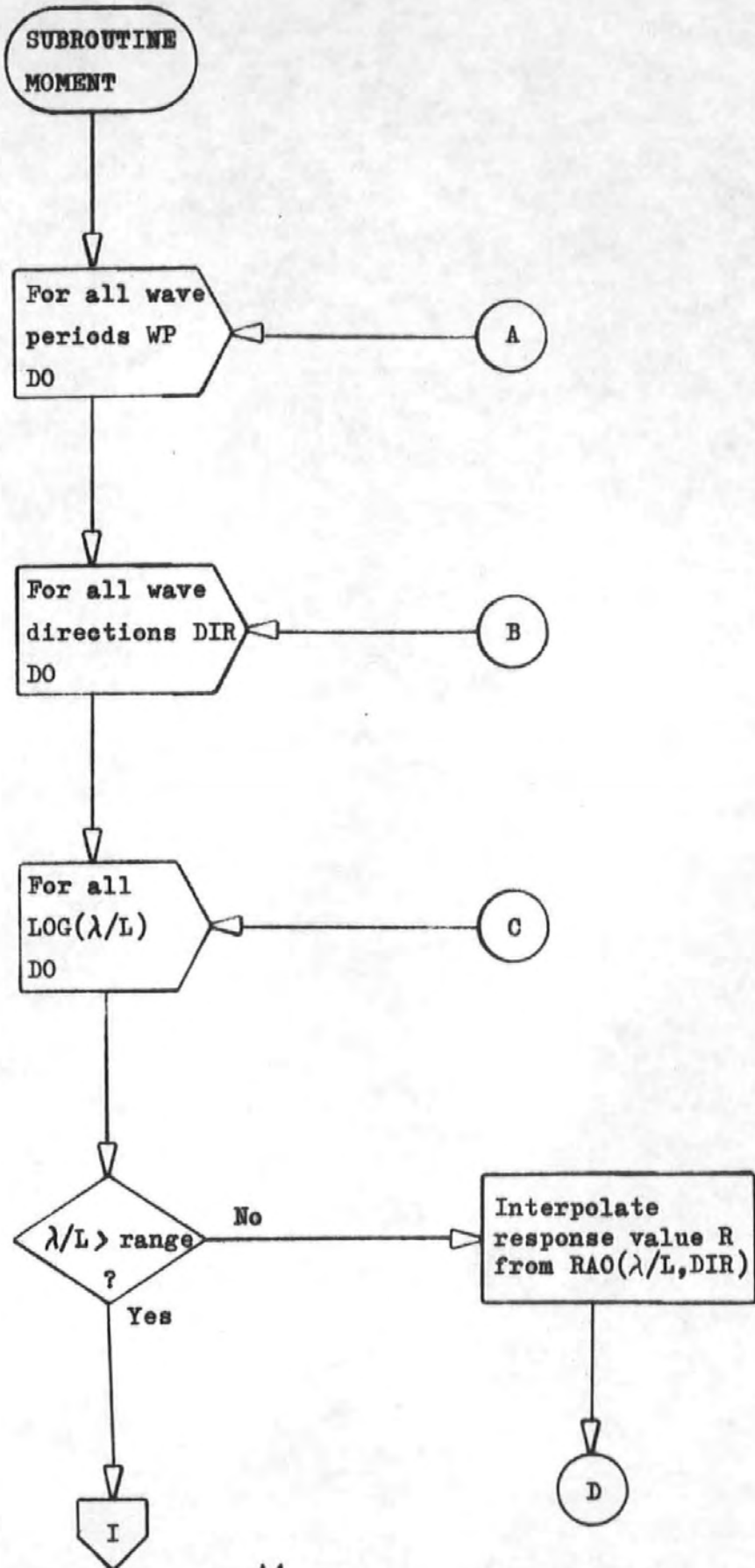
The first program is for calculation of responses in irregular waves for which the formulae may be found in Chapter 2. The second program describes the analysis of the full scale measurements from the tanker for which the mathematics are described in Chapter 5 under the headings of "the manual method" and "spectrum analysis".

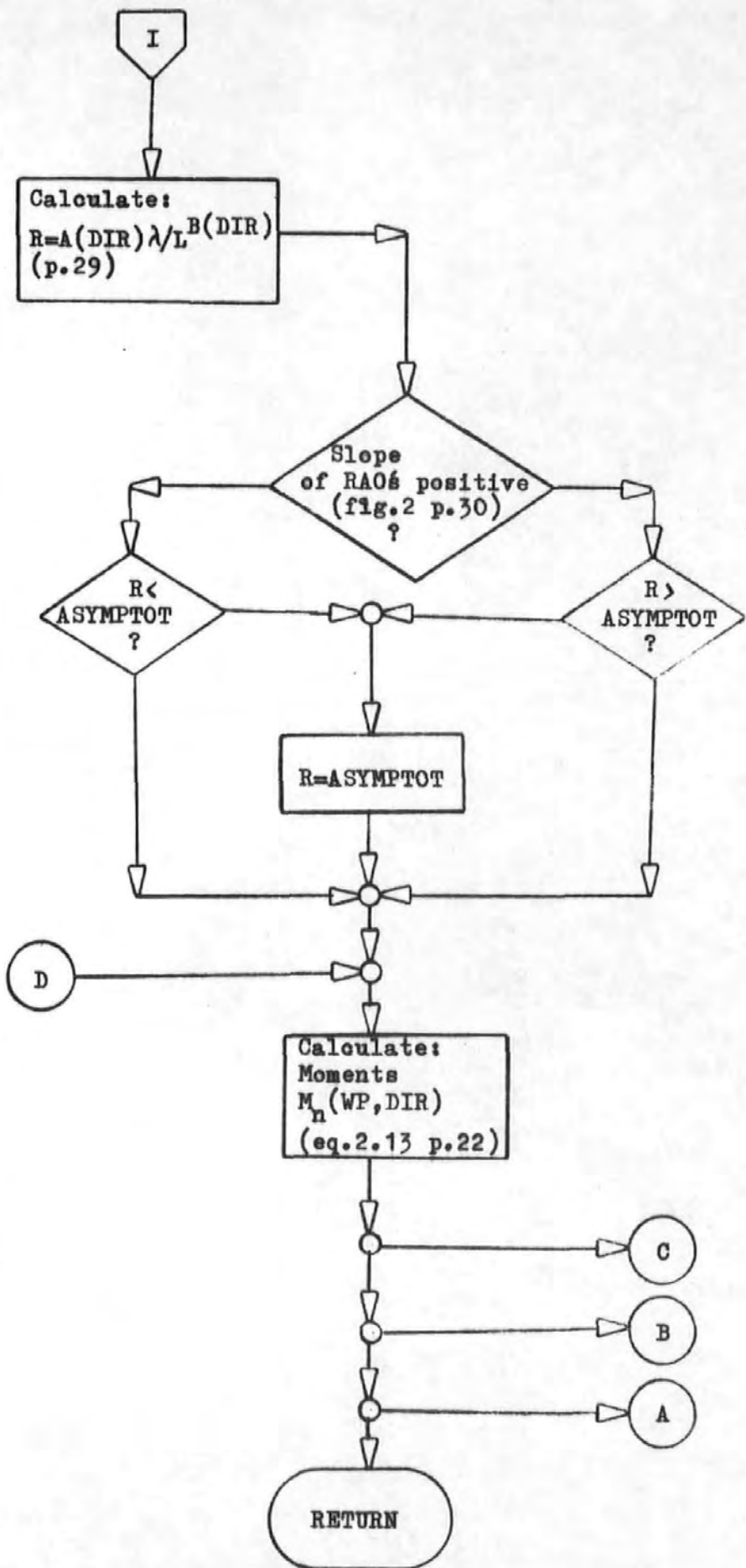
PROGRAM 1  
 RESPONSE IN IRREGULAR  
 WAVES

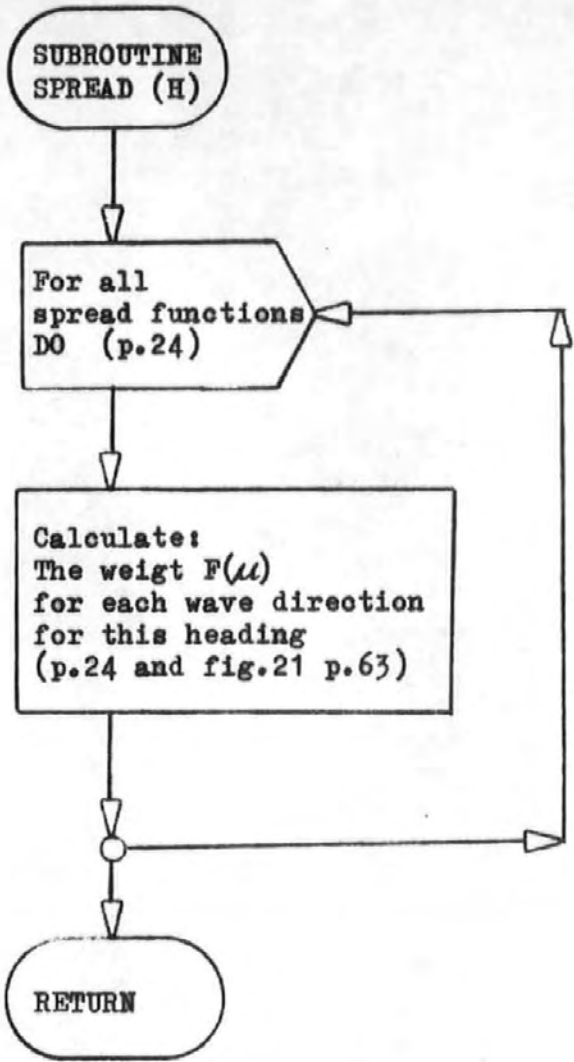


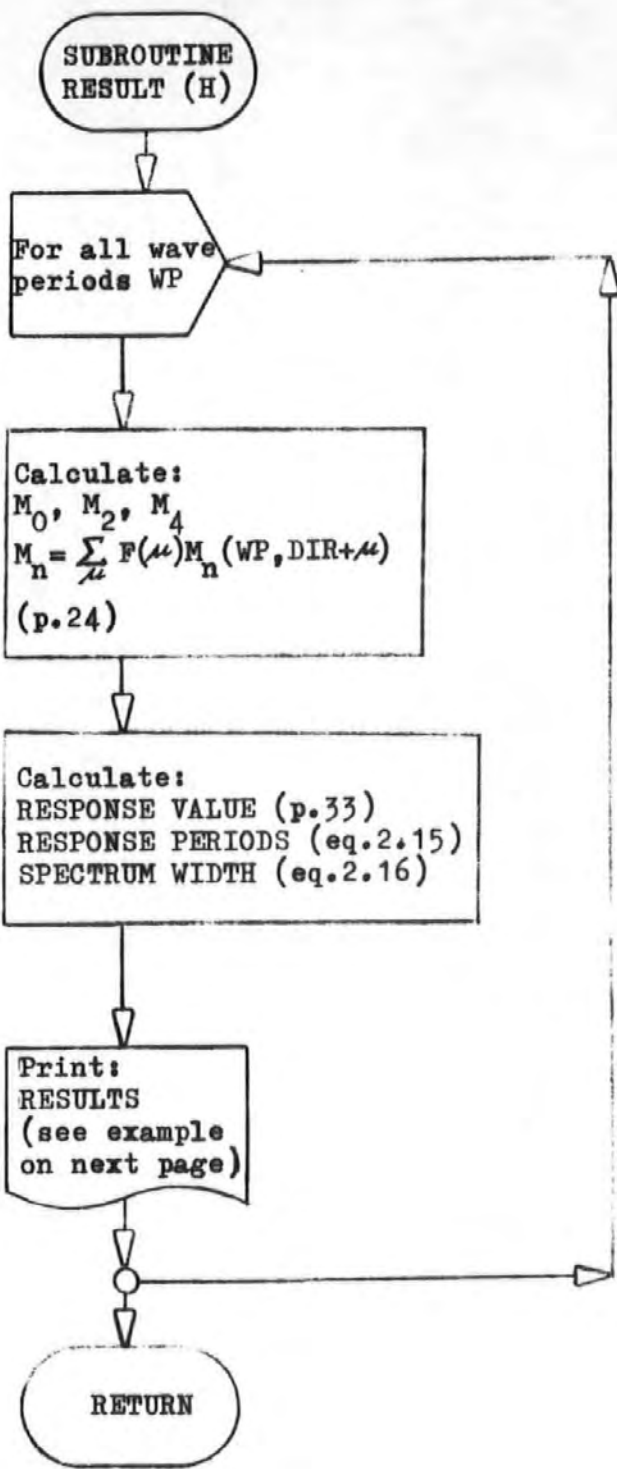












PITCH ANGLE            DEGREES/M            BALLAST  
 SPEED: 0 KNOTS  
 HEADING: 150 DEGREES

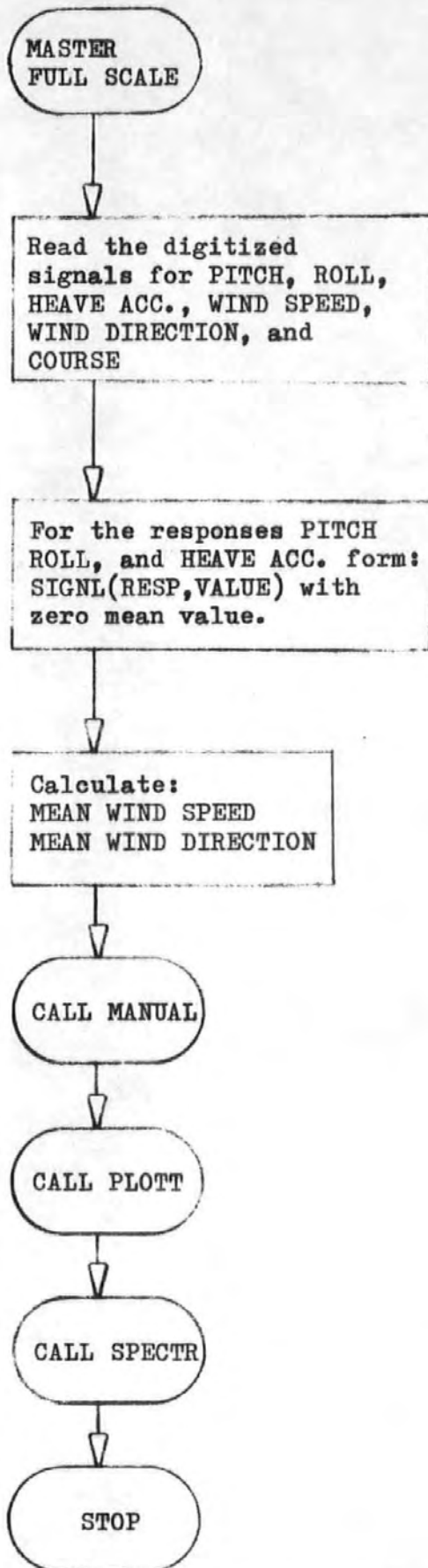
T2 PM	I            WITHOUT ENERGY SPREAD				I            WITH SPREAD FUNCTION 1				I            WITH SPREAD FUNCTION 2				I
	RESP. PERIOD	RESPONSE VALUE	ADJUSTED RESPONSE VALUE	RESP.- SPECTR WIDTH	RESP. PERIOD	RESPONSE VALUE	ADJUSTED RESPONSE VALUE	RESP.- SPECTR WIDTH	RESP. PERIOD	RESPONSE VALUE	ADJUSTED RESPONSE VALUE	RESP.- SPECTR WIDTH	
3.0	5.05	3.600E 01	3.510E 01	0.314	3.83	4.092E 01	3.311E 01	0.831	3.72	4.214E 01	3.409E 01	0.831	
5.0	6.24	7.547E 01	7.343E 01	0.327	6.09	7.434E 01	6.693E 01	0.615	6.05	7.417E 01	6.610E 01	0.641	
7.0	7.43	7.271E 01	6.908E 01	0.441	7.33	7.082E 01	6.406E 01	0.568	7.26	6.965E 01	6.342E 01	0.585	
8.0	7.86	6.623E 01	6.274E 01	0.453	7.73	6.269E 01	5.752E 01	0.563	7.66	6.141E 01	5.602E 01	0.579	
8.5	7.99	6.240E 01	5.391E 01	0.466	7.90	5.998E 01	5.504E 01	0.562	7.84	5.385E 01	5.370E 01	0.579	
9.0	8.09	5.755E 01	5.426E 01	0.471	8.06	5.660E 01	5.196E 01	0.561	8.01	5.356E 01	5.072E 01	0.577	
9.5	8.18	5.328E 01	5.018E 01	0.476	8.19	5.296E 01	4.803E 01	0.560	8.15	5.206E 01	4.752E 01	0.577	
10.0	8.26	4.952E 01	4.660E 01	0.478	8.29	4.946E 01	4.542E 01	0.560	8.26	4.576E 01	4.449E 01	0.579	
10.5	8.31	4.597E 01	4.325E 01	0.479	8.39	4.618E 01	4.241E 01	0.560	8.40	4.375E 01	4.170E 01	0.582	
11.0	8.34	4.278E 01	4.028E 01	0.477	8.47	4.311E 01	3.958E 01	0.561	8.55	4.300E 01	3.913E 01	0.586	
11.5	8.38	4.016E 01	3.782E 01	0.476	8.55	4.024E 01	3.690E 01	0.565	8.68	4.057E 01	3.681E 01	0.595	
12.0	8.43	3.758E 01	3.539E 01	0.476	8.64	3.735E 01	3.417E 01	0.571	8.86	3.314E 01	3.445E 01	0.607	
13.0	8.50	3.227E 01	3.038E 01	0.476	8.84	3.328E 01	3.041E 01	0.574	9.11	3.417E 01	3.077E 01	0.615	
14.0	8.50	2.843E 01	2.676E 01	0.477	8.96	2.952E 01	2.690E 01	0.582	9.36	3.094E 01	2.772E 01	0.628	
15.0	8.56	2.474E 01	2.326E 01	0.482	9.15	2.669E 01	2.425E 01	0.590	9.65	2.616E 01	2.511E 01	0.640	
20.0	8.54	1.415E 01	1.331E 01	0.478	9.37	1.569E 01	1.426E 01	0.590	10.01	1.694E 01	1.509E 01	0.644	

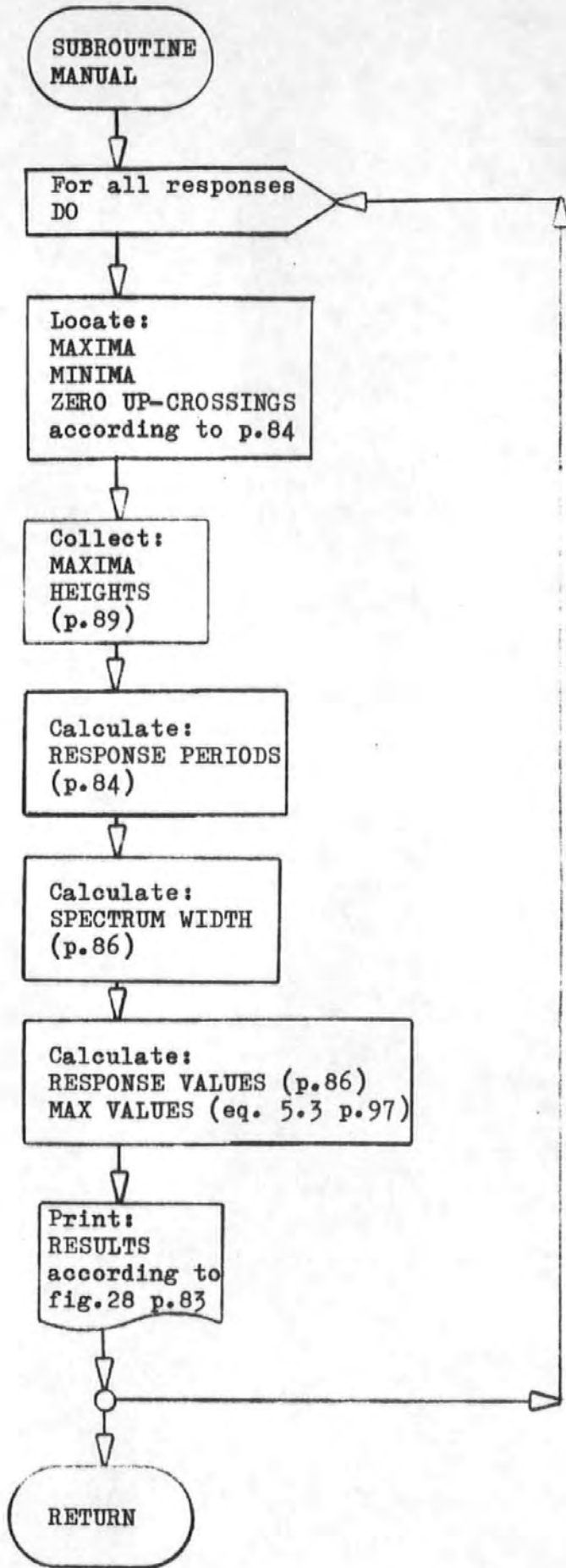
AB

HEADING: 165 DEGREES

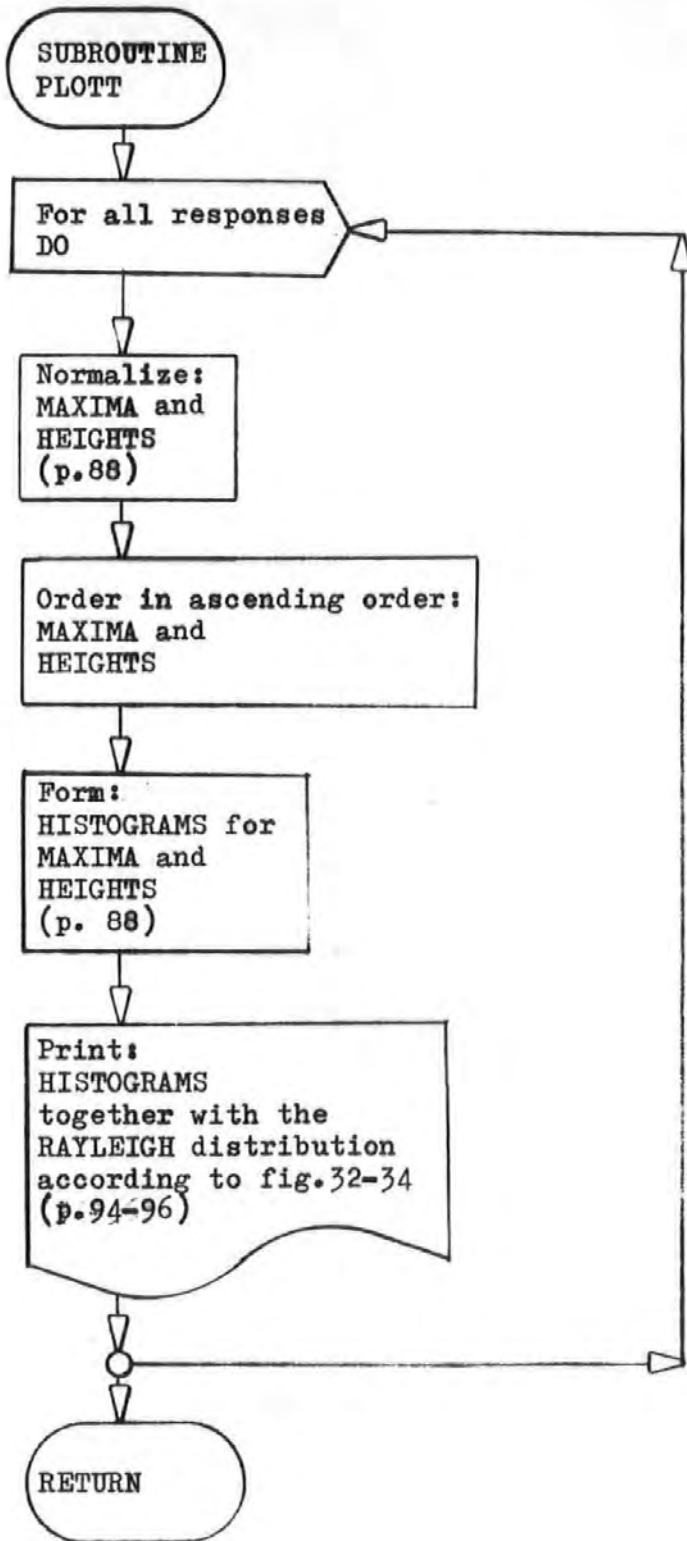
3.0	4.83	3.679E 01	3.237E 01	0.672	4.17	3.755E 01	3.058E 01	0.821	3.71	4.279E 01	3.421E 01	0.831	
5.0	6.21	7.511E 01	7.229E 01	0.384	6.19	7.395E 01	6.843E 01	0.536	6.05	7.419E 01	6.605E 01	0.644	
7.0	7.49	7.342E 01	6.925E 01	0.470	7.42	7.134E 01	6.635E 01	0.519	7.26	6.967E 01	6.330E 01	0.587	
8.0	7.91	6.502E 01	6.104E 01	0.487	7.82	6.335E 01	5.893E 01	0.519	7.66	6.142E 01	5.600E 01	0.581	
8.5	8.12	6.329E 01	5.924E 01	0.498	7.98	6.058E 01	5.628E 01	0.523	7.84	5.886E 01	5.368E 01	0.580	
9.0	8.33	6.064E 01	5.672E 01	0.502	8.13	5.716E 01	5.370E 01	0.523	8.01	5.556E 01	5.070E 01	0.579	
9.5	8.47	5.725E 01	5.348E 01	0.505	8.24	5.345E 01	4.965E 01	0.524	8.15	5.206E 01	4.750E 01	0.579	
10.0	8.57	5.356E 01	5.002E 01	0.506	8.33	4.981E 01	4.648E 01	0.523	8.26	4.576E 01	4.447E 01	0.580	
10.5	8.64	4.993E 01	4.661E 01	0.507	8.41	4.634E 01	4.308E 01	0.523	8.40	4.375E 01	4.168E 01	0.583	
11.0	8.68	4.626E 01	4.318E 01	0.508	8.45	4.307E 01	4.003E 01	0.522	8.53	4.300E 01	3.912E 01	0.587	
11.5	8.67	4.236E 01	3.956E 01	0.507	8.49	3.984E 01	3.707E 01	0.522	8.68	4.057E 01	3.660E 01	0.596	
12.0	8.63	3.836E 01	3.582E 01	0.506	8.51	3.664E 01	3.406E 01	0.523	8.85	3.313E 01	3.442E 01	0.607	
13.0	8.85	3.486E 01	3.254E 01	0.507	8.66	3.252E 01	3.041E 01	0.524	9.11	3.417E 01	3.074E 01	0.616	
14.0	8.77	2.972E 01	2.775E 01	0.507	8.68	2.836E 01	2.632E 01	0.526	9.36	3.093E 01	2.771E 01	0.629	
15.0	8.94	2.724E 01	2.541E 01	0.507	8.81	2.549E 01	2.364E 01	0.524	9.65	2.616E 01	2.510E 01	0.641	
20.0	8.94	1.545E 01	1.443E 01	0.506	8.89	1.468E 01	1.353E 01	0.525	10.01	1.694E 01	1.509E 01	0.644	

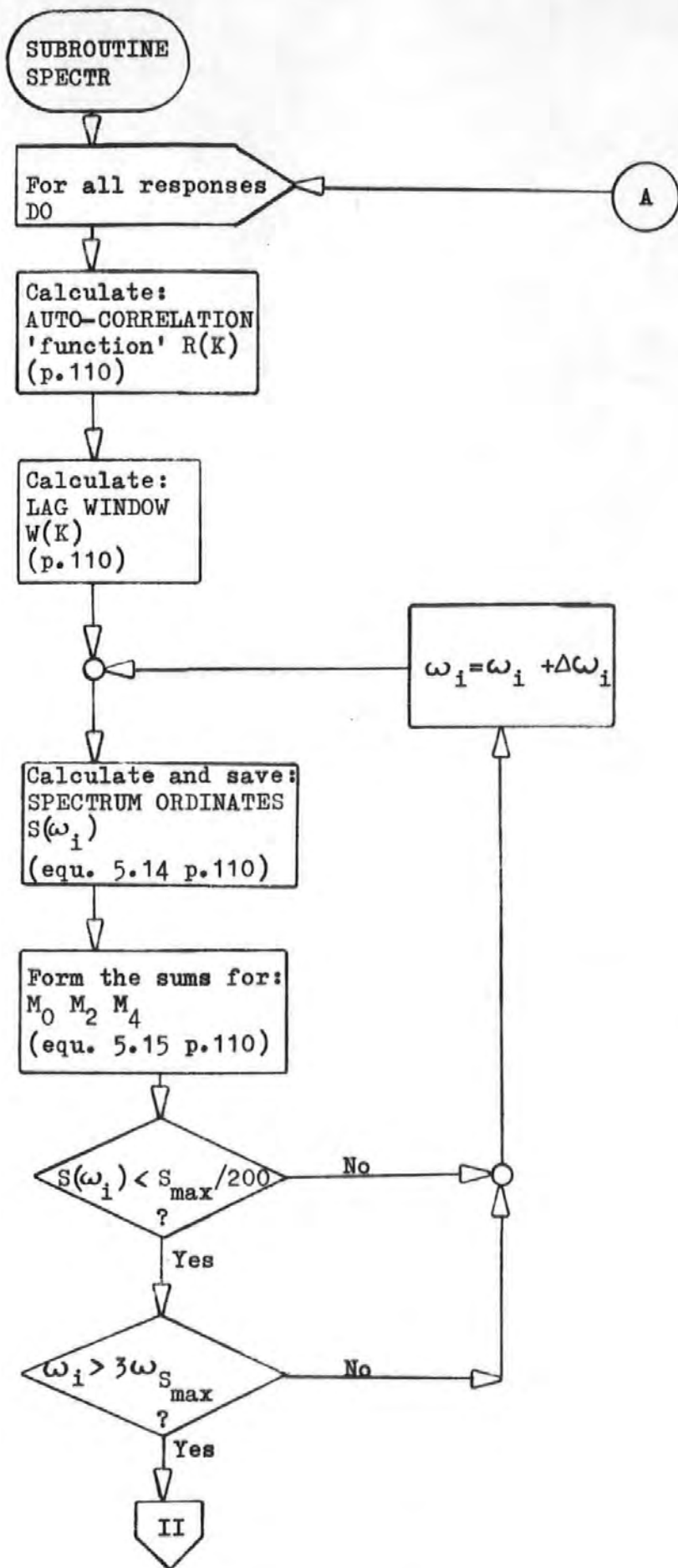
PROGRAM 2  
ANALYSIS OF  
FULL-SCALE DATA

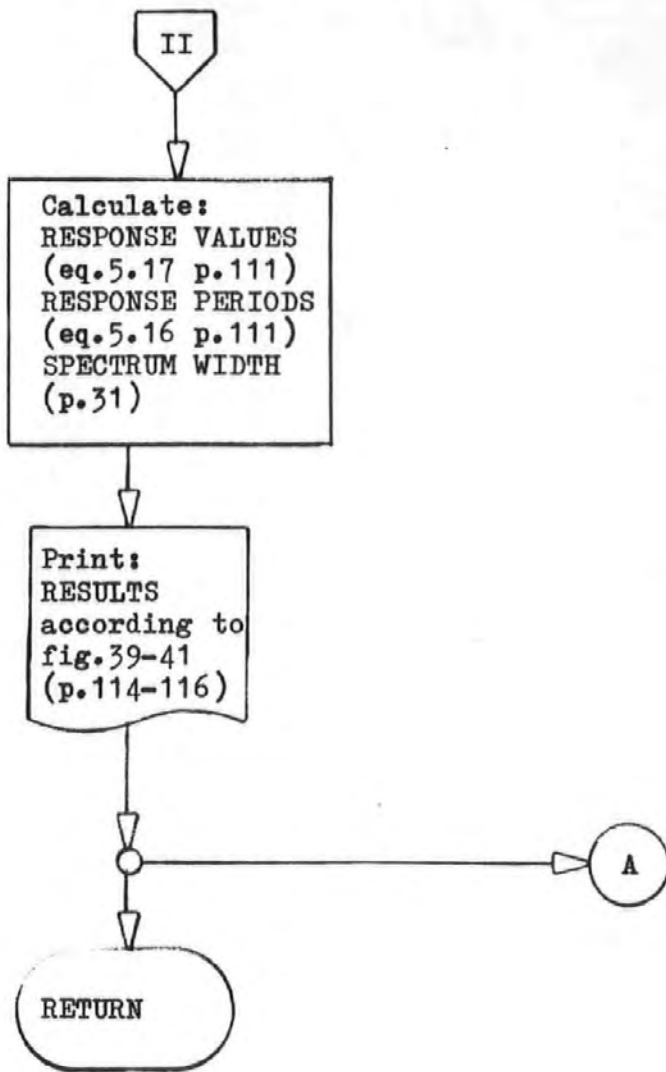












## SYMBOLS

$\alpha$	Phase displacement between wave and ship response	radians
$\alpha_i$	Phase displacement of wave component with frequency $\omega_i$	radians
$a$	Wave amplitude	m
$a_i$	Wave amplitude of wave compared with frequency $\omega_i$	m
$A$	Vertical acceleration	$\text{m sec}^{-2}$
$\beta$	Ship heading relative to direction of wave propagation	degrees
$b$	Wave breadth	m
$c$	Spectrum width parameter	
$E$	Energy of gravitational wave	$\text{kg m}^2 \text{sec}^{-2}$
$f_n(\mu)$	A spreading function	
$F$	Local freeboard	m
$F_n$	Froude Number	
$g$	Acceleration due to gravity	$\text{m sec}^{-2}$
$H$	Wave height	m
$\lambda$	Wave length	m
$L$	Ship length	m
$\mu$	Angle of a wave component to the axis of symmetry of the system	degrees
$m_n$	$n^{\text{th}}$ spectral moment	
$P$	Pitch angle	degrees
$\rho$	Mass density	$\text{kg m}^{-3}$
$R$	Roll angle	degrees
$r$	Relative bow motion amplitude	m
$r(t)$	Ship response as a function of time	
$R_P$	Pitch response amplitude	degrees
$R_R$	Roll response amplitude	degrees
$R_A$	Vertical acceleration response amplitude	$\text{m sec}^{-2}$
$\sigma^2$	Variance	
$S$	Power spectral density	

t	Time	sec
$T_2$	Mean wave period	sec
$T_P$	Mean pitch period	sec
$T_R$	Mean roll period	sec
$T_A$	Mean acceleration period	sec
$T_{P-M}$	Period of 'equivalent' spectrum	sec
U	Ship speed	m sec <sup>-1</sup>
$\omega$	Wave frequency	radians sec <sup>-1</sup>
$\omega_e$	Encounter frequency	radians sec <sup>-1</sup>
$Y_P$	Pitch response amplitude operator	
$Y_R$	Roll response amplitude operator	
$Y_A$	Vertical acceleration response amplitude operator	
$Y(\omega)$	Transfer function	
RM	Relative Bow motion	m